

AD-A084 641

BELL TELEPHONE LABS INC WHIPPANY N J  
BLAST TRANSPORT OF DEBRIS FROM SCALE MODEL BUILDINGS, VOLUME 1 --ETC(U)  
JAN 79 E F WITT

F/6 18/3

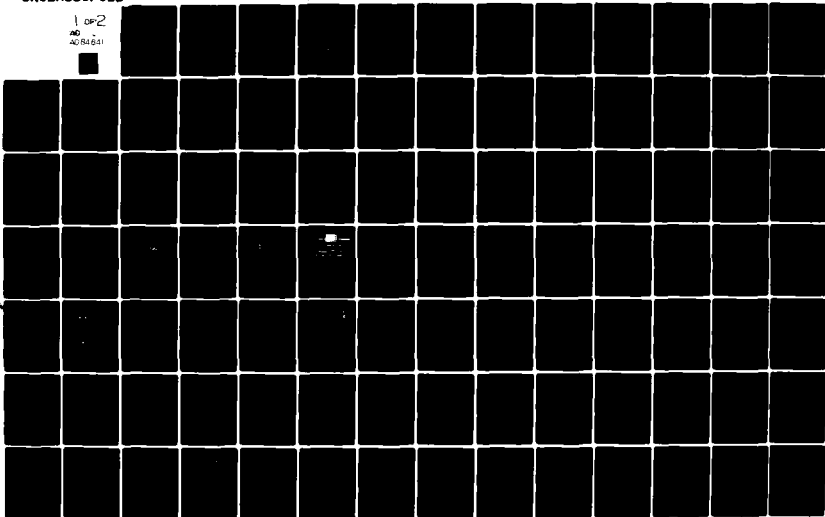
UNCLASSIFIED

SBIE -AD-E300 762

NL

1 of 2

AD  
AD 84 641



LEVEL III

AD-E 390 762

12

ADA 084641

# BLAST TRANSPORT OF DEBRIS FROM SCALE MODEL BUILDINGS

## Volume I - Chapters 1 through 5

Eugene F. Witt

Bell Telephone Laboratories, Inc.

Whippany, New Jersey 07981

18 January 1979

APPROVED FOR PUBLIC RELEASE;  
DISTRIBUTION UNLIMITED.

DDC FILE COPY

Prepared for  
Director  
DEFENSE NUCLEAR AGENCY  
Washington, D. C. 20305

DTIC  
ELECTRONIC  
MAY 23 1980

D

80 4 7 188

Destroy this report when it is no longer  
needed. Do not return to sender.

PLEASE NOTIFY THE DEFENSE NUCLEAR AGENCY,  
ATTN: STTI, WASHINGTON, D.C. 20305, IF  
YOUR ADDRESS IS INCORRECT, IF YOU WISH TO  
BE DELETED FROM THE DISTRIBUTION LIST, OR  
IF THE ADDRESSEE IS NO LONGER EMPLOYED BY  
YOUR ORGANIZATION.



UNCLASSIFIED

SECURITY CLASSIFICATION OF THIS PAGE (When Data Entered)

REPORT DOCUMENTATION PAGE		READ INSTRUCTIONS BEFORE COMPLETING FORM
1. REPORT NUMBER	2. GOVT ACCESSION NO.	3. RECIPIENT'S CATALOG NUMBER
	AD-A084642	
4. TITLE (and Subtitle)		5. TYPE OF REPORT & PERIOD COVERED
BLAST TRANSPORT OF DEBRIS FROM SCALE MODEL BUILDINGS Volume 1— Chapters 1 through 5		
7. AUTHOR(s)		6. PERFORMING ORG. REPORT NUMBER
Eugene F. Witt		
9. PERFORMING ORGANIZATION NAME AND ADDRESS		8. CONTRACT OR GRANT NUMBER(s)
Bell Telephone Laboratories, Inc. Whippany, New Jersey 07981		
11. CONTROLLING OFFICE NAME AND ADDRESS		10. PROGRAM ELEMENT PROJECT, TASK AREA & WORK UNIT NUMBERS
Director Defense Nuclear Agency Washington, D.C. 20305		
14. MONITORING AGENCY NAME & ADDRESS (if different from Controlling Office)		12. REPORT DATE
		18 January 1979
		13. NUMBER OF PAGES
		178
		15. SECURITY CLASS (of this report)
		UNCLASSIFIED
		15a. DECLASSIFICATION DOWNGRADING SCHEDULE
16. DISTRIBUTION STATEMENT (of this Report)		
Approved for public release; distribution unlimited.		
17. DISTRIBUTION STATEMENT (of the abstract entered in Block 20, if different from Report)		
18. SUPPLEMENTARY NOTES		
19. KEY WORDS (Continue on reverse side if necessary and identify by block number)		
Nuclear Effects	Operation SNOWBALL	TNT Tests
Scaling Debris	Operation DISTANT PLAIN	
Blast Effects	Event PAIRIE FLAT	
Scaling	Event DIAL PACK	
20. ABSTRACT (Continue on reverse side if necessary and identify by block number)		
<p>These tests were conducted to simulate in small scale, 1/140 to 1/8, the flight and ground distributions of debris ripped from masonry and wooden buildings by nuclear blasts. Those simulated in these tests had peak overpressures of 10 to 35 psi from detonations of 0.1 to 12 megatons. Scaled up test results are that wood debris can be carried over 2,000 feet with the blast, can travel over 1,000 feet to the side, can be lofted over 300 feet into the air above the building and can attain as much as 0.7 of the peak</p>		

20. ABSTRACT (Continued)

air particle velocity. These bounds are correspondingly less for denser masonry debris. Such effects can be a serious hazard to blast resistant facilities and these tests were part of a study to define these debris hazards. In all, 125 scale buildings were exposed to test blasts from up to 500 tons of TNT. The scaling factor, model debris density, and location from the test blast were determined by a scaling theory specifically developed for these tests. These models were specially constructed of loose pieces which simulated masonry blocks, plywood panels, beams and rafters. Some models were placed in groupings with one model building width between models. Less debris was carried away from the interior model buildings than from models on the periphery or from models placed by themselves. Tests were conducted on level terrain except in Event DIAL PACK where 15 degree slopes were constructed. These had limited effects on debris travel and slopes cannot be used to protect vulnerable facilities. The terminal locale of each piece of debris collected in these tests are presented along with information on the initial position in the building model of origin. All observed trajectories of wood debris are also presented. Some data is presented in statistical form. Most of the experimental data is in the volume of appendices.

<b>Accession For</b>	
NTIS GRA&I	<input checked="" type="checkbox"/>
DDC TAB	<input type="checkbox"/>
Unannounced	<input type="checkbox"/>
Justification	
By _____	
Distribution/	
Availability Codes	
Dist.	Avail and/or special
A	

DTIC  
ELECTE  
MAY 23 1980  
S D D

## INTRODUCTION

This two-volume report covers nine years of high-explosive field tests with scale-model buildings. The tests were designed to simulate, in miniature, the transport of debris from actual buildings by nuclear blasts.

The first volume contains the report itself — the scaling theory developed for the tests (Chapter 1), a description of the experimental techniques employed (Chapter 2), representative results regarding debris displacement from ground distributions (Chapter 3) and from debris trajectories as recorded by high-speed motion-picture cameras (Chapter 4), and a review of the results in terms of their simulated full-scale equivalents (Chapter 5). The second volume comprises ten appendices that present, in various formats, all the data obtained from all the tests conducted.

The tests incorporated 125 scale-model buildings, all square in plan, either as high or half as high as their horizontal dimensions, ranging in size from 3.3 to 60 inches on a side. These models were exposed to high-explosive TNT or gas-filled balloon detonations that simulated full-scale peak free-field overpressures of 10 to 35 psi and nuclear blast yields of 0.1 to 12 MT. The scale-model tests were part of a larger program of debris studies carried out by Bell Laboratories to determine how debris is formed and transported from actual buildings and other objects by nuclear blasts. Some of the results obtained from the scale-model tests supported other parts of the program; much information, however, is directly applicable to actual nuclear effects, as reviewed in Chapter 5. To the author's knowledge, this is the first detailed study of its kind and may be a stepping-stone to further studies.

Many people at Bell Laboratories supported this work during the years of the test series and thereafter. Don Cable, Jack Caroline, Dan Olatin, and Jerry Logan constructed models and operated cameras. Nick DeCapua directed the White Sands tests. Chen Fu, Martha Malone, and Kathy Holtz helped with data analysis. The report itself was

prepared with the help of Bob Goller, assisted by Jean Volz, Ann Wasser, and Kathy Willmot, all of the Technical Publication Department at Whippany,

Outside organizations contributed significantly to the tests. The blast-wave susceptibility of some of the models was checked at the Shock Tube Facility of Ballistic Research Laboratories. The vinyl blocks used to construct many of the model walls were prepared by the Hall Manufacturing Company; Harry Shaw Model Makers, Inc., preassembled and packed the block walls and prepared wooden parts for most of the models.

The U. S. Army SAFEGUARD System Command and its predecessors provided the funds for this report and for most of the experimental work itself. Additional support came from the Defense Research Establishment at Suffield, Canada, where most of the tests were performed, and from the Defense Nuclear Agency. Their cooperation is greatly appreciated.

Eugene F. Witt  
Bell Laboratories  
Whippany, New Jersey  
October 1974

## TABLE OF CONTENTS

	<u>Page</u>
Volume I	
Preface	iii
Chapter 1. BACKGROUND AND SCALING PROCEDURES	
1.1 Introduction	1-1
1.2 Objectives	1-3
1.2.1 SNOWBALL	1-3
1.2.2 DISTANT PLAIN	1-3
1.2.3 White Sands SOTRAN	1-3
1.2.4 PRAIRIE FLAT	1-3
1.2.5 DIAL PACK	1-3
1.3 Significance and Background	1-4
1.4 Theory of Scaling	1-4
1.4.1 Debris Flight in Blast	1-4
1.4.2 Equations of Motion	1-7
1.5 Scaling Schemes	1-10
1.5.1 Scheme with Debris Velocity Much Less Than Shock-Front Velocity	1-10
1.5.2 Scheme That Maintains Shock-Front Parameters	1-10
1.5.3 Scheme That Uses Scaling for Debris and Shock-Front Velocities	1-11
1.6 Assumptions and Approximations	1-11
1.6.1 Similarity of Blast Waves	1-11
1.6.2 Air-Velocity and Density Variations in the Blast Wave	1-12
1.6.3 Drag Coefficients	1-15
1.7 Graphical Method to Determine Test Conditions	1-16
1.8 Simulated Blast Conditions Corresponding to Tests	1-18

## TABLE OF CONTENTS (continued)

	<u>Page</u>
<b>Chapter 2. MODEL CONSTRUCTION AND DEBRIS COLLECTION</b>	
2.1 Model Building Characteristics and Requirements	2-1
2.2 Block Building Models	2-2
2.2.1 SNOWBALL	2-2
2.2.2 DISTANT PLAIN, Event 1	2-3
2.2.3 DISTANT PLAIN, Event 2a	2-6
2.2.4 DISTANT PLAIN, Event 2 (repeat)	2-8
2.2.5 White Sands SOTRAN	2-9
2.2.6 PRAIRIE FLAT	2-9
2.3 Frame Building Models	2-9
2.3.1 PRAIRIE FLAT	2-9
2.3.2 DIAL PACK	2-11
2.4 Packing and Shipping of Buildings	2-13
2.4.1 SNOWBALL	2-13
2.4.2 DISTANT PLAIN and White Sands SOTRAN	2-14
2.4.3 PRAIRIE FLAT	2-14
2.4.4 DIAL PACK	2-15
2.5 Model Layouts	2-15
2.5.1 SNOWBALL	2-15
2.5.2 DISTANT PLAIN	2-15
2.5.3 White Sands SOTRAN	2-15
2.5.4 PRAIRIE FLAT	2-15
2.5.5 DIAL PACK	2-20
2.6 Data Collection	2-23
2.6.1 Cameras	2-23
2.6.2 Identification of Building Elements	2-29
2.6.3 Debris Collection	2-34
<b>Chapter 3. DISTRIBUTION OF DEBRIS</b>	
3.1 Data Presentation	3-1
3.1.1 Bar Graphs	3-1
3.1.2 Statistical Representations	3-1
3.1.3 X-Y Plots	3-2
3.1.4 Terminal-Position Mapping on Representations of Building Surfaces	3-2

TABLE OF CONTENTS (continued)

	<u>Page</u>
3.2 Block Buildings, 1/120 Scale (SNOWBALL and PRAIRIE FLAT)	3-2
3.2.1 Distribution of Block Debris from Isolated Buildings	3-2
3.2.2 Distribution of Block Debris from Buildings in Complexes	3-4
3.2.3 Distribution of Roof Debris from Isolated Buildings	3-13
3.2.4 Distribution of Roof Debris from Buildings in Complexes	3-13
3.3 Larger Models at Low-Overpressure Sites: 1/8-Scale (PRAIRIE FLAT) and 1/33-Scale (White Sands SOTRAN) Buildings	3-18
3.3.1 Distribution of Block Debris from Isolated Buildings	3-19
3.3.2 Distribution of Block Debris from Buildings in Complex	3-20
3.3.3 Distribution of Roof Debris from Isolated Block Buildings	3-24
3.3.4 Distribution of Debris from 1/8-Scale Frame Buildings	3-27
3.4 Larger Models at High-Overpressure Sites: 1/8-Scale (PRAIRIE FLAT) and 1/33-Scale (White Sands SOTRAN) Block Buildings	3-27
3.4.1 Distribution of Block Debris	3-29
3.4.2 Distribution of Roof Debris	3-33
3.5 Block Buildings of 1/140 Scale (DISTANT PLAIN) and 1/20 Scale (PRAIRIE FLAT)	3-33
3.5.1 Distribution of Block Debris from Isolated Buildings	3-33
3.5.2 Distribution of Block Debris from Buildings in Complex	3-46
3.5.3 Distribution of Roof Debris from 1/20-Scale Models (PRAIRIE FLAT and DIAL PACK)	3-47
3.6 Effects of Sloping Terrain on Debris Transport (DIAL PACK)	3-47
 Chapter 4. DEBRIS IN FLIGHT	
4.1 Velocity-versus-Time Plots	4-1
4.1.1 Data Presentation	4-3
4.1.2 SNOWBALL 1/120-Scale Buildings	4-3
4.1.3 DISTANT PLAIN, Event 2a, 1/50-Scale Buildings and PRAIRIE FLAT 1/8-Scale Buildings; High-Overpressure Sites	4-4
4.1.4 DISTANT PLAIN, Event 2a, 1/50-Scale Buildings and PRAIRIE FLAT 1/8-Scale Buildings; Low-Overpress Sites	4-10
4.1.5 DISTANT PLAIN, Event 2a, 1/140-Scale Buildings and PRAIRIE FLAT 1/20-Scale Buildings	4-14
4.2 Debris Clouds	4-16
4.2.1 DIAL PACK 1/120-Scale Buildings	4-19
4.2.2 DIAL PACK 1/20-Scale Buildings	4-21
4.2.3 PRAIRIE FLAT 1/8- and 1/20-Scale Buildings	4-21

TABLE OF CONTENTS (continued)

	<u>Page</u>
Chapter 5. SUMMARY, CONCLUSIONS, AND RECOMMENDATIONS	
5.1 Hazard Prediction	5-1
5.1.1 Relating Model Elements to Real Materials	5-1
5.1.2 Predicted Bounds of Roof-Debris Distributions	5-3
5.1.3 Predicted Bounds of Block-Debris Distributions	5-5
5.1.4 Maximum Height of Debris Trajectories	5-7
5.1.5 Influence of Site Factors on Debris Distribution	5-10
5.2 Experimental Techniques	5-12
5.2.1 Model Construction	5-12
5.2.2 Instrumentation and Data Collection	5-12
5.3 Reproducibility and Consistency of Data	5-14
5.3.1 Roof-Panel Distributions — 1/120-Scale Models	5-14
5.3.2 Consistency with Other Data	5-16

Volume II

Appendix A. SNOWBALL, DISTANT PLAIN, and PRAIRIE FLAT 1/120-Scale Buildings: Post-Blast Locations of Wall Blocks	
Appendix B. SNOWBALL 1/120-Scale Complex: Post-Blast Locations of Roof Panels and Rafters	
Appendix C. PRAIRIE FLAT 1/120-Scale Buildings: Post-Blast Locations of Roof Panels and Rafters	
Appendix D. White Sands SOTRAN 1/33-Scale Buildings: Post-Blast Locations of Wall Blocks	
Appendix E. PRAIRIE FLAT 1/8- and 1/20-Scale Buildings: Post-Blast Locations of Wall Blocks	
Appendix F. White Sands SOTRAN 1/33-Scale Buildings: Post-Blast Locations of Roof Panels and Rafters	
Appendix G. PRAIRIE FLAT 1/8- and 1/20-Scale Buildings: Post-Blast Locations of Roof Panels and Rafters from Block Buildings and of All Debris from Frame Buildings	
Appendix H. DIAL PACK 1/20-Scale Buildings: Post-Blast Locations of All Debris	
Appendix I. DIAL PACK 1/120-Scale Buildings: Post-Blast Locations of All Debris	
Appendix J. Velocity-versus-Time Plots: Panels and Rafters	

## LIST OF ILLUSTRATIONS

<u>Figure</u>		<u>Page</u>
1.1	Representation of debris object in a blast wave.	1-5
1.2	Comparison of nuclear and high-explosive blast waveforms.	1-12
1.3	Time decay of dimensionless air density and particle velocity parameters.	1-13
1.4	Variation of positive phase duration with range.	1-14
1.5	Variation of blast air density . . . with time and shock strength.	1-14
1.6	Reynolds number as a function of diameter and velocity.	1-15
1.7	Graphical method of finding the scaling factor . . . for a 500-ton TNT blast.	1-18
2.1	SNOWBALL 40-building complex and isolated building before detonation.	2-4
2.2	Relative sizes and shapes of the plastic wall blocks used in the various tests.	2-5
2.3	Block construction methods used in the various tests.	2-6
2.4	Roof construction methods used in the various tests.	2-7
2.5	SNOWBALL block buildings after detonation.	2-8
2.6	PRAIRIE FLAT 1/120-scale block-building complex before detonation.	2-10
2.7	PRAIRIE FLAT 1/8-scale frame buildings.	2-11
2.8	Construction details, PRAIRIE FLAT 1/8-scale frame building.	2-12
2.9	Exterior construction, DIAL PACK 1/120-scale frame buildings.	2-13
2.10	Interior construction, DIAL PACK 1/20-scale frame buildings.	2-14
2.11	Camera locations in Operation SNOWBALL.	2-16
2.12	Plan view of the SNOWBALL model layout.	2-16
2.13	Camera locations, forward pad; DISTANT PLAIN, Event 2a.	2-17
2.14(a)	Camera locations, rear pad; DISTANT PLAIN, Event 2a.	2-18
2.14(b)	Plan view of the 1/140-scale buildings on the rear pad; DISTANT PLAIN, Event 2a.	2-18
2.15	Plan views of the forward and rear pads; White Sands SOTRAN.	2-19
2.16	General plan views of 1/20- and 1/8-scale layouts: PRAIRIE FLAT.	2-20
2.17	Plan views of large pad and a typical small pad, 1/8-scale low-overpressure site, and 1/20-scale site; PRAIRIE FLAT.	2-21

LIST OF ILLUSTRATIONS (continued)

<u>Figure</u>		<u>Page</u>
2.18	Plan view of 1/120-scale complex and isolated buildings: PRAIRIE FLAT.	2-22
2.19	DIAL PACK 1/20-scale buildings before detonation.	2-23
2.20	Plan view of the 1/20-scale building layout: DIAL PACK.	2-24
2.21	DIAL PACK 1/120-scale buildings before detonation.	2-25
2.22	Plan view of the 1/120-scale building layout: DIAL PACK.	2-26
2.23	Blast-proof camera housing.	2-29
2.24	Wall-block colors; SNOWBALL complex.	2-31
2.25	Exterior building colors; SNOWBALL complex.	2-32
2.26	Wall-block colors; DISTANT PLAIN, Event 2a.	2-33
2.27	Wall-block colors, full- and half-height isolated buildings: White Sands SOTRAN.	2-35
2.28	Wall-block colors; White Sands complex.	2-36
2.29	Wall-block colors, 1/120-scale buildings; PRAIRIE FLAT.	2-39
3.1	Block distribution from SNOWBALL 1/120-scale isolated block building.	3-3
3.2	Block distribution from front full-height 1/120-scale isolated building; PRAIRIE FLAT.	3-4
3.3	Block distribution from rear full-height 1/120-scale isolated building; PRAIRIE FLAT.	3-5
3.4	Block distribution from front half-height 1/120-scale isolated building; PRAIRIE FLAT.	3-6
3.5	Block distribution from rear half-height 1/120-scale isolated building; PRAIRIE FLAT.	3-7
3.6	Tangential block transport, SNOWBALL 1/120-scale buildings.	3-8
3.7	Radial block transport, SNOWBALL 1/120-scale buildings.	3-9
3.8	Tangential block transport, PRAIRIE FLAT 1/120-scale buildings.	3-10
3.9	Radial block transport, PRAIRIE FLAT 1/120-scale buildings.	3-11
3.10	Comparison of tangential block transport data, SNOWBALL.	3-12
3.11	Comparison of radial block transport data, SNOWBALL.	3-14
3.12	Comparison of roof-debris distributions, SNOWBALL and PRAIRIE FLAT 1/120-scale isolated buildings.	3-15
3.13	Comparison of tangential roof-debris transport, SNOWBALL and PRAIRIE FLAT 1/120-scale buildings within complex.	3-16
3.14	Comparison of radial roof-debris transport, SNOWBALL and PRAIRIE FLAT 1/120-scale buildings within complex.	3-17
3.15	Comparison of radial roof-debris transport, PRAIRIE FLAT 1/120-scale front-row buildings of complex.	3-19

LIST OF ILLUSTRATIONS (continued)

<u>Figure</u>		<u>Page</u>
3.16	Full-height isolated building after detonation; White Sands low-overpressure site.	3-20
3.17	Full-height isolated block building, 1/8 scale, after detonation; PRAIRIE FLAT low-overpressure site.	3-21
3.18	Block distributions, full-height isolated building; White Sands low-overpressure site.	3-22
3.19	Block distributions, forward full-height isolated building, 1/8 scale; PRAIRIE FLAT low-overpressure site.	3-23
3.20	White Sands complex after detonation.	3-24
3.21	Comparison of block distributions from complex and isolated building; White Sands.	3-25
3.22	Comparison of roof-debris transport; PRAIRIE FLAT (1/8 scale) and White Sands SOTRAN low-overpressure sites.	3-26
3.23	Comparison of roof- and floor-debris transport; PRAIRIE FLAT 1/8-scale low-overpressure site.	3-28
3.24	Half-height and full-height isolated buildings after detonation; White Sands high-overpressure site.	3-30
3.25	Selected block distribution from full-height building; White Sands high-overpressure site.	3-31
3.26	Selected block distribution from 1/8-scale full-height building; PRAIRIE FLAT high-overpressure site.	3-32
3.27	Comparison of roof-debris transport; PRAIRIE FLAT and White Sands SOTRAN high-overpressure sites.	3-34
3.28	Post-blast view of 1/20-scale buildings; PRAIRIE FLAT.	3-35
3.29	Front wall, 1/20-scale full-height building nearer the blast, showing distance contours; PRAIRIE FLAT.	3-36
3.30	Right side wall, 1/20-scale full-height building nearer the blast, showing distance contours; PRAIRIE FLAT.	3-37
3.31	Back wall, 1/20-scale full-height building nearer the blast, showing distance contours; PRAIRIE FLAT.	3-38
3.32	Left side wall, 1/20-scale full-height building nearer the blast, showing distance contours; PRAIRIE FLAT.	3-39
3.33	Front wall, 1/20-scale full-height building farther from the blast, showing distance contours; PRAIRIE FLAT.	3-40
3.34	Front and back walls, 1/20-scale half-height building nearer the blast, showing distance contours; PRAIRIE FLAT.	3-41
3.35	Left and right side walls, 1/20-scale half-height building nearer the blast, showing distance contours; PRAIRIE FLAT.	3-42
3.36	Post-blast view of 1/140-scale models; DISTANT PLAIN, Event 2a.	3-43
3.37	Block distribution from rear 1/140-scale isolated building; DISTANT PLAIN, Event 2a.	3-44
3.38	Block distribution from forward full-height 1/20-scale building; PRAIRIE FLAT.	3-45

LIST OF ILLUSTRATIONS (continued)

<u>Figure</u>		<u>Page</u>
3.39	Post-blast view of four-building 1/140-scale complex; DISTANT PLAIN, Event 2a.	4-46
3.40	Roof-debris transport from 1/20-scale buildings: PRAIRIE FLAT and DIAL PACK.	3-48
3.41	DIAL PACK 1/120-scale buildings after detonation.	3-49
3.42	DIAL PACK 1/20-scale buildings after detonation.	3-50
3.43	Radial debris transport from DIAL PACK 1/120-scale buildings.	3-51
3.44	Comparison of roof-debris transport from DIAL PACK 1/120- and 1/20-scale buildings.	3-52
3.45	Comparison of radial debris transport from roofs, back walls, and floors; DIAL PACK 1/20-scale buildings.	3-54
4.1	Debris lofting in Operation SNOWBALL.	4-2
4.2	Roof-debris trajectories; SNOWBALL.	4-3
4.3	Roof-panel velocity-versus-time bounds; SNOWBALL.	4-5
4.4	Roof-rafter velocity-versus-time bounds; SNOWBALL.	4-6
4.5	Roof-debris trajectories: DISTANT PLAIN, Event 2a, 1/50-scale buildings and PRAIRIE FLAT 1/8-scale buildings; high-overpressure sites.	4-7
4.6	Roof-debris velocity-versus-time bounds; DISTANT PLAIN, Event 2a, 1/50-scale buildings; high-overpressure site.	4-8
4.7	Roof-debris velocity-versus-time bounds and plots; PRAIRIE FLAT 1/8-scale buildings; high-overpressure site.	4-9
4.8	Comparison of full-scale velocity-versus-time bounds; DISTANT PLAIN, Event 2a, 1/50-scale buildings and PRAIRIE FLAT 1/8-scale buildings; high-overpressure sites.	4-10
4.9	Roof-debris trajectories; DISTANT PLAIN, Event 2a, 1/50-scale buildings and PRAIRIE FLAT 1/8-scale buildings; low-overpressure sites.	4-11
4.10	Roof-debris velocity-versus-time plots; DISTANT PLAIN, Event 2a, 1/50-scale buildings; low-overpressure site.	4-12
4.11	Roof-panel velocity-versus-time bounds; PRAIRIE FLAT 1/8-scale block and frame buildings, low-overpressure site.	4-13
4.12	Comparison of full-scale velocity-versus-time plots, DISTANT PLAIN, Event 2a, 1/50-scale buildings, and bounds, PRAIRIE FLAT 1/8-scale buildings; low-overpressure sites.	4-14
4.13	Roof-debris trajectories; DISTANT PLAIN, Event 2a, 1/140-scale buildings, and PRAIRIE FLAT 1/20-scale buildings.	4-15
4.14	Roof-debris velocity-versus-time bounds and plots; DISTANT PLAIN, Event 2a, 1/140-scale buildings.	4-17
4.15	Roof-debris velocity-versus-time bounds; PRAIRIE FLAT 1/20-scale buildings.	4-18

LIST OF ILLUSTRATIONS (continued)

<u>Figure</u>		<u>Page</u>
4.16	Comparison of full-scale velocity-versus-time bounds; DISTANT PLAIN, Event 2a, 1/140-scale buildings and PRAIRIE FLAT 1/20-scale buildings.	4-19
4.17	Airborne debris; DIAL PACK 1/120-scale buildings.	4-20
4.18	Airborne debris; DIAL PACK 1/20-scale buildings.	4-21
4.19	Airborne debris; PRAIRIE FLAT sites.	4-22
5.1	Maximum full-scale radial distances between roof-panel terminal locations and buildings of origin.	5-3
5.2	Maximum full-scale tangential distances between roof- and wall-panel terminal locations and buildings of origin.	5-4
5.3	Maximum full-scale radial distances between wall-block terminal locations and buildings of origin.	5-5
5.4	Maximum full-scale tangential distances between wall-block terminal locations and buildings of origin.	5-7
5.5	Ratios of maximum full-scale vertical debris velocities to simulated peak air velocity versus simulated weapon yield.	5-8
5.6	Maximum full-scale trajectory height versus simulated weapon yield.	5-9
5.7	Maximum full-scale tangential distances between roof-panel terminal locations and buildings of origin; SNOWBALL and PRAIRIE FLAT 1/120-scale buildings.	5-11
5.8	Maximum full-scale tangential distances between roof-panel terminal locations and buildings of origin; DIAL PACK 1/120-scale and 1/20-scale buildings.	5-12
5.9	Comparison of air-velocity waveforms from various tests with the predicted waveform.	5-13
5.10	Comparison of the radial and tangential mean displacements of roof panels; SNOWBALL, PRAIRIE FLAT, and DIAL PACK 1/120-scale buildings.	5-15
5.11	Comparison of the radial and tangential variances of roof panels; SNOWBALL, PRAIRIE FLAT, and DIAL PACK 1/120-scale buildings.	5-17

## LIST OF TABLES

<u>Table</u>		<u>Page</u>
1.1	Summary of building models in blast tests	1-2
1.2	Summary of scaling parameters	1-9
1.3	Summary of simulated nuclear-blast parameters	1-19
2.1	Dimensions and weights of building elements	2-2
2.2	Summary of site information	2-27
2.3	Camera data	2-28
5.1	Summary of specific gravities of model elements	5-2

## Chapter 1

### BACKGROUND AND SCALING PROCEDURES

#### 1.1 Introduction

Objects transported by a nuclear blast wave pose a serious threat to facilities designed to withstand such blasts — more serious, sometimes, than other nuclear weapon effects. For example, an antenna radome may be designed to resist blast pressure and thermal radiation, but chunks of material ripped from nearby buildings and traveling at hundreds of feet per second probably would destroy the radome.

The tests reported here were conducted to explore how such building debris is transported by nuclear blasts. It is a complicated problem, because the damaging potential is a function of the blast characteristics, the characteristics of the debris, and the characteristics of the source of the debris. A method was devised for reproducing the desired conditions in miniature: small models were blown apart by correspondingly small high-explosive detonations, the models and the scaled-down blasts designed to simulate the effects of a full-size nuclear blast on actual buildings.

This chapter includes background material on the various tests and an explanation of the scaling techniques that were developed for them. The models were simple cubes with flat roofs, ranging in size from 3.3 inches to 60 inches on a side. Many were constructed of interlocking blocks, though frame models were devised also. All were constructed of loose pieces, so that a blast could reduce the models to their constituent elements and scatter these as debris. The terminal location of debris was recorded after each blast, provided that external influences such as high winds did not destroy the validity of such data; high-speed motion pictures were taken during most of the tests. Five of the seven tests took place at the Defense Research Establishment in Suffield, Alberta, Canada; one test was conducted at the White Sands Proving Ground in New Mexico.

A brief summary of information pertaining to the models, detonations, and other field conditions is presented in Table 1.1.

Table 1.1  
SUMMARY OF BUILDING MODELS IN BLAST TESTS

Test	Yield (tons TNT)	Model Plan (in. x in.)	Number of Buildings in Complex	Number of Isolated Buildings			Distance from Blast (ft)	Peak Free-Field Overpressure (psig)	
				Block	Frame	Frame			
				Full Ht.	Half Ht.	Full Ht.	Half Ht.		
SNOWBALL	500	4 x 4	40	1	0	0	0	4200	1
DISTANT PLAIN									
Event 1	20	3.3 x 3.3	15	2	0	0	0	1000	1.7
		10 x 10	15	2	0	0	0	1000	1.7
		10 x 10	15	2	0	0	0	720	3.5
Event 20	20*	3.3 x 3.3	4	2	0	0	0	1000	1.7
		10 x 10	4	2	0	0	0	1000	1.7
		10 x 10	4	2	0	0	0	720	3.0
White Sands									
Day	50	14 x 14	4	1	1	0	0	1400	2.0
		14 x 14	0	1	1	0	0	1000	3.0
Night	50	14 x 14	12	1	1	0	0	1400	2.0
		14 x 14	0	1	1	0	0	1000	3.0
PRAIRIE FLAT									
	500	4 x 4	12	2	2	0	0	4231	1
		24 x 24	0	2	2	0	0	2174	3
		60 x 60	0	2	2	1	1	2120 to 2218	3
		60 x 60	0	2	2	0	0	1465 to 1526	6
DIAL PACK									
	500	4 x 4	0	0	0	12	0	4052	1
		24 x 24	0	0	0	10	0	2000	3

\*Gas-filled balloon.

## 1.2 Objectives

### 1.2.1 SNOWBALL

The first debris study took place in Operation SNOWBALL at Suffield in 1964. Its objective was to obtain a comparison between debris transport from buildings spaced close together and debris transport from a single building standing alone. The single isolated building suffered wind damage before the test; hence, the results were incomplete.

### 1.2.2 DISTANT PLAIN

The debris study in Operation DISTANT PLAIN at Suffield in 1966 was designed to provide data for three blast conditions. It was anticipated that the same three conditions could be simulated in a forthcoming test using larger models; comparing the field results would then determine the validity of the scaling technique. Isolated buildings and complexes of closely spaced buildings were used in this operation.

Winds again interfered with data collection. The initial test, in Event 1, was completely invalidated by wind damage; a modified test, Event 2a, was somewhat more successful but nevertheless yielded relatively little data.

### 1.2.3 White Sands SOTRAN

The SOTRAN tests were conducted at White Sands in 1967 to provide the data not obtained in Operation DISTANT PLAIN. Two debris tests took place. The first, conducted during the day, suffered complete wind damage, but the second, which took place during a dead calm at midnight, was a complete success.

### 1.2.4 PRAIRIE FLAT

Event PRAIRIE FLAT was conducted at Suffield in 1968 primarily to obtain better information on isolated buildings than had been obtained in Operation SNOWBALL. Other tests were conducted to add to the kinds of data obtained during DISTANT PLAIN and the SOTRAN tests at White Sands.

All model buildings up to the time of PRAIRIE FLAT were constructed of interlocking blocks of various sizes and shapes. Two models of frame construction were developed for use in PRAIRIE FLAT and used for the first time in that event. Successful information was obtained on both the block and the frame models.

### 1.2.5 DIAL PACK

The DIAL PACK event was conducted at Suffield in 1970 to determine the effect of hilly terrain on debris transport and deposition. Specifically, the results of this test were to show whether hilly terrain can provide buildings with enough protection to minimize debris from a nearby blast.

Two horizontal pads were built at different levels, with an inclined pad joining them. The models, all of frame construction, were placed in various configurations on the two levels and on the incline. Good results were obtained from this test.

### 1.3 Significance and Background

Debris from unhardened buildings and other sources can be a serious threat to antiballistic ground facilities and other military or civil communication facilities. Debris damage is also a factor in the study of post-attack recovery in cities. The threat can affect the design of hardened facilities, the location of these facilities, and the requirements to be placed on the sites.

Unfortunately, no direct experimental data existed to provide information on the nature of the threat of airborne debris. Trajectories of specific blast-induced airborne objects could be calculated, but the perturbations inherent in airborne building debris could not be simulated. These experiments were conducted to provide this vital information and to provide field data that could check computed predictions.

To the best of the author's knowledge the scaling technique used here is original and has not been used before.

### 1.4 Theory of Scaling

Several criteria governed the derivation of the scaling scheme discussed here:

1. The blast wave applied to the model must be similar to an actual wave from a nuclear blast.
2. The flight of debris must be similar in actual and scaled cases.
3. The equations of motion for debris must be similar in both cases.

It is assumed that the first criterion is satisfied if TNT is used for the scale-model blasts, since nuclear blasts and those produced by TNT are similar at the relatively low overpressures of interest here.

#### 1.4.1 Debris Flight in Blast

A piece of debris is assumed to be at rest at a certain distance from the blast. It is engulfed by the blast wave and sent into flight. The propelling force on the debris results from the differential between the debris velocity and the air velocity. This phenomenon is rather complex, because the air velocity and density are functions of both time and distance.

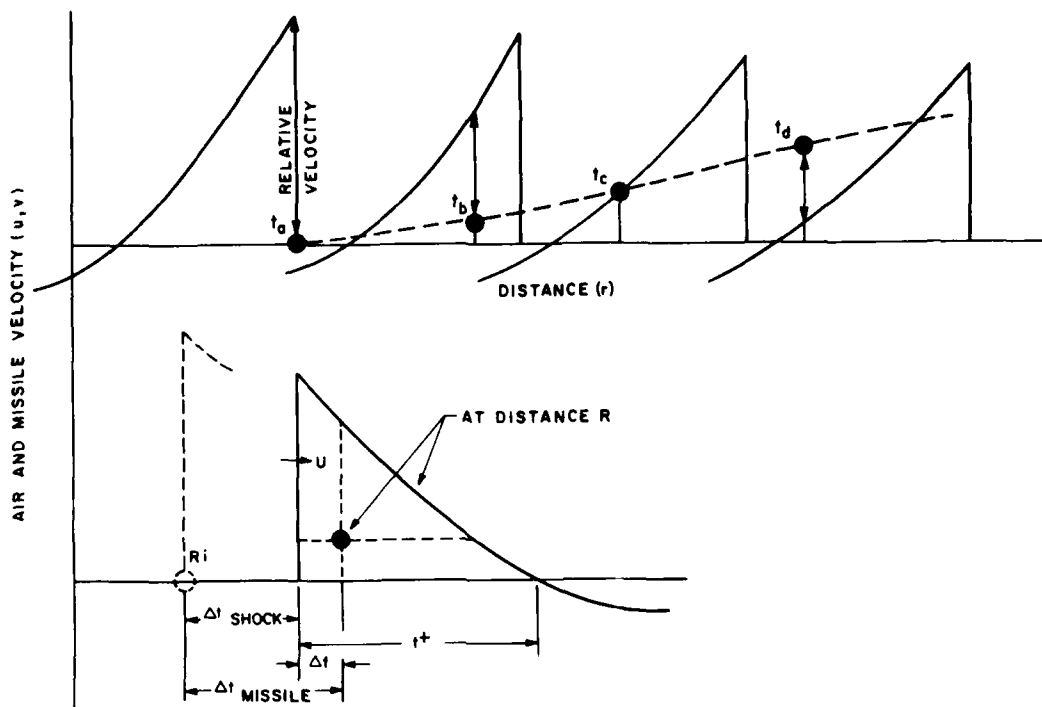


Figure 1.1. Representation of debris object in a blast wave.

Figure 1.1 represents the distance-versus-air-velocity characteristics of a blast wave at four points in time, just as if the blast effect were recorded by stop-motion photography. At time (a) the shock front reaches the material that becomes the debris. At time (b) the piece of debris is engulfed by the blast wave and falls behind the shock front. The debris accelerates as long as the air velocity is greater than that of the debris. At time (c) the velocities of the debris and the air are equal. At time (d) the debris decelerates.

The lower portion of Figure 1.1 represents the velocity of the air versus time at a fixed point,  $R$ ; this is the way blast measurements are made. The piece of debris appears at  $R$  only for an instant, because it is in motion; it arrives at  $R$  after the shock front.

The shock wave moves from an initial point,  $R_i$ , to  $R$  in time  $\Delta t_{\text{shock}}$ :

$$\Delta t_{\text{shock}} = \int_{R_i}^R \frac{dr}{U(r)}; \quad (1)$$

$U(r)$  is the shock-front velocity as a function of the variable  $r$ .

The piece of debris moves from  $R_i$  to  $R$  in time  $\Delta t_{\text{debris}}$ :

$$\Delta t_{\text{debris}} = \int_{R_i}^R \frac{dr}{v(r)}; \quad (2)$$

$v(r)$  is the debris velocity as a function of  $r$ .

The time lag between the arrival of the shock front and the arrival of the debris at point  $R$  is

$$\Delta t = \int_{R_i}^R \left[ \frac{1}{v(r)} - \frac{1}{U(r)} \right] dr. \quad (3)$$

The relative position of the debris at each such point  $R$  can be described by the ratio of  $\Delta t$  to the positive phase duration,  $t^+$ , which also is a function of  $R$ .

Consider two blast environments — for example, an actual, full-size environment and a scaled-down environment — with a piece of debris moving in each. If the two environments are similar, then at a distance  $R$  from a blast of yield  $W$  the relative position of the debris in the blast wave is the same as its counterpart's position at a distance  $R'$  from a blast of yield  $W'$ .

$$\frac{1}{t^+(R)} \int_{R_i}^R \left[ \frac{1}{v(r)} - \frac{1}{U(r)} \right] dr = \frac{1}{t^+(R')} \int_{R'_i}^{R'} \left[ \frac{1}{v'(r')} - \frac{1}{U'(r')} \right] dr'. \quad (4)$$

The integrands and variables of integration in Equation (4) can be related by constant proportions. Assume:

$$\frac{U'(R')}{U(R)} = \frac{v'(R')}{v(R)} = \alpha; \quad (5)$$

$$\frac{R'}{R} = \frac{r'}{r} = \beta.$$

Since

$$\frac{1}{U'(r')} = \frac{1}{\alpha[U(r)]},$$

$$\frac{1}{v'(r')} = \frac{1}{\alpha[v(r)]},$$

$$r' = \beta r,$$

$$R' = \beta R,$$

Equation (4) becomes

$$\frac{1}{t^+(R)} \int_{R_i}^R \left[ \frac{1}{v(r)} - \frac{1}{U(r)} \right] dr = \frac{\beta}{\alpha t^+(\beta R)} \int_{R_i}^R \left[ \frac{1}{v(r)} - \frac{1}{U(r)} \right] dr .$$

Thus,

$$\frac{t^+(\beta R)}{t^+(R)} = \frac{\beta}{\alpha} . \quad (6)$$

The ratio  $\beta/\alpha$  is an implied ratio of time in Equation (5); therefore, Equation (6) simply states that positive phase duration varies directly with time.

If both  $\alpha$  and  $\beta$  are allowed to vary, Equation (6) does not provide sufficient information to design a scale-model environment that simulates debris motion beginning at a given distance from a known explosion. The dynamic equations of motion impose further restrictions on this simulation.

#### 1.4.2 Equations of Motion

The general equations that describe two-dimensional trajectories of objects in horizontal blast flow are:

$$\begin{aligned} M\ddot{x} &= \frac{\rho A}{2} \left[ C_D (u - \dot{x}) - C_L (v - \dot{y}) \right] \left[ (u - \dot{x})^2 + (v - \dot{y})^2 \right]^{1/2} \\ M(\ddot{y} + g) &= \frac{\rho A}{2} \left[ C_D (v - \dot{y}) + C_L (u - \dot{x}) \right] \left[ (u - \dot{x})^2 + (v - \dot{y})^2 \right]^{1/2} \end{aligned} \quad (7)$$

where

- $C_D$  = drag coefficient;
- $C_L$  = lift coefficient;
- $A$  = cross-sectional area of object;
- $M$  = mass of object;
- $\rho$  = air density;
- $x$  = horizontal component of object displacement;
- $y$  = vertical component of object displacement;
- $\dot{x}$  = horizontal component of object velocity;
- $\dot{y}$  = vertical component of object velocity;
- $\ddot{x}$  = horizontal component of object acceleration;
- $\ddot{y}$  = vertical component of object acceleration;

- u = horizontal component of air velocity;
- v = vertical component of air velocity;
- g = gravitational acceleration.

A change in velocity requires that both the object and air velocities be multiplied by the same factor in these equations. It is not possible to do this and still maintain the proportion between shock-front and debris velocities given in Equations (5), since shock-front and air-particle velocities in a blast are not linearly related. It is not possible, therefore, to scale debris trajectories exactly.

A simplification of Equation (7), in which  $C_L = v = \dot{y} = 0$ , demonstrates the relationships between parameters:

$$M\ddot{x} = \frac{\rho A C_D}{2} (u - \dot{x})^2, \quad (8)$$

or

$$M\ddot{x} = \frac{\rho}{2\rho_f} A C_D \rho_f u_f^2 \left( \frac{u}{u_f} - \frac{\dot{x}}{u_f} \right)^2.$$

$\rho_f$  is the air density at the shock front and  $u_f$  is the air velocity at the shock front.

Again consider two blast environments with an object moving in the blast wave of each. The parameters for this situation are summarized on the right side of Table 1.2. Equation (8) for these debris objects then becomes the following:

$$\text{For object 1: } s^3 m = \frac{1}{2} C_D \rho_f u_f^2 s^2 \left[ \frac{\rho}{\rho_f} \left( \frac{u}{u_f} - \frac{\dot{x}}{u_f} \right)^2 \right]. \quad (9)$$

$$\text{For object 2: } \beta^3 s^3 m' = \frac{1}{2} \beta^2 C_D' \rho_f' \alpha^2 u_f'^2 s^2 \left[ \frac{\rho'}{\rho_f'} \left( \frac{u'}{u_f'} - \frac{\dot{x}'}{u_f'} \right)^2 \right]. \quad (10)$$

where

m = density of object;

s = typical dimension of object, e.g., the side of a cube.

If it is assumed that the quantities in brackets in Equations (9) and (10) have about the same variation with time divided by positive phase duration for a range of shock-front parameters, regardless of explosive yield, then Equations (9) and (10) are approximately equivalent if

$$\frac{C_D}{m} = \frac{C_D' \rho_f' \alpha^2}{m' \beta}. \quad (11)$$

Table 1.2  
SUMMARY OF SCALING PARAMETERS

Parameter	Actual Blast and Object 1 and Object 2		Scaling Schemes	
	$U$	$\alpha U$	$U \gg \dot{x}$	$\alpha = 1$ $u \gg \dot{x}$
Shock Velocity	$U$	$\alpha U$	Not applicable	$U$
Peak Air Velocity	$u_f$	$\alpha u_f$	$\alpha u_f$	$u_f$
Positive Phase Duration	$t^+$	$(\beta/\alpha)t^+$	$\alpha t^+$	$\beta t^+$
Peak Air Density	$\rho_f$	$\frac{C_D^m \beta \rho_f}{C_D^m \alpha^2}$	$\frac{C_D^m \rho_f}{C_D^m}$	$\rho_f$
Object Density	$m$	$\frac{C_D^m \rho_f \alpha^2 m}{C_D^m \beta^3}$	$\frac{C_D^m \rho_f m}{C_D^m}$	$\frac{C_D^m}{C_D^m \beta}$
Object Distance and Size	$x, s$	$\beta x, \beta s$	$\alpha^2 x, \alpha^2 s$	$\beta x, \beta s$
Object Velocity Components	$\dot{x}, \dot{y}$	$\alpha \dot{x}, \alpha \dot{y}$	$\alpha \dot{x}, \alpha \dot{y}$	$\dot{x}, \dot{y}$
Time	$t$	$(\beta/\alpha)t$	$\alpha t$	$\beta t$
Object Horizontal Acceleration	$\ddot{x}$	$(\alpha^2/\beta)\ddot{x}$	$\ddot{x}$	$\ddot{x}/\beta$

Equation (7) also depends on gravitational acceleration,  $g$ , which has the same units as  $\dot{x}/t$  in the real environment and  $(\alpha^2/\beta)\dot{x}/t$  in the scaled environment. It would be fortunate if  $\alpha^2/\beta = 1$ , since gravitational acceleration doesn't change with scaling.

## 1.5 Scaling Schemes

The scaling requirements that have been derived here and summarized in Table 1.2 are met to some degree by various scaling schemes, though no scheme satisfies all requirements completely. Three scaling schemes are presented here, the first scheme being the preferred one.

### 1.5.1 Scheme with Debris Velocity Much Less Than Shock-Front Velocity

This scheme assumes that the motion of the debris has little effect on its relative position in the blast wave because the debris velocity is so much less than that of the shock front. This certainly is true for the tests reported here. Therefore, the relation between the shock-front and debris velocities is ignored. It is also assumed that  $\alpha^2/\beta = 1$ , which means that debris acceleration in both the real and the scaled environments is simply that resulting from the force of gravity. From this,  $\beta = \alpha^2$ , and the parameters given in the column headed " $U \gg \dot{x}$ " in Table 1.2 are described by  $\alpha$  only. The test-blast peak particle velocity and positive phase duration both are derived by multiplying the corresponding values for the full-scale simulated blast by  $\alpha$ . Once the simulated blast and the test blast are specified, the value of  $\alpha$  and the range from the test blast are fixed. The details of these interrelationships are discussed in Section 1.7.

### 1.5.2 Scheme That Maintains Shock-Front Parameters

In this scheme,  $\alpha = 1$ . For example, assume that a blast to be simulated has a peak overpressure of 10 psi from a 1-MT explosion and that the test explosion is 1 kT. The scaled buildings then would be placed at a range from the test blast where the peak overpressure in this environment is also 10 psi.

The test blast would have one-tenth the duration of the 1-MT blast to be simulated, and the factor  $\beta$  in Table 1.2 would be 0.10. This leads to two serious scaling problems: The scaled debris would have to be ten times as dense as the debris, which may be impossible to achieve; further, the acceleration in the scaled environment should be ten times greater than that in the environment being simulated. Nature does not cooperate; the acceleration due to gravitational attraction is a constant and, therefore, the same in both environments.

### 1.5.3 Scheme That Uses Scaling for Debris and Shock-Front Velocities

Using the same scaling for debris and shock-front velocities will not satisfy the equations of motion, because the shock-front velocity,  $U$ , and the air-particle velocity,  $u_f$ , are not linearly related for varying shock strengths. However, if the debris velocity is small compared with the air-particle velocity, the equations of motion become principally functions of the air-particle velocity. The debris density then can be adjusted, as shown in Table 1.2, to compensate for the difference in velocity scaling by means of the parameter  $\alpha'$ , where

$$\alpha' = \frac{u_f' U}{u_f U'} = \frac{u_f'}{u_f} \alpha .$$

This third scaling scheme has little practical value, because it depends on the assumption of low debris velocities — debris velocities much lower than the shock-front velocity. This is the same assumption that forms the basis for the first scaling scheme, and that one is preferable to this one.

Since the second scheme leads to problems of simulation, and since the third scheme is based upon the same premise as the less complex first scheme, the first scheme is the one that was used in the model tests.

## 1.6 Assumptions and Approximations

A number of simplifications were employed in the design of the experiments in addition to those assumed in the preceding discussion. The background for these simplifications is presented here.

### 1.6.1 Similarity of Blast Waves

Tests have shown that TNT explosions from 1 to 1,000,000 pounds produce blast waves that can be made similar by cube root scaling; specifically, the same peak shock-front parameters will occur at a distance proportional to the cube root of the explosive mass. The time variation of blast parameters at this scaled range also vary with the cube root of the explosive mass.

Nuclear explosions can be scaled in much the same way; however, there can be considerable scatter from one explosion to another. There are also similarities between nuclear and high-explosive blast waves. For example, 500 tons of TNT will produce lower-overpressure blast waves that are similar to those predicted for a 1000-ton (1 MT) nuclear detonation.<sup>1</sup> On the other hand, there are differences in positive phase durations and some later-time blast characteristics for these

---

<sup>1</sup>Glasstone, Samuel, ed., Effects of Nuclear Weapons, U. S. Atomic Energy Commission, April 1962; p. 126.

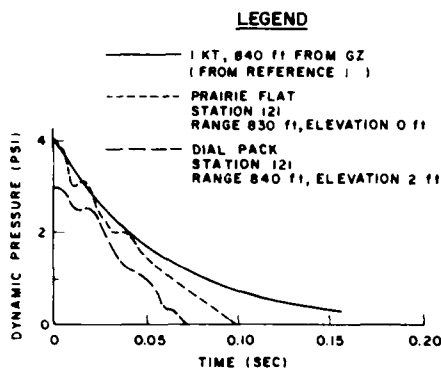


Figure 1.2. Comparison of nuclear and high-explosive blast waveforms.

explosions. When high explosives and nuclear detonations are compared, as in Figure 1.2, it is better to use a time measure other than positive phase duration (the time required for the air-particle velocity to decay to  $1/e$  of the peak value rather than zero).

The difference between dynamic measurements in two of the high-explosive events — DIAL PACK<sup>2</sup> and PRAIRIE FLAT<sup>3</sup> (see Figure 1.2) — indicate that experimental results can vary between tests that are geometrically identical. Clearly, it is impossible to simulate debris blast transport exactly even if perfect scaling were achieved, because of variations among the test blasts. Actual nuclear detonations are themselves subject to this inherent irreproducibility.

#### 1.6.2 Air-Velocity and Density Variations in the Blast Wave

The equations of motion for the debris depend upon the air velocity and density in the blast wave. For the equations to be similar in the two blasts being considered, the time variations of air velocity and density also should be similar. This is certainly the case if both blast waves have the same shock-front parameters and differ only in phase duration.

In these experiments, however, long-duration blast waves that are assumed to be produced by a nuclear explosion are compared with short-duration blast waves from a TNT explosion. The TNT explosion has a lower peak overpressure than the blast being simulated, a consequence of the scaling requirement that blast velocity and duration be scaled similarly. Short-duration test blasts require that the experiments be performed where the overpressures are less than those being simulated.

<sup>2</sup>Middle North Series, PRAIRIE FLAT Event, Project Officers Report, Project LN-101 — Fundamental Blast Studies; POR 2100 (WT2100), Headquarters, Defense Atomic Support Agency, Washington, D. C., 1 March 1971; p. 73.

<sup>3</sup>Advance Information, Event DIAL PACK, Project Officers Report, Project LN-101 — Fundamental Air Blast Measurements.

It is convenient to convert air velocity and density to the following dimensionless parameters:

$$\left[ \frac{u(t)}{u_f} \right]_R ;$$

$$\left[ \frac{\frac{\rho(t) - 1}{\rho_0}}{\frac{\rho_f - 1}{\rho_0}} \right]_R .$$

These parameters have a similar time decay over a range of peak overpressures. This is shown in Figure 1.3, which consists of correlations constructed by the author from data calculated by H. L. Brode, a well known nuclear effects authority. The constructions utilized the positive phase durations given in Figure 1.4. The dashed portion of the velocity positive phase curve was constructed to minimize variations with overpressure in the decay curves. Similar curves have been constructed for the negative phase regions but are not presented in this report.

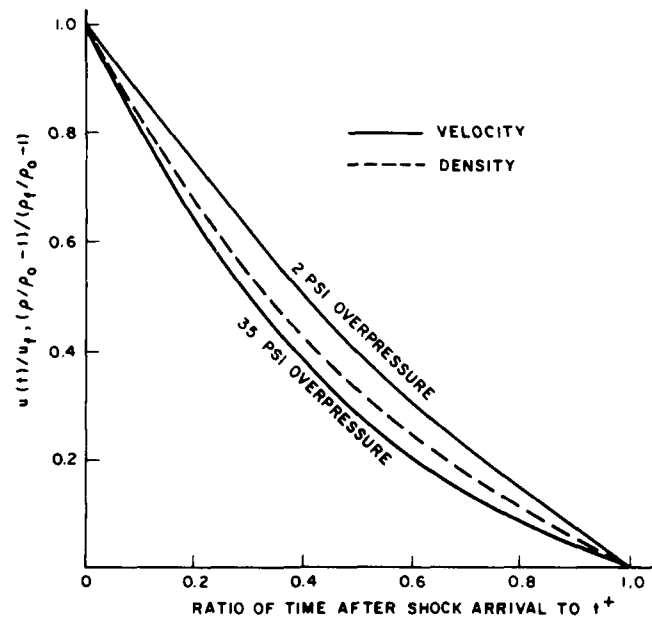


Figure 1.3. Time decay of dimensionless air density and particle velocity parameters.

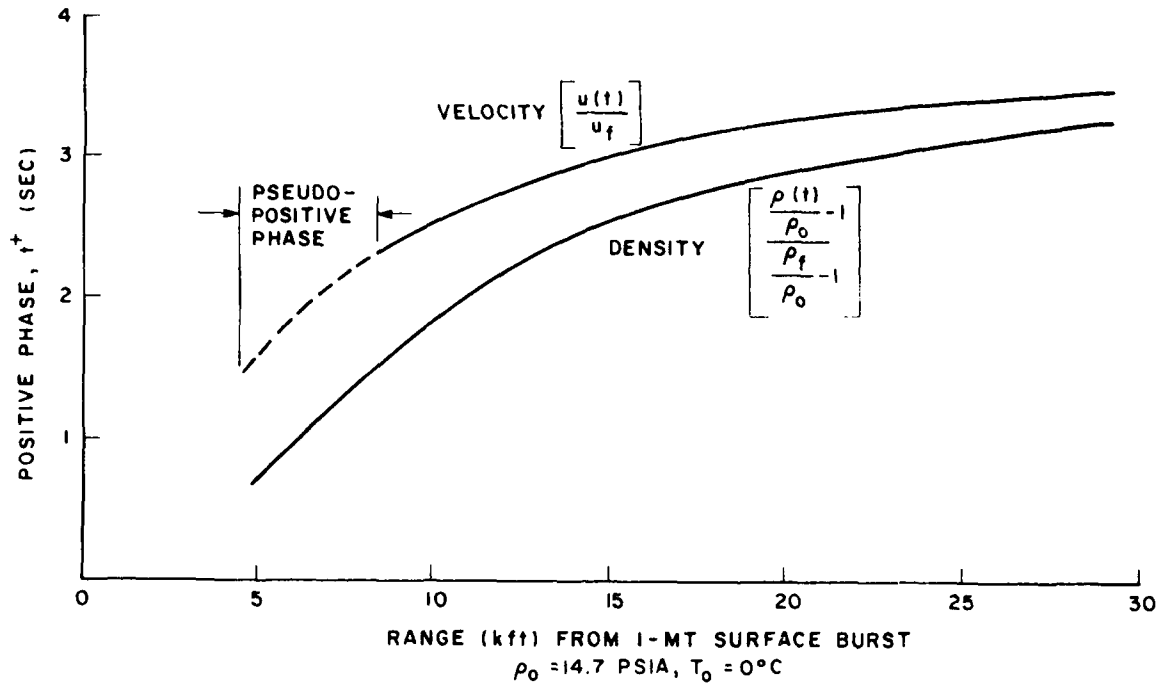


Figure 1.4. Variation of positive phase duration with range.

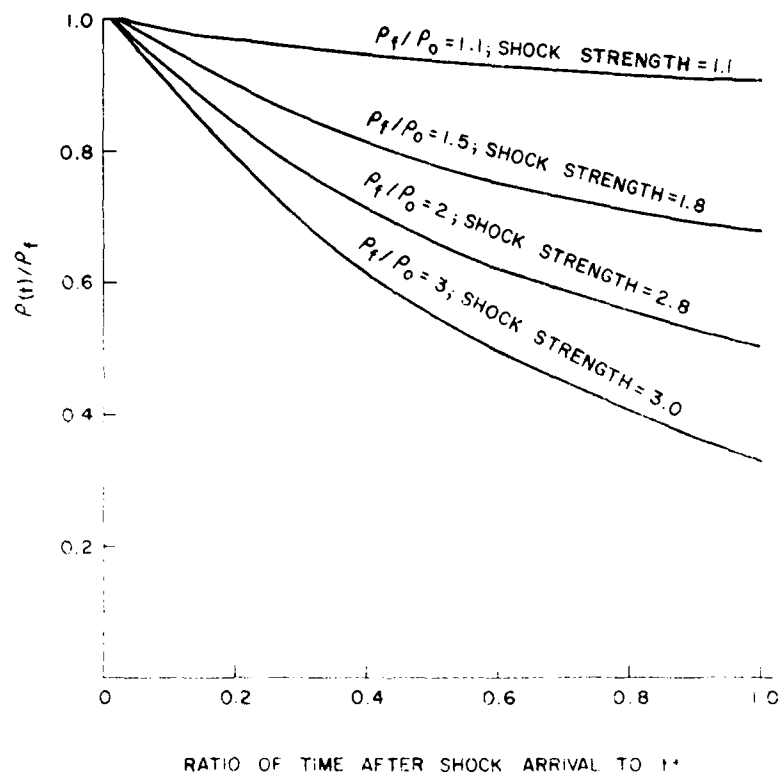


Figure 1.5. Variation of blast air density, reduced to a dimensionless parameter, with time and shock strength.

The density decay curve in Figure 1.3 is nearly independent of peak overpressures in the range between 2 and 35 psig. Unfortunately, the equations of motion depend upon  $\rho(t)/\rho_0$ , not  $\{[\rho(t)/\rho_0] - 1\}/\{[\rho_f/\rho_0] - 1\}$ . As a result, the ratio  $\rho(t)/\rho_0$  is not independent of peak overpressure — a fact well illustrated in Figure 1.5. An inaccuracy results, therefore, if density variations are assumed to be independent of peak overpressure, as in this report. However, variations in blast waves easily can overshadow this density phenomenon.

### 1.6.3 Drag Coefficients

In scaling the density of the debris in a model environment relative to debris in an actual nuclear environment, the drag coefficients for the full-size and the model debris must be taken into account. It would be convenient if the drag coefficients for objects in the two environments were equal. In fact, the drag coefficients become approximately constant above a Reynolds number of  $10^3$  for plates, rough spheres, and cylinders — the kinds of objects that generally approximate blast debris. Figure 1.6 illustrates this  $10^3$  lower bound, above which drag coefficients become constant.

Some of the smallest objects used in these tests, the 1/120 scale blocks used in Operation SNOWBALL, had a length of a bit over 0.01 foot. Thus, a velocity of about 20 ft/sec corresponds to a Reynolds number of  $10^3$  (from Figure 1.6).

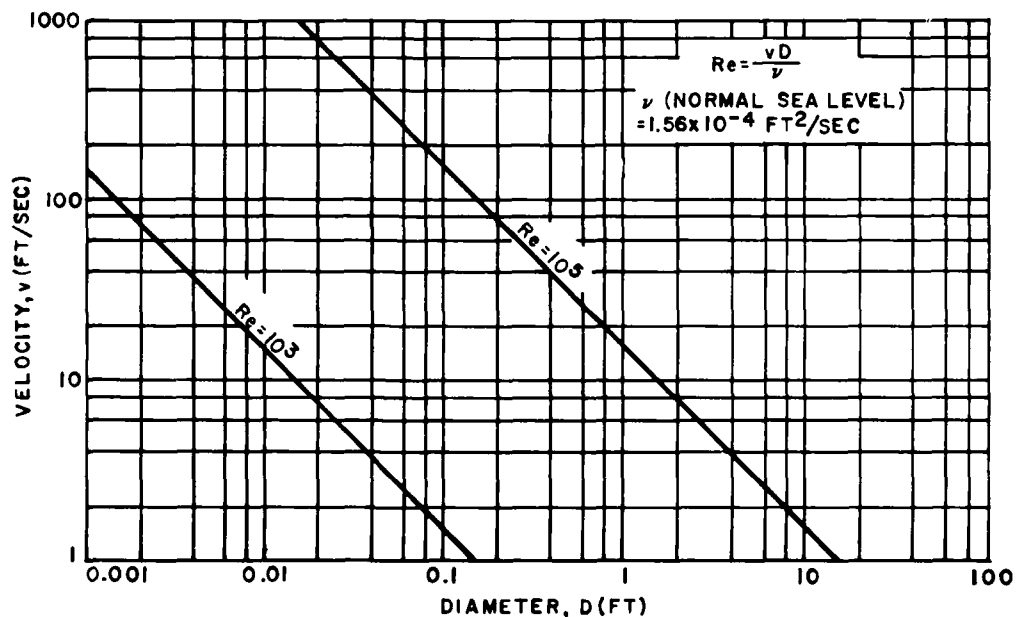


Figure 1.6. Reynolds number as a function of diameter and velocity.

The peak air velocity in this experiment was about 60 ft/sec, so that drag on the blocks was independent of Reynolds number during the period of greatest block acceleration. The drag coefficients, then, can be assumed to have been constant in all cases.

### 1.7 Graphical Method to Determine Test Conditions

The technique used here requires that the peak air-particle velocity and positive phase duration of the dynamic pressure can be scaled down by the same factor ( $\alpha$ ) in going from a full-scale simulated blast environment to the model blast environment. For a given explosion, both are functions of range and generally are expressed graphically. This information can be used to fix the range from a test explosion for a setup of model buildings, given the blast conditions to be simulated.

The two curves in Figure 1.7 are used to make the site determination. The upper curve shows John Dewey's<sup>4</sup> fit to experimental data obtained at the Defense Research Establishment, Suffield. The lower curve represents the author's fit of a 1-kT nuclear blast calculation by H. L. Brode. The upper curve, representing a 500-ton TNT blast, has been extended to lower velocities along the dashed portion parallel to the nuclear blast curve.

(The author received data on a blast with a peak overpressure of 1 psi from John Dewey; this is represented by the isolated point in Figure 1.7. Since it is far from agreement with the other data, it will not be considered in this discussion. Obviously, more and better low-overpressure data are needed.)

Given the nuclear-blast conditions to be simulated and the yield of the test TNT detonation, the curves in Figure 1.7 are used as follows:

1. Determine the ratio of the peak air-particle velocity to the sonic velocity in ambient air from the peak overpressure using the following relationship,<sup>5</sup> which has been simplified for the condition in which  $\gamma$  (for air), the ratio of specific heat at constant pressure to that at constant volume, is equal to 1.4.

$$\frac{u_f}{c_o} = \frac{5}{6} \left( \frac{y - 1}{\left[ \frac{7}{6} \left( y + \frac{1}{6} \right) \right]^{1/2}} \right),$$

<sup>4</sup>Dewey, John M., The Air Velocity and Density in Blast Waves from TNT Explosions, Defence Research Board, Canada; Suffield Report No. 207, 4 March 1964; p. 40.

<sup>5</sup>Wright, J. K., Shock Tubes, Methuen's Monographs on Physical Subjects, London, 1961; p. 19.

where

$$y = (p + p_0)/p_0;$$

$p$  = peak overpressure;

$p_0$  = absolute ambient pressure;

$u_f$  = peak air particle velocity;

$c_0$  = sonic velocity in ambient air

2. Having determined the appropriate value of  $u_f/c_0$ , one can read the corresponding value of  $t^*$  as defined in Figure 1.7 from the lower (1-kT nuclear blast) curve. This value of  $t^*$  then must be multiplied by the cube root of the simulated yield in kT. For example, assume that the blast being simulated is a 1-MT (1000-kT) nuclear explosion with 30 psi overpressure. The corresponding value of  $u_f/c_0$  is about 0.88, for which  $t^*$  on the 1-kT curve is about 0.07. This is then multiplied by 10 (the cube root of 1000) to obtain a  $t^*$  of 0.7 sec for a 1000-kT explosion.
3. It is required that the positive phase duration and the air-particle velocity be scaled by the same factor; therefore, the test condition will be at some point on a straight line passing through the origin and the point at  $t^* = 0.7$  sec and  $u_f/c_0 = 0.88$ ; this is the dashed line in Figure 1.7. If the test yield is 500 tons of TNT, the test conditions are represented by the intersection of the dotted line and the TNT curve. For the example used, this would mean that  $u_f/c_0 = 0.2$ , which corresponds to a peak overpressure of 4.3 psi in a 13.6-psia atmosphere and a  $t^*$  of 0.16 sec. The scaling factor  $\alpha$  [Equation (5)], therefore, is  $0.16 \text{ sec}/0.7 \text{ sec} = 0.023$ . Dimensions for the scale-model sites — buildings and distances — are derived by multiplying full-scale dimensions of  $\alpha^2$ . (See Table 1.2.)
4. If a test yield other than 500 tons of TNT were used, the appropriate curve would replace the 500-ton curve in Figure 1.7. The same end can be achieved if the ordinate ( $t^*$ ) is adjusted to read values of  $t^*$  for the actual test yield, in which case the same TNT curve could be used. For example, if the test yield were one-eighth as large — 125,000 lb, or 62.5 tons — all values of  $t^*$  would be divided by 2 (the cube root of 8). The dashed straight line also should be drawn with this modified ordinate. The determination of the nuclear characteristics is not affected by such a modification.

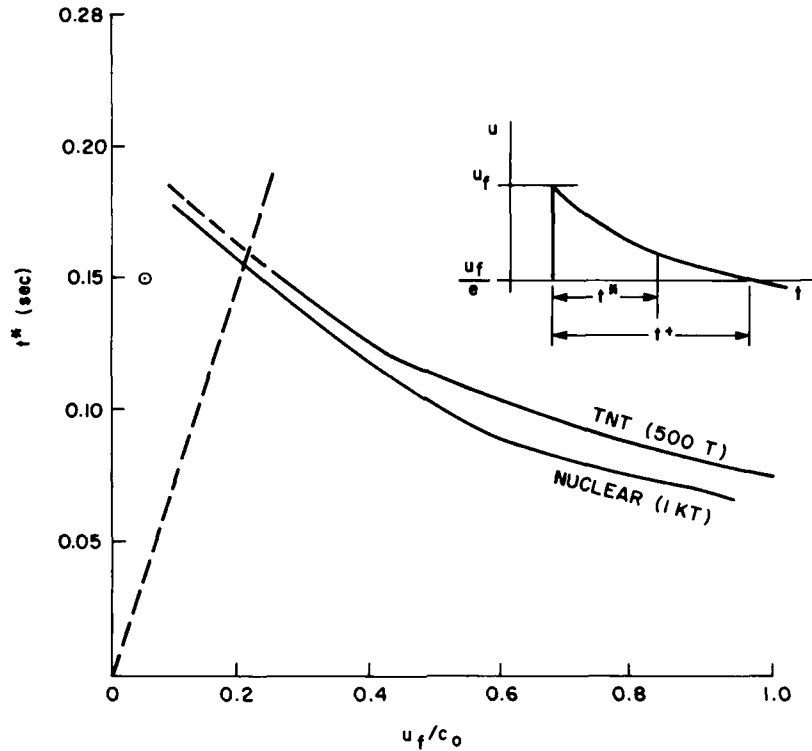


Figure 1.7. Graphical method of finding the scaling factor that determines model sizes and distances from ground zero for a 500-ton TNT test blast.

1.8 Simulated Blast Conditions Corresponding to Tests

The tests described in this report were designed to represent a variety of simulated blast conditions; blast data varying in source and interpretation were used to fix the test parameters. So that the results of all tests could be compared with the same data — the data of Figure 1.7 — the procedure developed in Section 1.7 was reversed. From given test parameters, simulated blasts were constructed, with the results shown in Table 1.3. The figures are not claimed to be accurate, but they are, at least, based uniformly on the same data.

The reader should bear in mind that these simulated blast conditions, which will be referred to in the discussion to follow, represent a range of blast parameters rather than a specific set.

Table 1.3  
SUMMARY OF SIMULATED NUCLEAR-BLAST PARAMETERS

Yield (tons TNT)	Peak Over- pressure (psig) <sup>†</sup>	$\frac{u}{c_0}$	$t^*$ (sec) <sup>‡</sup>	Scale Factor	$\sqrt{\text{S.F.}}$	Peak Over- pressure (psig) <sup>§</sup>	$t^*$ 1 kT (sec) <sup>¶</sup>	$t^*$ test (sec)	$\frac{t^* \text{ test } \sqrt{\text{S.F.}}}{t^* 1 \text{ kT}}$	Yield (MT)
500	1	0.055	0.190	120:1	11	17.6	0.088	2.09	23.7	12
	3	0.14	0.173	20:1	4.5	18.7	0.085	0.78	9.2	0.8
	3	0.14	0.173	8:1	2.8	10.3	0.117	0.48	4.1	0.07
	6	0.27	0.140	8:1	2.8	24.6	0.077	0.39	5.1	0.13
50	2	0.10	0.083	33:1	5.8	16.8	0.090	0.48	5.3	0.15
	3	0.14	0.079	33:1	5.8	26.7	0.070	0.46	6.6	0.3
20	1.7	0.09	0.062	50:1	7	18.7	0.085	0.43	5.1	0.13
	1.7	0.09	0.062	140:1	12	37.3	0.060	0.74	12.3	1.8
	3	0.14	0.058	50:1	7	35.2	0.065	0.40	6.1	0.23

<sup>†</sup>Based on  $p_0 = 13.7$  psia.

<sup>‡</sup>From chart with yield corrections.

<sup>§</sup>Based on  $p_0 = 14.7$  psi.

<sup>¶</sup>From chart.

## Chapter 2

### MODEL CONSTRUCTION AND DEBRIS COLLECTION

This chapter describes the construction of the model buildings used in the various high-explosive tests, giving details of how model designs evolved from field experience, and relates how the models performed under field conditions. It also describes the field layouts and the methods of collecting and identifying post-blast debris that were used in these tests.

#### 2.1 Model Building Characteristics and Requirements

The tests were designed to show, on reduced scales, the manner in which buildings subjected to blast are blown apart. It was not possible, with the small-scale buildings used, to simulate all types of debris that would come from actual buildings; only the larger components of typical buildings were studied.

Low-overpressure locations for the model buildings had to be used because of the restrictions imposed by the scaling laws described in Chapter 1 of this report. The models had to be sufficiently fragile, therefore, to be blown apart by the required low-level blasts. On the other hand, the models had to be sturdy enough to resist pre-shot wind damage. Model designs evolved that reasonably satisfied these conflicting requirements.

The elements of each model building were coded in some way so that specific debris could be traced back to the building and the location within the building from which it came. Usually the way this was done was to paint all the elements of a particular building a distinctive color and to further identify each element by means of a second color or the use of a number-letter combination.

All of the models simulated a full-size building with a plan of 40 by 40 feet and a height of either 40 or 20 feet. Each model had a flat roof and no windows; most had no interiors, although the frame buildings tested in DIAL PACK and PRAIRIE FLAT did have some interior structure.

Some buildings were arranged in groups, and others were placed alone, with no objects nearby to disturb the natural deposition of debris. In the groups, or complexes, buildings were spaced one building width apart; the buildings, therefore, occupied one-quarter of the complex area.

Table 2.1  
DIMENSIONS AND WEIGHTS OF BUILDING ELEMENTS

Test	Model Scale	Model Plan (in. × in.)	Wall Elements							
			Block Dimensions				Panel Dimensions			
			Ht. (in.)	Wdth. (in.)	Lngh. (in.)	Wt. (gm)	Lngh. (in.)	Wdth. (in.)	Thk. (in.)	Wt. (gm)
SNOWBALL	1/120	4 × 4	0.13	0.12	0.25	0.075	—	—	—	—
DISTANT PLAIN (All three shots)	1/140	3.3 × 3.3	0.010*	0.11*	0.19*	0.033*	—	—	—	—
	1/50	10 × 10	0.30	0.31	0.60	1.22	—	—	—	—
	1/50	10 × 10	0.33*	0.31*	0.60*	0.95*	—	—	—	—
White Sands	1/33	14 × 14	0.40	0.42	0.87	3	—	—	—	—
	1/33	14 × 14	0.33*	0.31*	0.60*	0.95*	—	—	—	—
PRAIRIE FLAT	1/120	4 × 4	0.13	0.12	0.25	0.075	—	—	—	—
	1/20	24 × 24	0.63*	0.63*	1.23*	9*	—	—	—	—
	1/8	60 × 60	1.5	1.5	3.0	148	—	—	—	—
	1/8	60 × 60	1.5*	1.5*	3.0*	107*	—	—	—	—
	1/8	60 × 60	—	—	—	—	12.0	6.0	0.12	48
DIAL PACK	1/120	4 × 4	—	—	—	—	0.8	0.4	0.07	0.06
	1/20	24 × 24	—	—	—	—	4.80	2.40	0.07	1.7

\*Hollow blocks.

Table 2.1 contains all the dimensions pertinent to the models used in these tests, as well as the weight of each building element.

## 2.2 Block Building Models

### 2.2.1 SNOWBALL

The first model buildings composed of blocks were used in Operation SNOWBALL. These consisted of a complex of 40 buildings and a single isolated building, placed as shown in Figure 2.1. Each building wall was made up of 500 vinyl blocks that were designed to interlock, as shown in Figure 2.2, thus allowing the wall to stand without support; the blocks at corners were glued to uprights, however, as shown in Figure 2.3. The bottom row of blocks was not interlocked with the fixed member at the base. This allowed the wall to bow under the pressure of a blast force. Each roof was made up of panels representing plywood sheets, which rested loosely on rafters, as shown in Figure 2.4.

Before the field test took place, the fragility of these buildings was checked with the shock tube at Ballistics Research Laboratories. It was discovered there that glue used between roof elements prevented the 1-psi-overpressure blast from separating them and that the overpressure was not great enough to demolish the block walls completely. The walls were so flimsy that they could barely stand, however; hence, this wall construction technique was continued.

Table 2.1  
DIMENSIONS AND WEIGHTS OF BUILDING ELEMENTS (continued)

Roof Elements								Interior Elements							
Panel Dimensions				Rafter Dimensions				Floor Panel Dim.				Joist Dimensions			
Lngth. (in.)	Wdth. (in.)	Thk. (in.)	Wt. (gm)	Lngth. (in.)	Wdth. (in.)	Thk. (in.)	Wt. (gm)	Lngth. (in.)	Wdth. (in.)	Thk. (in.)	Wt. (gm)	Lngth. (in.)	Wdth. (in.)	Thk. (in.)	Wt. (gm)
1.1	0.55	0.040	0.19	4.4	0.12	0.030	0.12	-	-	-	-	-	-	-	-
0.8	0.5	0.033	0.04	3.5	0.15	0.033	0.06	-	-	-	-	-	-	-	-
2.17	1.17	0.044	0.9	10.4	0.25	0.076	1.5	-	-	-	-	-	-	-	-
2.17	1.17	0.035	0.3	10.3	0.25	0.064	0.7	-	-	-	-	-	-	-	-
2.85	1.40	0.065	2.2	14	0.25	0.065	1.70	-	-	-	-	-	-	-	-
2.85	1.40	0.065	2.2	14	0.25	0.065	1.70	-	-	-	-	-	-	-	-
0.8	0.4	0.03	0.04	4	0.15	0.03	0.07	-	-	-	-	-	-	-	-
4.8	2.4	0.05	4.0	24	0.6	0.15	15.0	-	-	-	-	-	-	-	-
12.0	6.0	0.12	48	60	1.5	0.38	240	-	-	-	-	-	-	-	-
12.0	6.0	0.12	48	60	1.5	0.38	240	-	-	-	-	-	-	-	-
12.0	6.0	0.12	48	60	1.5	0.38	240	12.0	6.0	0.12	48	-	-	-	-
0.8	0.4	0.07	0.06	4.1	0.14	0.07	0.10	-	-	-	-	-	-	-	-
4.87	2.43	0.07	5.3	2.44	0.68	0.12	14	4.63	2.32	0.07	1.6	23.9	0.62	0.12	5.4

The field test substantiated the shock tube findings: All the roofs blew off, but 50 percent or more of each building wall remained standing. The field results are shown in Figure 2.5.

### 2.2.2 DISTANT PLAIN, Event 1

The block construction of the larger buildings in this test was modified as shown in Figure 2.3 to eliminate the vertical support at the wall corners. Each wall was built up separately; the four walls then were brought together and the end blocks of corresponding courses glued to each other. This resulted in a free-standing unit. Only every other course of blocks came together for gluing, since blocks were staggered and no half blocks were used to fill the partial spaces at the ends of alternate courses.

No glue was to be used between courses within a wall — only between adjoining end blocks at the same elevation. Actually, however, glue was drawn into the cracks between blocks, producing locked groups. In spite of this, a model tested at Ballistics Research Laboratories was reduced to rubble by the blast from the low-pressure 2-foot-diameter shock tube. This model was placed outside the tube, near the muzzle. The roof elements were loose, as in Operation SNOWBALL, but were held down with metal washers to prevent wind displacement.

Since wind damage was a constant threat in these tests, the model buildings were erected in protected areas and covered by boxes. The boxes were removed

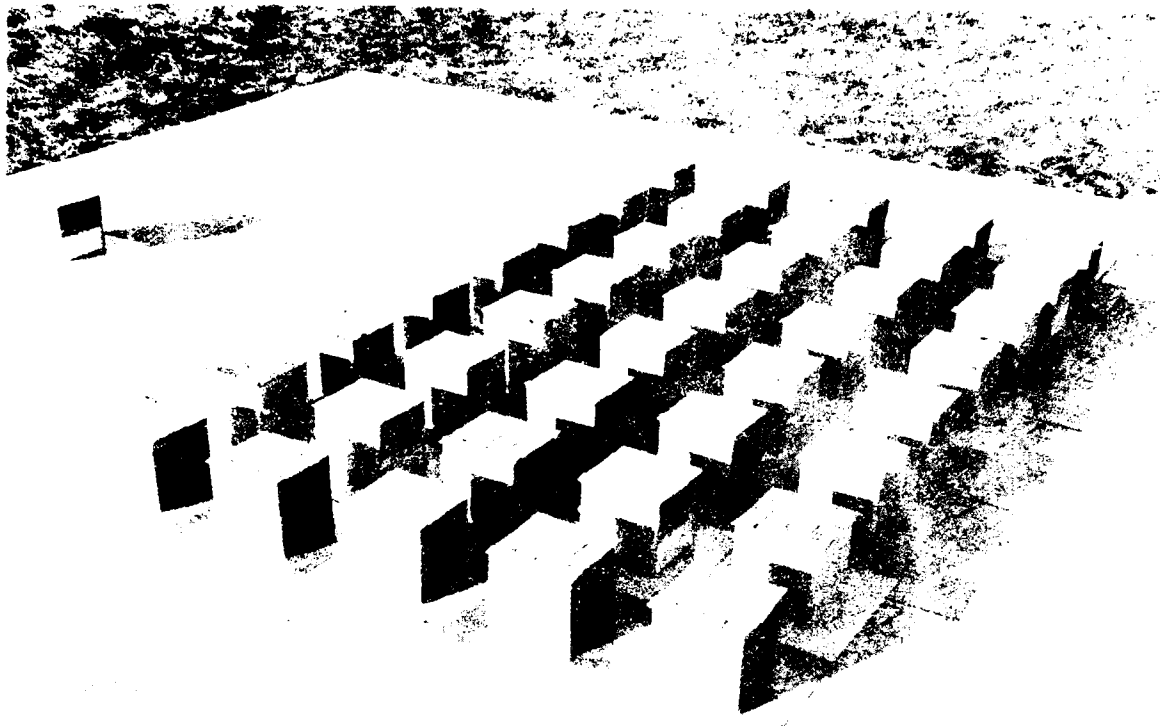


Figure 2.1. Operation SNOWBALL 1/120-scale block buildings:  
40-building complex and isolated building before detonation.

as close to the time of the blast as field regulations allowed. In Operation SNOWBALL, for example, the models were erected under cover of a tent and then covered with boxes before tent removal. These boxes were removed about 20 minutes before the detonation.

Successful results were obtained from SNOWBALL, but the conditions in DISTANT PLAIN, Event 1, were not as fortuitous. The boxes covering the models were removed about 45 minutes before time zero, whereupon the 12- to 15-mph wind blew down the larger buildings almost as fast as they were uncovered. The weakness of these buildings was in the block walls, which bowed and buckled readily under the wind pressure. The smaller buildings, 3.3 inches on a side, were similar to the 4-by-4 inch buildings used in SNOWBALL, but were more wind-resistant. Their rigid corner posts, shown in Figure 2.3, probably saved them: examination of the high-speed motion pictures taken during the test showed that they appeared to be intact for the detonation, though it was not certain that all roof members were

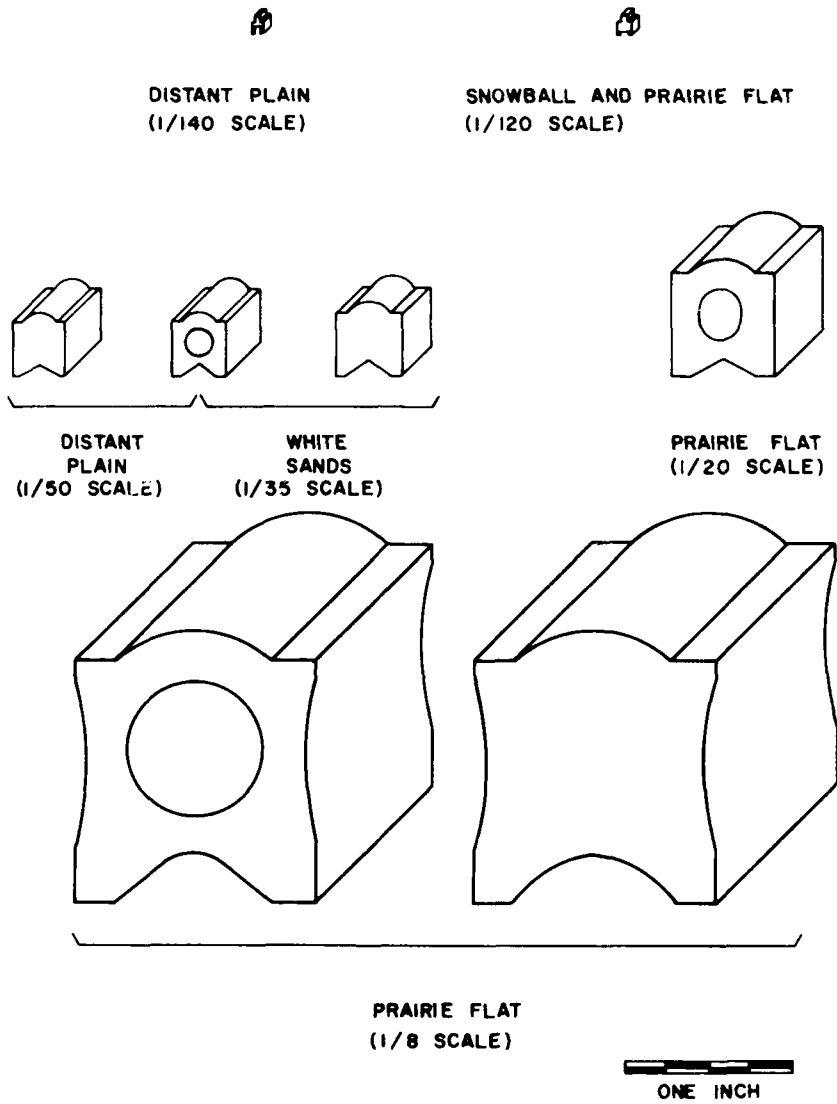


Figure 2.2. Relative sizes and shapes of the plastic blocks used in the various tests.

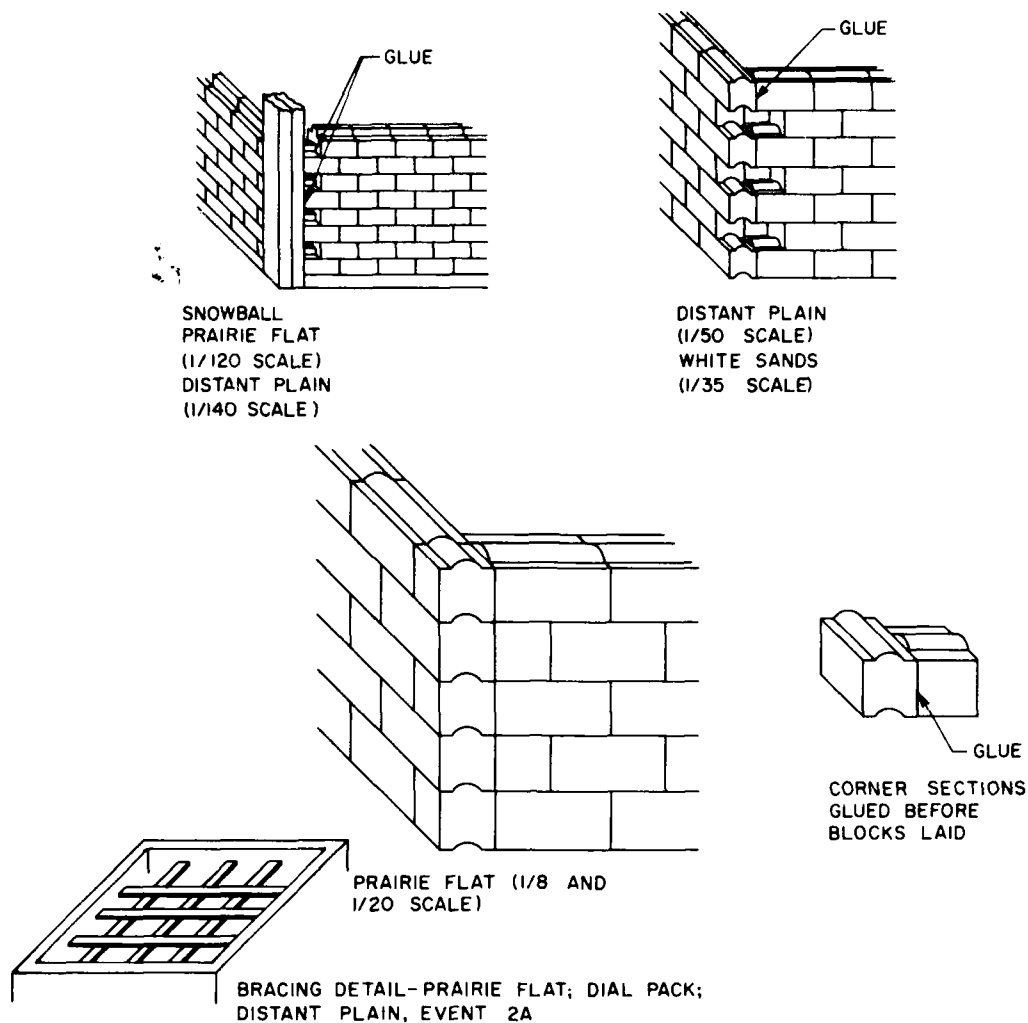


Figure 2.3. Block construction methods used in the various tests.

in place. Unfortunately, winds after the blast altered the debris distribution from these small buildings, and significant data could not be obtained.

### 2.2.3 DISTANT PLAIN, Event 2a

The same types of large and small model buildings were used in DISTANT PLAIN, Event 2a, except that reinforcement was added at three levels in the larger buildings to strengthen the walls against wind pressure. This reinforcement is shown in detail in Figure 2.3. Three wood strips running from the front to the back wall and three wood strips running between side walls were placed at approximately the same elevation. The end of each strip was glued to a block in the wall, and the strips all were glued together at their intersections. This reinforcement acted like a floor and was repeated at two other elevations in each of the larger model

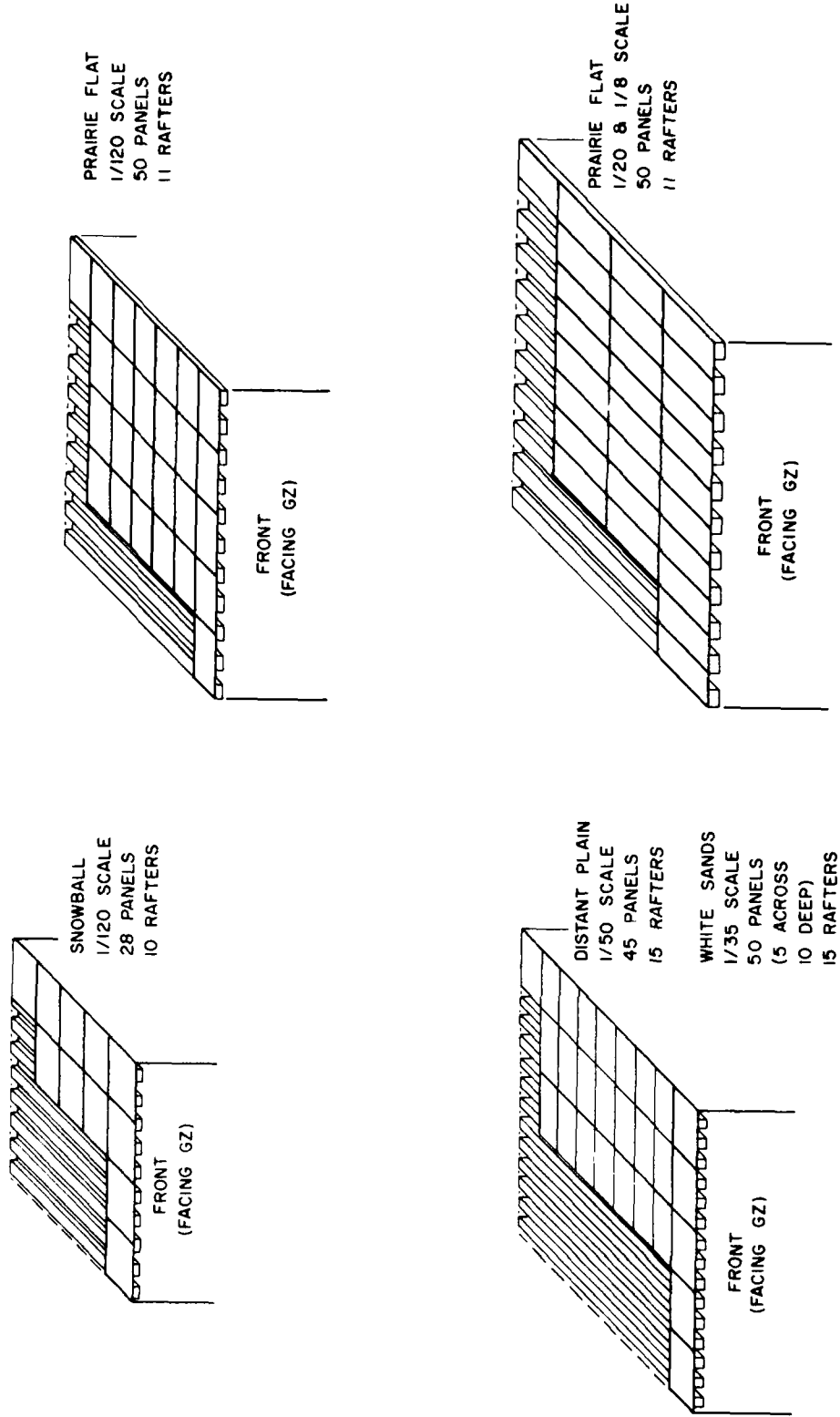


Figure 2.4. Roof construction methods used in the various tests.

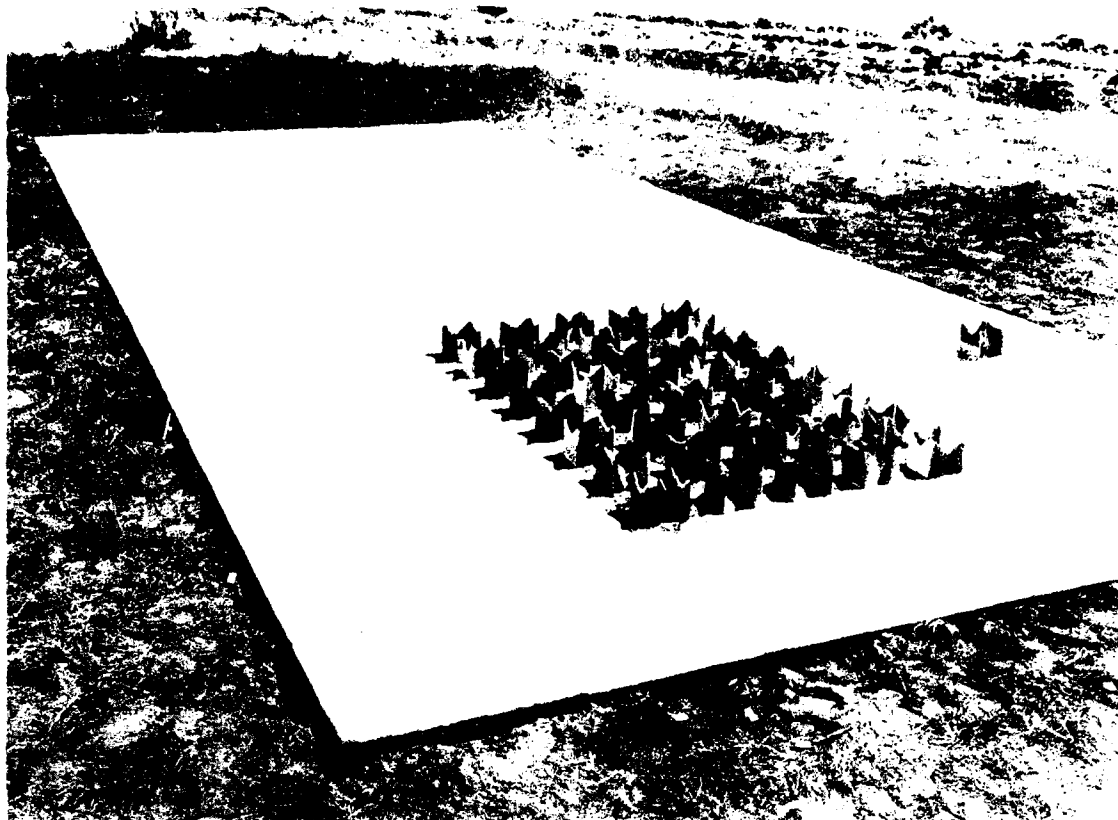


Figure 2.5. SNOWBALL 1/120-scale block buildings after detonation.

buildings. The smaller buildings were not reinforced, since they apparently survived the high wind in Event 1.

Strong wind preceded this shot also, but this time the larger buildings withstood it while they were uncovered. Some wind damage did occur, as the record of the high-speed motion picture cameras showed, but enough of some buildings remained intact to support part of their roofs, and some trajectories of roof elements were recorded on film. Ground distributions were not considered valid.

#### 2.2.4 DISTANT PLAIN, Event 2 (repeat)

The elevated gas-filled balloon shot was repeated with identical groups of model buildings and the addition of "half-height" buildings. The half-height models had the same square floor plan but had walls only half as high as those of the comparative full-height models.

In this test the balloon misfired, and no useful information was obtained.

### 2.2.5 White Sands SOTRAN

6 This test duplicated part of the DISTANT PLAIN test to provide the data not obtained previously because of high winds. Only the ground distribution of debris from the larger buildings was ascertained. In this test, the larger buildings were 14 by 14 inches in plan, as compared with buildings 10 by 10 inches in plan used in the DISTANT PLAIN shots. The increase in size was necessary because of the higher-yield blast — 50 tons versus 20 tons for DISTANT PLAIN.

Two detonations took place; one during the day, the other at midnight. As anticipated, wind damage again destroyed the value of the data in the daytime shot; not many buildings had been placed during this shot because of the likelihood of wind interference. Calm conditions were expected for the midnight event; hence, most of the buildings were placed then. The weather proved to be as favorable as anticipated, and excellent data were obtained.

### 2.2.6 PRAIRIE FLAT

The PRAIRIE FLAT event used 1/120-scale buildings of essentially the same construction as those tested in Operation SNOWBALL except that bracing was added between opposite walls and the roof members were weighted down with washers. The 12-building complex is shown in Figure 2.6. PRAIRIE FLAT also used 1/8- and 1/20-scale buildings similar in construction to those tested at White Sands and in the DISTANT PLAIN shots, except that half blocks were used to fill the gaps in alternate courses at the wall corners, as shown in Figure 2.3. The absence of these corner blocks in the buildings tested in White Sands SOTRAN and DISTANT PLAIN caused alternate courses of their walls to shift; corner blocks tended to increase the rigidity of the model buildings in PRAIRIE FLAT.

The 1/8- and 1/120-scale buildings tested in PRAIRIE FLAT were assembled at the site; the 1/120-scale buildings were shipped assembled as were all model buildings previously tested. Good data were obtained from all models.

## 2.3 Frame Building Models

Buildings of frame construction were used first in the PRAIRIE FLAT event and proved to be successful there, which influenced the subsequent course of the test program.

### 2.3.1 PRAIRIE FLAT

Two 1/8-scale frame buildings, shown in Figure 2.7, were built on a large concrete pad originally intended for a complex of 1/8-scale block buildings. The block building complex was canceled because the material for the models was too expensive.

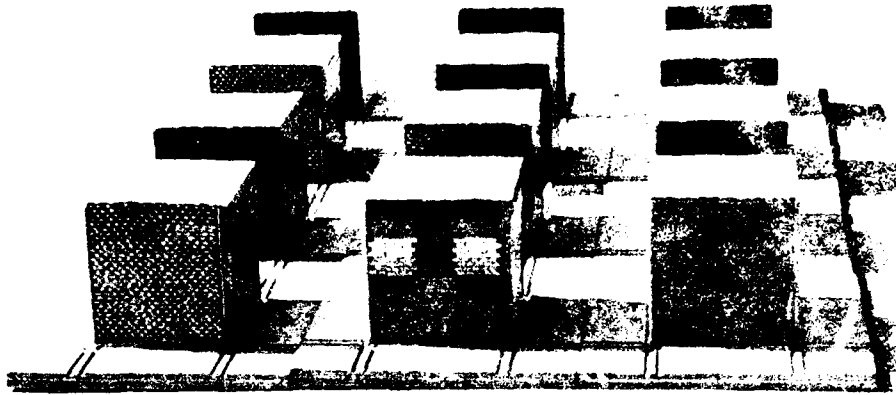


Figure 2.6. PRAIRIE FLAT 1/120-scale block-building complex before detonation.

The frame models were constructed as shown in Figure 2.8. The walls and roof of each building were made of 6-by-12-inch panels; those for the walls all were glued to a frame made of 1/4-by-1/2-inch strips. This approximated full-size construction consisting of plywood sheets attached to studs and other framing members.

Interior framing was provided to add support to the walls and to support floors also made of 6-by-12-inch panels. The floor panels were laid on the interior framing. The full-height (5-foot) building had two floors; the half-height (2.5-foot) building had one.

These frame buildings were almost completely broken into individual elements by the blast, though some of the wall panels stayed together.

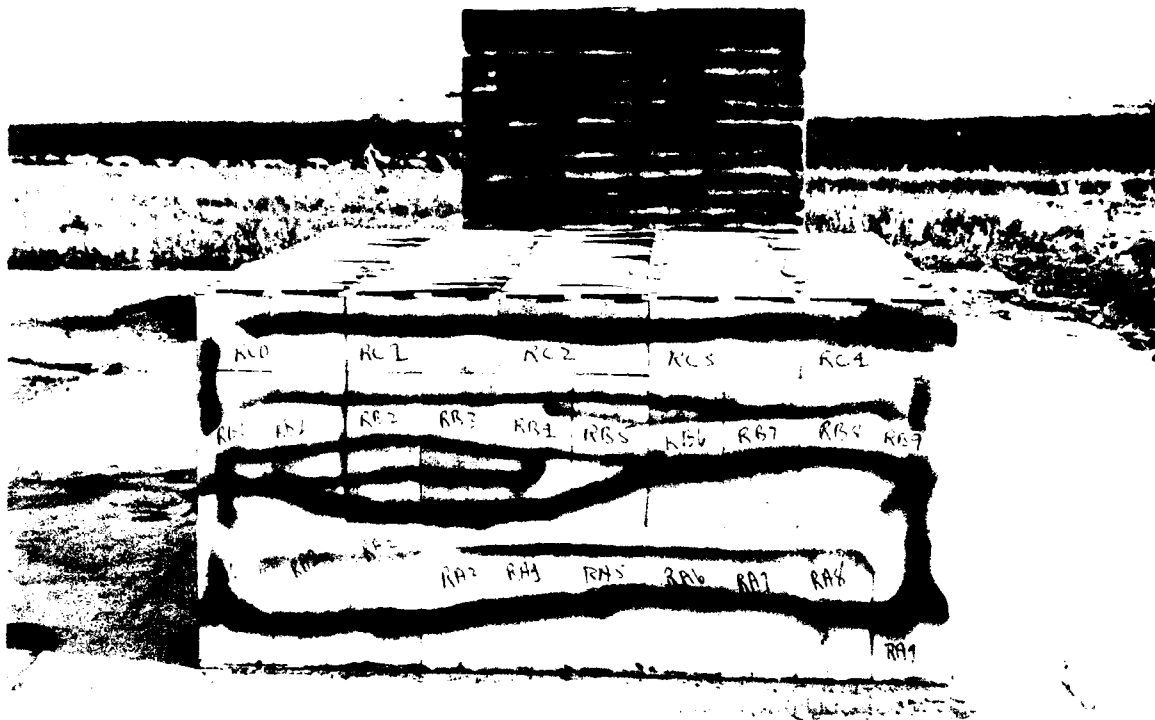


Figure 2.7. PRAIRIE FLAT 1/8-scale frame buildings:  
half-height model in the foreground.

### 2.3.2 DIAL PACK

The successful testing of frame buildings in PRAIRIE FLAT led to the exclusive use of this type of construction in the DIAL PACK event. The frame models, easier to construct than block models, were assembled in 1/120- and 1/20-scale sizes.

Figure 2.9 shows how the 1/120-scale buildings were constructed. A single sheet of 1/16-inch-thick balsa wood was used for each of the four walls. Each sheet was cut into 50 rectangles, each of which represented a 4-by-8-foot sheet of plywood in full size.

A constraint in this test, as in all the others, was that each wall had to be strong enough to withstand environmental damage before the blast, yet fragile enough to be demolished completely by the blast. The Bell Laboratories shock tube at Chester, New Jersey, was used to evaluate the performance of various building designs under the 1-psi blast intended for the DIAL PACK event. None of the models tested was demolished completely under this loading; the best design used

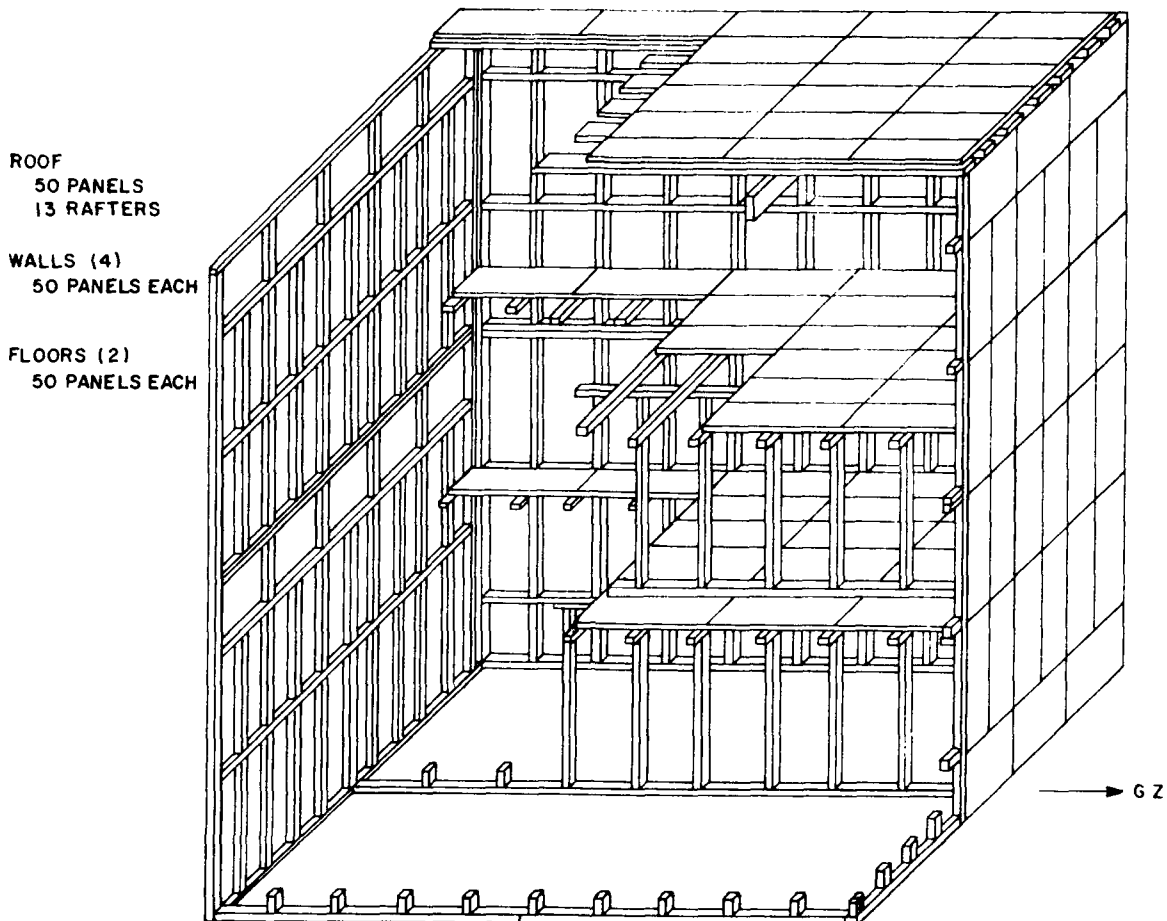


Figure 2.8. Construction details of the PRAIRIE FLAT 1/8-scale full-height frame building. The half-height building was built in a similar fashion.

balsa-wood sheets cut almost all the way through (scored) in two directions to form the 50 simulated rectangular panels. These models, their walls held together only by a few fibers of wood at the corners of the scored rectangles, were very flimsy indeed; some of them required repair in the field while the models were being put together.

The walls of the 1/20-scale buildings were made of individual balsa-wood panels glued together on a very weak balsa-wood frame. They were assembled and reinforced with cross braces as shown in Figure 2.10. The roofs and interior floors were added without the use of glue. These models also were tested at the Chester shock tube. All wall panels were blown free during these tests, and many individual panels were broken into pieces.

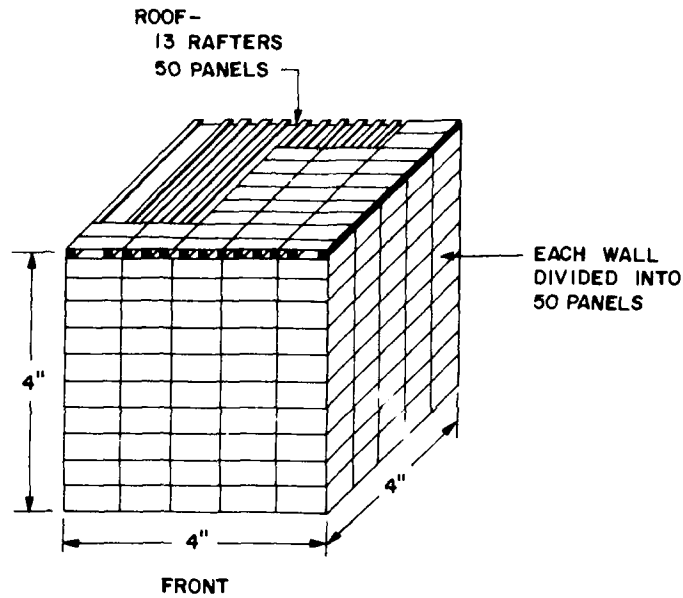


Figure 2.9. Exterior construction of the DIAL PACK 1/120-scale frame buildings.

Model buildings of both scales were subjected to a steady air stream to determine whether they could survive winds of at least 10 mph. They did, provided that the roof panels were properly weighted with washers.

The DIAL PACK field results agreed with the results of the Chester shock-tube tests: The 1/20-scale models were completely demolished, and the 1/120-scale models were partially demolished. Some walls were badly torn apart, and others were hardly damaged — an indication of the variability introduced by the balsa wood and the method of construction.

## 2.4 Packing and Shipping of Buildings

### 2.4.1 SNOWBALL

The methods of packaging the model buildings evolved during the various tests. In Operation SNOWBALL, all four walls of each building were assembled on a Plexiglas base and placed in a cardboard box. Temporary wood strips were glued between the vertical corner members across the top of the walls to keep the blocks in place. The assembled walls were surrounded by polystyrene foam blocks inside and outside the model; the packed box was effectively a solid cube. In the field, the block fitting inside the walls was the most difficult to remove. The temporary strips across the top of the walls broke free during transit in some instances, causing blocks to fall out during the unpacking. Many hours of tedious work with

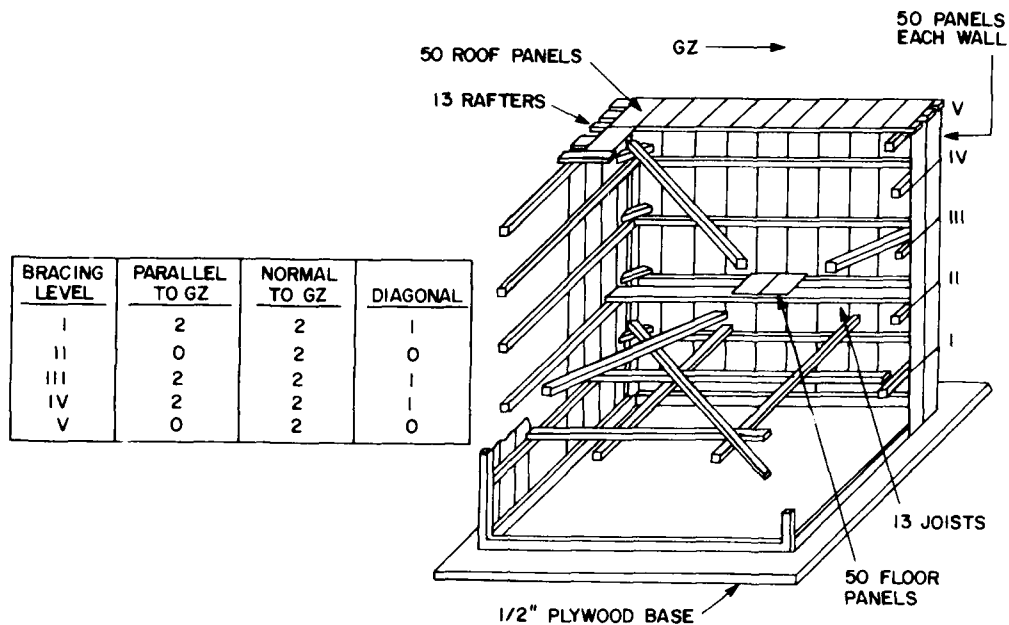


Figure 2.10. Interior construction of the DIAL PACK 1/20-scale frame buildings.

tweezers were spent in getting the walls of damaged models back together. The roof panels were set atop the walls at the site after the models had been unpacked and repaired.

#### 2.4.2 DISTANT PLAIN and White Sands SOTRAN

In packing the models for DISTANT PLAIN and White Sands SOTRAN, the polystyrene foam blocks were replaced by masonite sheets inside and outside the walls. These sheets fitted in grooves in two plywood plates; one plate was the model building base, the other a removable top fastened to the bottom plate with a tie rod. A felt filler was placed between the top of the walls and the top plywood plate. Removal of the plywood plates, felt filler, and masonite sheets would then leave the buildings standing free. However, this method of packing also left much to be desired: during shipment, walls separated, bricks shifted, and considerable repair work was necessary in the field.

#### 2.4.3 PRAIRIE FLAT

The 1/120-scale buildings used in PRAIRIE FLAT were shipped in a similar way to the method above. The 1/20- and 1/8-scale buildings, however, were constructed at the site. This was time consuming but probably the only practical way to construct these larger models.

#### 2.4.4 DIAL PACK

For the DIAL PACK event, the walls of the buildings were either precut or prefabricated before shipment. The other parts of the buildings were shipped loose. The models were then assembled at the site.

### 2.5 Model Layouts

The model buildings in all these experiments were placed on paved areas called pads. These provided a good footing for the buildings, kept down the dust in the vicinity of the models, and provided a good surface upon which to mark a grid system for the convenient location and collection of debris after a blast. In most of the tests, information was also recorded during the blast on high-speed motion-picture film. Cameras were mounted near the ground on stub poles, to the side of the pad with the line of sight approximately perpendicular to a line from ground zero.

#### 2.5.1 SNOWBALL

In Operation SNOWBALL, one of the cameras was placed behind the models, as shown in Figure 2.11. The model locations, with respect to the 1-foot grid spacings, are shown in Figure 2.12.

#### 2.5.2 DISTANT PLAIN

Two pads were used in the DISTANT PLAIN events. The forward pad, Figure 2.13, contained some of the 10-by-10-inch models; the rear pad, Figure 2.14(a) and (b), contained the remainder of the 10-by-10-inch models and all of the 3.3-by-3.3-inch models.

#### 2.5.3 White Sands SOTRAN

Two pads were used in the White Sands event also. These are shown in Figure 2.15. The forward pad, left, was used only for isolated buildings; the larger rear pad, right, accommodated a 12-building complex as well as two isolated buildings. Two grid spacings were used to identify the post-shot debris locations: one was a 35-inch gridwork over each entire pad, the other a 7-inch subdivision applied only near the models. No cameras were used in this test.

#### 2.5.4 PRAIRIE FLAT

Event PRAIRIE PLAT used a complex setup of four test locations, frame buildings of half height and full height, and block buildings in three scales, half height and full height.

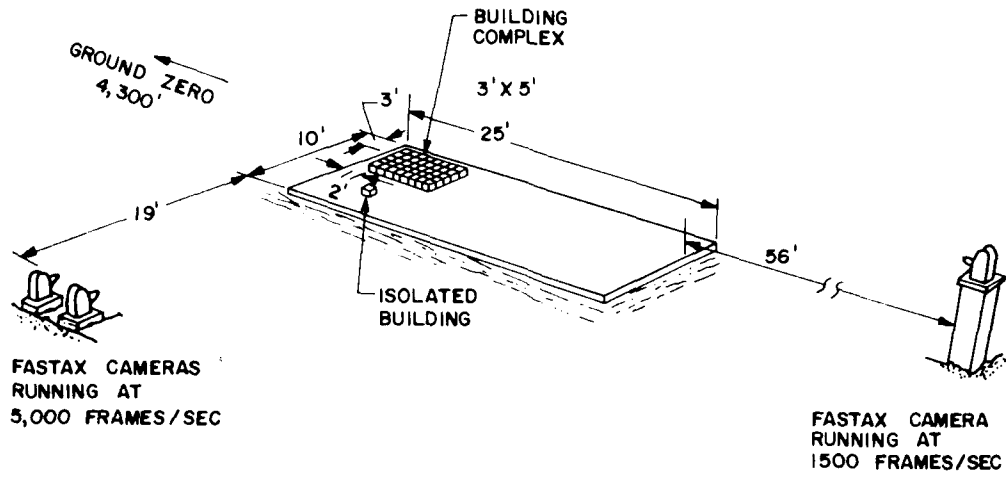


Figure 2.11. Camera locations in Operation SNOWBALL.

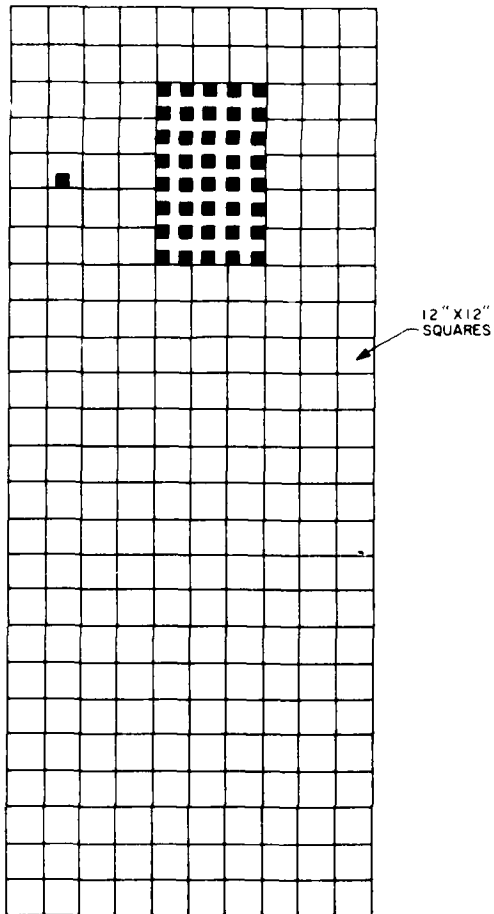


Figure 2.12. Plan view of the SNOWBALL model layout.

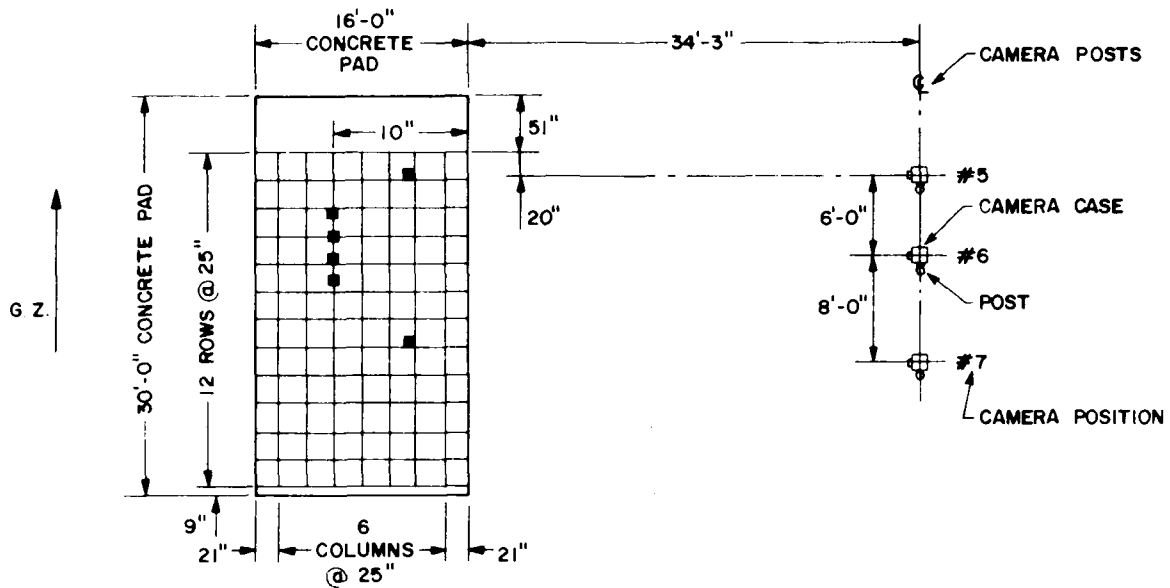


Figure 2.13. Plan view of the forward pad; DISTANT PLAIN, Event 2a, showing camera locations.

One location was at a distance from ground zero that would subject the models to a peak free-field overpressure of 6 psi — a relatively high overpressure. The models at this location were built to 1/8 scale (5 feet square) and comprised two full-height and two half-height block buildings individually located on small concrete pads 10 feet square. The areas surrounding the building models were each divided into a gridwork with a 2.5-foot spacing.

Another group of 1/8-scale models and a group of 1/20-scale models were located at a distance from ground zero that would subject them to a peak overpressure of 3 psi — a relatively low overpressure. The 1/8-scale models comprised a full-height and a half-height frame building on a large concrete pad and four block buildings — two full height and two half height — individually located on small concrete pads 10 feet square, placed symmetrically around the large pad. The large pad and the areas surrounding the small pads were divided into a 2.5-foot grid, as at the 6-psi location. The overall layout of buildings and cameras at the 6- and 3-psi locations is shown in Figure 2.16. The detailed layout of the large pad at the 3-psi location and a typical small pad for the 1/8-scale buildings are shown on left in Figure 2.17; the four 1/20-scale block buildings (2 feet square) were separated sufficiently to be considered isolated buildings but were located on a single large pad divided into a 2-foot gridwork, as shown on the right in Figure 2.17. Two of these were full-height buildings; the other two were half-height buildings.

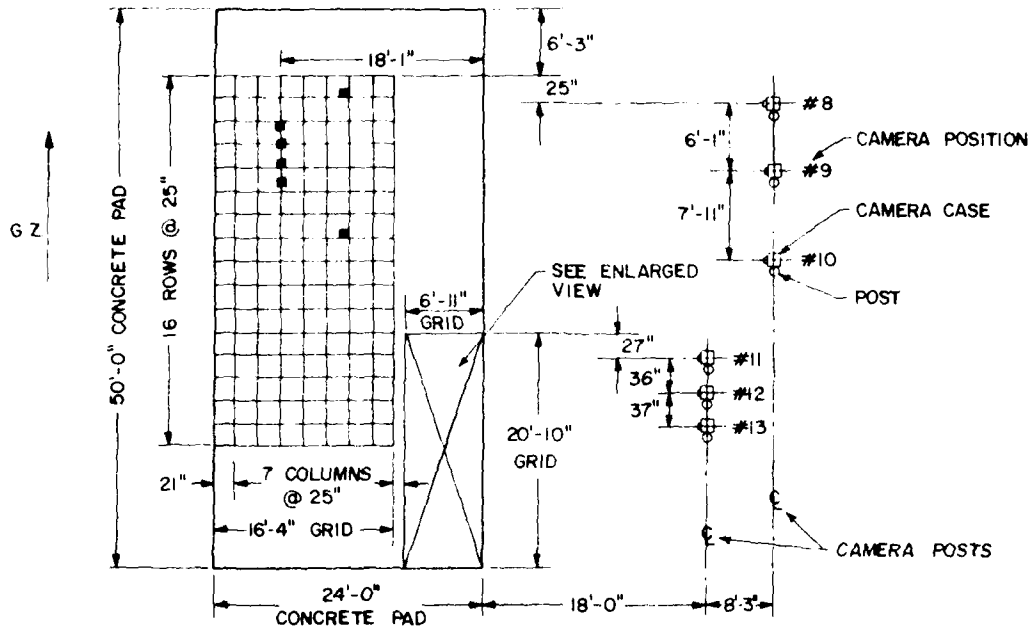


Figure 2.14(a). Plan view of the rear pad; DISTANT PLAIN, Event 2a, showing camera locations.

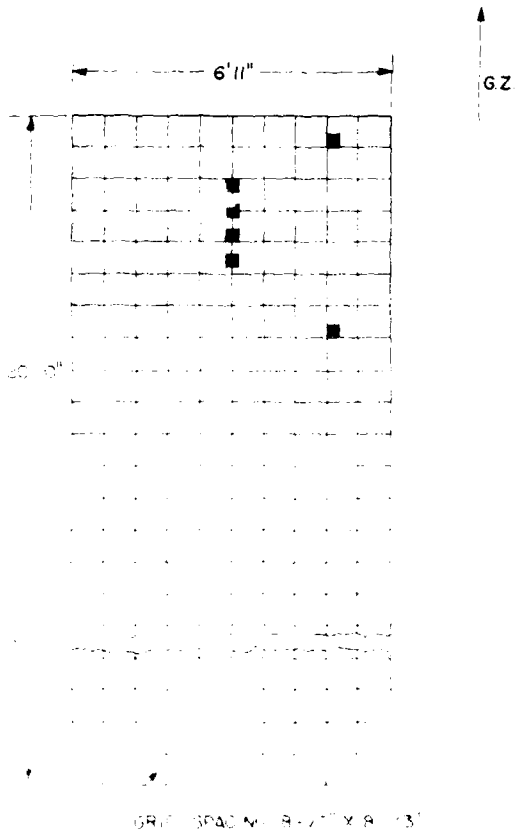


Figure 2.14(b). Plan view of the 1/40-scale buildings on the rear pad; DISTANT PLAIN, Event 2a.

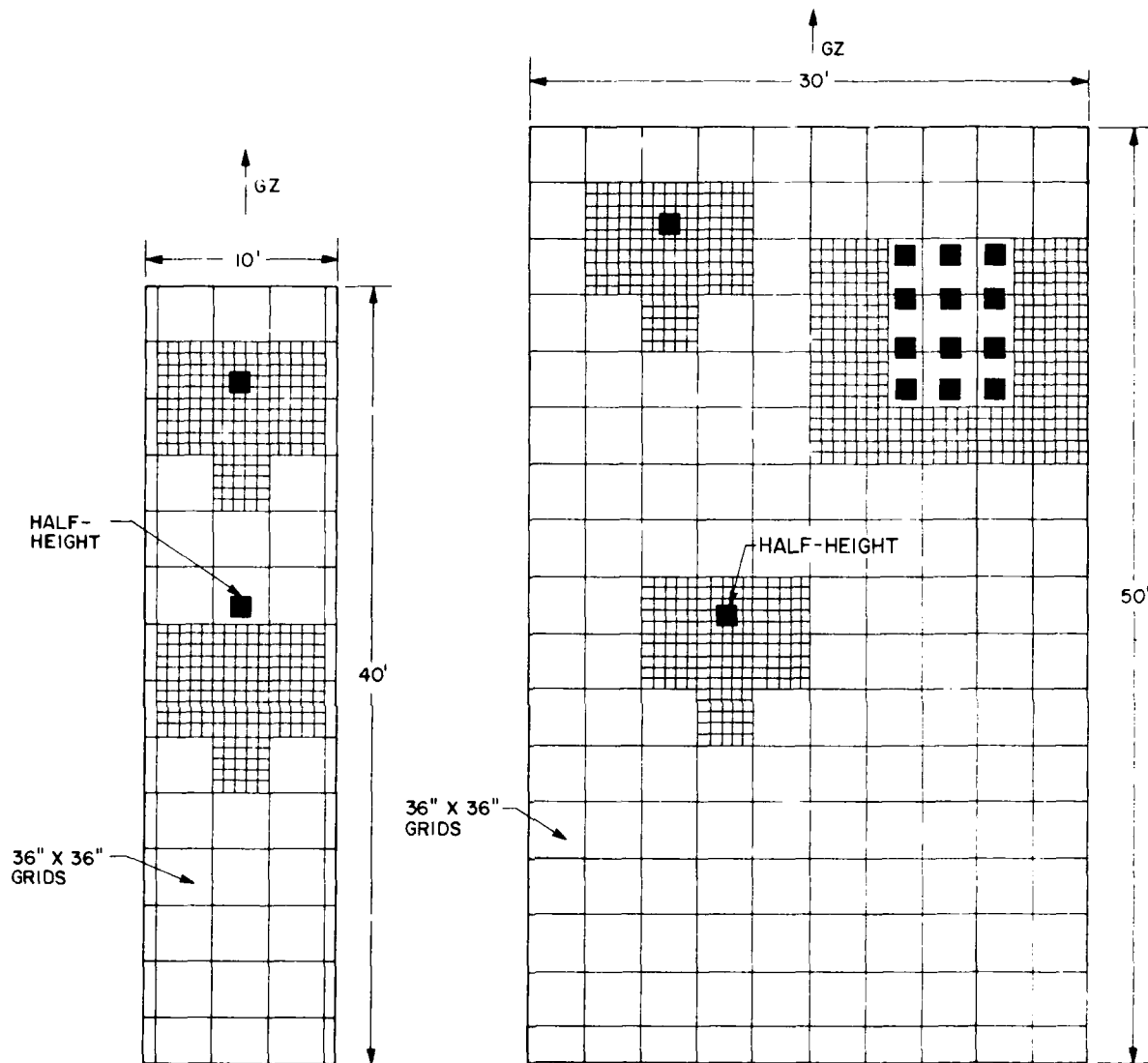


Figure 2.15. Plan views of the forward (left) and rear (right) pads:  
White Sands SOTRAN.

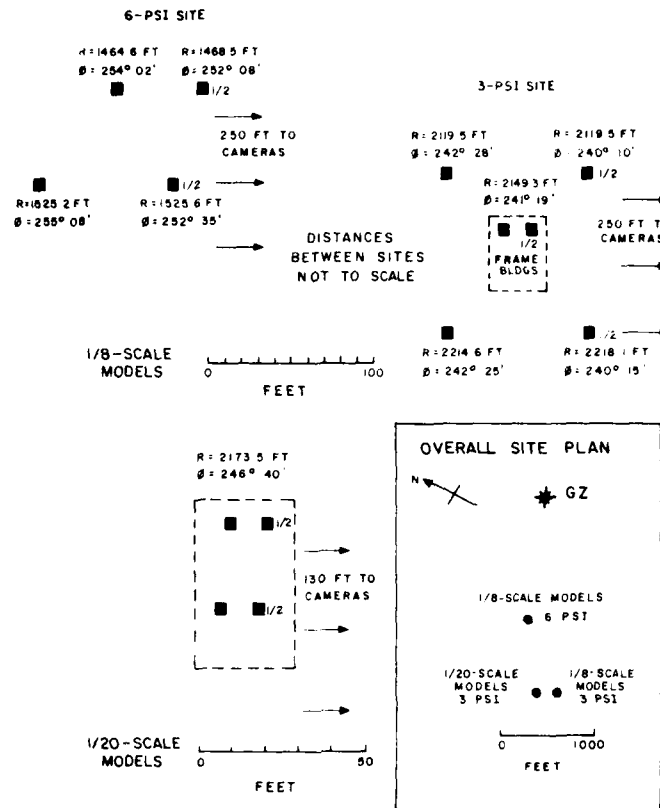


Figure 2.16. General plan views of 1/20-scale and 1/8-scale building layouts, indicating distances to cameras; PRAIRIE FLAT.

The fourth location was at a distance from ground zero that would subject the models to a peak overpressure of 1 psi. The buildings here were 1/120 scale (4 inches square) block models: a complex of 12 full-height buildings and four isolated buildings, two of which were half height, located on a large pad, as shown in Figure 2.18. There was no camera coverage at this location.

### 2.5.5 DIAL PACK

One of the objects of the DIAL PACK event was to observe the effect of sloping terrain on debris transport. To accomplish this, models were placed on pads at two elevations connected by a 15-degree slope.

At the site where 1/20-scale frame buildings were used, shown in Figure 2.19, the slope rose 10 feet. Models were placed in front of the slope at the base, midway up, and at the crest, as shown in Figure 2.20. Two additional buildings were placed on a flat pad to the side of the main pad at the lower level.

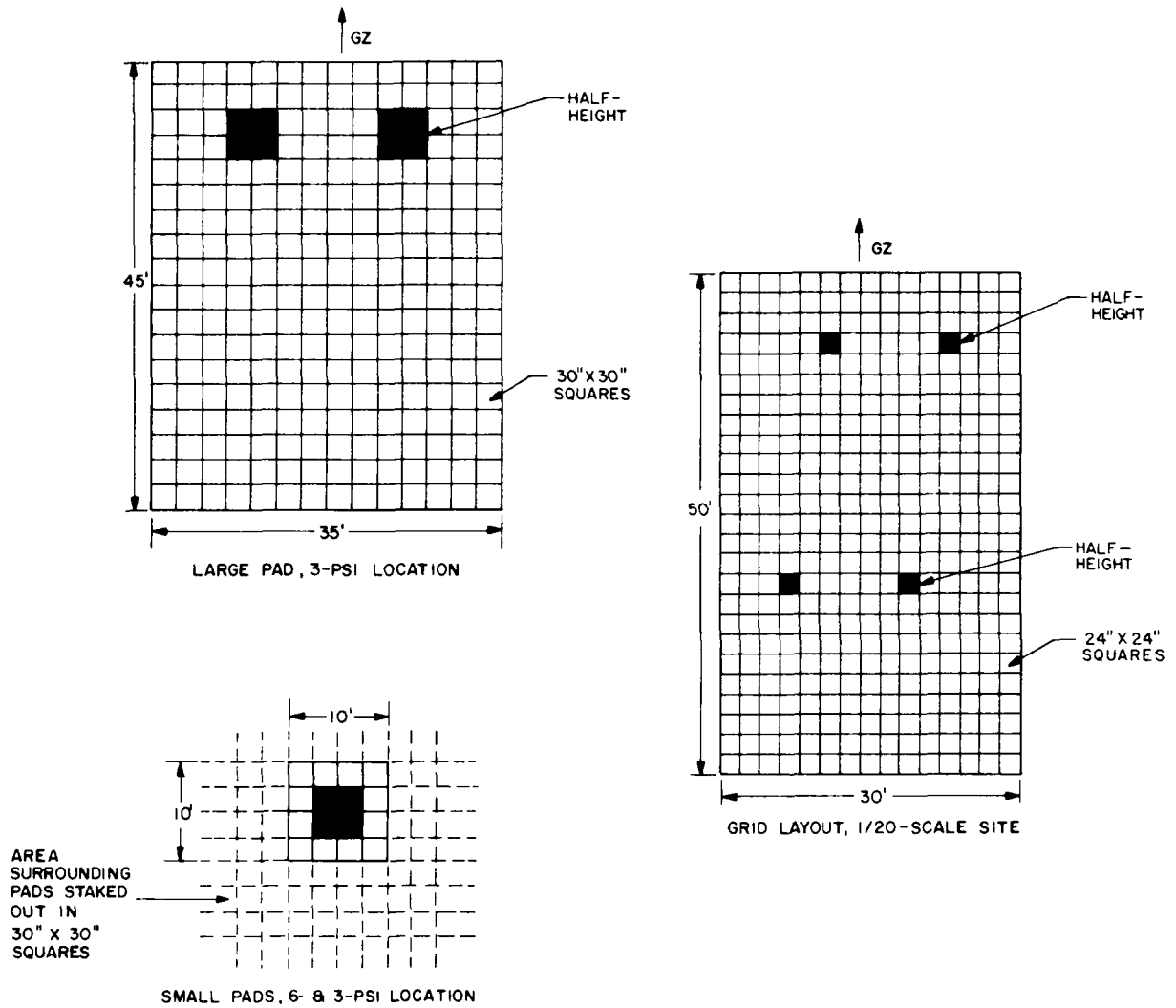
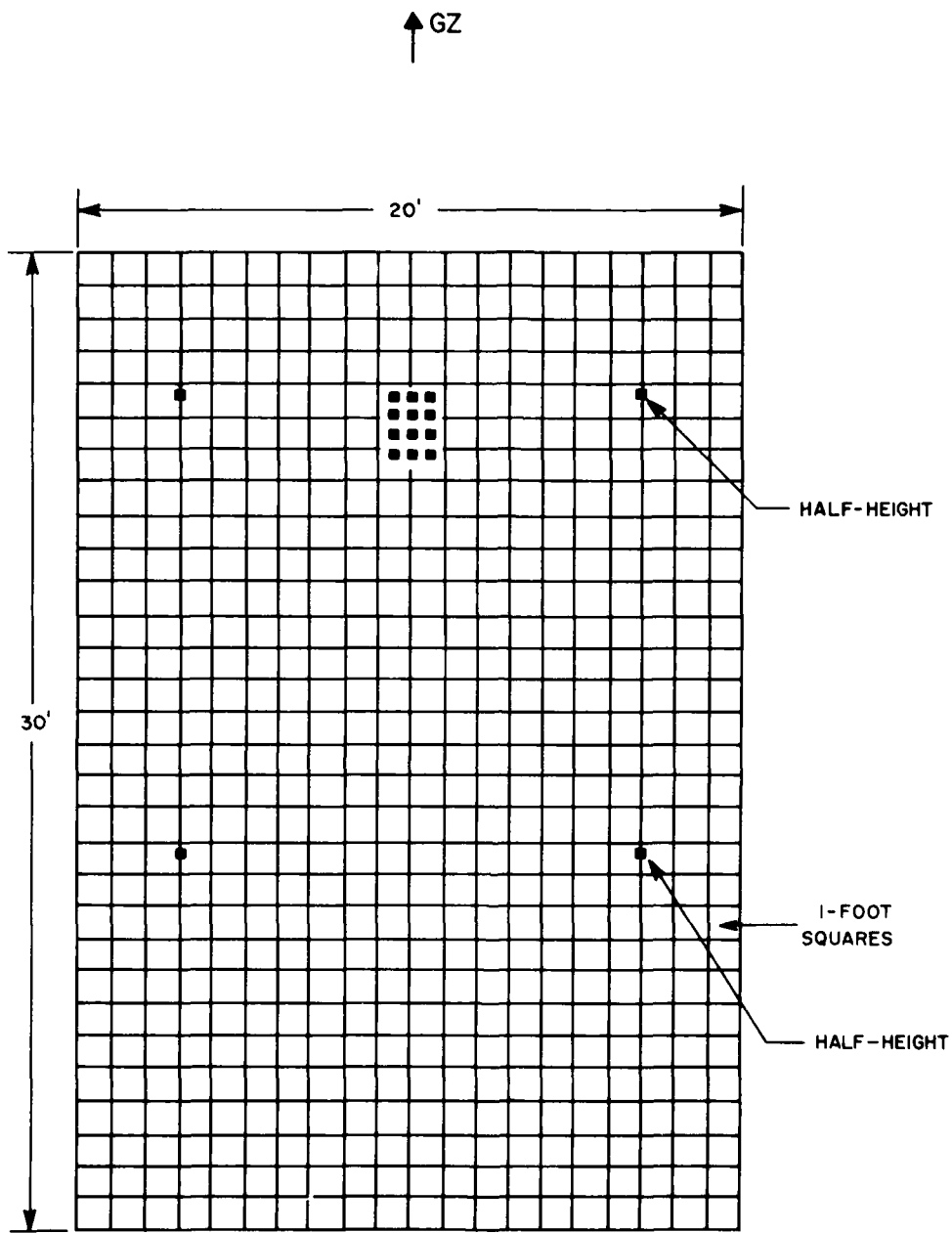


Figure 2.17. Plan views of the large pad (upper left) and typical small pad (lower left), low-overpressure site with 1/8-scale buildings, and 1/20-scale building site (right); PRAIRIE FLAT.



NO CAMERA COVERAGE AT THIS LOCATION

Figure 2.18. Plan view of complex and isolated buildings,  
1/120-scale buildings; PRAIRIE FLAT.

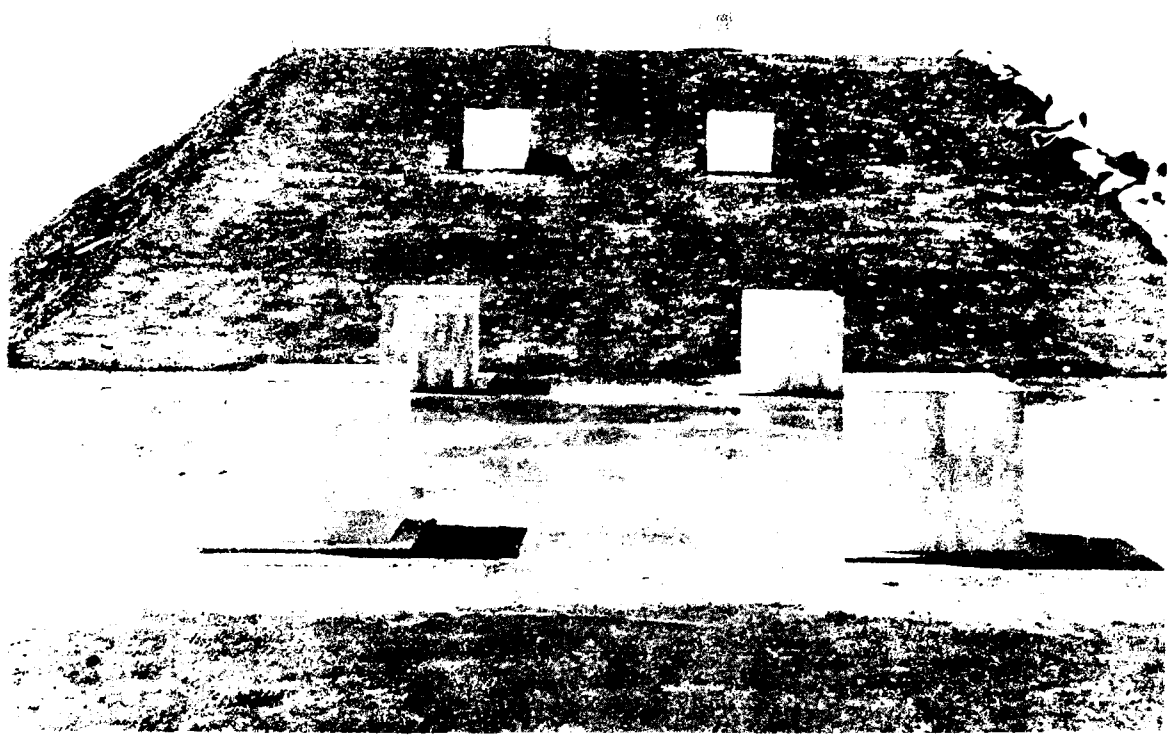


Figure 2.19. DIAL PACK 1. 20-scale buildings before detonation.

At the site where 1/120-scale models were used, shown in Figure 2.21, the slope between elevations rose 2 feet. The locations of models on the lower elevation, the slope, and the higher elevation are indicated in Figure 2.22. The pads were made of asphalt, which is cheaper than concrete, but not as satisfactory. The

asphalt pads were placed on the slope and the higher elevation. The pads were

placed on the slope and the higher elevation. The pads were

placed on the slope and the higher elevation. The pads were

placed on the slope and the higher elevation. The pads were

placed on the slope and the higher elevation. The pads were

placed on the slope and the higher elevation. The pads were

placed on the slope and the higher elevation. The pads were

placed on the slope and the higher elevation. The pads were

placed on the slope and the higher elevation. The pads were

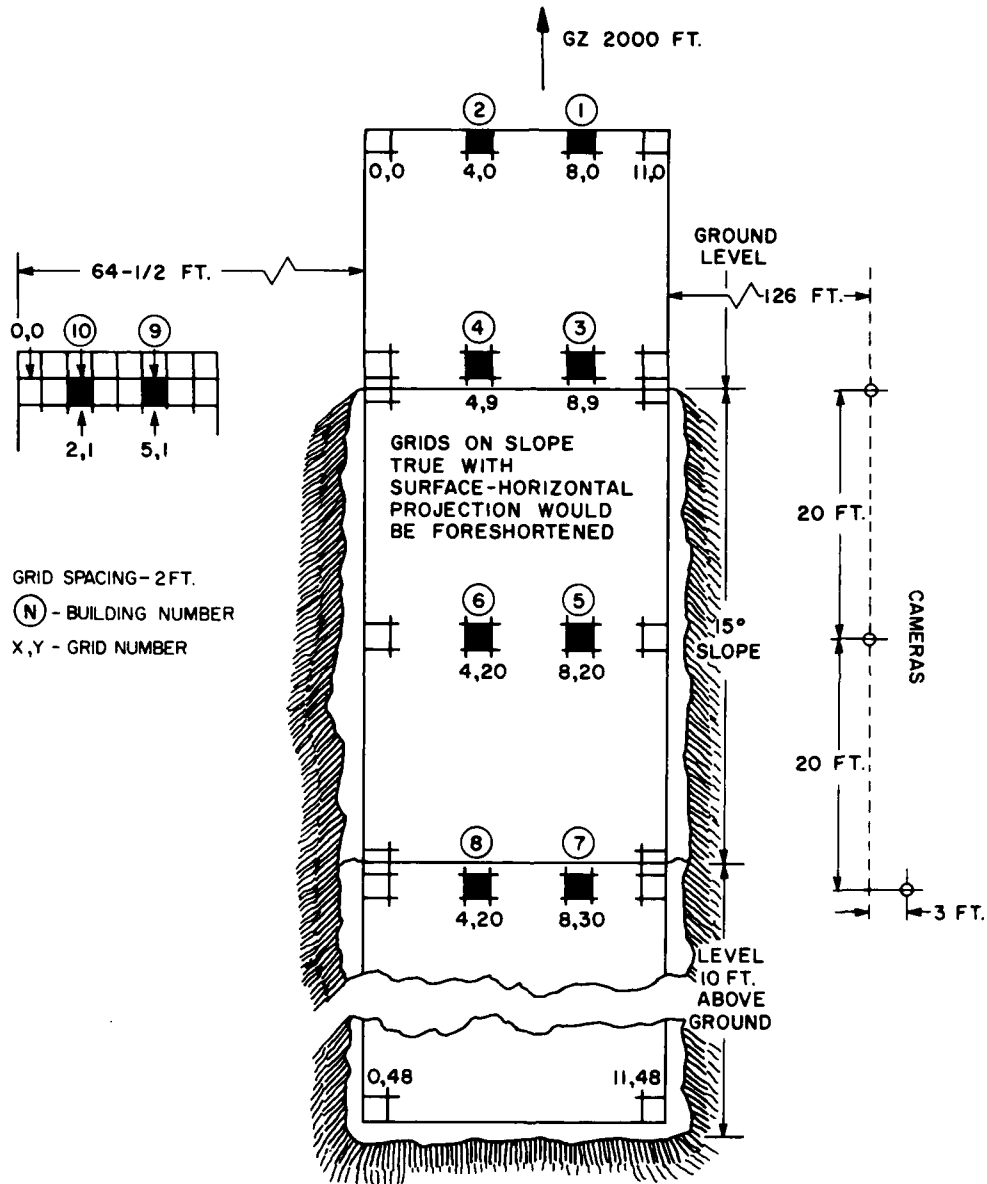


Figure 2.20. Plan view of the 1/20-scale building layout; DIAL PACK.

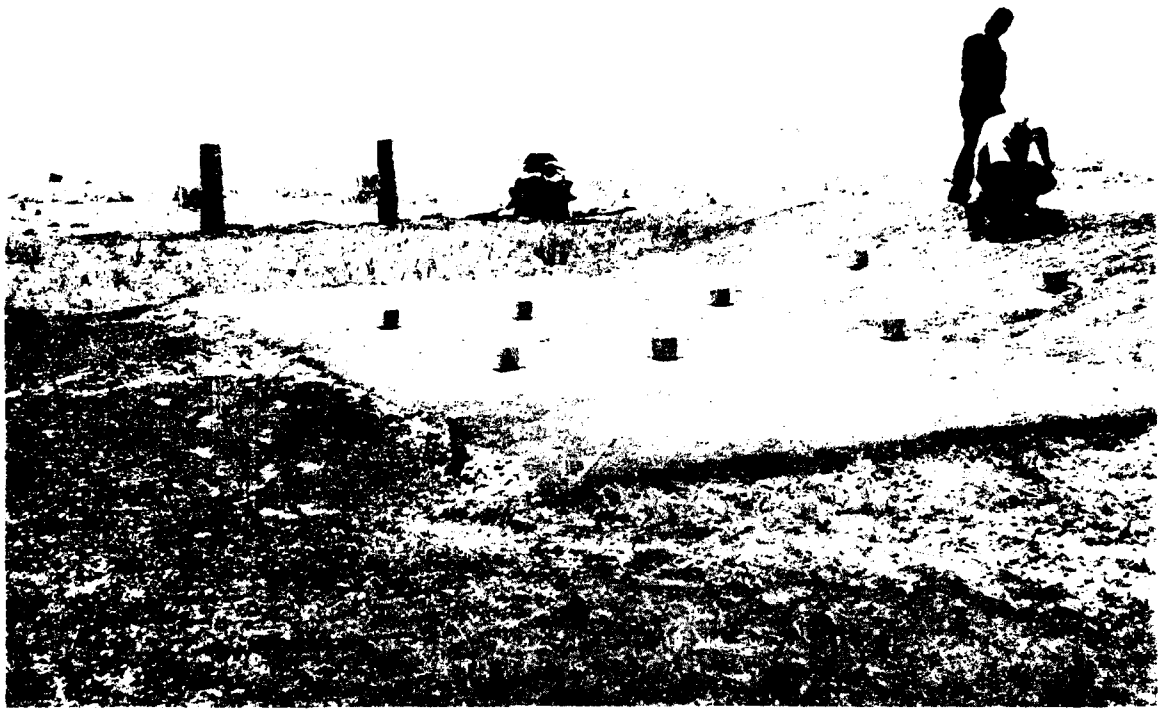


Figure 2.21. DIAL PACK 1/120-scale buildings before detonation.

Three Fastax cameras were used in Operation SNOWBALL, protected from the blast by sandbags. All three worked satisfactorily. The camera at the rear of the complex was powered by 24 Vdc supplied by batteries and ran at about 1300 frames/sec; the two cameras to the side of the complex were supplied by 120 Vac and ran at about 5000 frames/sec, the entire 100-foot reel of film being exposed in about one second. Timing for these extremely fast side cameras was critical.

In Operation DISTANT PLAIN three cameras were used at each of the two pads. The forward camera at each pad operated on 300 Vac and ran at about 7000 frames/sec. These cameras were to record the motion of the blocks during early building breakup, but this information was not obtained. The other two cameras at each site operated on 220 Vac and ran at about 5000 frames/sec. Their objective was to view the action of the roof elements during each blast. In these and in all subsequent events the cameras were mounted in blast-proof boxes of the type shown in Figure 2.23.

A new model Hycam camera was used in PRAIRIE FLAT. Operating on only 120 Vac, this type of camera was able to run at 4000 frames/sec.

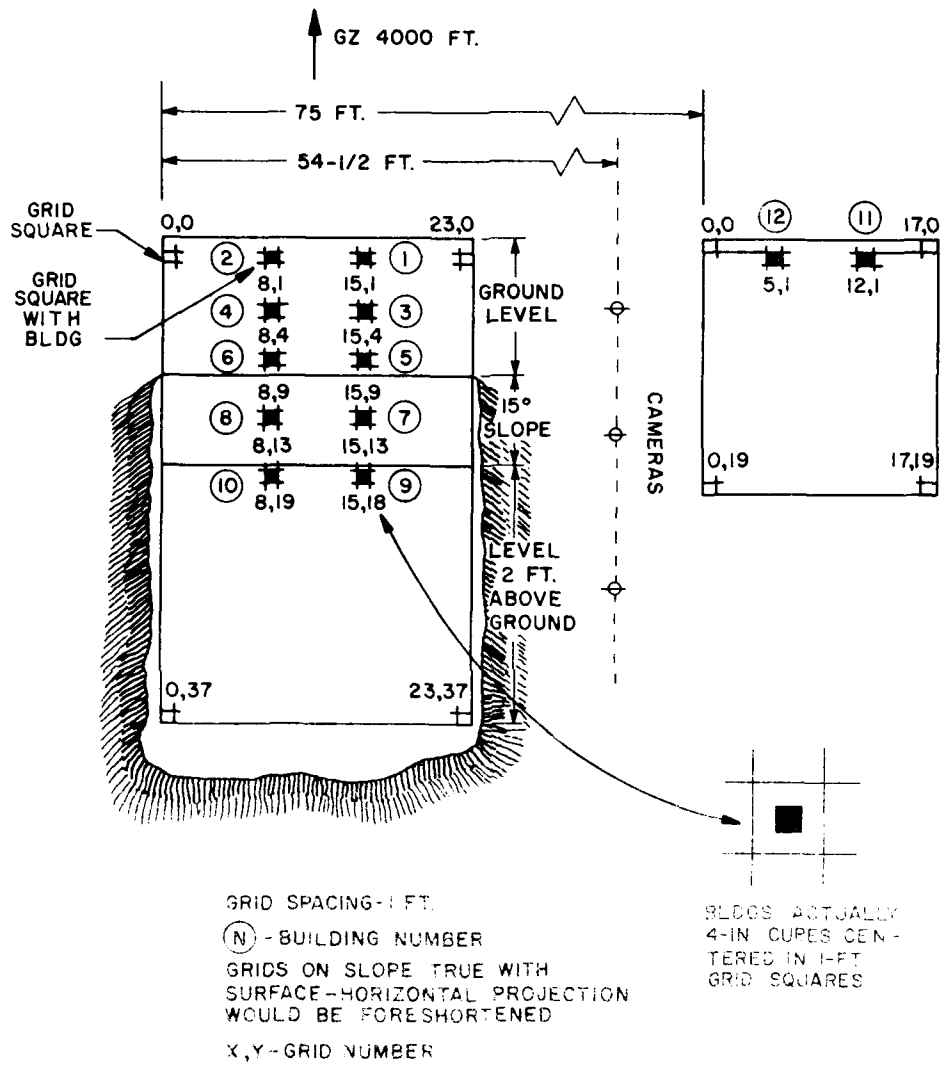


Figure 2.22. Plan view of the 1/120-scale building layout: DIAL PACK.

Table 2.2  
SUMMARY OF SITE INFORMATION

Test	Model Plan (in. x in.)	Peak Free-Field Overpressure (psi)	Pad Dimensions (ft x ft)	Grid Spacing (in. x in.)	Number of Cameras	Camera-to- Model Distance (ft)	Lens Focal Length (ft)
SNOWBALL	4 x 4	1	10 x 25	12 x 12	3	~24 (side) ~76 (rear)	Not Recorded
DISTANT PLAIN (All shots)	3.3 x 3.3	1.7	24 x 50	8.3 x 8.3	3	21	4 (1) 4 (2)
	10 x 10	1.7		25 x 25	3		
White Sands	10 x 10	3.0 - 3.5	16 x 30	25 x 25	3	42	(1) 4 (2) 1-3/8
	14 x 14	2	30 x 50	36 x 36	0	NA*	NA
PRAIRIE FLAT	14 x 14	3	10 x 40	7.2 x 7.2	0	NA	NA
	4 x 4	1	20 x 30	12 x 12	0	NA	NA
DIAL PACK	24 x 24	3	30 x 50	24 x 24	3	130	2
	60 x 60 (frame)	3	35 x 45	30 x 30	3	250	2
	60 x 60 (block)	3	10 x 10†	30 x 30	3	250	2
	60 x 60	6	10 x 10†	30 x 30	3	250	2
DIAL PACK	4 x 4	1	25 x 40	12 x 12	3	42	2
	4 x 4	1	20 x 22	12 x 12	0	NA	NA
	24 x 24	3	30 x 100	24 x 24	3	140	2
	24 x 24	3	10 x 20	24 x 24	0	NA	NA

\*NA † not applicable.

† For each building, 4 pads per overpressure location.

Table 2.3  
CAMERA DATA

Test	Number of Cameras	Overpressure at Camera Station (psi)	Camera Voltage (volts)	Max. Speed (frames/sec)		Lens Opening	Camera Model	Film	Timing (sec after blast)	
				Est.	Meas.				Camera Start	Blast Arrival
SNOWBALL Side Cameras	2	1	120 ac	6000	5000	-	Fastax WF3	Ansco D200	+2.7	3.0
Back Camera	1	1	24 dc	1500	1300	-	Fastax WF3	Ansco D200	+2.0	3.0
DISTANT PLAIN	3	1.7	220 ac	5000	-	-	Hycam K100	Ansco D200	+0.5	-
	3	1.7	{(1) 220 ac {(2) 300 ac	5000 7000	-	-	Hycam K100 Hycam K100	Ansco D200 Ansco D200	+0.5	-
	3	3.0 - 3.5	{(1) 220 ac {(2) 300 ac	5000 7000	-	-	Hycam K100 Hycam K100	Ansco D200 Ansco D200	0	-
	3	3*	120 ac	4000	-	-	Hycam 2001R	Ansco D500	+0.1	-
PRAIRIE FLAT	3	3†	120 ac	4000	-	-	Hycam 2001R	Ansco D500	+0.1	-
	3	6	120 ac	4000	-	-	Hycam 2001R	Ansco D500	0	-
	3	1	{(1) 120 ac {(2) 120 ac	4000 4000	-	f/2.8 f/2.8	(1) Fastax WF3 (2) Hycam 2001R	Ansco D500 Ansco D500	+2.0	-
DIAL PACK	3	3	120 ac	4000	-	f/2.8	Hycam 2001R	Ansco D500	0	-

\*24-in. models  
†60-in. models

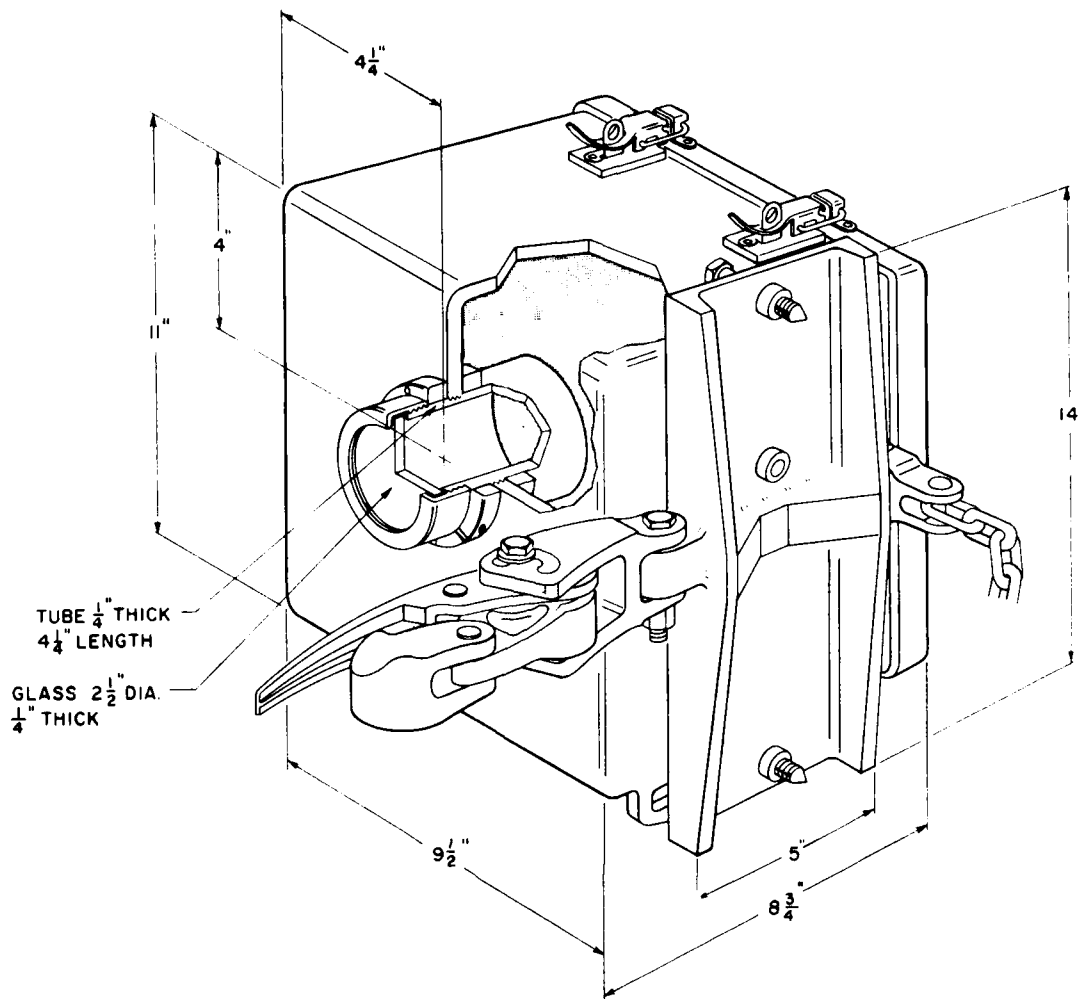


Figure 2.23. Blast-proof camera housing.

Similar cameras were used in DIAL PACK, with the exception that a Fastax camera without a camera box was used at the 1-psi location.

The fastest color film available, Anscochrome D500, was used in the PRAIRIE FLAT and DIAL PACK events. This film was slightly overexposed at first, but became slightly underexposed when the camera reached its rated speed. A better record would have been obtained if the camera speed had been reduced.

### 2.6.2 Identification of Building Elements

Some means of identification was necessary in these experiments so that debris collected after each blast could be traced back to the particular building and the location within that building from which it came.

To identify the building itself, all the elements of each building were painted a particular color, distinct from the colors of the other buildings in the experiment. Secondary markings of various kinds were used to identify specific elements within each building. The methods used are discussed below.

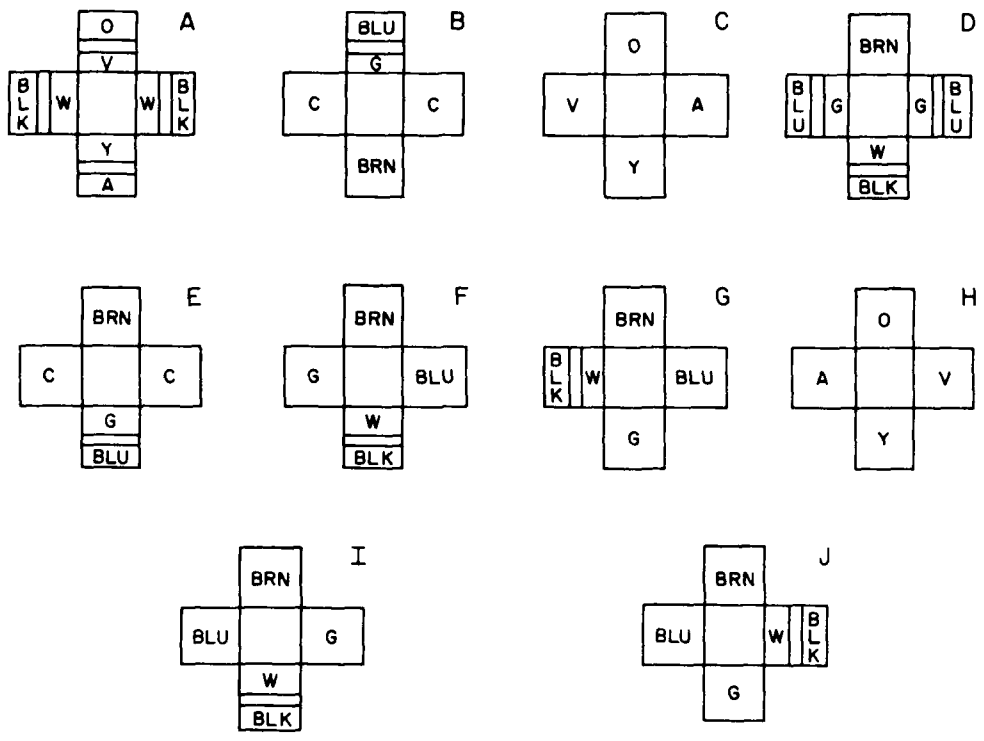
In Operation SNOWBALL the roof elements, except those in the isolated building, were not individually marked. In all subsequent tests, however, each roof panel and rafter was numbered.

The blocks used for the buildings in SNOWBALL, DISTANT PLAIN, and the 1/120-scale buildings in PRAIRIE FLAT were made in various colors by the addition of dyes to the rigid vinyl resin. Walls were made from various colored blocks so that a specific color of block would represent a specific wall or section within a wall. Each piece of debris, therefore, exhibited two colors: the plastic color of the block, indicating the specific location of that block within the building, and the painted color applied to the exterior of the entire building, indicating the particular building from which the block came.

A compromise in this method had to be made for the 40-building complex of Operation SNOWBALL. It was not possible to find 40 separately identifiable paint colors; to simplify the task of discriminating among pieces of debris, therefore, only 12 distinctly different exterior paints were used, each color being common to several buildings in the complex. The complex consisted of five columns of buildings, the center column on a line through ground zero. Thus, the first two columns were symmetrically placed with respect to the fourth and fifth columns and, consequently, painted the same colors. This reduced the number of colors needed from 40 to 24. The further reduction to 12 colors was made by segregating the colors of the plastic blocks so that two models could have the same exterior color but no plastic colors in common. In all, ten arrangements of colored blocks were used to construct the model buildings. These are shown in Figure 2.24; the walls of each building are shown rotated outward as though each building were partially disassembled with the walls lying flat. The 40-building complex followed the grid pattern of Figure 2.25, in which the color of each building is indicated by a number from 1 through 12.

In DISTANT PLAIN, Event 1, 13 color combinations were used for the complex of 15 buildings and two isolated buildings at each of the three test sites. Further information on these models is not given, because wind damage destroyed the validity of the debris distribution.

DISTANT PLAIN, Event 2a, was a repeat of this experiment. A group of four buildings and two isolated buildings were erected at the three test sites from material salvaged from Event 1. All models were built according to the plan of an isolated building shown in Figure 2.26.



**NOTES:**

- 1) VIEWS ARE FROM ABOVE WITH TOP OF WALLS ROTATED DOWN
- 2) UNMARKED AREAS INDICATE BLOCKS MADE FROM PLASTIC IN WHICH ADJACENT COLORS WERE MIXED
- 3) BLOCK ARRANGEMENT PER BUILDING:

**PAINT IDENTIFICATION CODE**

- A - APRICOT
- BLK - BLACK
- BLU - BLUE
- BRN - BROWN
- C - CLEAR
- G - GREEN
- O - ORANGE
- V - VIOLET
- W - WHITE
- Y - YELLOW

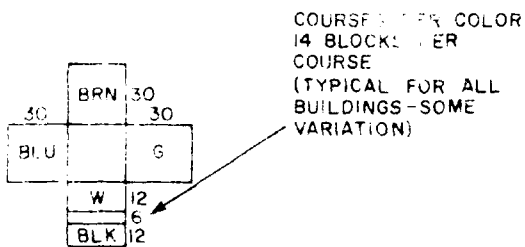


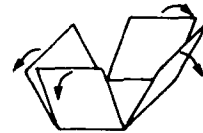
Figure 2.24. Wall-block color arrangements in the ten basic models used in the 40-building SNOWBALL complex.

GZ ↑

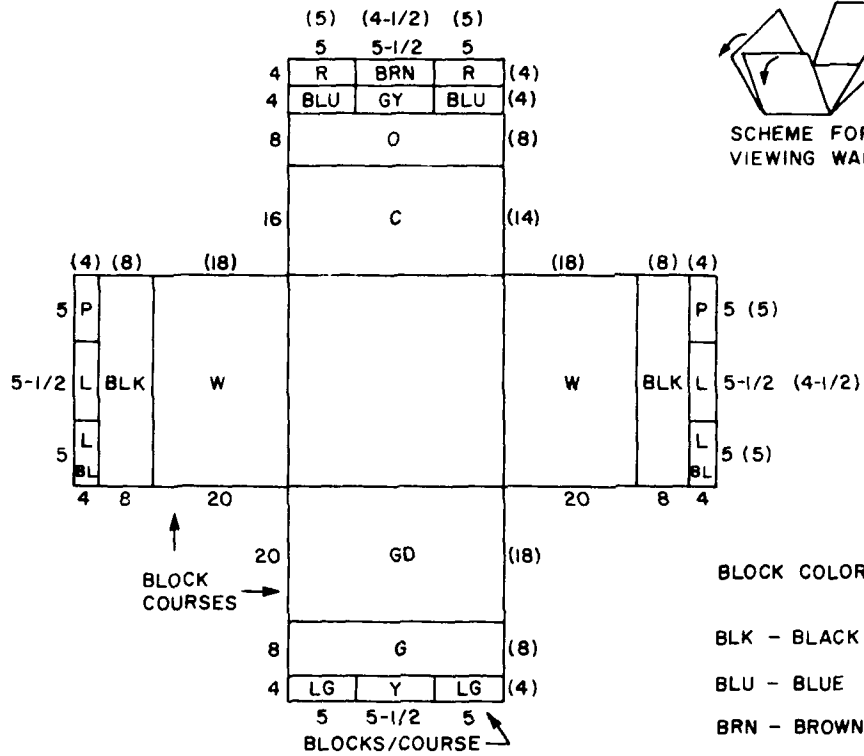
B RED SPOT	A CERISE	A RED	A CERISE	B RED SPOT
G YEL/ORANGE SPOT	C GRAY	D GRAY SPOT	H GRAY	J YEL/ORANGE SPOT
E CERISE SPOT	A COPPER	B COPPER SPOT	A COPPER	E CERISE SPOT
C BLUE	J BLUE SPOT	C YEL/ORANGE	G BLUE SPOT	H BLUE
A YELLOW	E SILVER SPOT	A SILVER	E SILVER SPOT	A YELLOW
J GREEN SPOT	C GREEN	C RED/ORANGE	H GREEN	G GREEN SPOT
B PINK SPOT	A PINK	E YELLOW SPOT	A PINK	B PINK SPOT
F GOLD SPOT	C GOLD	D RED SPOT	H GOLD	I GOLD SPOT

A-J BLOCK PATTERN  
FROM FIGURE  
2.24

Figure 2.25. Exterior building colors in relation to building positions in the SNOWBALL complex.



SCHEME FOR VIEWING WALLS



NOTE:

NUMBERS IN PARENTHESES  
ARE FOR THE SMALL  
(3.3" x 3.3") BUILDINGS

BLOCK COLORS

- BLK - BLACK
- BLU - BLUE
- BRN - BROWN
- C - CLEAR
- GD - GOLD
- GY - GRAY
- G - GREEN
- L - LAVENDER
- LBL - LT. BLUE
- LG - LT. GREEN
- O - ORANGE
- P - PINK
- R - RED
- W - WHITE
- Y - YELLOW

Figure 2.26. Wall-block color arrangements used in the DISTANT PLAIN, Event 2a, buildings.

This basic configuration was used in the White Sands tests as well. Half-height buildings were introduced here, the wall arrangements of which followed a similar pattern. Color combinations for the full-height and half-height buildings are shown in Figure 2.27. The models at the two sites differed in that those at the forward location were composed of smaller blocks and thus had a greater number of each color in each section. A number of block arrangements, shown in Figure 2.28, were used in the 12 buildings forming the complex constructed at the rear pad.

Twelve color combinations were used for the walls of the 12 1/120-scale buildings in the complex and the four 1/120-scale isolated buildings in the PRAIRIE FLAT event. The wall arrangements are shown in Figure 2.29. Each of the 12 buildings in the complex was given a spattering of a unique paint color on its exterior walls. Post-shot debris identification, then, involved the rather tedious identification of combinations of 18 plastic colors and 12 paint colors. In the 1/8- and 1/20-scale buildings of PRAIRIE FLAT, the 500 blocks in each wall of each building were identified by a number-letter code. Each of a building's four walls was composed of blocks of a different color, and the exterior of each building was given a unique paint color. Debris was identified, then, by the paint color, which determined the building of origin; the block color, which determined the wall within the building; and the number-letter code, which determined the specific location of the block within the wall.

The walls of the frame buildings in DIAL PACK and PRAIRIE FLAT were individually identified by a letter-number code; interior parts were identified in the same way.

The actual codes used in these experiments are not discussed here. Several techniques were used, and an explanation of them is not necessary for the purposes of this report. Whenever information is presented here, an index will be used so that data can be associated with a building and location within that building without the need to resort to the actual codes.

### 2.6.3 Debris Collection

The original method of collecting debris was to pick up each piece within a grid and put it in an envelope marked with the grid identification. This technique was used in SNOWBALL, DISTANT PLAIN, White Sands SOTRAN, and PRAIRIE FLAT (the 1/120-scale buildings only).

If the winds are mild, this technique is satisfactory. In DISTANT PLAIN, however, a number of small tornadoes were observed; these could and did destroy the value of data.

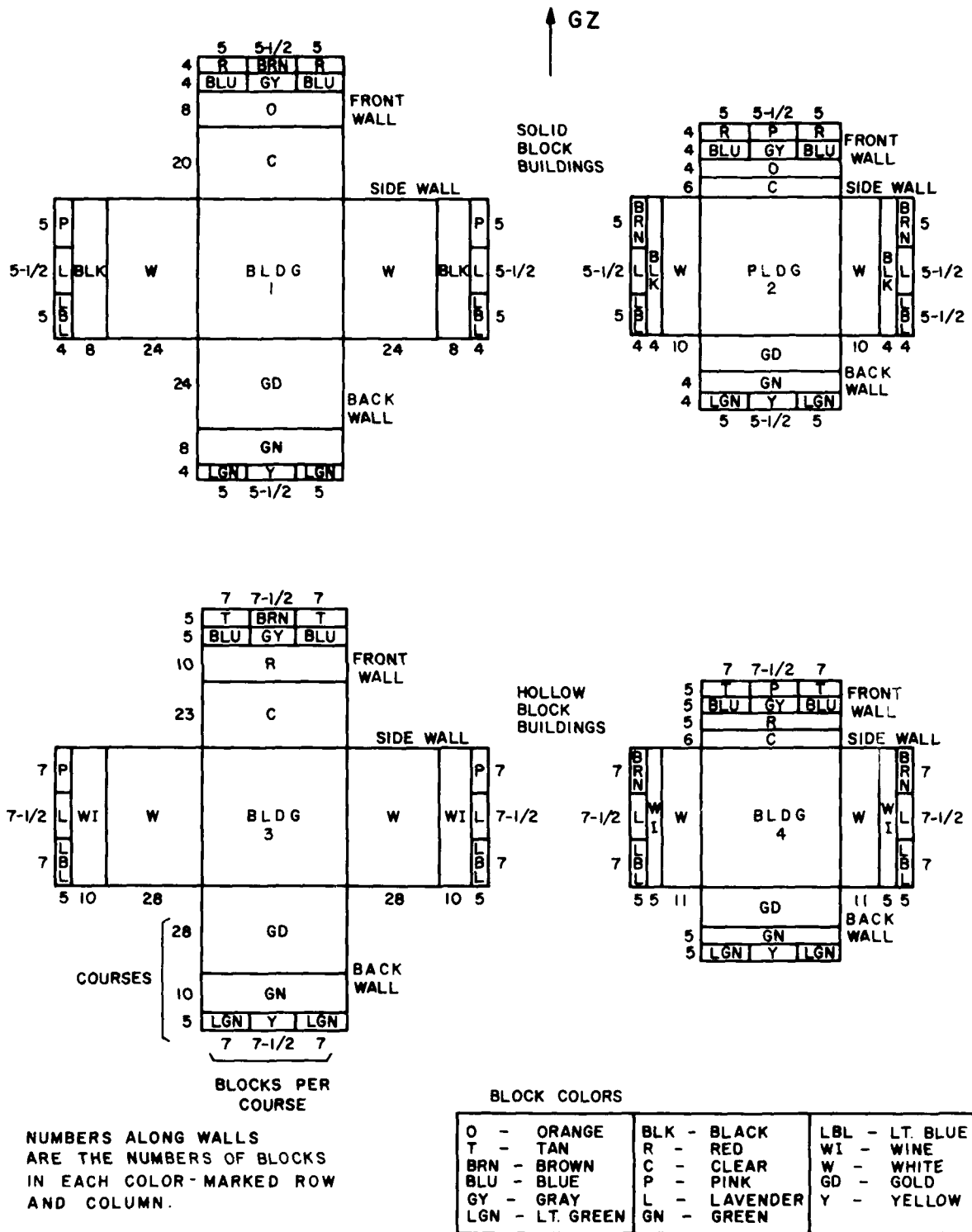


Figure 2.27. Wall-block color arrangements for full- and half-height isolated buildings used in White Sands SOTRAN.

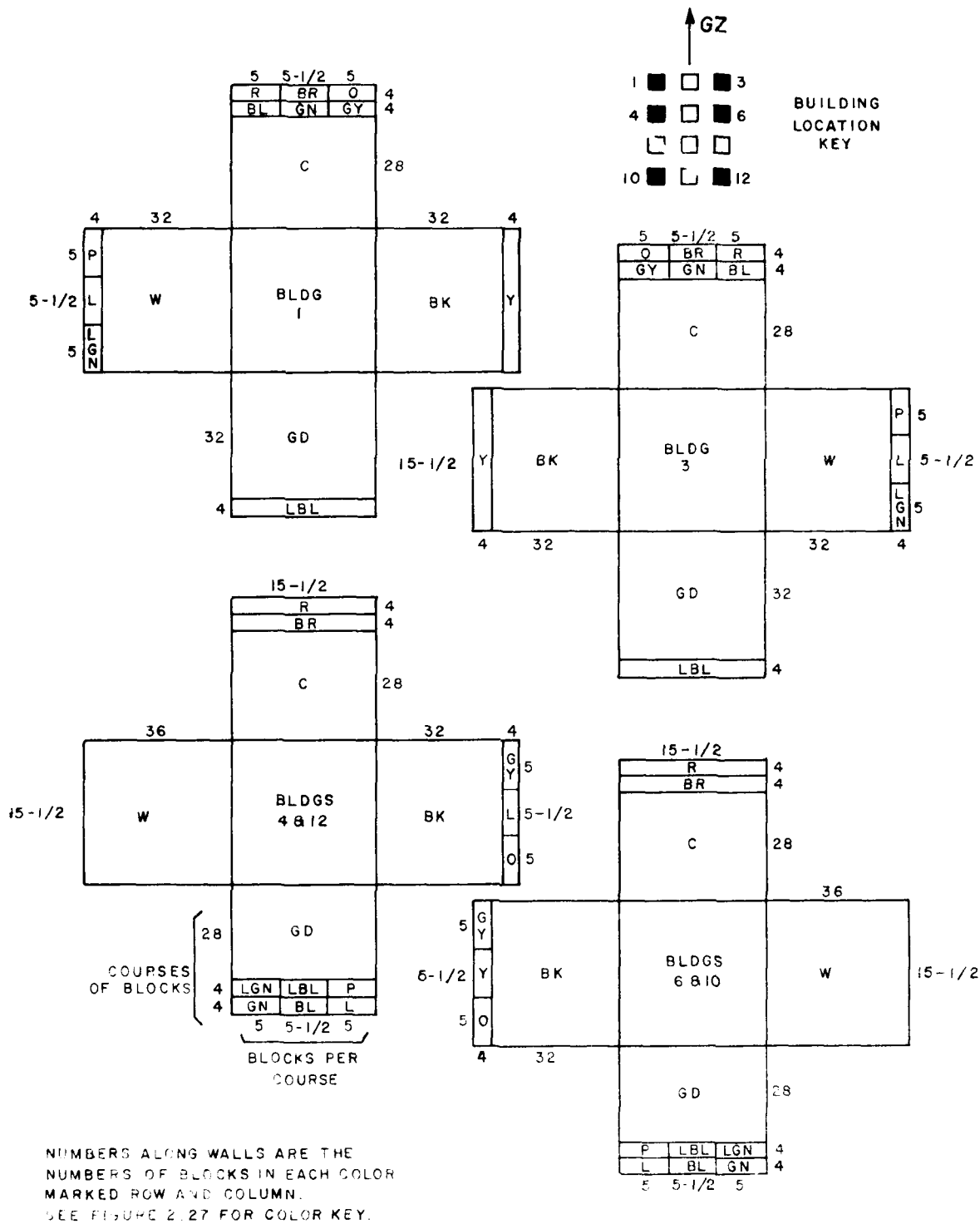


Figure 2.28. Wall-block color arrangements used in the 12-building White Sands complex.

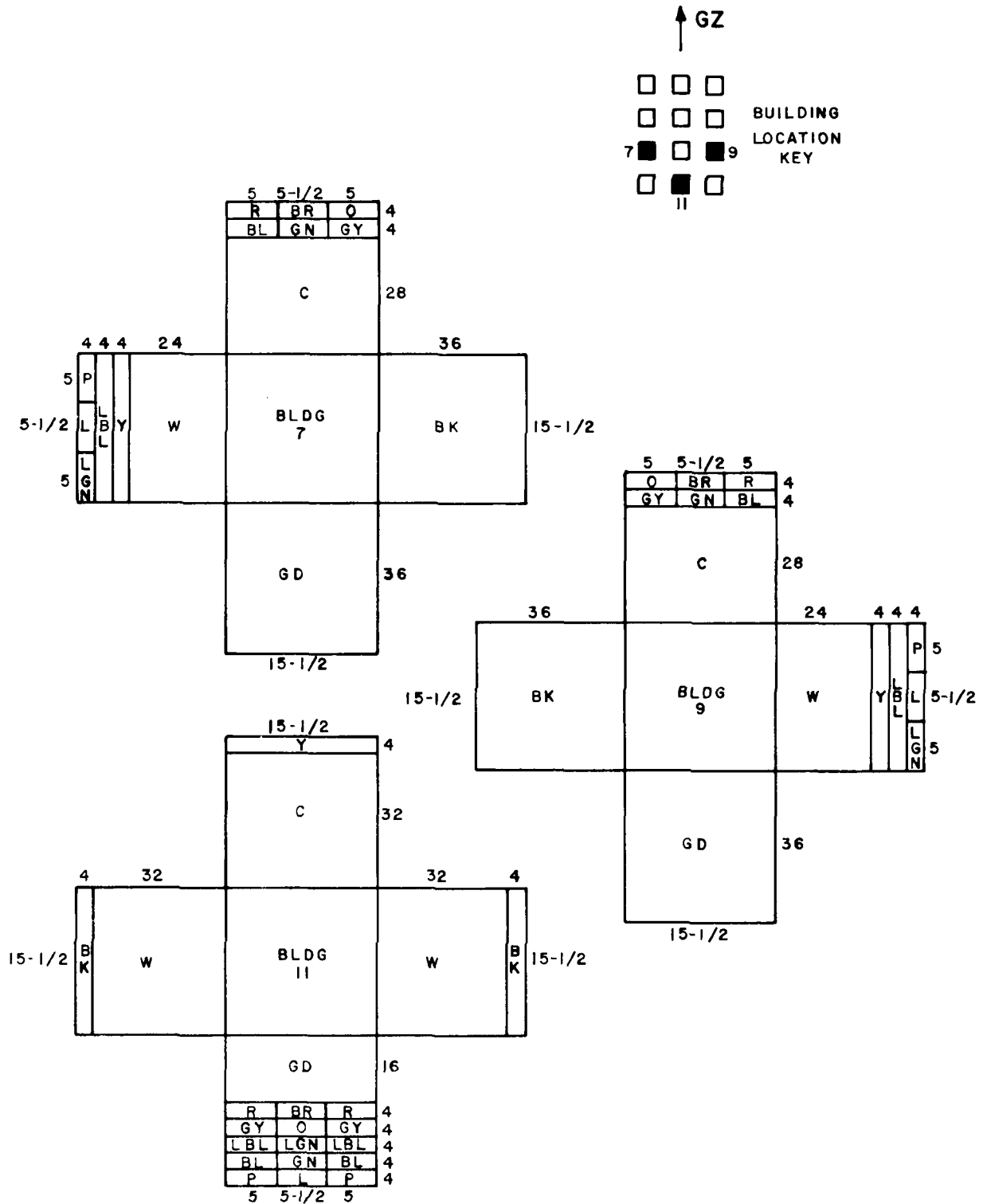


Figure 2.28. Wall-block color arrangements used in the 12-building White Sands complex (continued).

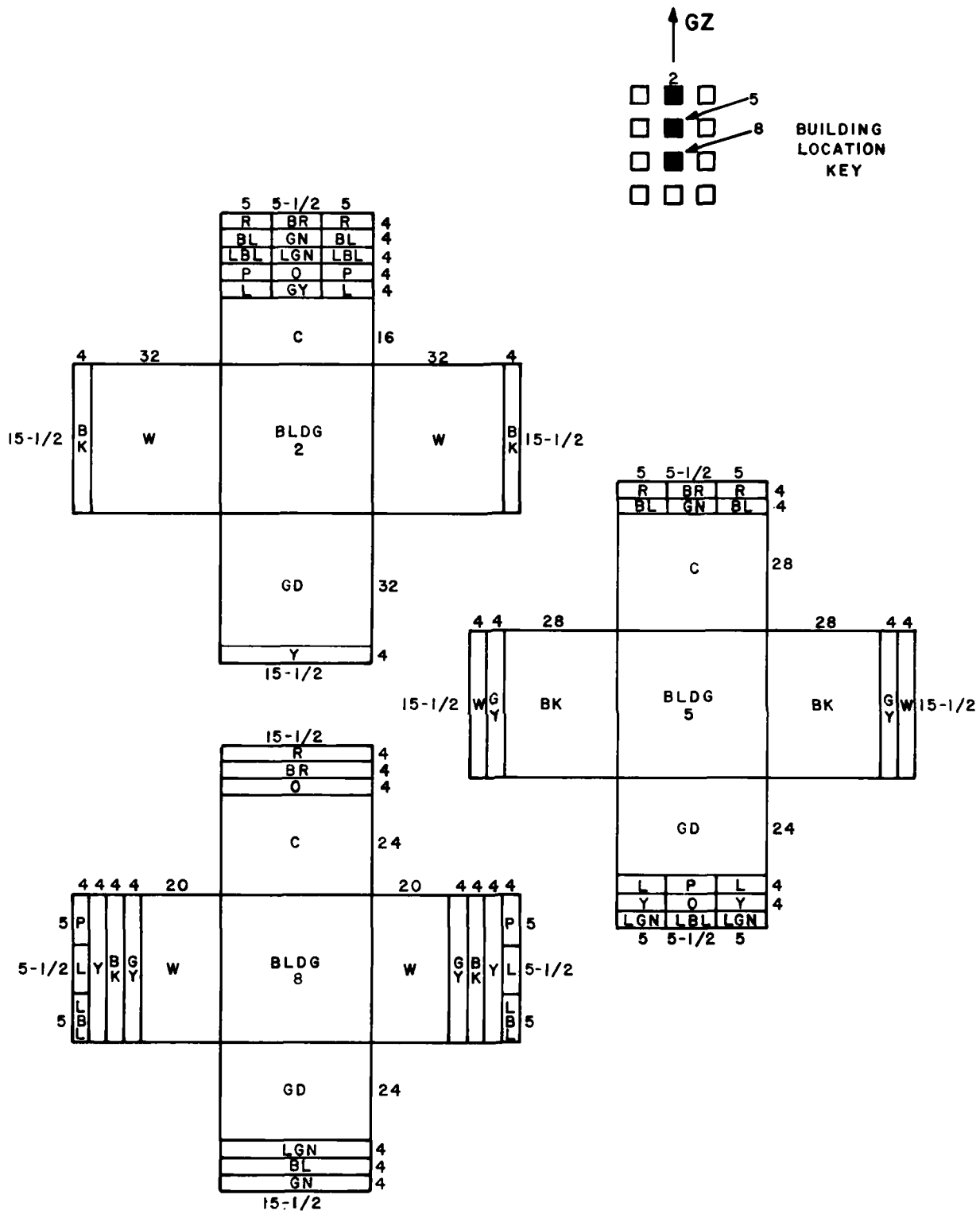


Figure 2.28. Wall-block color arrangements used in the 12-building White Sands complex (continued).

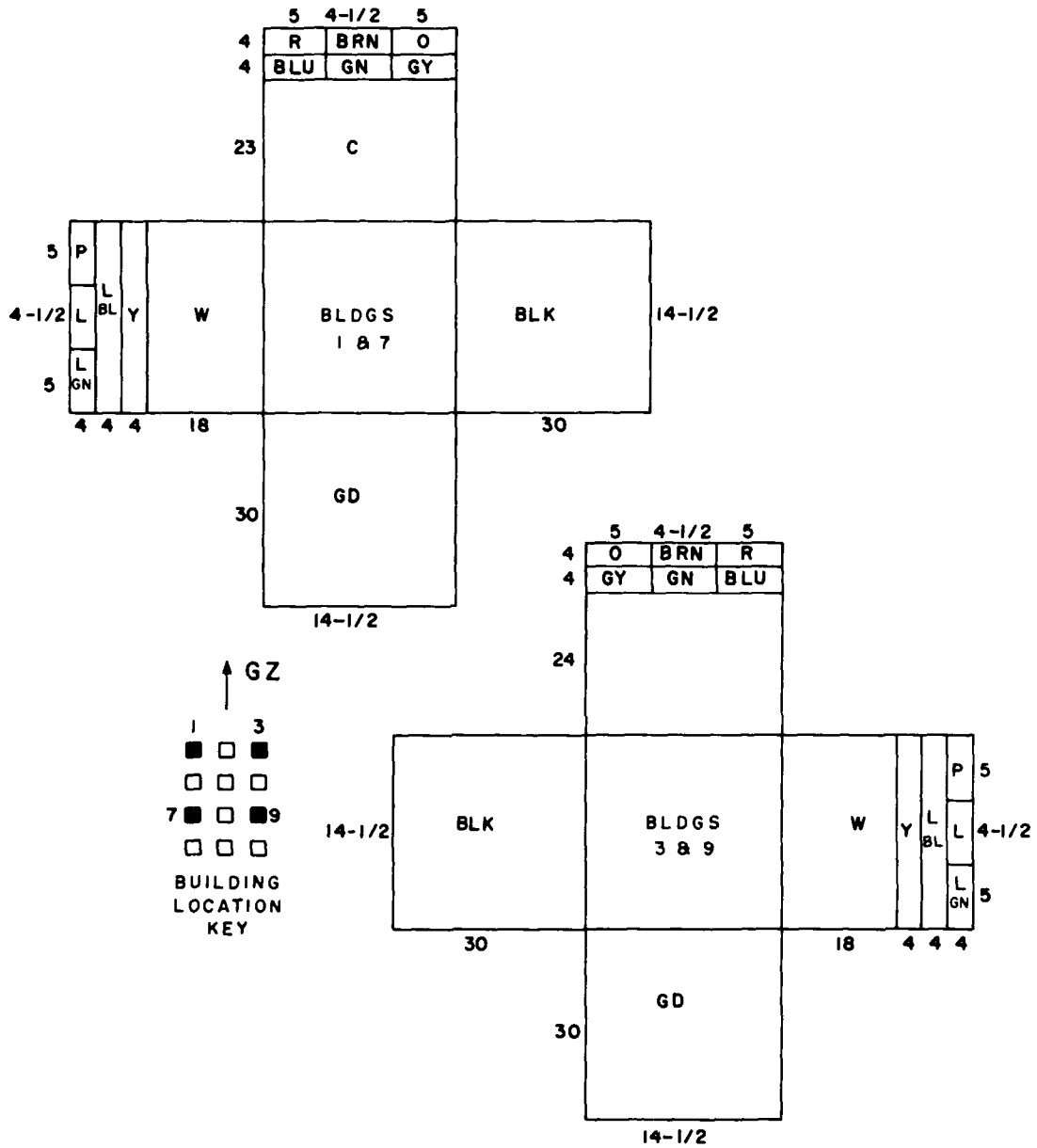


Figure 2.29. Wall-block color arrangements for the 1/120-scale PRAIRIE FLAT buildings.

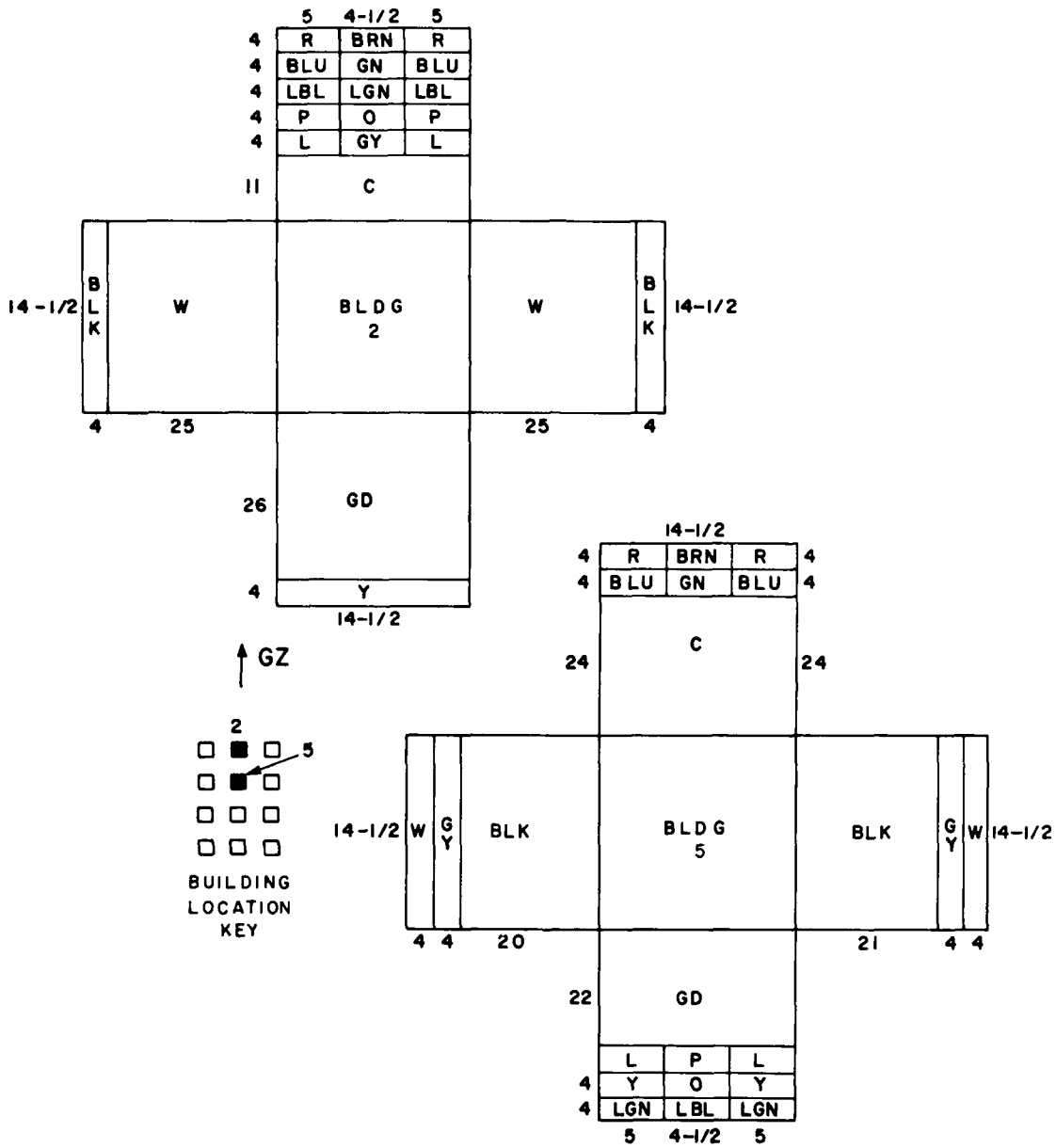


Figure 2.29. Wall-block color arrangements for the 1/120-scale PRAIRIE FLAT buildings (continued).

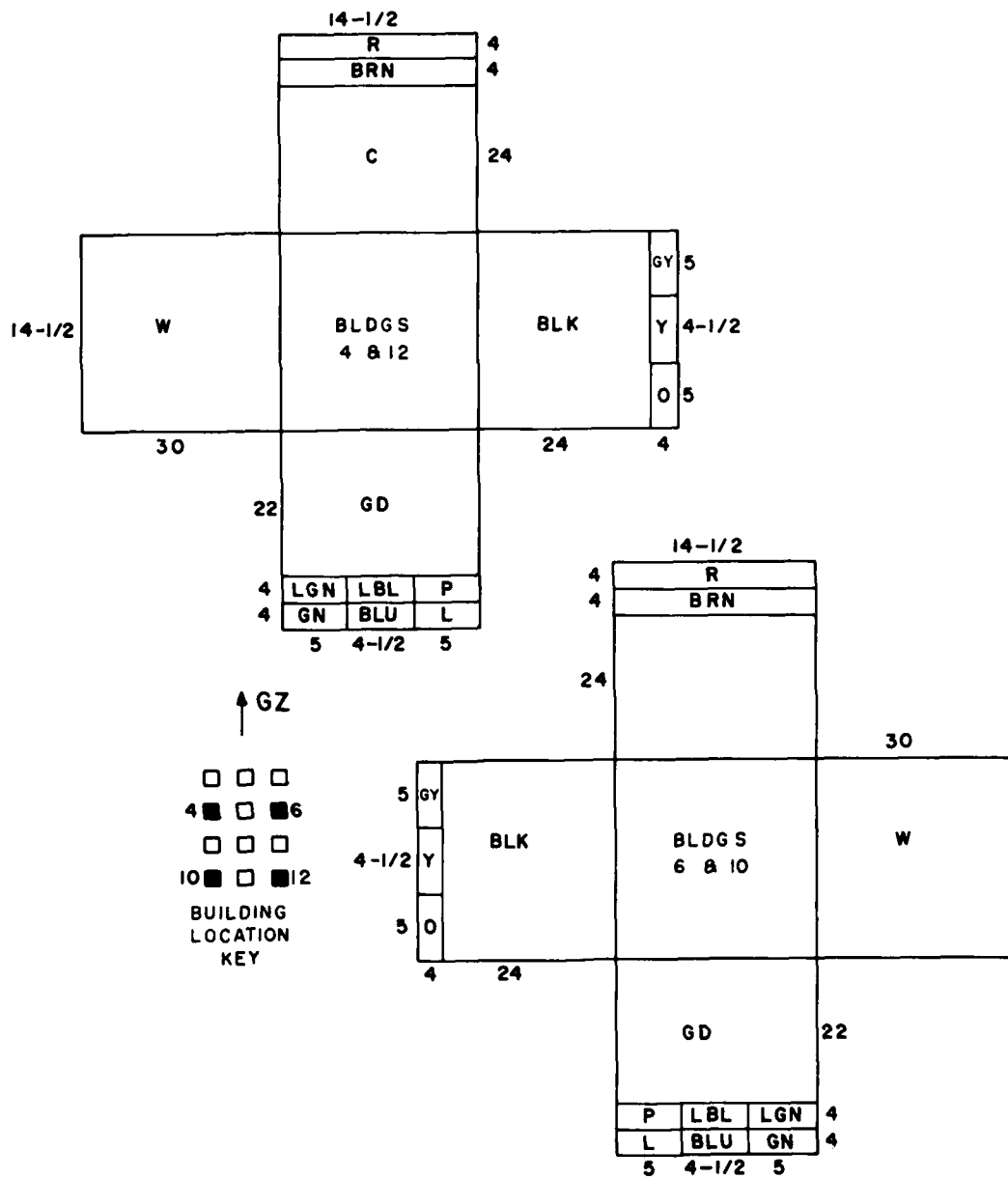


Figure 2.29. Wall-block color arrangements for the 1/120-scale PRAIRIE FLAT buildings (continued).

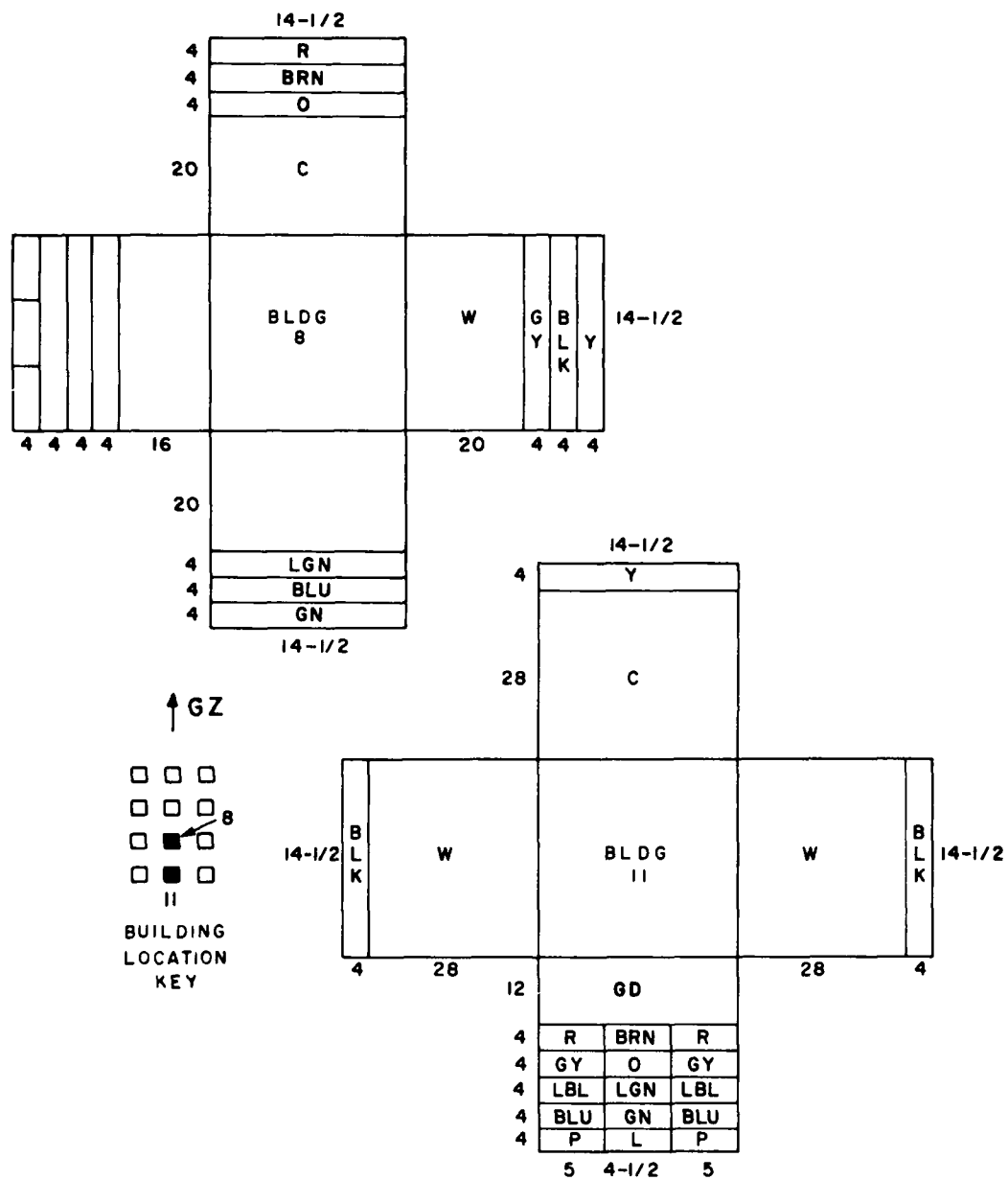


Figure 2.29. Wall-block color arrangements for the 1/120-scale PRAIRIE FLAT buildings (continued).

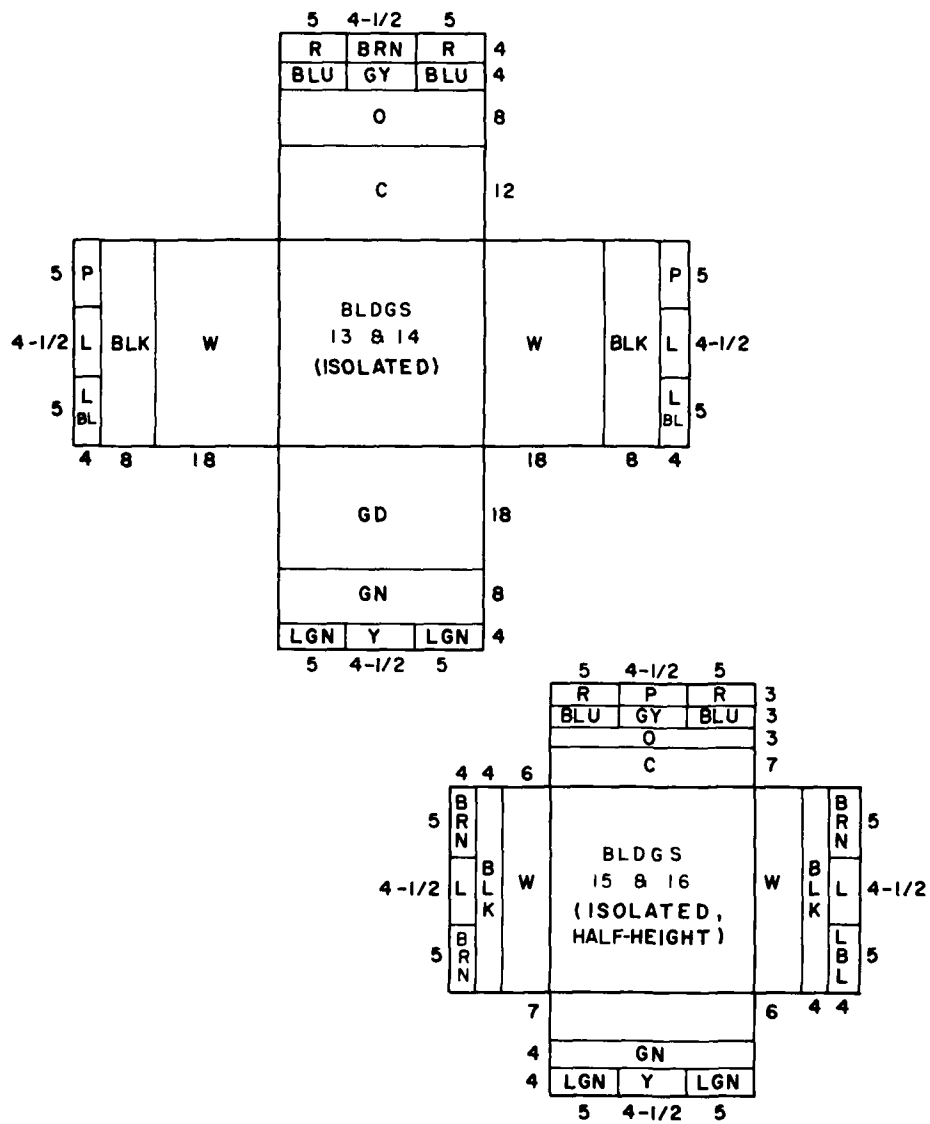


Figure 2.29. Wall-block color arrangements for the 1/120-scale PRAIRIE FLAT buildings (continued).

A new technique was used for the 1/8- and 1/20-scale buildings in PRAIRIE FLAT. At these sites the pad and adjacent area were covered with plastic sheets as soon after the shot as possible. The sheets were held down with sandbags. Pieces that fell beyond the extent of the sheets were weighted down with bricks and whatever else happened to be handy. The debris was logged as it was uncovered; the unlogged debris, therefore, remained protected until its turn came to be identified.

The same procedure was used in DIAL PACK -- with good results. Very high winds came up after the blast, which would have been particularly damaging to the debris deposited on the elevated portions of the pads, had not the plastic sheets been used.

## Chapter 3

### DISTRIBUTION OF DEBRIS

The way that elements of the model buildings were carried and distributed by the scaled-down blast waves provided information useful in predicting how real buildings would be affected in an actual attack. This chapter explores the patterns of distribution — how far and in what directions the blast waves carried the blocks, panels, rafters, and other model-building elements that became debris.

Each building element was coded in some way (by color, for example) so that its building of origin and position within that building could be determined after it had been blown free. The terminal position of each piece of debris was fixed by an x-y or alphanumeric grid at each test site, and individual x-y coordinate systems determined each element's position with respect to its building of origin. The x coordinate was defined as the "tangential" distance (oriented in a direction tangent to the blast wave), and the y coordinate was defined as the "radial" distance (oriented along the radius of the blast wave).

#### 3.1 Data Presentation

The appendices to this report contain all the data collected in the study of debris distributions. This chapter includes samplings of these data where they are appropriate. Four ways of representing data are used here, described briefly below.

##### 3.1.1 Bar Graphs

Bars are used to represent the number of pieces of debris found between incremental values of x and y. Each bar represents a certain range of x or y values — for example, all the pieces found between y and y+1 feet in a radial direction from the origin for a particular model building. All debris may be tabulated together, or separate graphs may be used to portray debris distributions from different parts of a building.

##### 3.1.2 Statistical Representations

The statistical graphs show the mean and the standard deviation of each distribution as points along a horizontal. Again, the distribution is in terms of x or y distances from the building of origin. The width of the horizontal line indicates the extent of the distribution in the x or y direction — except for anomalies, as will be explained.

### 3.1.3 X-Y Plots

Plan views of the various model configurations and their associated x-y grids include, in each grid square, the number of pieces of debris found in that square. In instances where it is useful to study the distribution of debris from only a portion of a building, a separate x-y plot is provided for that part of the distribution.

### 3.1.4 Terminal-Position Mapping on Representations of Building Surfaces

Some of the figures show a square or rectangle that represents a model-building surface. This can be a wall, a roof, or an interior floor. On this representation the terminal x-y coordinates of each dislodged element of that surface are mapped in the element's position of origin. For walls, separate maps are presented for the tangential (x) and radial (y) coordinates; for roofs and floors, each map shows both x and y coordinates.

## 3.2 Block Buildings, 1/120-Scale (SNOWBALL and PRAIRIE FLAT)

The 1/120-scale buildings in Operation SNOWBALL were arranged in a 40-building complex along with one isolated building. The model construction is described in Section 2.2.1, and the layout is shown in Figure 2.1. Following the test blast the buildings appeared as shown in Figure 2.5.

In Event PRAIRIE FLAT the 1/120-scale buildings consisted of a 12-building complex and four isolated buildings. (See Section 2.2.6.) The model layout is shown in Figure 2.6.

### 3.2.1 Distribution of Block Debris from Isolated Buildings

For the isolated SNOWBALL building, the ground distribution of blocks is shown in the x-y plot of Figure 3.1. The grid represents the one-foot grid actually used. Each square in this figure contains three numbers: the top figure gives the number of blocks from the front wall that were collected in that square; the middle figure gives the number of blocks from the two side walls; and the bottom figure gives the number of blocks from the rear wall. Figures 3.2, 3.3, 3.4, and 3.5 show similar x-y plots for the four isolated buildings tested in PRAIRIE FLAT.

Some blocks — from the SNOWBALL isolated building and from the rear full-height building in PRAIRIE FLAT — traveled up to nine feet in the direction of the blast wave from their origins; this is equivalent to an 1100-foot distance for full-size debris. The test results suffered from considerable variability, however: blocks from the front full-height isolated building in PRAIRIE FLAT traveled a maximum radial distance of only five feet. (The front full-height isolated building may have been exposed to a localized blast anomaly or may have collapsed partially before the test blast took place.)

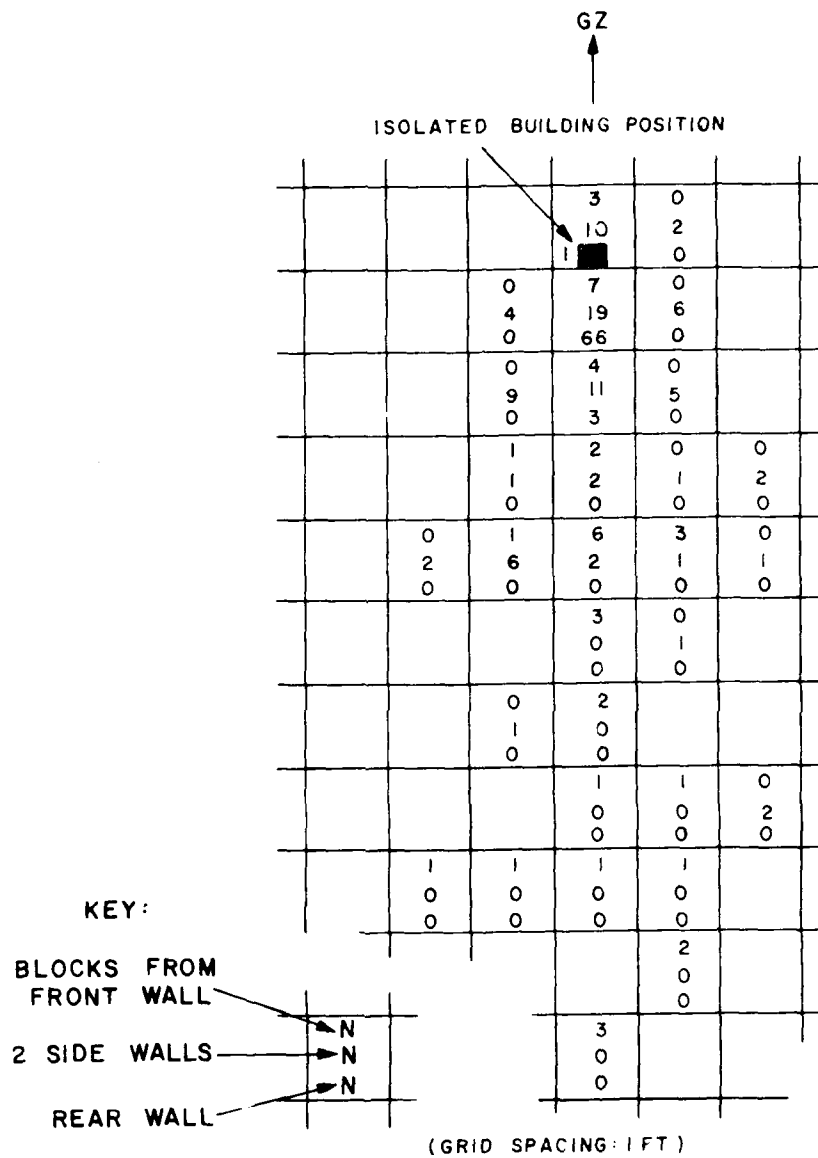


Figure 3.1. Block distribution from SNOWBALL  
1/120-scale isolated block building.

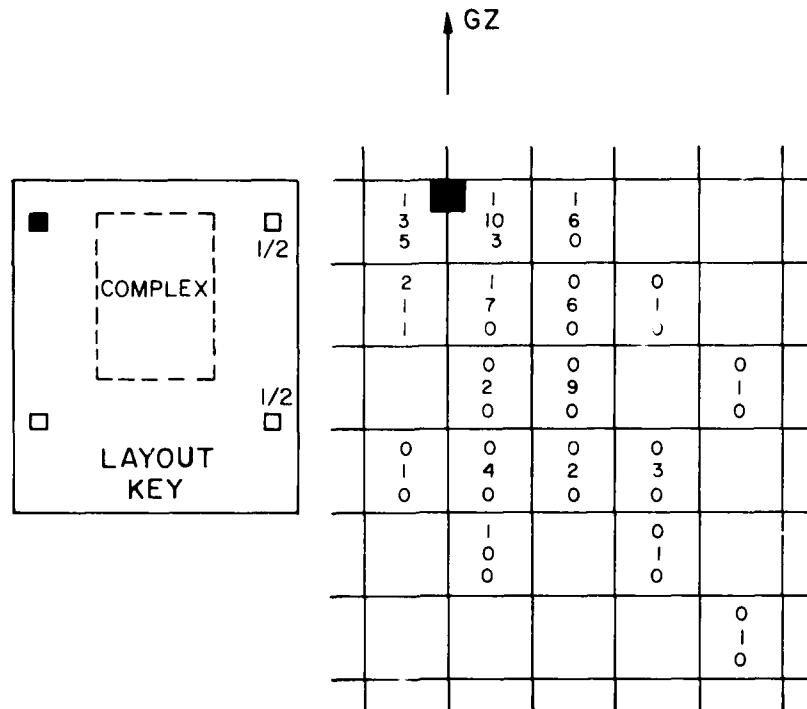


Figure 3.2. Block distribution from front full-height 1/120-scale isolated building; PRAIRIE FLAT.

The blast wave would be expected to affect the lower half-height buildings less than the full-height buildings. Results from the two half-height isolated buildings in PRAIRIE FLAT, Figures 3.4 and 3.5, do show greater similarity with each other: both distributions were lower than those from the rear full-height isolated building and the SNOWBALL isolated building, but not as low as that from the front full-height isolated building.

### 3.2.2 Distribution of Block Debris from Buildings in Complexes

The SNOWBALL complex comprised five columns of eight buildings each. Figure 3.6 is a collection of bar graphs, one for each building, showing the number of blocks found at various x distances — distances tangent to the blast wave — from their buildings of origin. Because the complex was centered with respect to ground zero, the figure has been simplified by symmetry: The right column, labeled "III," corresponds to the eight-building center column of the complex. However, column I in the figure represents the averaged data from corresponding buildings in the first and fifth columns of the complex; likewise, column II represents averaged data from corresponding buildings in the second and fourth columns of the complex. The bar graph pertaining to the isolated building, discussed in Section 3.2.1, is included at the left.

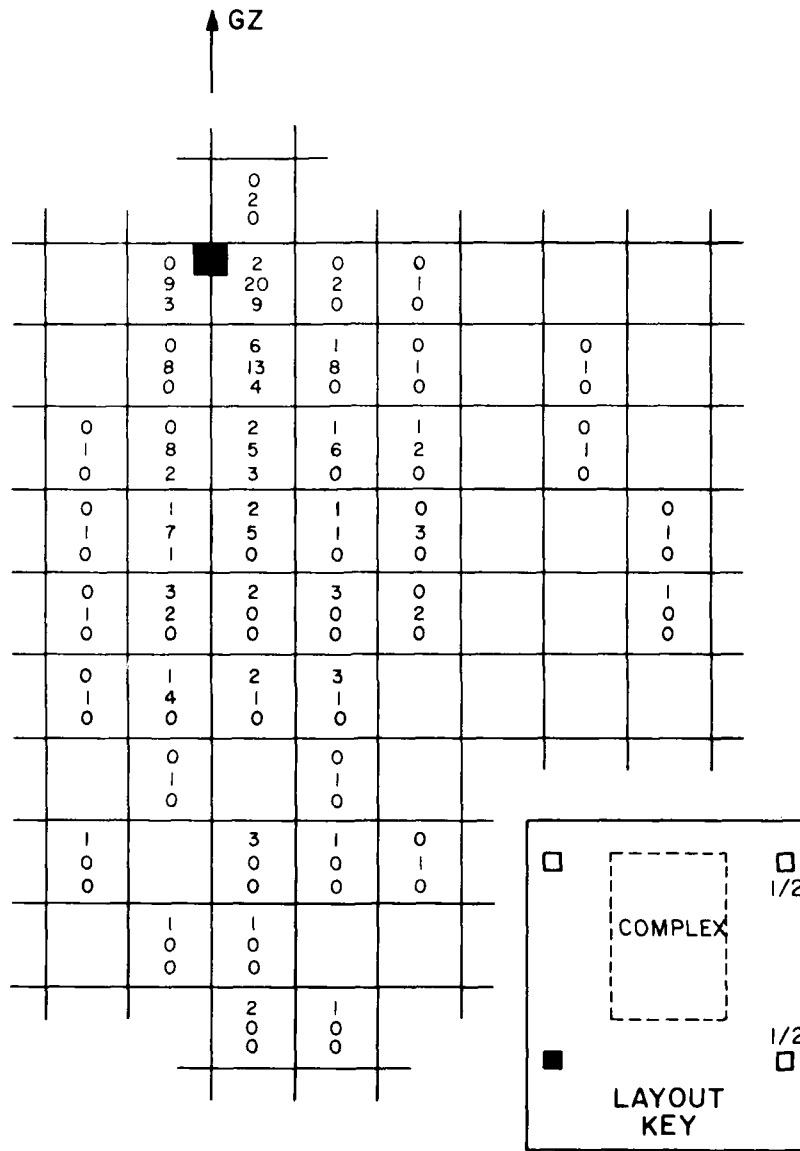


Figure 3.3. Block distribution from rear full-height 1/120-scale isolated building; PRAIRIE FLAT.

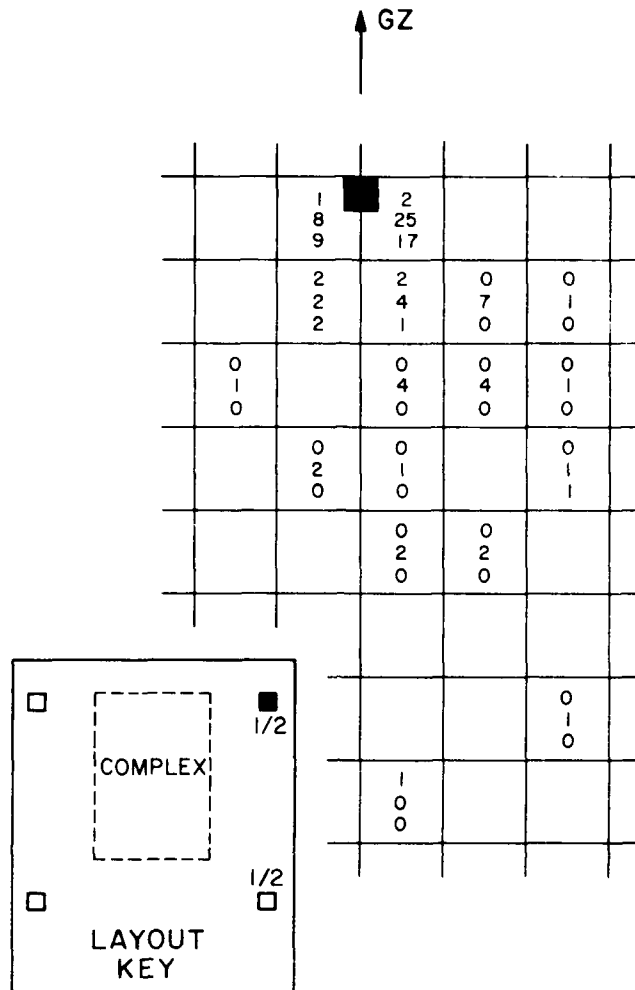


Figure 3.4. Block distribution from front half-height 1/120-scale isolated building: PRAIRIE FLAT.

Figure 3.7 is the companion to Figure 3.6. In this case the bar graphs show the numbers of blocks found at various y distances — distances along the radius of the blast wave — from their buildings of origin. The format is reoriented but follows the same logic as that of Figure 3.6.

Figures 3.8 and 3.9 show similar bar graphs, which, in these cases, represent the tangential and radial distributions of blocks from each of the 12 buildings in the PRAIRIE FLAT complex. The figures include bar graphs for each of the four isolated buildings as well. Blocks originating with models in the front row of the complex traveled the greatest distances, both tangentially and radially. The maxima, however, fall short of those associated with most of the isolated buildings. Debris from the latter was able to travel unobstructed, while debris from buildings in the

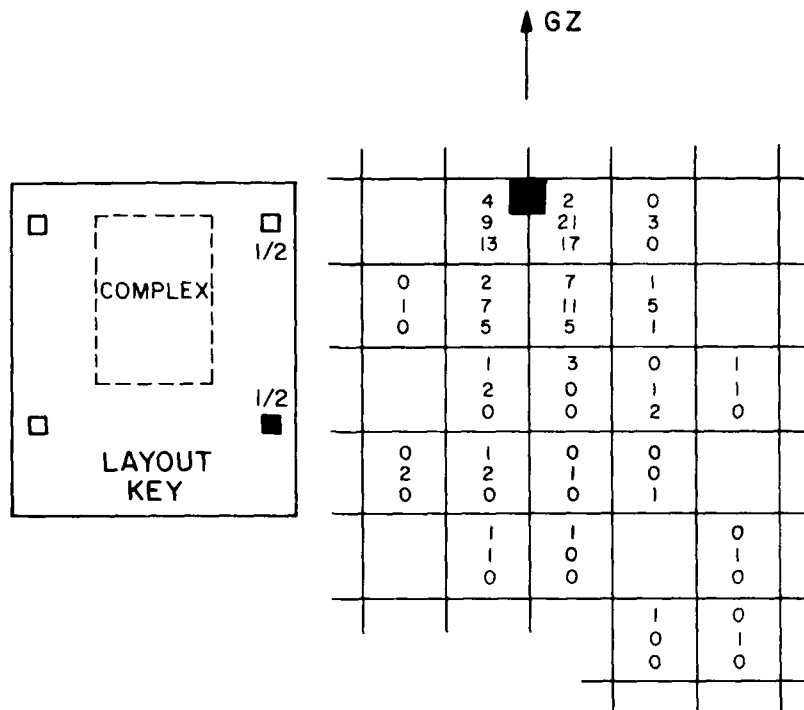
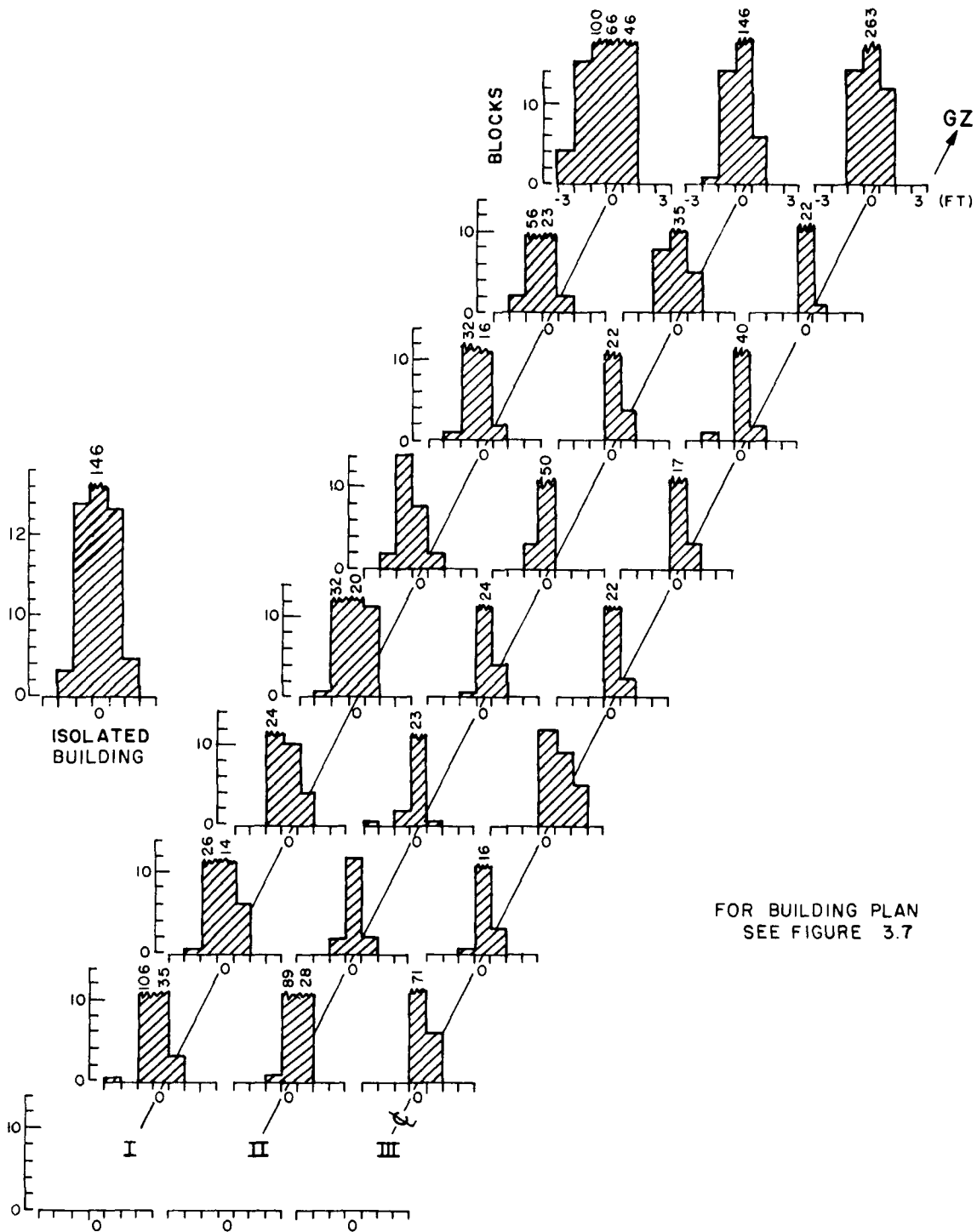


Figure 3.5. Block distribution from rear half-height 1/120-scale isolated building; PRAIRIE FLAT.

complex was obstructed by other debris and by portions of models still standing. (The blast wave itself must have been modified by its passage over the complex.) In both SNOWBALL and PRAIRIE FLAT the buildings in the interior of the complex, being the most shielded, suffered the least.

Most real buildings, however, would be leveled by the 18-psi peak overpressure simulated in these tests. In a real situation, therefore, destruction would be so extensive that the shielding of some buildings by others would not be as significant.

The one-foot grid used on the concrete pad for the SNOWBALL experiment was subdivided into four-inch squares within the area of the 40-building complex, so that the pattern of debris distribution within the complex could be studied in greater detail. Figure 3.10 consists of bar graphs showing the tangential distributions of blocks from six buildings in the SNOWBALL complex. Again, blocks found within four inches of their wall of origin were not counted; those blocks noted at zero distance tangentially, for example, had traveled at least four inches radially. The upper left quarter of the figure shows the number of blocks from the front, rear, and side walls for two front-row buildings versus the tangential distance, in four-inch grid squares, from the building; data for one building is given above the distance scale, the other below. The distributions at corresponding distances are



FOR BUILDING PLAN  
SEE FIGURE 3.7

Figure 3.6. Tangential block transport, SNOWBALL 1/120-scale buildings: abscissa represents grid squares to right and left of building with respect to building centered at 0; ordinate represents blocks counted.

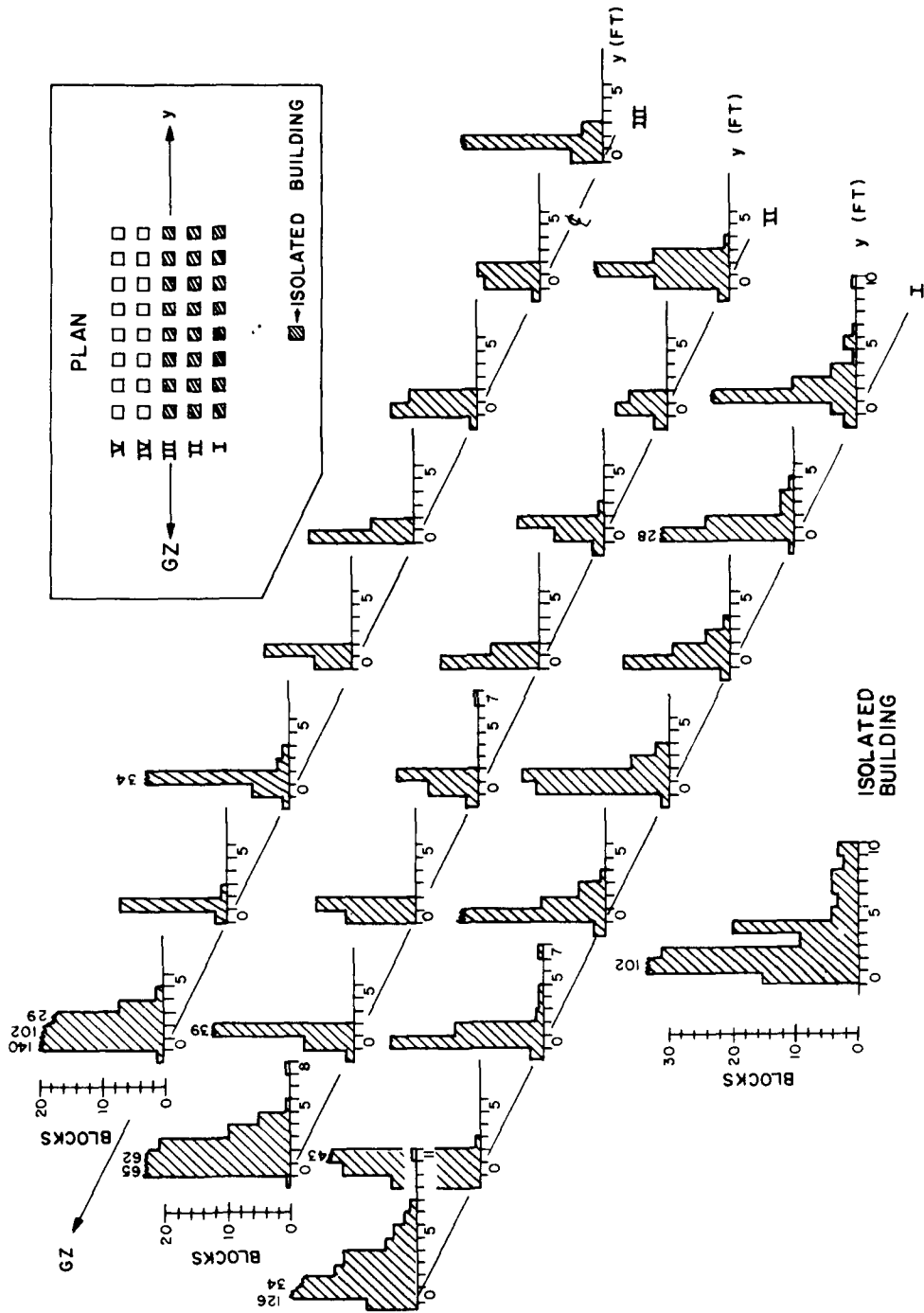


Figure 3.7. Radial block transport, SNOWBALL 1/120-scale buildings: abscissa represents grid squares along column line with respect to building centered at 0; ordinate represents blocks counted.

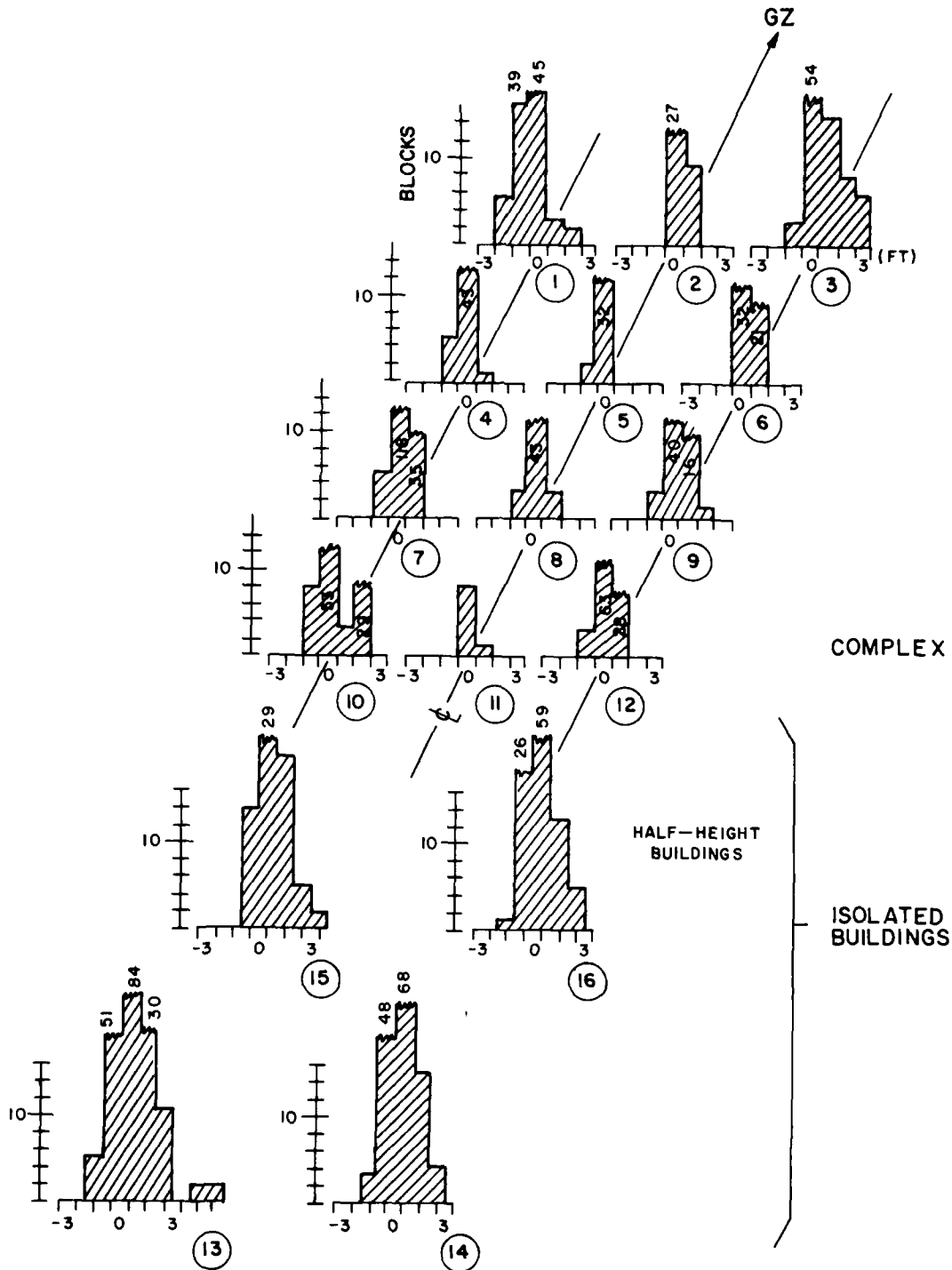


Figure 3.8. Tangential block transport, PRAIRIE FLAT 1/120-scale buildings: abscissa represents grid squares to right and left of building with respect to building centered at 0; ordinate represents blocks counted.

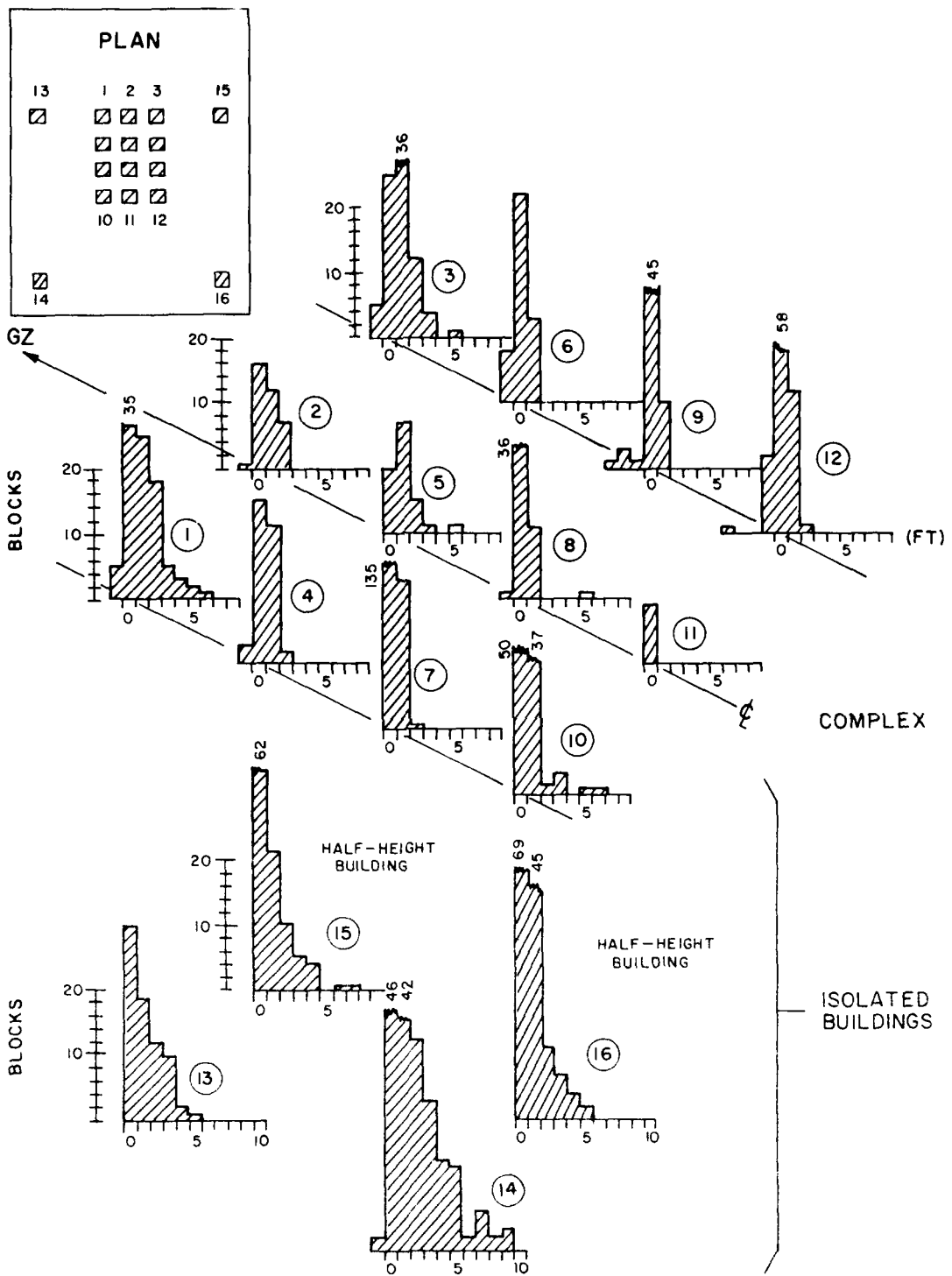


Figure 3.9. Radial block transport, PRAIRIE FLAT 1/120-scale buildings: abscissa represents grid squares along column line with respect to building centered at 0; ordinate represents blocks counted.



similar for the two buildings. This is to be expected, since the two buildings were in symmetrical locations. The upper right quarter of the figure presents similar data for the middle building in the front row. The lower half of the figure compares buildings in the fourth row of the complex; again, the effect of symmetry shows in the bar graphs for the buildings in the second and fourth columns. Notice, however, that the transport of blocks is strikingly lower for these buildings somewhat back in the complex (i.e., the fourth row) compared with the transport of blocks from the buildings at the front of the complex.

Figure 3.11 compares radial block distributions — i.e., distributions with respect to grid squares in the direction of the blast wave — for the same six buildings. The same effects of symmetry and greatly reduced block transport from interior buildings are clear in these bar graphs.

The information presented in this chapter on block distribution is only a portion of the data collected. A complete tabulation is given in Appendix A.

### 3.2.3 Distribution of Roof Debris from Isolated Buildings

The roofs of the model buildings in Operation SNOWBALL consisted of panels simulating rectangular sheets of plywood and wood strips simulating rafters. Roofs of the 1/120-scale PRAIRIE FLAT models were similar but contained more panels weighted down with washers.

Figure 3.12 shows plan views of the roof-debris distributions from the isolated SNOWBALL building and two of the isolated 1/120-scale PRAIRIE FLAT buildings, one being a half-height model and the other a full-height model. Only those panels shown shaded in the roof diagrams were collected; the others were blown away before the blast by ambient winds. The roofs of the SNOWBALL buildings were damaged extensively this way, as high-speed motion pictures taken during the test indicate: adding the washers as weights in PRAIRIE FLAT saved considerably more of the roof members. (Note the more nearly complete shaded areas on the PRAIRIE FLAT isolated-building roof diagrams.)

The distributions of debris from the PRAIRIE FLAT buildings were considerably more dense than that from the SNOWBALL building, but the maximum distance traveled and the overall spread of debris were similar in all cases. Comparing the data for the full-height and the half-height building of PRAIRIE FLAT indicates that building height had little effect, if any, on roof-debris distribution. Data concerning all four PRAIRIE FLAT isolated buildings are given in Appendix C.

### 3.2.4 Distribution of Roof Debris from Buildings in Complexes

Figures 3.13 and 3.14 show statistical comparisons of the roof-debris distributions from selected buildings in the SNOWBALL and PRAIRIE FLAT



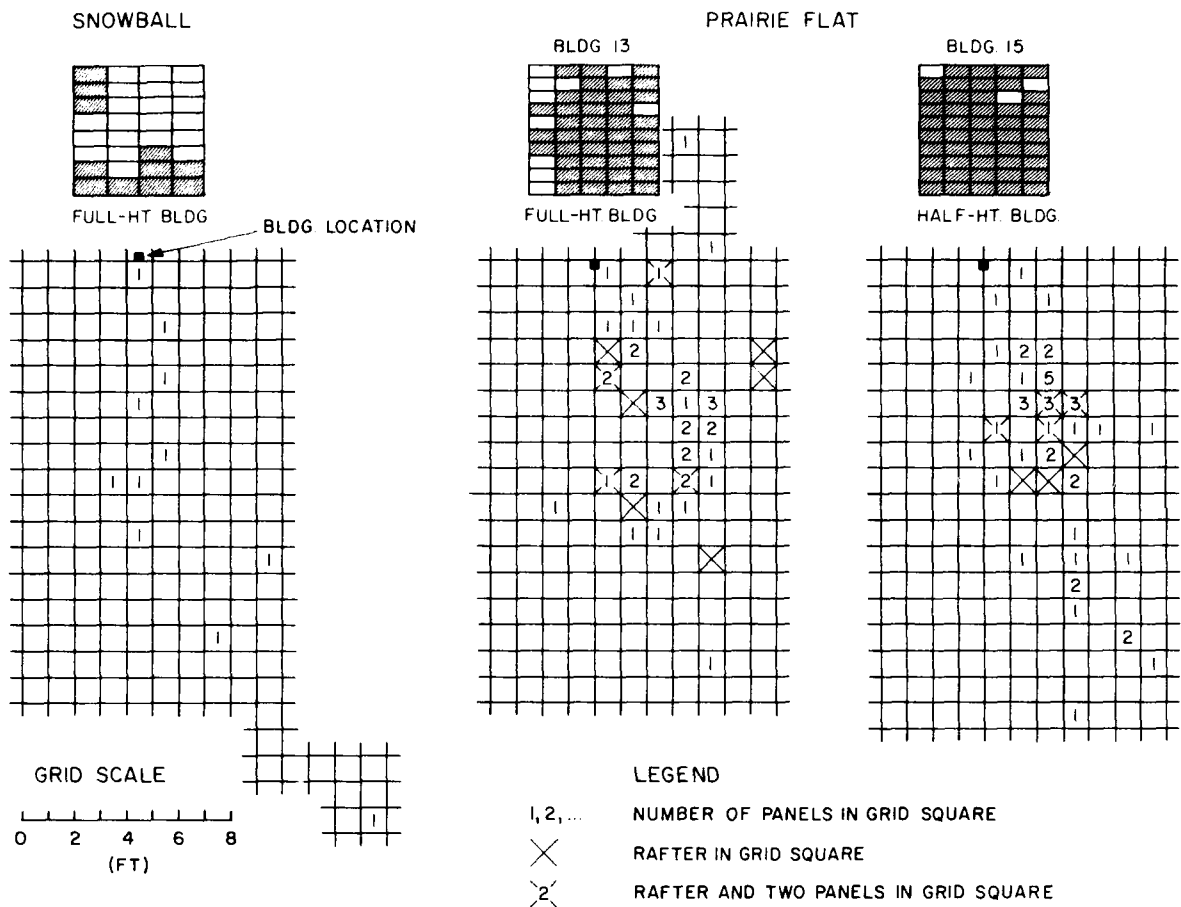


Figure 3.12. Comparison of roof-debris distributions, SNOWBALL and PRAIRIE FLAT 1/120-scale isolated buildings.

complexes — in each case, the buildings in the center column. (Appendices B and C include data for all buildings in these complexes, showing the tangential and radial coordinates of distance traveled superimposed on representations of the corresponding roof panels.)

Figure 3.13 concerns the tangential, or x, components of distances traveled by roof panels from the eight center-column SNOWBALL buildings and the four center-column PRAIRIE FLAT buildings. The buildings are represented at the left. To the right are corresponding straight lines that connect the extremes, along the x axis, at which roof-panel debris from each of these buildings was found. The large vertical mark in each line represents the mean tangential distance traveled, and the two smaller vertical marks to the right and left represent plus and minus one standard deviation from the mean, respectively. The mean values and the standard deviations are given at the right side of the figure.

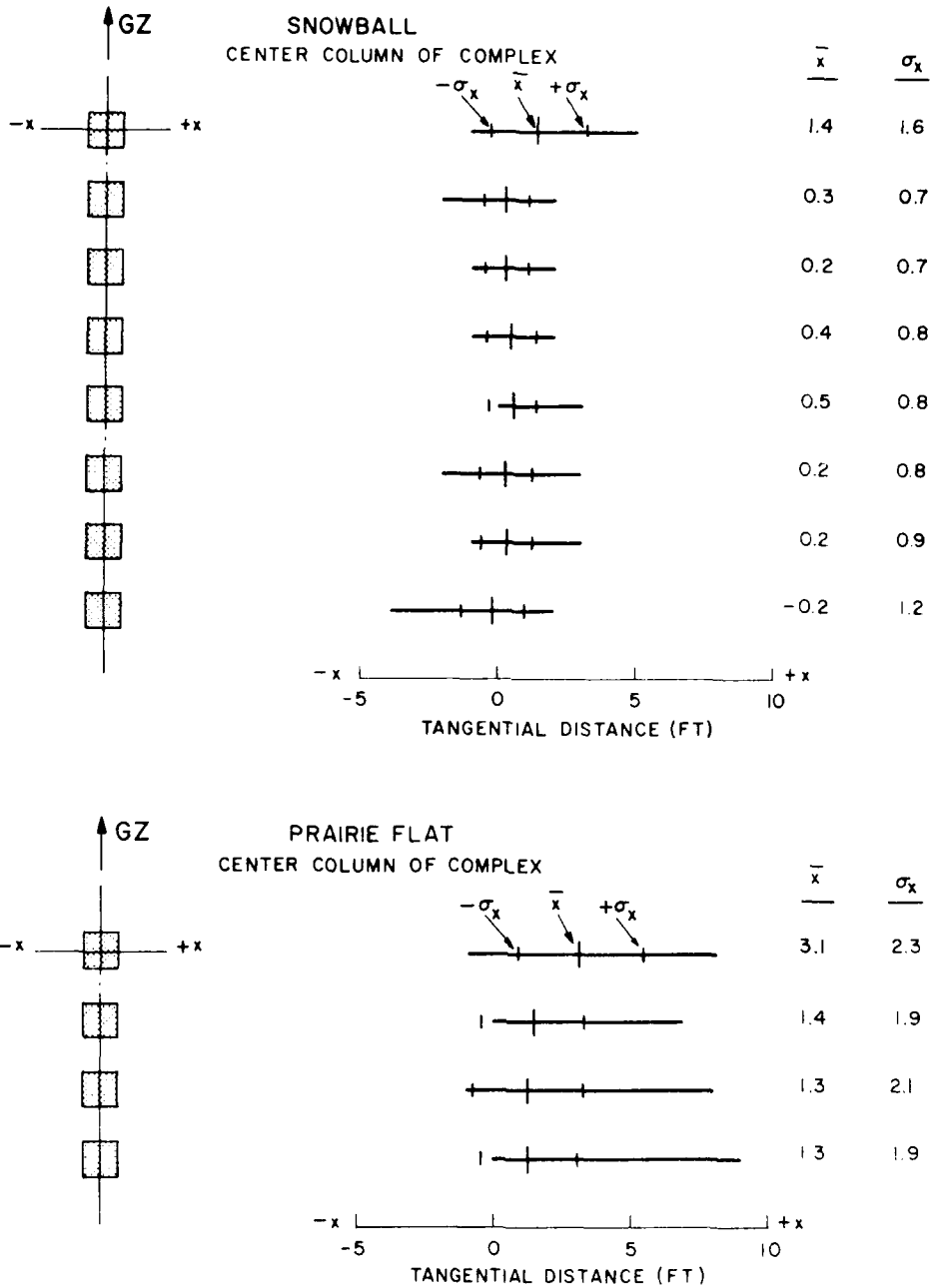


Figure 3.13. Comparison of tangential roof-debris transport, SNOWBALL and PRAIRIE FLAT 1/120-scale buildings from center column of complex.

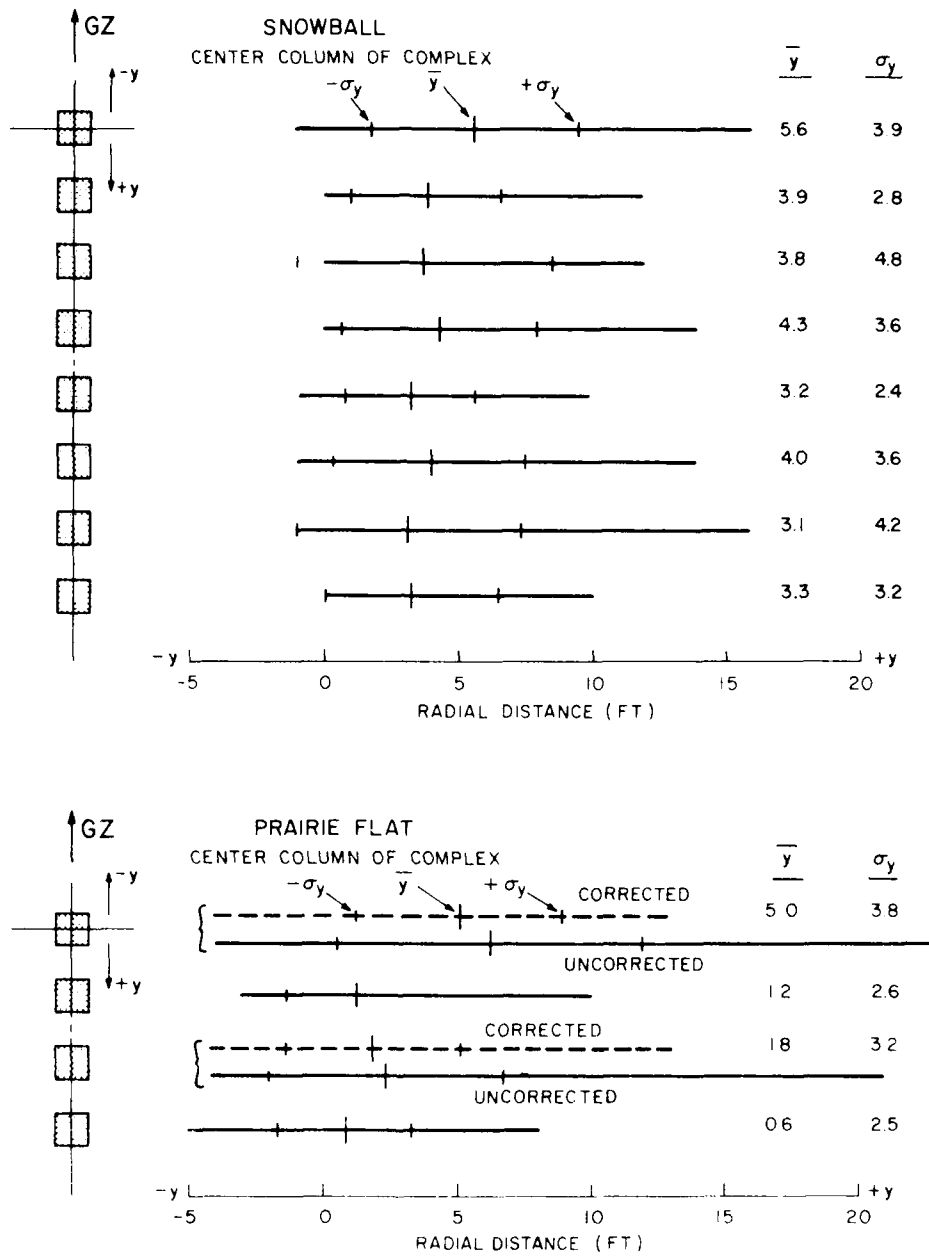


Figure 3.14. Comparison of radial roof-debris transport, SNOWBALL and PRAIRIE FLAT 1/120-scale buildings from center column of complex.



The tangential mean ( $\bar{x}$  in the figure) depends on ambient winds and the direction of the blast. It can vary from test to test, therefore, but should be about the same for all buildings at one test site. Significantly, roof debris from the front building in the SNOWBALL column was distributed over a wider area than debris from the other buildings, and the tangential mean for this building was greater. This indicates that debris was in flight longer than the roof debris from the other seven buildings, for which the statistics all are similar. These trends applied also to the center column of buildings in the PRAIRIE FLAT complex; the values of the means and standard deviations, however, consistently exceeded those measured in SNOWBALL.

Figure 3.14 presents a similar analysis of the radial, or y, components of roof-debris travel from the same buildings. The debris that traveled the greatest distances in the y direction came from the front building in each column; data from the front PRAIRIE FLAT building showed the greatest standard deviation.

Less uniformity was evident in these radial data than was evident in the tangential data. Notice, however, that two sets of statistics are given for the first and third buildings of the PRAIRIE FLAT complex, and that the "corrected" results agree more closely with the results for the second and fourth buildings. Figure 3.15 reveals how and why the corrections were made. The figure gives data pertaining to the radial transport of debris from the three buildings in the front row of the PRAIRIE FLAT complex, the center one being the front building of the column shown in Figure 3.14. Some roof debris from the three front buildings was transported radially more than 20 feet; the big gap between most of the debris and these farthest pieces suggests that the latter probably were blown from their buildings by winds before the blast took place. (This was true also for the third building in the center column, not shown.) The corrected results in Figure 3.14, therefore, simply ignore those pieces of roof debris thought to have been transported by ambient winds rather than by the blast wave.

### 3.3 Larger Models at Low-Overpressure Sites: 1/8-Scale (PRAIRIE FLAT) and 1/33-Scale (White Sands SOTRAN) Buildings

The PRAIRIE FLAT and White Sands SOTRAN events included tests of larger models in high- and low-overpressure environments. Block buildings were used in both events — 1/8-scale in PRAIRIE FLAT and 1/33-scale in White Sands SOTRAN; in addition, 1/8-scale frame buildings were devised and added to one of the low-overpressure PRAIRIE FLAT setups. This section is devoted to a discussion of the low-overpressure sites.

These experiments were designed to simulate the same full-scale, or real, blast conditions with test blasts and the scaling factors discussed in Chapter 1. The

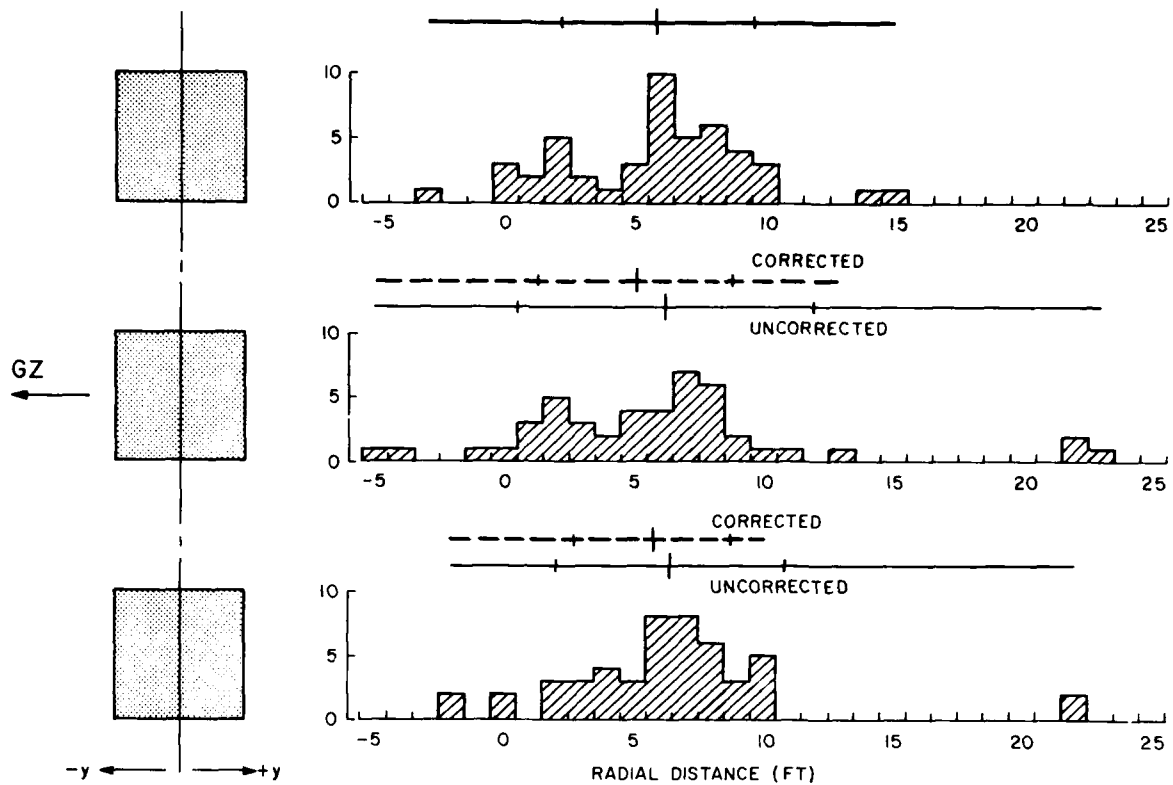


Figure 3.15. Comparison of radial roof-debris transport, PRAIRIE FLAT 1/120-scale buildings from front row of complex.

actual results varied somewhat: In PRAIRIE FLAT the blast being simulated would have had a peak overpressure of 10 psi produced by a 0.07-MT detonation; in White Sands SOTRAN the corresponding values were 17 psi and 0.15 MT.

The PRAIRIE FLAT field layout (Figure 2.15) comprised four isolated block buildings — two of full height, two of half height — and two isolated frame buildings. At White Sands the layout (Figure 2.14) comprised a full-height and a half-height isolated block building and a complex of 12 full-height block buildings.

### 3.3.1 Distribution of Block Debris from Isolated Buildings

Figure 3.16 shows the destroyed full-height isolated building at White Sands, and Figure 3.17 shows one of the destroyed full-height isolated block buildings of the PRAIRIE FLAT event. Debris distributions from selected parts of these buildings are given in Figures 3.18 and 3.19, respectively. An isometric sketch accompanies each plan view, with the relevant wall or walls shown shaded and the portions of the wall or walls from which the debris originated shown black. The figures are drawn so that the simulated full-scale distance dimensions can be compared directly.



Figure 3.16. Full-height isolated block building, 1/33 scale, after detonation:  
White Sands low-overpressure site.

In terms of the full-scale dimensions, the maximum transport of blocks from the side walls of the White Sands building was 120 feet in both directions along the x axis, tangent to the blast wave; that from the corresponding PRAIRIE FLAT building was 100 feet, also in both directions along the x axis. Blocks from the front wall of the White Sands building traveled rearward with the blast wave a distance equivalent to 160 feet in full scale; in PRAIRIE FLAT the corresponding debris traveled the equivalent of 90 feet. The fact that the White Sands SOTRAN blast environment was relatively more severe than the PRAIRIE FLAT environment may account for the greater radial transport of blocks from the White Sands building. Complete block distribution data for these buildings are given in Appendices D and E.

### 3.3.2 Distribution of Block Debris from Buildings in Complex

The complex of twelve 1/33-scale block buildings used in the White Sands SOTRAN event is shown in Figure 3.20 as it appeared after the blast. Data regarding the debris that fell within the complex were not recorded, but the distribution of blocks outside the complex was mapped; the results are contained in Appendix D. Figure 3.21 summarizes some of this information, including a comparison of the debris distribution from buildings in the complex with that of the full-height building.

The figure shows a similarity between the tangential (x) distributions from the side walls of the isolated building and the outside walls of the buildings in the front



Figure 3.17. Full-height isolated block building, 1/8 scale, after detonation:  
PRAIRIE FLAT low-overpressure site.

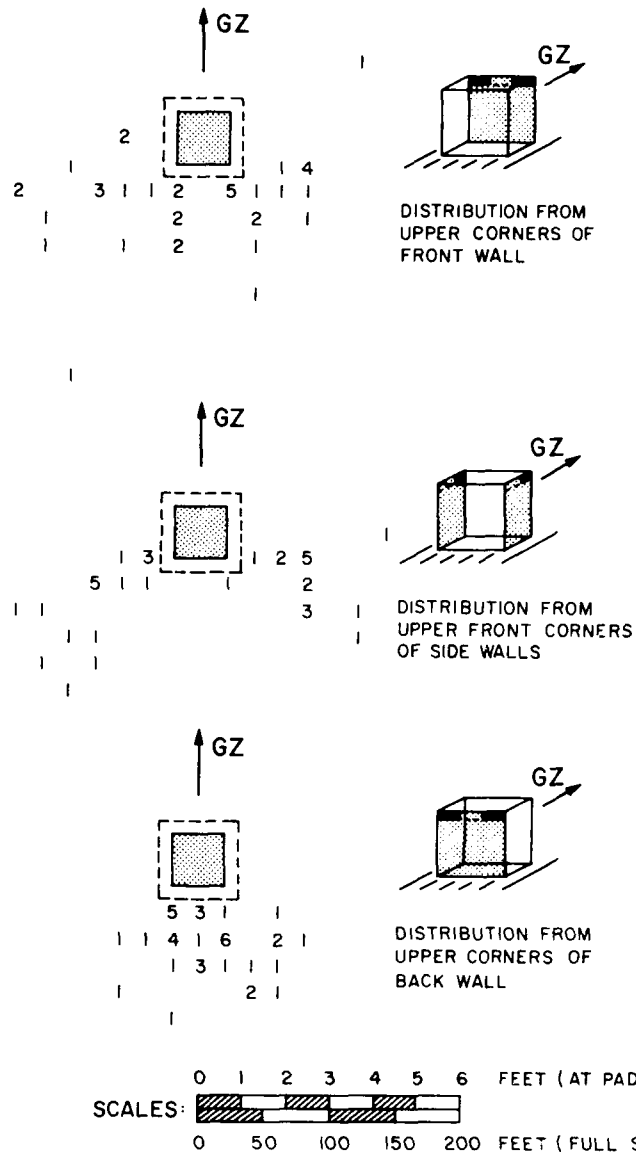


Figure 3.18. Block distribution from selected locations, full-height isolated block building, 1/33 scale: White Sands low-overpressure site.

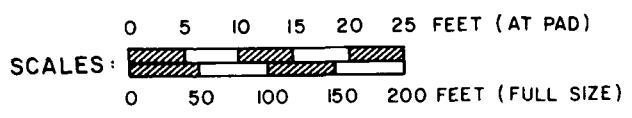
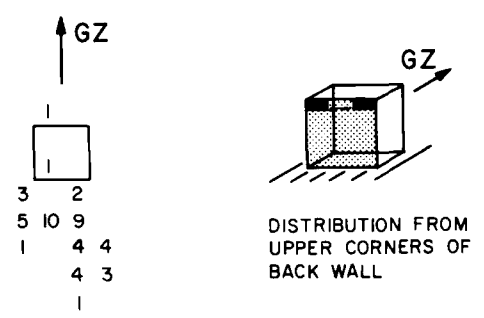
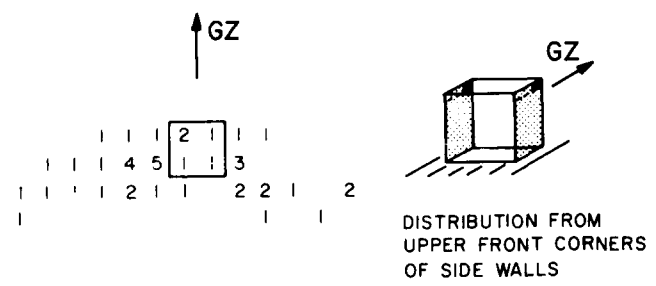
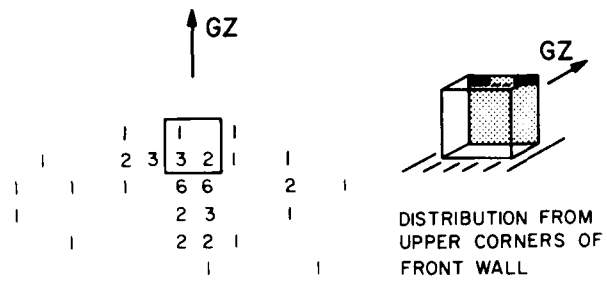


Figure 3.19. Block distribution from selected locations, forward full-height isolated building, 1/8 scale; PRAIRIE FLAT low-overpressure site.

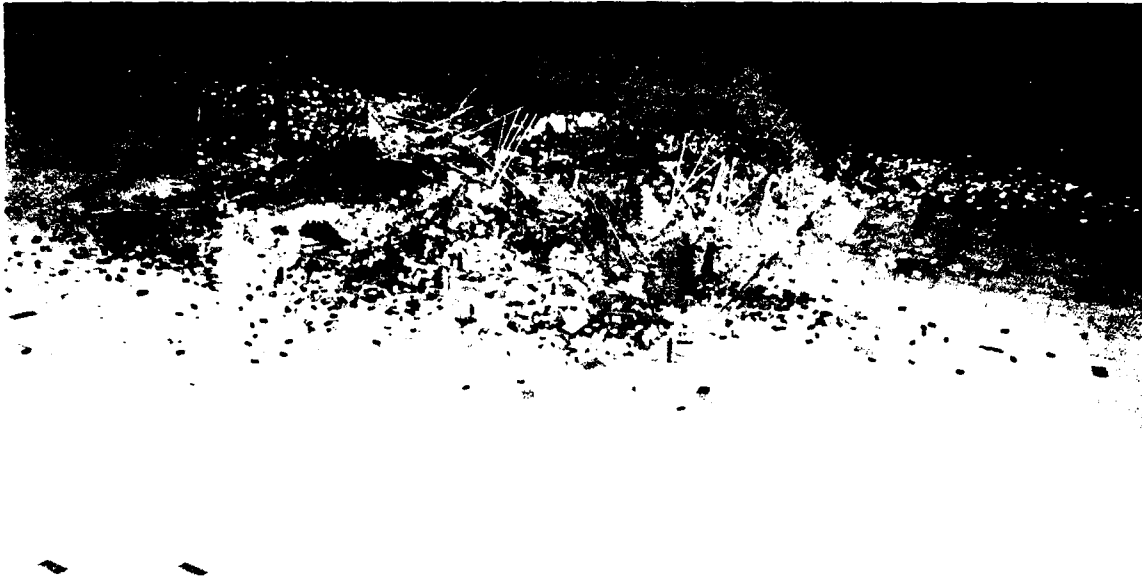


Figure 3.20. Complex of twelve 1/33-scale block buildings after detonation:  
White Sands low-overpressure site.

row of the complex. There also is some similarity between the radial ( $y$ ) distributions from the back wall of the isolated building and the back walls of the buildings in the last row of the complex. It appears that the front row of the complex had some effect in shielding the other buildings, since the tangential distributions from the outside walls of buildings in the second, third, and last rows are markedly lower. However, no such shielding effect seems evident in the distributions from the back walls of buildings in the last row. No data were collected within the complex: no observations are possible, therefore, about the effect of shielding there.

### 3.3.3 Distribution of Roof Debris from Isolated Block Buildings

Figure 3.22 shows statistical comparisons of the roof-panel distributions from the isolated buildings at the PRAIRIE FLAT and White Sands low-overpressure sites. The upper part of the figure compares the tangential ( $x$ ) distances traveled, while the lower part compares the radial ( $y$ ) distances traveled. As in Figures 3.13 and 3.14, straight lines connect the extremes, along the  $x$  or  $y$  axis, along which roof panels from particular buildings were found, the large vertical mark on each line again representing the mean distance traveled and the smaller vertical marks to the right and left representing plus and minus one standard deviation from the mean.



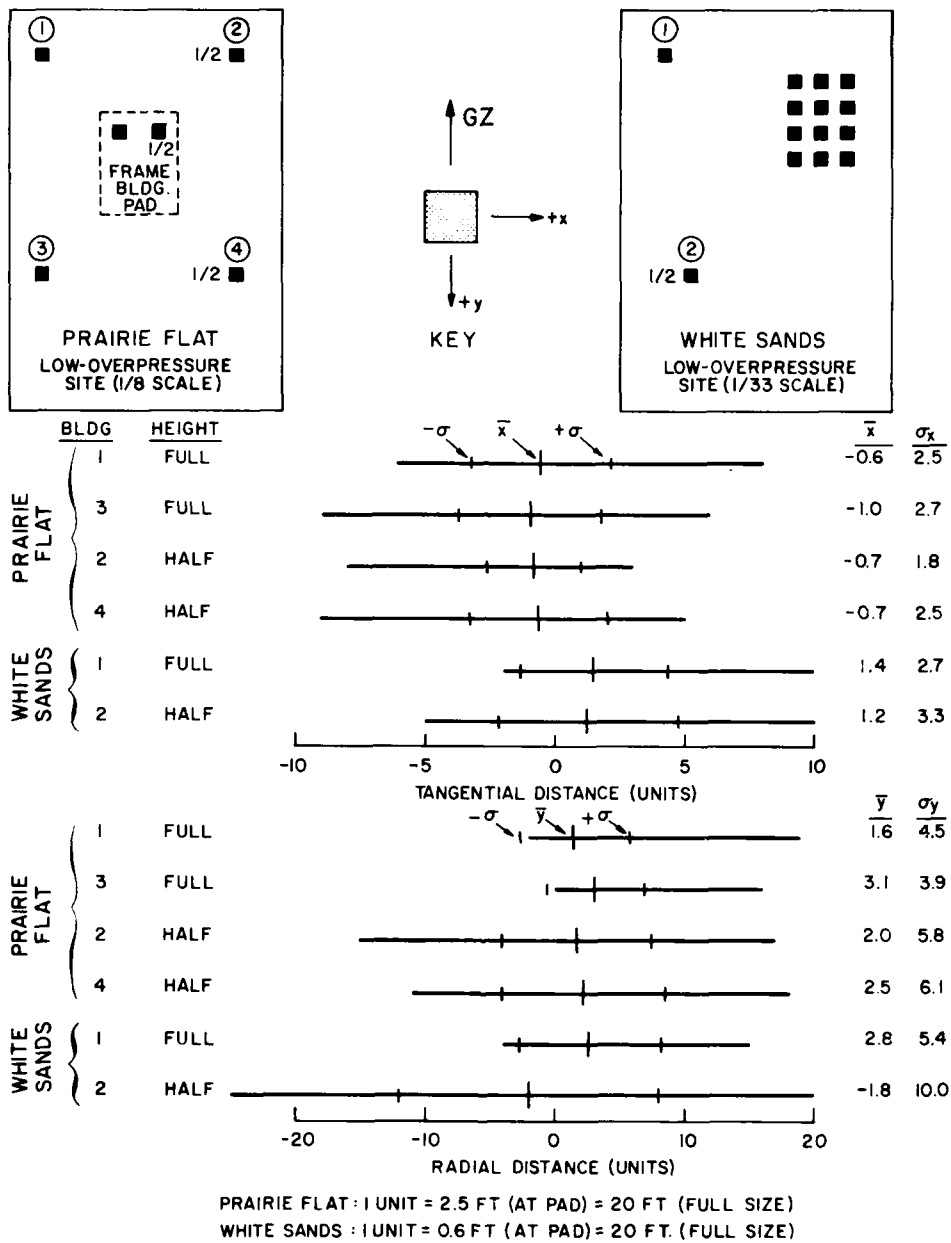


Figure 3.22. Comparison of roof-debris transport from isolated block buildings, PRAIRIE FLAT (1/8 scale) and White Sands SOTRAN (1/33 scale); low-overpressure sites.

respectively. Complete data on the displacement of roof elements are given in Appendices F and G.

Ideally, the tangential distribution should be symmetrical about the radial axis, in which case the tangential mean,  $\bar{x}$ , would be zero. Deviations of  $\bar{x}$  from zero indicate the degree to which the debris distributions have been affected by ambient wind conditions or by blast misalignment. The means for the PRAIRIE FLAT data indicate very calm wind conditions. Standard deviations,  $\sigma_x$ , are similar for the PRAIRIE FLAT and White Sands SOTRAN data.

The radial means,  $\bar{y}$ , are similar for the four PRAIRIE FLAT buildings and the full-height White Sands SOTRAN building, as are the standard deviations,  $\sigma_y$ . The half-height White Sands building has a considerably lower mean and greater standard deviation; however, the sum of the mean and the standard deviation for this building agrees well with those of the other buildings, which indicates that distributions far from the buildings were similar.

#### 3.3.4 Distribution of Debris from 1/8-Scale Frame Buildings

The wood frame models in PRAIRIE FLAT simulated buildings composed of plywood sheets mounted on appropriate framing. Walls of the models were glued together to provide some structural strength, while the roofs and floors simply were laid on supporting members without glue.

Figure 3.23 compares the tangential and radial distributions of roof- and floor-panel debris from these frame models with corresponding distributions from the four 1/8 scale block models. The tangential means and standard deviations for the frame models are similar to those of the block models, but the radial means are greater and the radial standard deviations are smaller. Hence, the net effect is that the sums of the radial means and standard deviations are quite similar for the frame and the block buildings — the same effect noted in the comparison of block buildings discussed at the end of the preceding section.

The mean tangential and radial travel distances for floor-panel debris are quite similar to those for the roof-panel debris; the standard deviations, however, are considerably lower. This indicates that there was less time for random lift to disperse the debris; hence, flight times were short and trajectories were shallow.

Appendix G contains all the data on debris distribution from the two frame buildings.

#### 3.4 Larger Models at High-Overpressure Sites: 1/8-Scale (PRAIRIE FLAT) and 1/33-Scale (White Sands SOTRAN) Block Buildings

The high-overpressure sites in the PRAIRIE FLAT and White Sands SOTRAN events contained block-building models like those of 1/8 and 1/33 scales that were

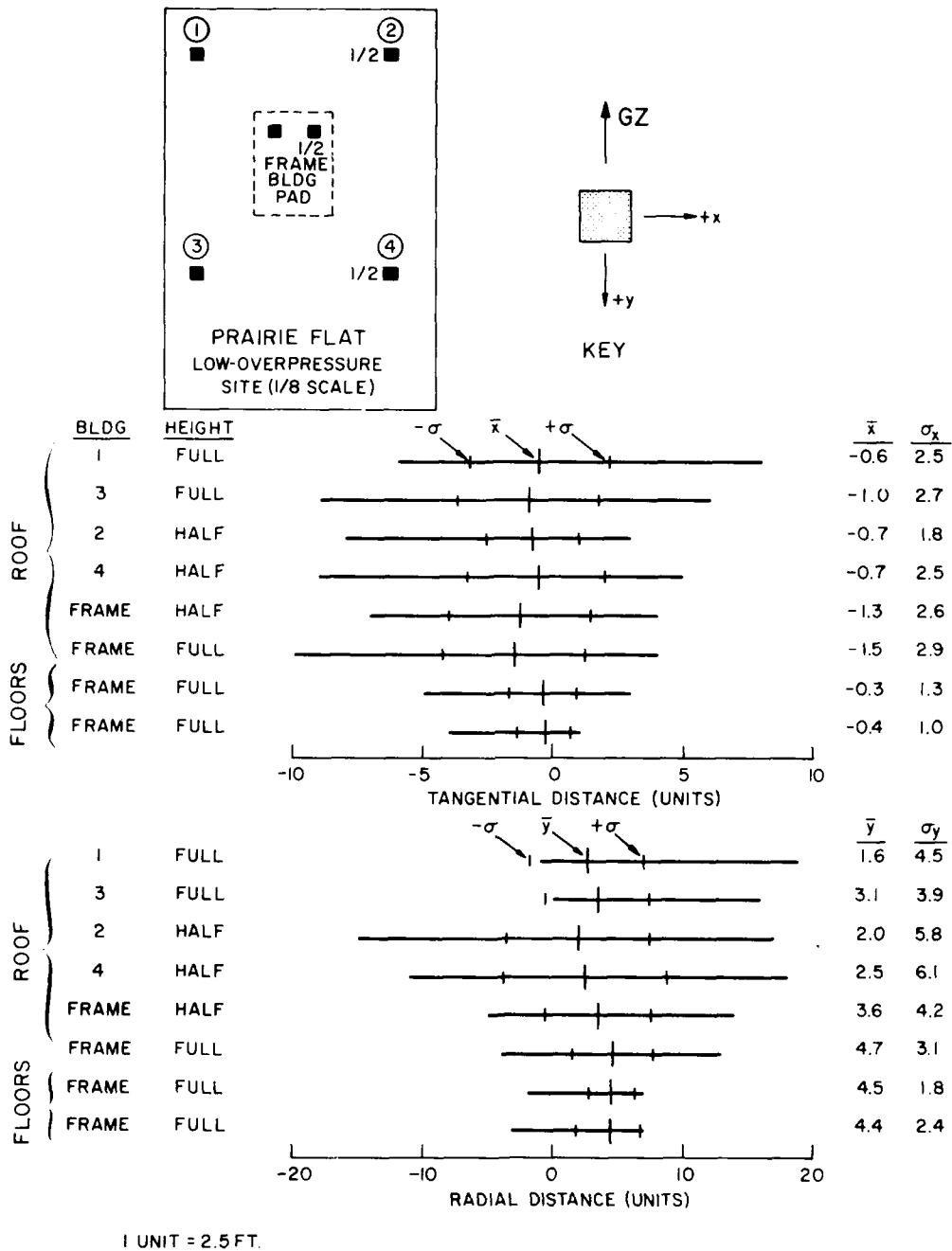


Figure 3.23. Comparison of roof- and floor-debris transport from 1/8-scale isolated block and frame buildings: PRAIRIE FLAT low-overpressure site.

used at the low-overpressure sites. These were placed closer to ground zero, of course, and thus subjected to a higher overpressure (6 psi in PRAIRIE FLAT, versus 3 psi at the low-overpressure site). The test blast at White Sands simulated a full-scale 0.3-MT detonation producing a peak overpressure of 27 psi; that in PRAIRIE FLAT simulated a full-scale 0.13-MT detonation — about one-half the intensity of the White Sands simulation — yet the PRAIRIE FLAT blast produced a simulated peak overpressure of 25 psi — nearly equal to the simulation at White Sands.

All models at both sites were isolated buildings: i.e., models were sufficiently far apart that one model did not interfere with the debris distribution of another. The PRAIRIE FLAT site (Figure 2.15) comprised four block buildings — two of half height and two of full height — and that at White Sands (Figure 2.13) comprised a full-height building in front of a half-height building.

Figure 3.24 shows the debris of the two 1/33-scale isolated buildings at White Sands after the blast. The base of the half-height building is near the center of the picture; the base of the full-height building is in the background, about at the edge of the visible area.

#### 3.4.1 Distribution of Block Debris

Figure 3.25 is a plan view of the grid at the full-height White Sands building, showing the distribution of blocks from a selected portion of the front wall. Comparable data for the forward full-height PRAIRIE FLAT building are given in Figure 3.26. The data are reproduced so that full-scale distances are the same in both figures.

The maximum tangential and radial block displacements, converted to full-scale distances, are 240 feet and 670 feet, respectively, for the White Sands building, and 310 and 510 feet, respectively, for the PRAIRIE FLAT building. The radial transport of debris at White Sands (670 feet) was greater than that in PRAIRIE FLAT (510 feet); this was expected, because of the higher-yield blast simulated at White Sands (0.3 MT versus 0.13 MT). Assume that distances along the radius of the blast wave vary as the cube root of the weapon yield. This proportion can be expressed for these test results as

$$510 \sqrt[3]{\frac{0.3}{0.13}} = 670 ,$$

which happens to be exactly correct. This is coincidental, of course, since test results generally cannot be expected to agree this well with a theoretical assumption.

There is an anomaly — the PRAIRIE FLAT distribution is wider (greater tangential transport) than that for the White Sands building. If one applies a yield



Figure 3.24. Half-height (center) and full-height (rear) isolated blue bullbores, 1-33 scale, after detonation: White sands high-overpressure site.

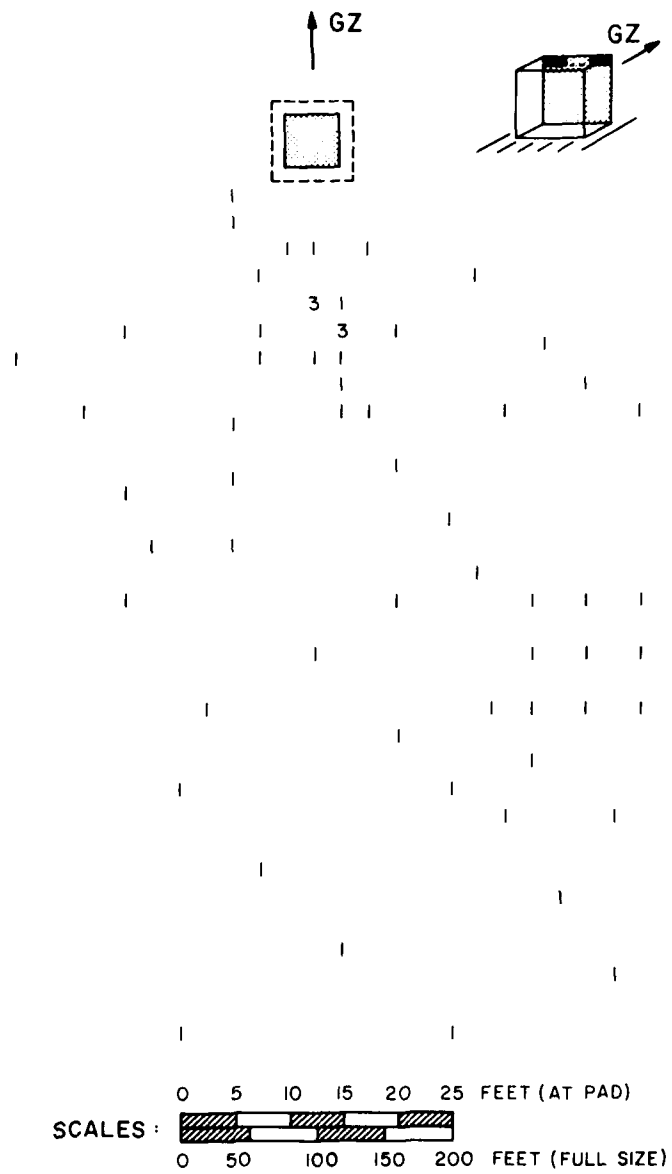


Figure 3.25. Block distribution from upper corners of front wall (shown here as black areas on shaded wall), 1/33-scale full-height building; White Sands high-overpressure site.

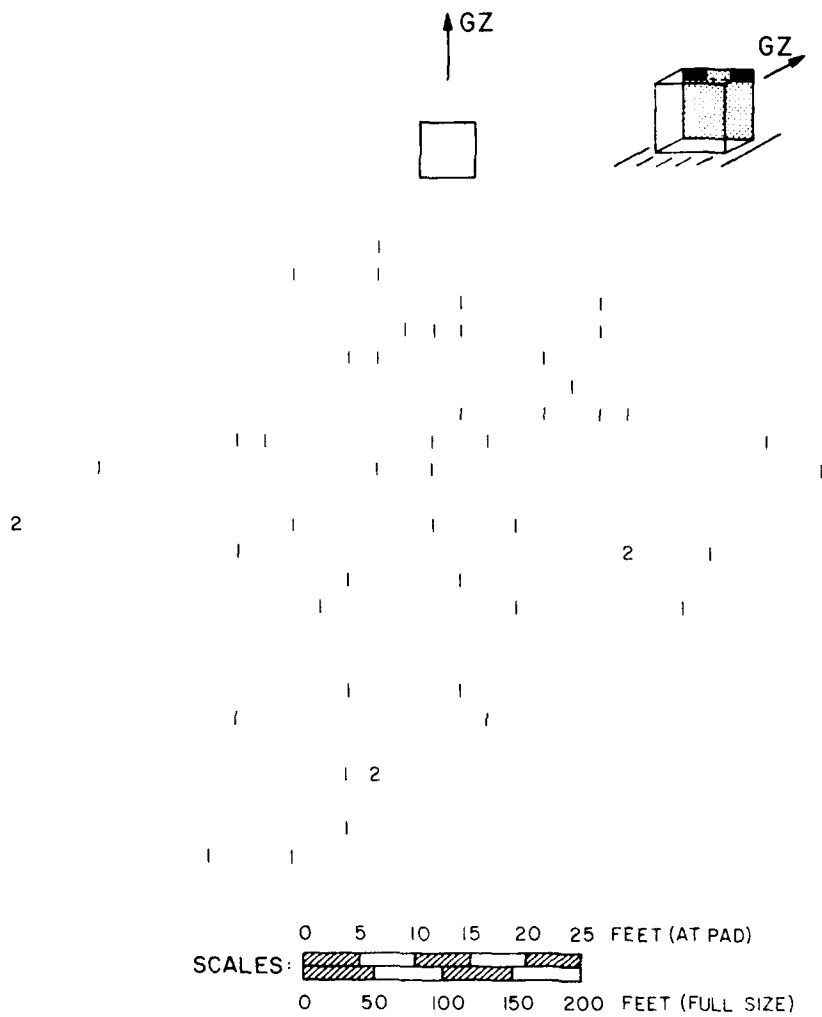


Figure 3.26. Block distribution from upper corners of front wall (shown here as black areas on shaded wall), 1/8-scale full-height building: PRAIRIE FLAT high-overpressure site.

factor in the scaling calculations that determined these distributions, the discrepancy would be even greater. (However, it is shown in Chapter 5 that the tangential transport of debris is not strongly yield-dependent.)

### 3.4.2 Distribution of Roof Debris

A statistical comparison of the roof-debris distribution from the four PRAIRIE FLAT models and the two White Sands SOTRAN models is given in Figure 3.27, in the same format as used in Figures 3.22 and 3.23. The distribution components tangent to the blast wave (x direction) are similar for the four PRAIRIE FLAT buildings: the near-zero mean distributions indicate that there was little cross-wind effect. The tangential distribution components for the two White Sands buildings show greater means and standard deviations. There is considerably more variability among the radial-component distributions: That from the White Sands full-height building shows the largest mean and the largest standard deviation by far. This variability among results within a test site was evident also in the data for the 1/120-scale isolated buildings in PRAIRIE FLAT.

### 3.5 Block Buildings of 1/140 Scale (DISTANT PLAIN) and 1/20 Scale (PRAIRIE FLAT)

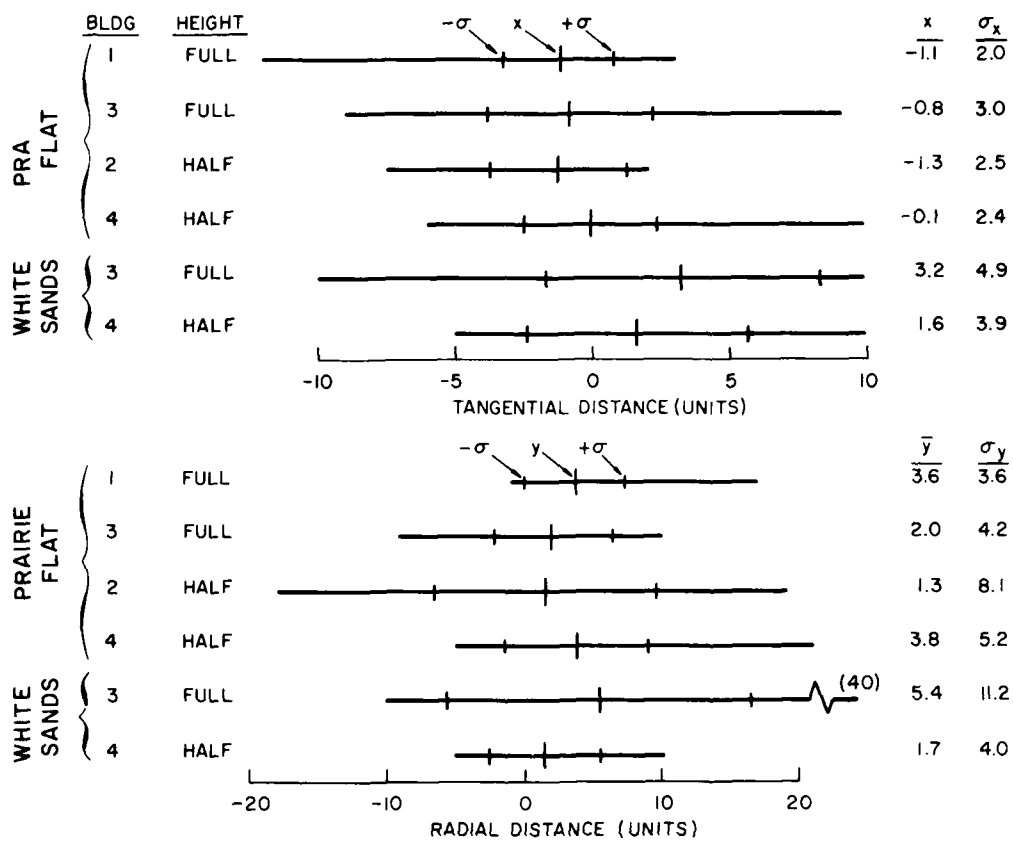
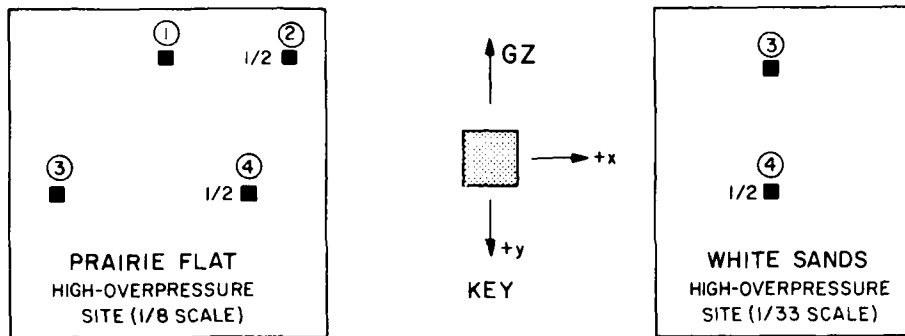
A test site of models was set up in Operation DISTANT PLAIN and another was set up in Event PRAIRIE FLAT, both designed to simulate the same actual, full-scale blast environment; this was not accomplished, however, as was discussed in Chapter 1. Results showed that the DISTANT PLAIN test simulated an over-pressure of 37 psi produced by a 1.8-MT detonation: the corresponding values in the PRAIRIE FLAT test were 20 psi and 0.8 MT.

Event 2a of Operation DISTANT PLAIN incorporated six 1/140-scale buildings — two isolated buildings and a four-building complex. Wind caused much damage to the models both before and after the blast: The roof elements of all buildings were blown completely clear of the test area. Because of this, the results were considered to be of questionable value, and complete records were not retained.

The test site in Event PRAIRIE FLAT incorporated four isolated 1/20-scale buildings. Figure 3.28 shows the post-blast condition of these models: block distributions from them showed some correspondence with the DISTANT PLAIN results.

#### 3.5.1 Distribution of Block Debris from Isolated Buildings

A method of contour-mapping block distances on representations of the walls from which the blocks came was used for the four PRAIRIE FLAT buildings. Figure 3.29 is such a map for the front wall of the full-height building nearer the blast. Each of the two squares represents the front wall of the model: the upper square



PRAIRIE FLAT : 1 UNIT = 2.5 FT. (AT PAD) = 20 FT. (FULL SIZE)  
 WHITE SANDS : 1 UNIT = 0.6 FT. (AT PAD) = 20 FT. (FULL SIZE)

Figure 3.27. Comparison of roof-debris transport from block buildings, PRAIRIE FLAT (1/8 scale) and White Sands SOTRAN (1/33 scale): high-overpressure sites.



Figure 3.28. Post-blast view of test pad and four demolished 1/20-scale buildings; PRAIRIE FLAT.

shows data pertaining to the tangential, or x, components of block distances, while the lower square shows data pertaining to the radial, or y, components. The x or y distance traveled by each block was plotted on the appropriate square in the relative position of that block's original location in the wall; contours then connected common distances, thereby delineating areas from which blocks traveled greater or lesser distances. Extremely large values are shown as isolated numbers. All values shown are in feet; these should be multiplied by 20 to obtain the comparable values for debris from a full-size building. Notice that the blocks blown furthest to the right and left of the front wall originated near the upper side edges, while those blown furthest back originated near the top edge.

Additional maps follow in succeeding figures. Figure 3.30 shows maps of the block distribution from the right side wall of the same model ("right" with respect to an observer facing ground zero). Blocks were blown appreciable distances only from the upper front area of the wall, probably because of vortex formation. Figure 3.31 shows the results for the back wall of this model, and Figure 3.32 shows the results for the left side wall. The latter maps are quite symmetrical with those for the right side wall.

An important measure of the validity of tests like these is their reproducibility: Are the results consistent from test to test? One would expect the pattern of block distribution from the half-height buildings to follow that of the full-height

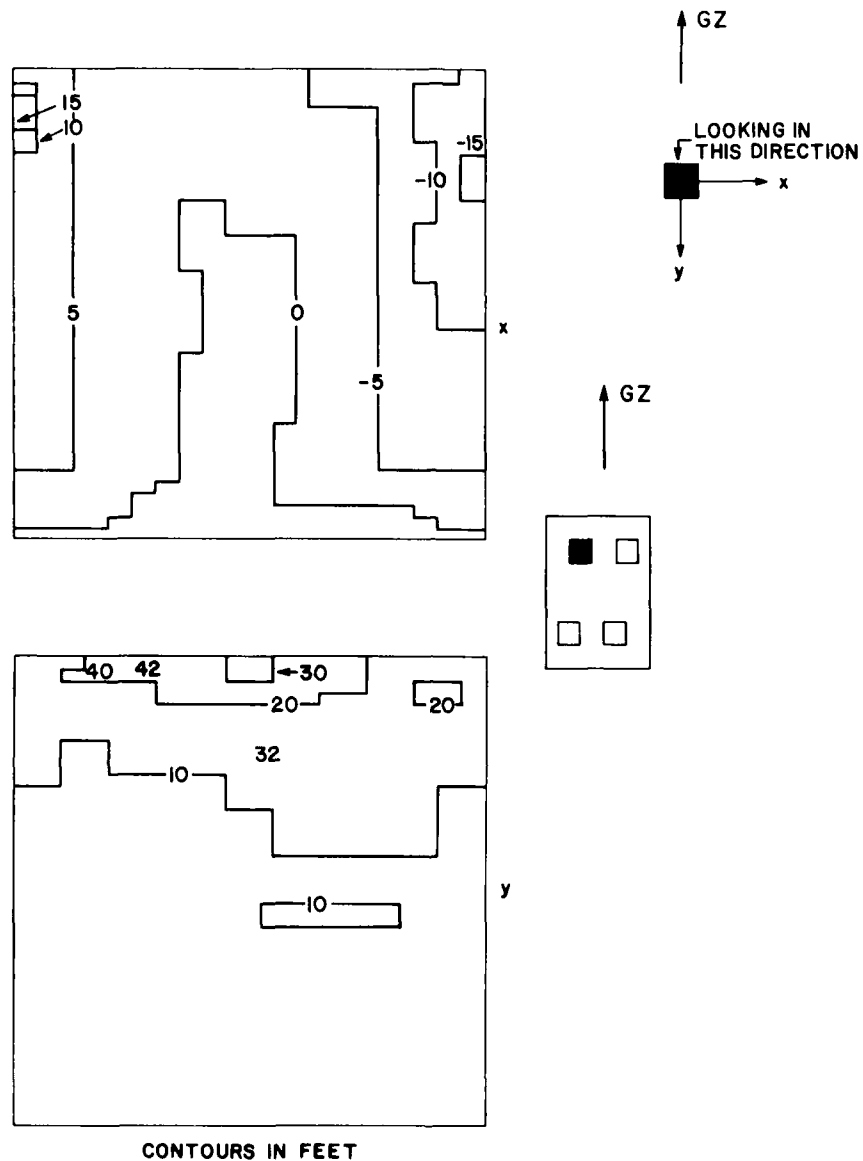


Figure 3.29. Front wall of 1/20-scale full-height building nearer the blast, showing x and y block-distance contours; PRAIRIE FLAT.

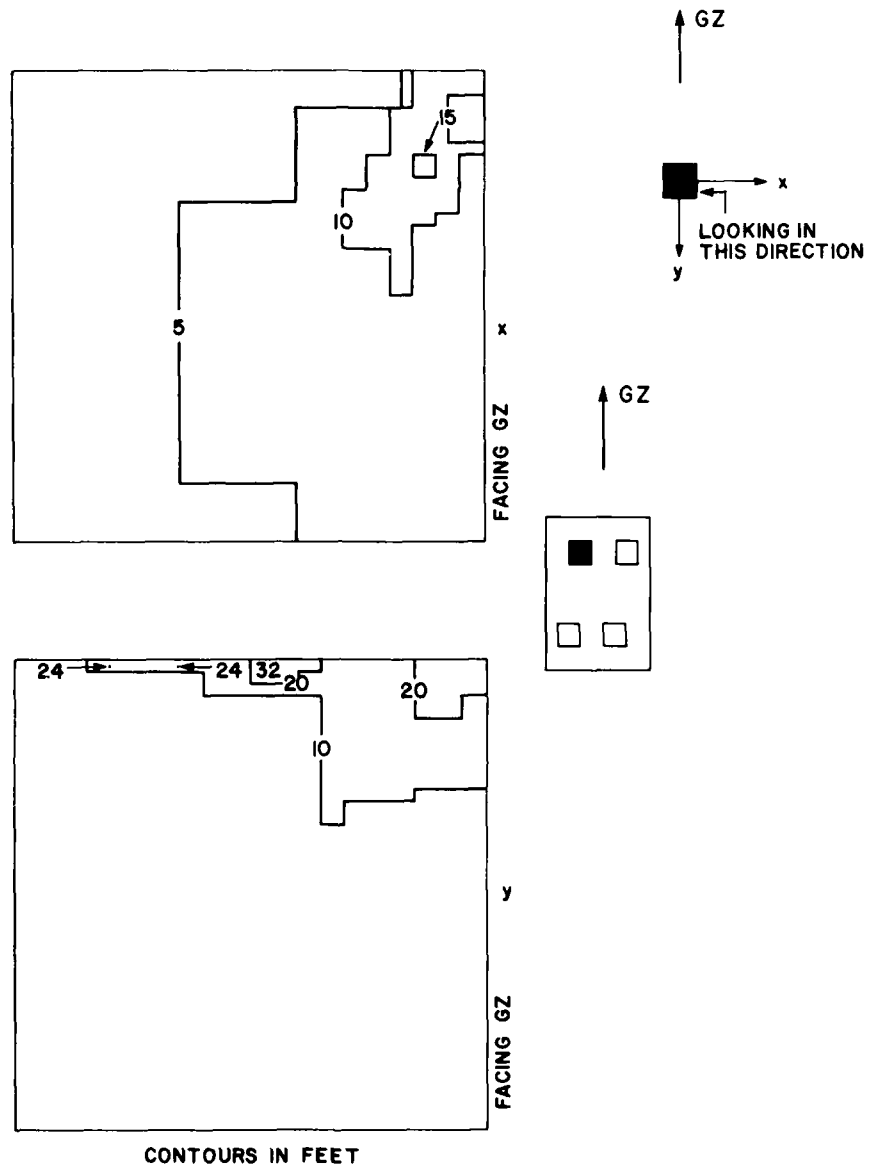


Figure 3.30. Right side wall of 1/20-scale full-height building nearer the blast, showing x and y block-distance contours; PRAIRIE FLAT.

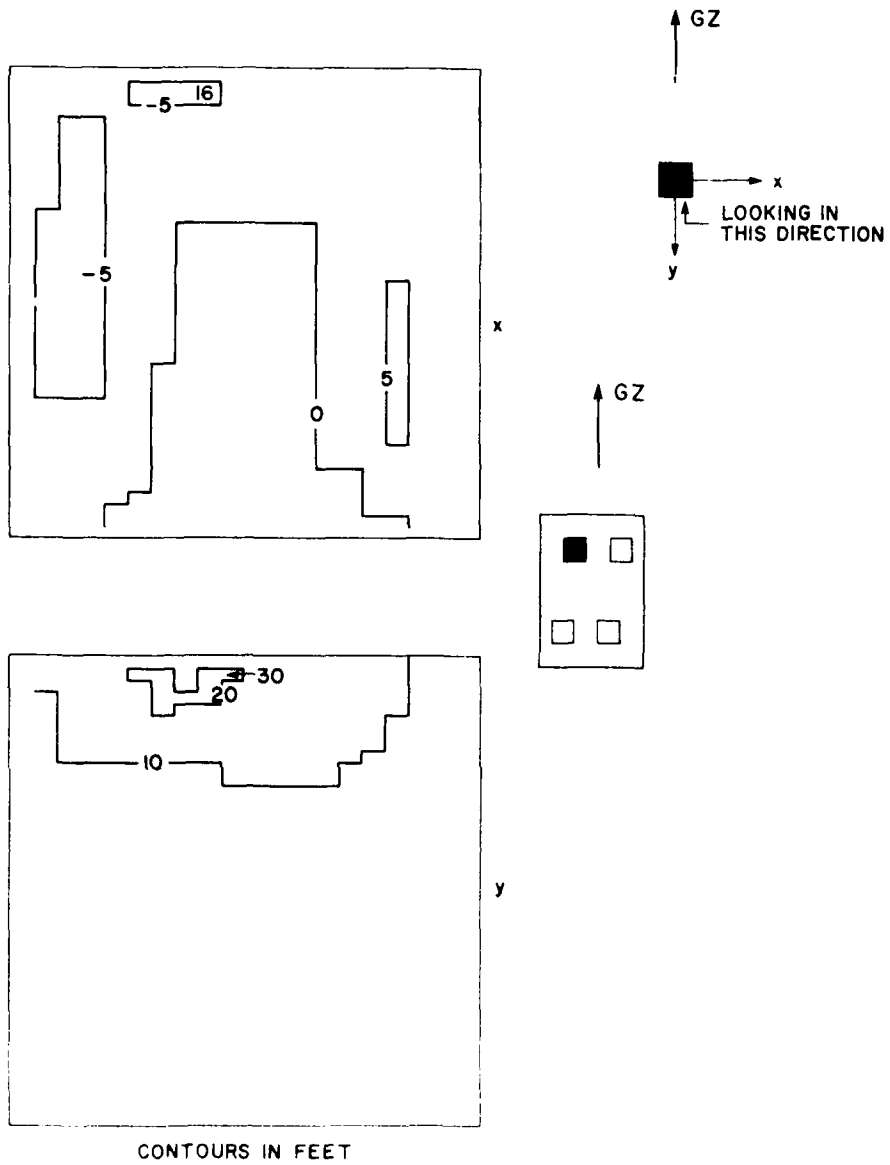


Figure 3.31. Back wall of 1/20-scale full-height building nearer the blast, showing x and y block-distance contours: PRAIRIE FLAT.

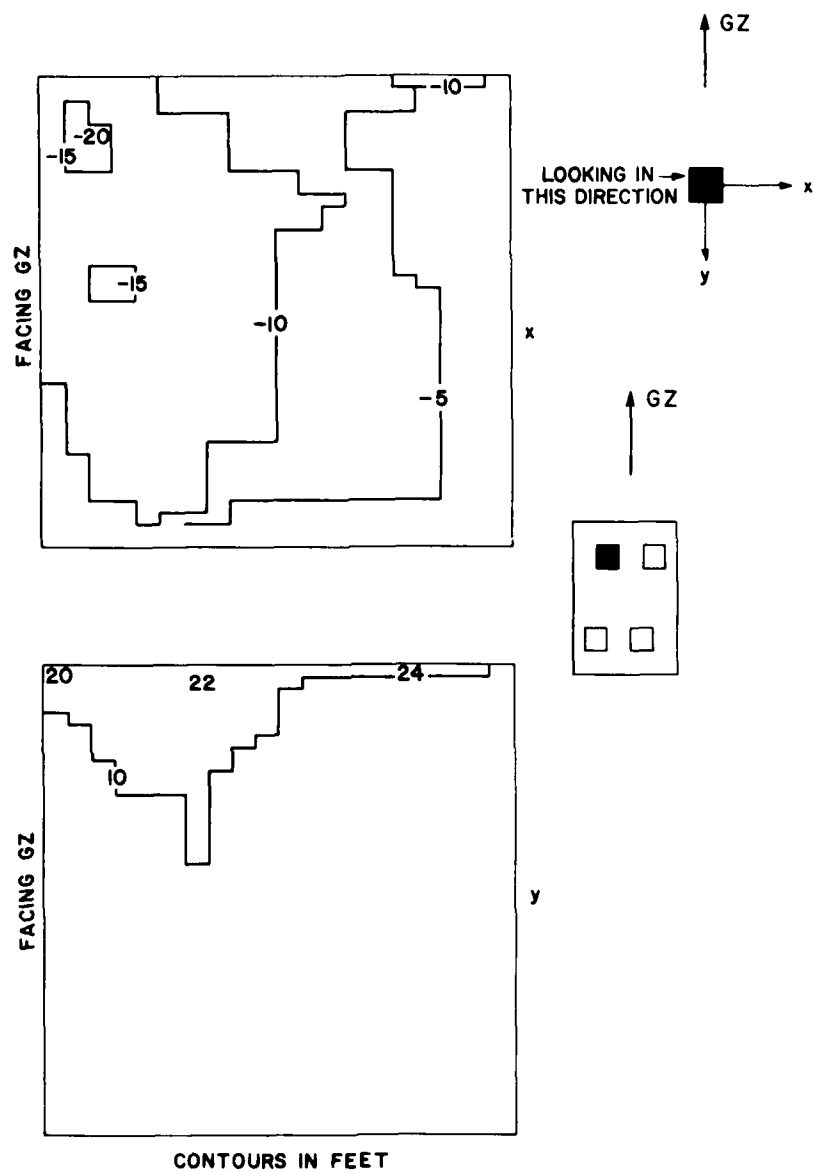


Figure 3.32. Left side wall of 1/20-scale full-height building nearer the blast, showing x and y block-distance contours; PRAIRIE FLAT.

buildings except that the distances traveled should be shorter. If the model were farther away from ground zero, one would expect a decrease in block transport distances also. Figure 3.33 shows the mapped x and y transport distances from the front wall of the full-height model farther from the blast; the contour patterns are similar to those for the corresponding wall of the model nearer to ground zero (Figure 3.29).

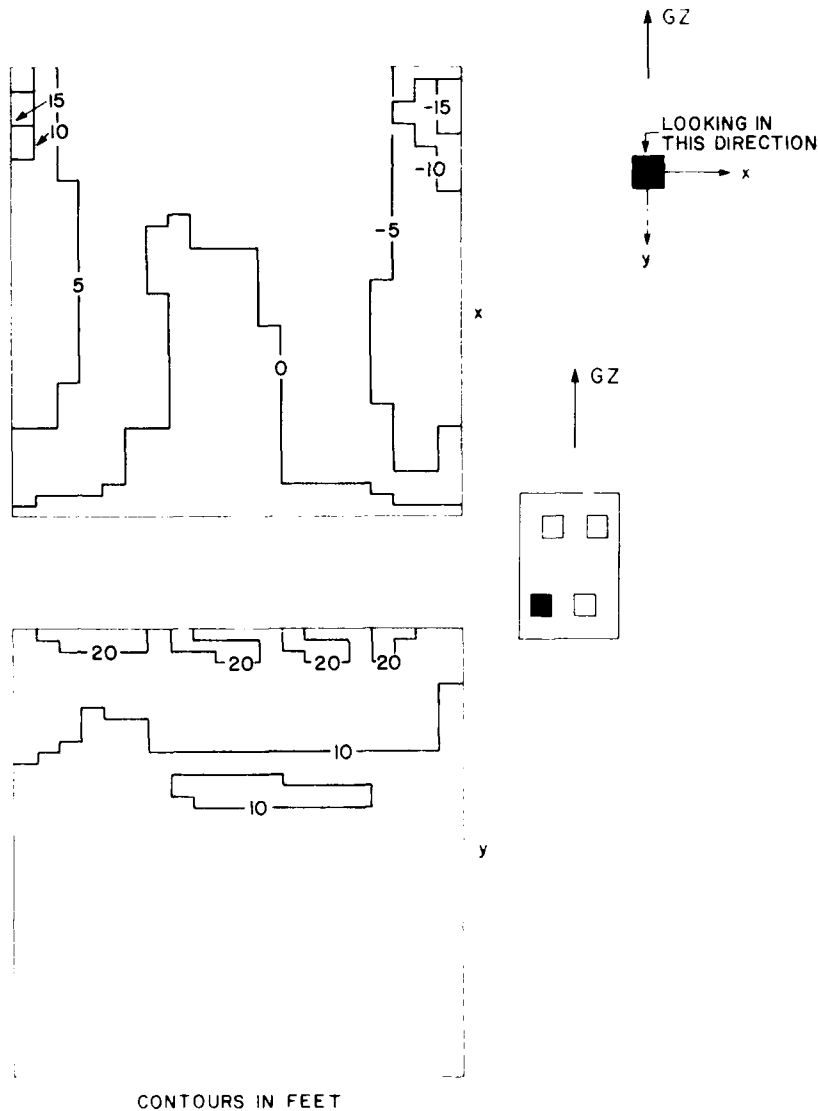


Figure 3.33. Front wall of 1/20-scale full-height building farther from the blast, showing x and y block-distance contours; PRAIRIE FLAT.

Figures 3.34 and 3.35 show maps of the x and y block transport distances from the four walls of the half-height model nearer the blast. The contour patterns are similar to the corresponding ones for the full-height building nearer the blast, although, as expected, the maximum distances traveled are almost always lower.

The roof elements of the 140-scale buildings in Operation DISTANT PLAIN, Event 2a, were not found at the site; many may have been blown away by winds before the blast. The walls of these buildings apparently withstood these winds.

The walls of the rear isolated building were destroyed most completely by the blast, as Figure 3.36 shows. Figure 3.37 shows the distribution of blocks from this building.

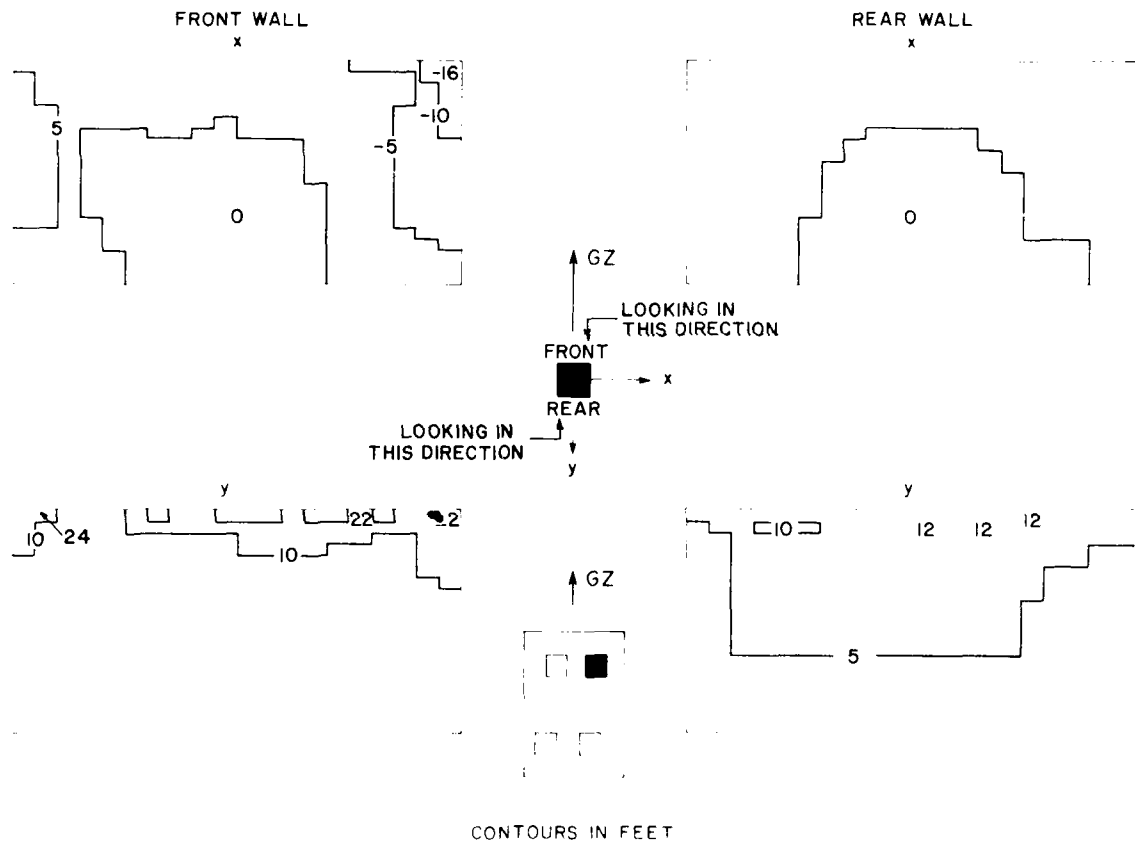


Figure 3.34. Front and back walls of 1/20-scale half-height building nearer the blast, showing x and y block-distance contours; PRAIRIE FLAT.

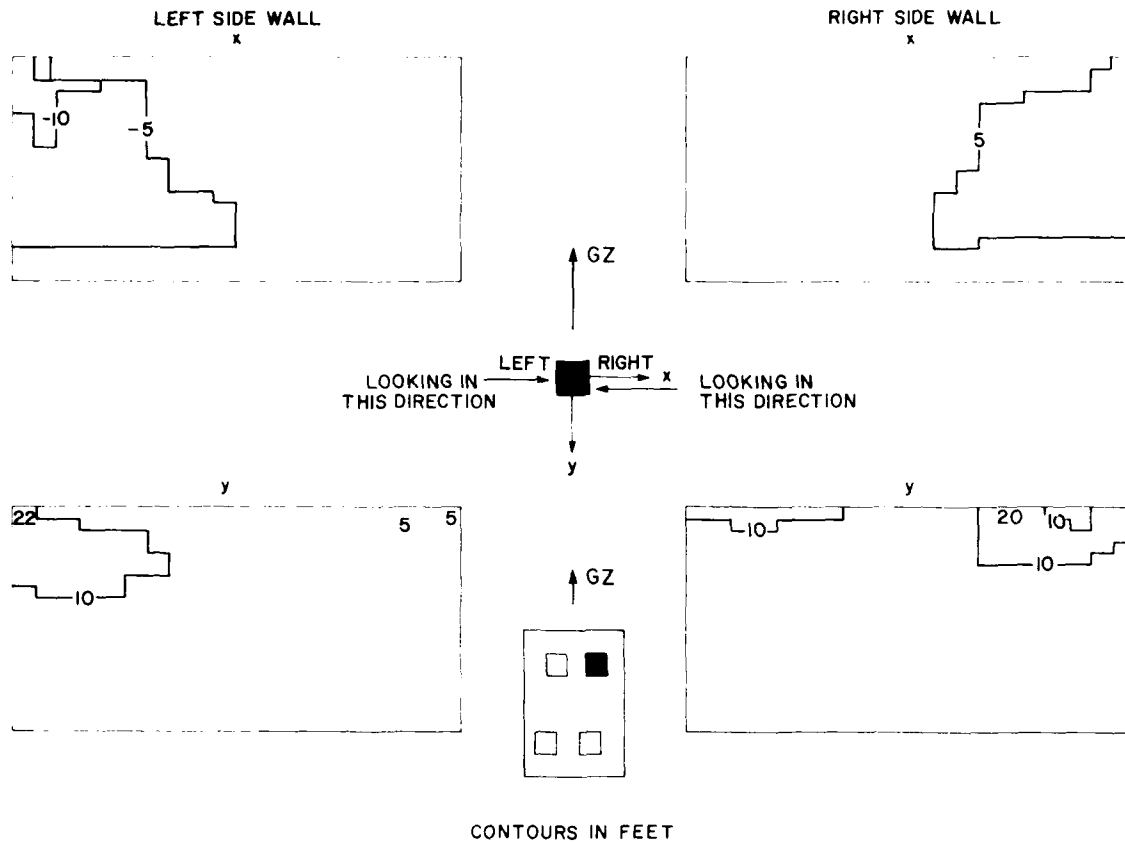


Figure 3.35. Left and right side walls of 1/20-scale half-height building nearer the blast, showing x and y block-distance contours; PRAIRIE FLAT.

Figure 3.38 shows the block distribution for the 1/20-scale forward full-height PRAIRIE FLAT building, scaled so that the grid size represents the same full-scale value as that in Figure 3.37. This required restructuring of the PRAIRIE FLAT grid pattern: The 2-foot grids, representing 40-foot full-scale grids, were overlaid with 100-foot full-scale grids; all the data of the 40-foot grids that spanned the 100-foot grid lines were averaged and reallocated accordingly.

Blocks from the DISTANT PLAIN building were spread over a greater area — an indication of the correspondingly more severe blast conditions (37 psi simulated peak overpressure from a 1.8-MT detonation, compared with values of 20 psi and 0.8 MT in PRAIRIE FLAT). Despite this difference in area spread, the maximum simulated full-scale radial distances that blocks traveled were about the same — approximately 900 feet — in both experiments. It may be that some blocks from the DISTANT PLAIN building were beyond the field of view of the photograph.



Figure 3.13. Models of 1/40-scale in Operation DISTANT PLAIN,  
Event 2a, after detonation.



GZ  
↑

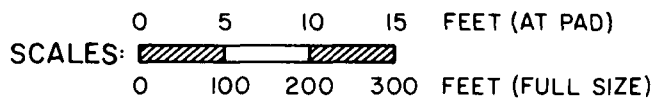
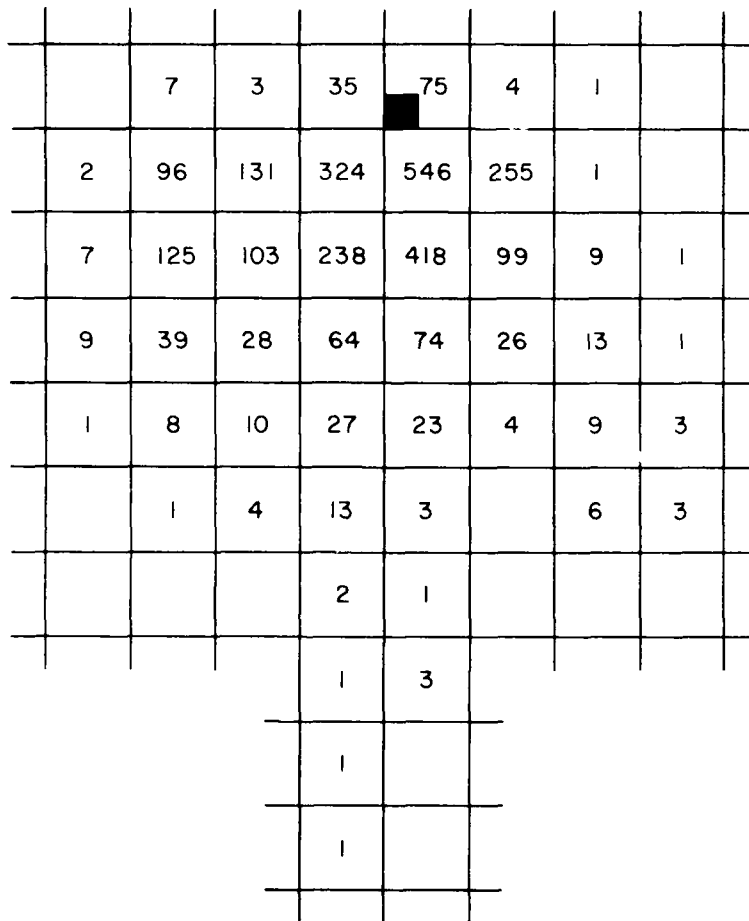


Figure 3.38. Block distribution from forward full-height 1/20-scale building; PRAIRIE FLAT (grid rescaled for comparison with Figure 3.37).

### 3.5.2 Distribution of Block Debris from Buildings in Complex

Figure 3.39 shows the four 1/140 scale buildings in the DISTANT PLAIN complex as they appeared after the blast. Evidently the three buildings in line behind the front one were shielded somewhat; the front building suffered much greater damage.

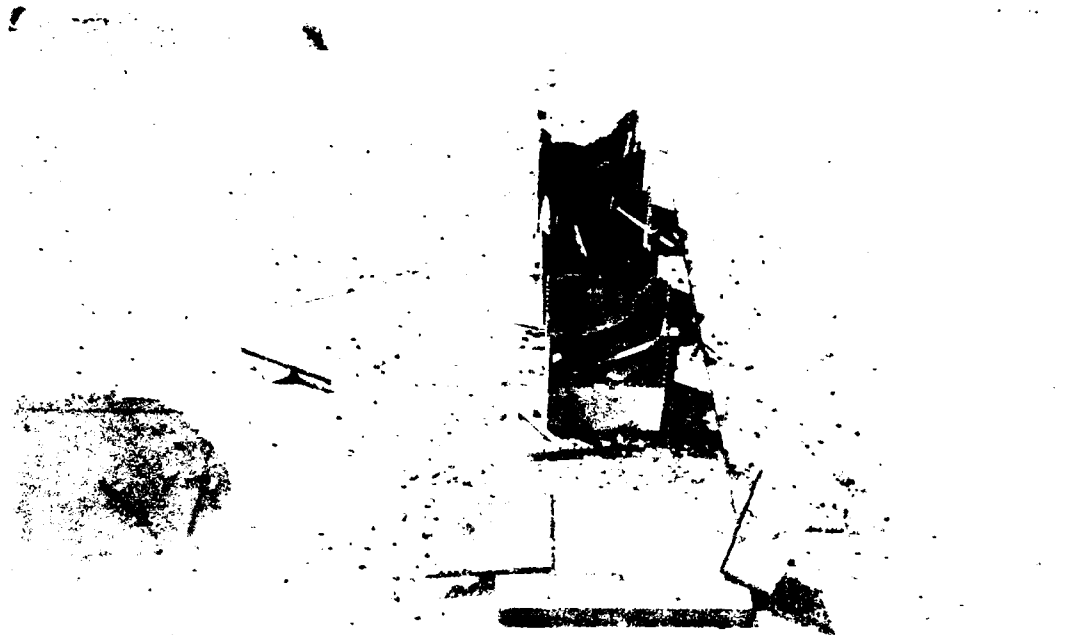


Figure 3.39. Complex of four 1/140-scale block buildings after detonation; DISTANT PLAIN, Event 2a.

These 1/140-scale models were constructed like the 1/120-scale models of Operation SNOWBALL, described in Chapter 2: The end blocks of all walls were glued to vertical supports, which tended to make the models more rigid than was desirable. It is possible that the rigidity and small size of the models, coupled with the relatively short blast duration in this test, may have created a situation in which the damage done to the models was more dependent on the construction of the models than on the level of the blast. Consequently, one should not assume that the apparent "shielding" of the second, third, and rear buildings would occur in a real, full-scale blast environment.

### 3.5.3 Distribution of Roof Debris from 1/20-Scale Models (PRAIRIE FLAT and DIAL PACK)

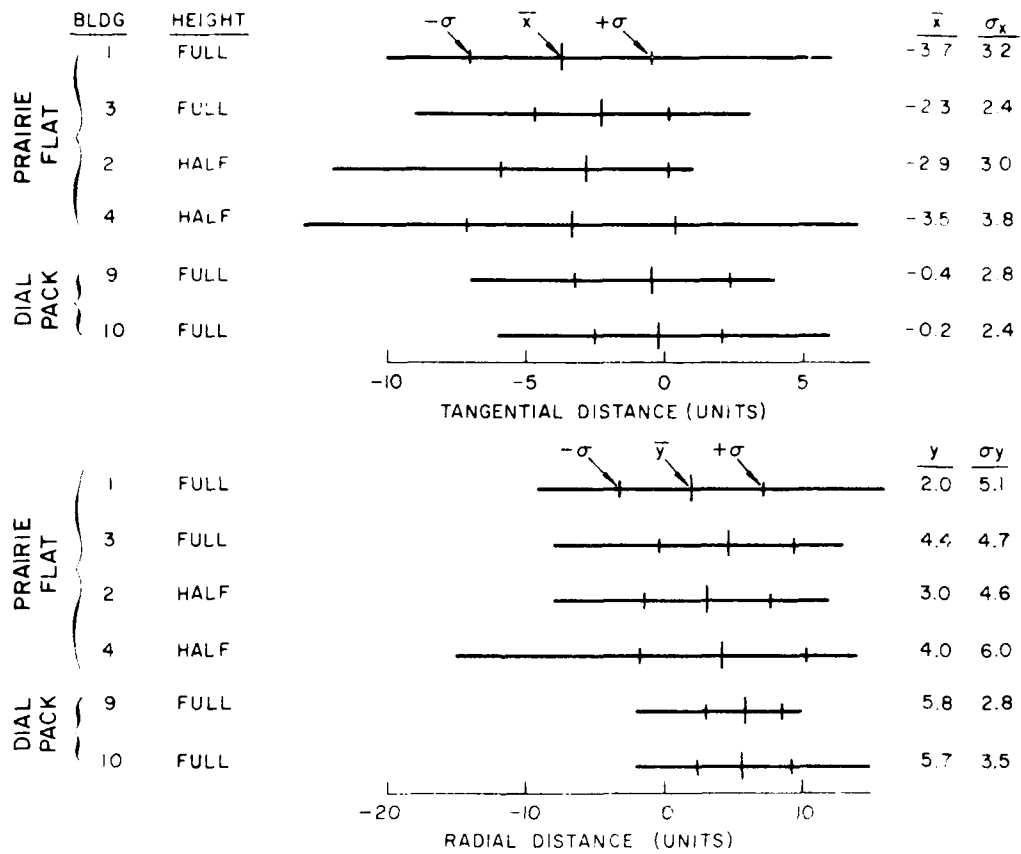
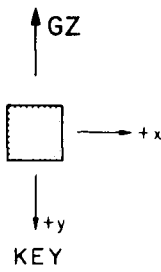
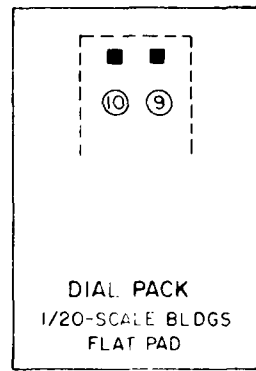
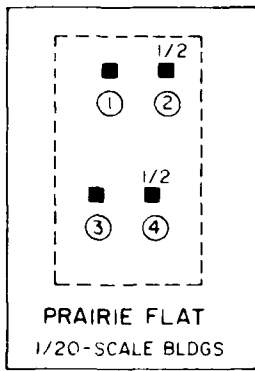
Wind damage before and after the DISTANT PLAIN test destroyed all data relevant to the behavior of roof panels; hence, results are available only for the 1/20-scale PRAIRIE FLAT models, and a comparison between DISTANT PLAIN and PRAIRIE FLAT cannot be made. However, the DIAL PACK test site discussed in the next section included two 1/20-scale frame models on a flat pad: the roof debris from these are compared statistically with the roof debris from the 1/20-scale PRAIRIE FLAT models in Figure 3.40.

The figure follows the same format as previous figures of the same type. Roof-panel distributions are separated into tangential (x) and radial (y) travel distances; the horizontal bar associated with each building contains a large vertical mark designating the mean distribution and two smaller vertical marks designating plus and minus one standard deviation. The standard deviations for tangential distributions,  $\sigma_x$ , are similar for all buildings. The two DIAL PACK models exhibit smaller standard deviations for radial distributions,  $\sigma_y$ , than those of the PRAIRIE FLAT models; however, the DIAL PACK models also exhibit larger means than those of the PRAIRIE FLAT models. Hence, the sums of the mean and the standard deviation are similar, both tangentially and radially, for all buildings. This has been observed in the results for almost all other roof-panel distributions.

Appendix G and H contain complete data on the roof-debris distributions from the 1/20 scale PRAIRIE FLAT and DIAL PACK buildings.

### 3.6 Effects of Sloping Terrain on Debris Transport (DIAL PACK)

The DIAL PACK experiment was designed specifically to study the influence of sloping terrain on the transport of debris from buildings located there — to find whether hills reduce debris travel. Two test sites were prepared, each with frame models on horizontal and on inclined pads; the models were of 1/20 scale at one



1 UNIT = 2 FEET (AT PAD) = 40 FEET ( FULL SIZE )

Figure 3.40. Comparison of roof-debris transport from 1/20-scale buildings: PRAIRIE FLAT and DIAL PACK (horizontal pad).

site (Figure 2.20) and of 1/120 scale at the other (Figure 2.22). Figures 3.41 and 3.42 show the two sites after the test blast. In each view personnel are placing plastic sheets over the debris to protect the distributions from any disruption by local winds.

Figure 3.43 gives statistical information regarding the radial (y) debris distributions from the 1/120-scale buildings. Refer to Figure 2.22 for a plan view of this site: note that buildings were arranged in pairs at each position lengthwise along the main pad — at the top, on the slope, and at ground level — and on the separate smaller pad designed to represent flat terrain. Figure 3.43 shows the side views of these pads, turned on end, with the information for each pair of buildings



Figure 3.41. DIAL PACK 1/120-scale buildings after detonation.



Figure 3.42. DIAL PACK 1/20-scale buildings after detonation.

opposite the side view. The set of lines associated with a pair of buildings shows the radial distribution from each building roof and the combined radial distributions from the two front walls, the two pairs of side walls, and the two back walls. Each line represents the limits of debris travel radially, along the direction of blast-wave travel; the large vertical mark indicates the mean distribution, and the two smaller vertical marks indicate plus and minus two standard deviations (previous figures indicated plus and minus one standard deviation). The data for the building walls were combined to obtain better statistical distributions, because the walls tended to break apart in clumps of elements rather than in individual pieces. Roofs did break apart into individual panels, and their distributions are shown for each building to demonstrate data consistency.

The data for the separate pad, at the top of the figure, are inconsistent with the data for other buildings on flat pads. Probably this was the result of an anomalous wind condition at the smaller pad, which Figure 3.44 tends to confirm. The

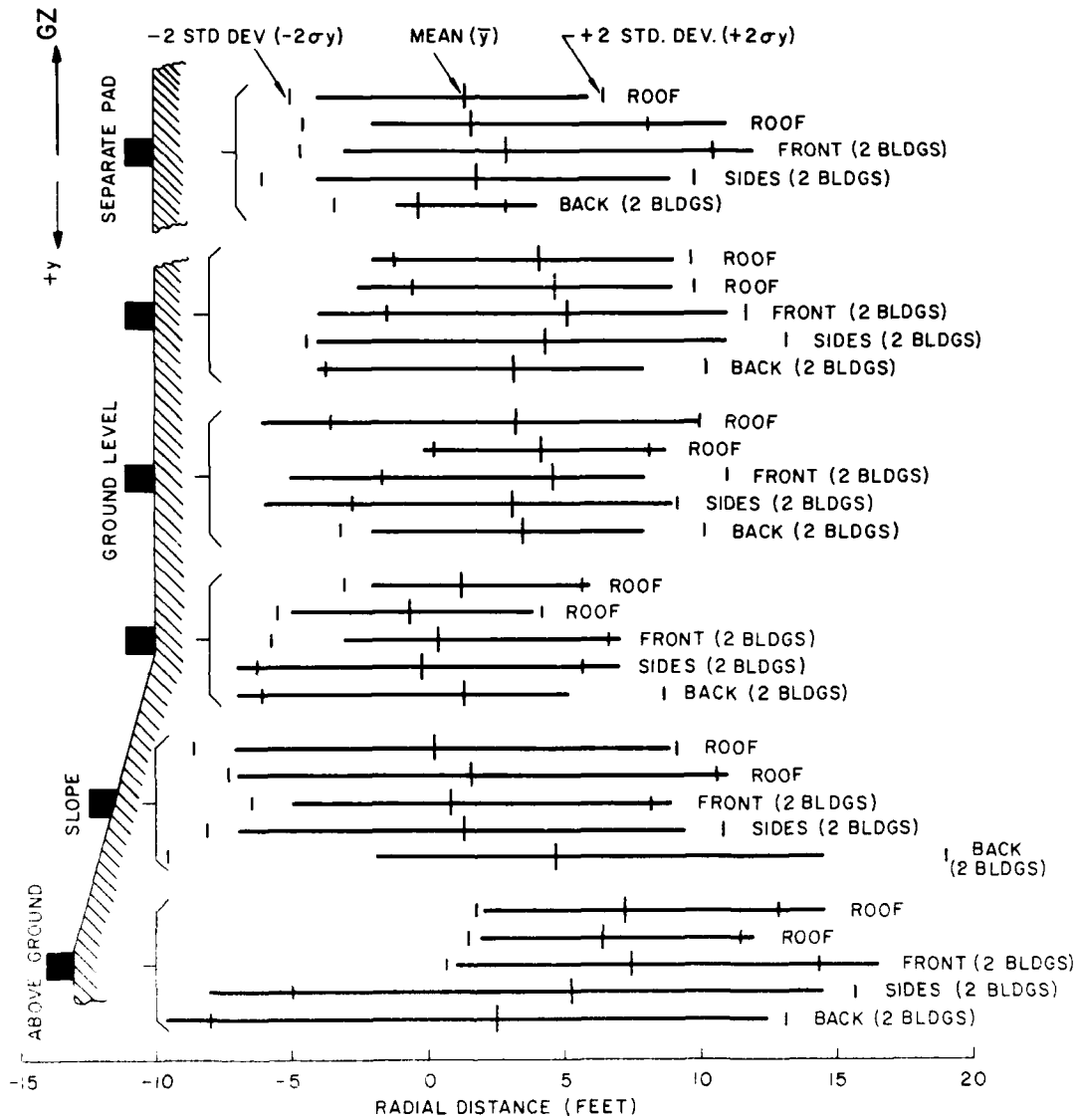


Figure 3.43. Radial debris transport from DIAL PACK 1/120-scale buildings.

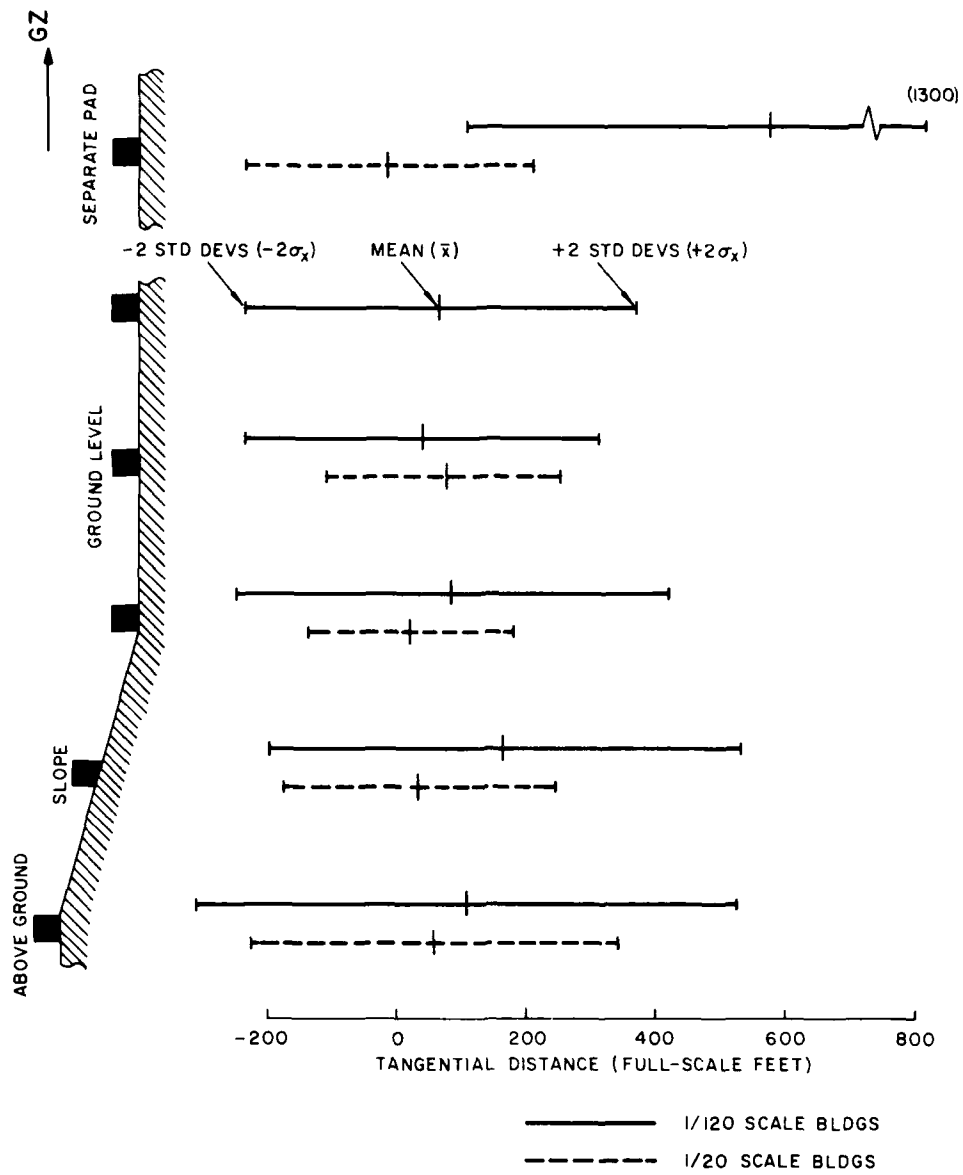


Figure 3.44. Comparison of roof-debris transport from DIAL PACK 1/120- and 1/20-scale buildings

evidence indicates that the data for the buildings on the flat portion of the main pad, forward of the slope, are more representative of flat-terrain debris transport.

Refer again to Figures 2.22 and 3.43. The transport of debris from the buildings forward of the slope (buildings 1, 2, 3, and 4) was similar for all four buildings. The mean roof-debris distributions from buildings at the base of the slope were near zero, and the standard deviations for these distributions were lower than those associated with the buildings forward of the slope. These effects can be attributed to flow disturbances. The mean distributions from buildings on the slope were lower than those from buildings on the separate horizontal pad, but the corresponding standard deviations were somewhat higher; hence, the net effect was that debris traveled about the same maximum distances from both groups of buildings. The mean distributions from buildings at the top of the slope were greater than those from all other buildings. Generally, the line lengths show that the  $2\sigma$  band represents the spread of data fairly well.

Figure 3.44 compares the tangential (x) roof-debris distributions, combined for each pair of buildings along the pad, from the buildings at both test sites. Distribution distances have been converted to full-scale feet so that the results from the 1/120-scale buildings can be compared directly with those from the 1/20-scale buildings. Figure 2.20 shows the plan view of the test site at which the 1/20-scale models were located; note that the pattern is similar but that there were no buildings occupying the positions forward of the slope corresponding to buildings 1 and 2 of 1/120 scale, Figure 2.22. In Figure 3.44 the side view turned on end serves to represent both test sites. The solid lines pertain to the pairs of 1/120-scale buildings, and the dashed lines pertain to the pairs of 1/20-scale buildings in corresponding positions.

Figure 3.45 is a statistical comparison of the radial (y) debris distributions from the roofs, back walls, and floors of the ten 1/20-scale buildings. The six lines associated with each building silhouette represent the extent of debris distribution from each roof, back wall, and floor of the two buildings at that location along the pad.

Panel distributions were similar for the pair of buildings on the separate flat pad (buildings 9 and 10) and the pair of buildings forward of the slope (buildings 1 and 2). Also, distributions were similar for the pair at the base of the slope (buildings 3 and 4) and the pair on the slope (buildings 5 and 6), through the debris from these did not travel as far as the debris from the buildings on the flat areas.

Debris from the pair of buildings at the top of the slope (buildings 7 and 8) tended to travel in the negative y direction — that is, toward ground zero rather than away from it. Film records show the probable reason for this. Debris from buildings 7 and 8 was lofted higher than debris from the other buildings; this debris

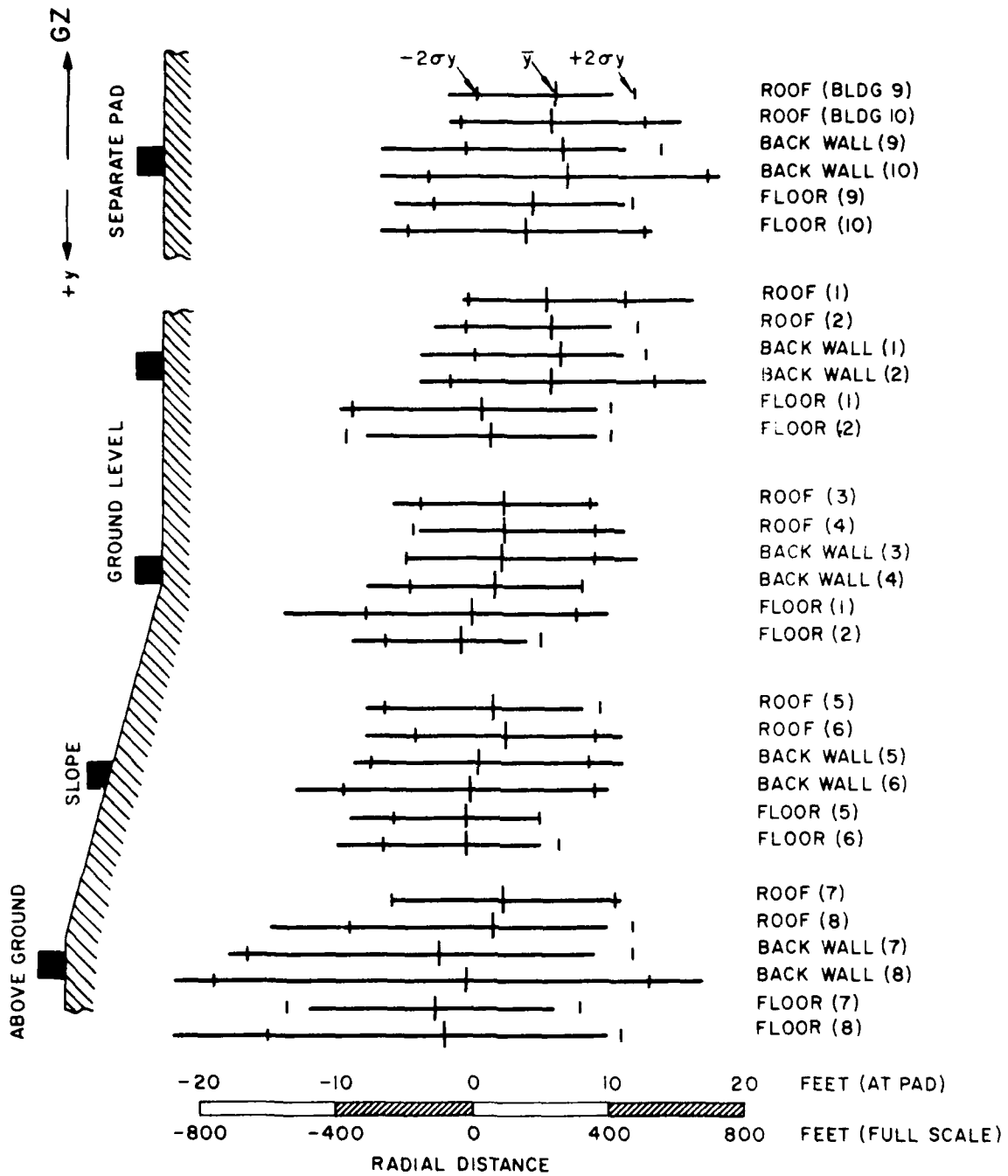


Figure 3.45. Comparison of radial debris transport from roofs, back walls, and floors: DIAL PACK 1/20-scale buildings.

was still in the air, therefore, after the positive phase of the blast wave had passed and the negative phase occurred: air rushing back to fill the low-pressure void left by the blast wave carried the most highly lofted debris with it, depositing it in many instances on the side of the buildings toward ground zero.

The opposite seems to have occurred at the site occupied by the 1/120-scale buildings. Here the blast's positive phase lasted long enough to carry the debris from the buildings at the top of the slope the longest distances in the positive y direction.

Panels from the 1/20-scale buildings on the slope tended to travel shorter distances than panels from the buildings on flat areas, while the distributions from the 1/120-scale buildings did show a reduction in mean travel but not in maximum travel. The explanation in this case is not obvious. Perhaps blast-flow disturbances originating at the relatively close edges of the slope had some effect on the 1/20-scale models; the edges of the slope on which the 1/120-scale models rested were farther away, relative to the size of the buildings.

Finally, the results from both sites show little differences among the distributions of debris from different parts of the buildings. The maximum travel distances were comparable for debris from back walls, roofs, and floors.

## Chapter 4

### DEBRIS IN FLIGHT

High-speed motion-picture films recorded the flight of debris from model buildings during most of the tests. Timing marks that were recorded simultaneously, along with the position of debris in each film frame, determined displacement and time data for those pieces of airborne debris that were discernible. The only pieces that could be followed in this way were the wooden elements — the panels and rafters; individual wall blocks in flight were impossible to distinguish on the films.

These records of debris in flight are more useful, in some ways, than terminal debris locations. (The terminal distributions, discussed in Chapter 3, revealed little about the simulated nuclear blast wave if they were influenced by ambient winds or by the negative phase of the scaled-down blasts.) Film records, giving an account of debris displacement versus time, provide information about the aerodynamic characteristics of debris in flight and about the statistical variations inherent in debris distribution.

The most significant effect observed in the films was lofting — debris carried high in the air by the disturbed blast wave passing over the model buildings. Figure 4.1, a series of frames from the high-speed films made during Operation SNOWBALL, illustrates this.

Statistical differences exist between information from debris distributions and information from film records. In most cases, all the pieces of debris were accounted for in the recording of terminal positions, but by no means all the pieces could be seen during flight on the film records. Some pieces were out of camera range and could not be followed: some pieces were masked by others or obscured by raised dust; some, especially the small wall blocks, were missed because of the relatively poor film resolution. Usually, pieces that remained close to the ground during flight were missed.

#### 4.1 Velocity-versus-Time Plots

All of the data obtained in SNOWBALL, DISTANT PLAIN, and PRAIRIE FLAT were reduced to plots of debris velocity versus time. These plots, each of which covers the duration of the film record, are presented in Appendix J.

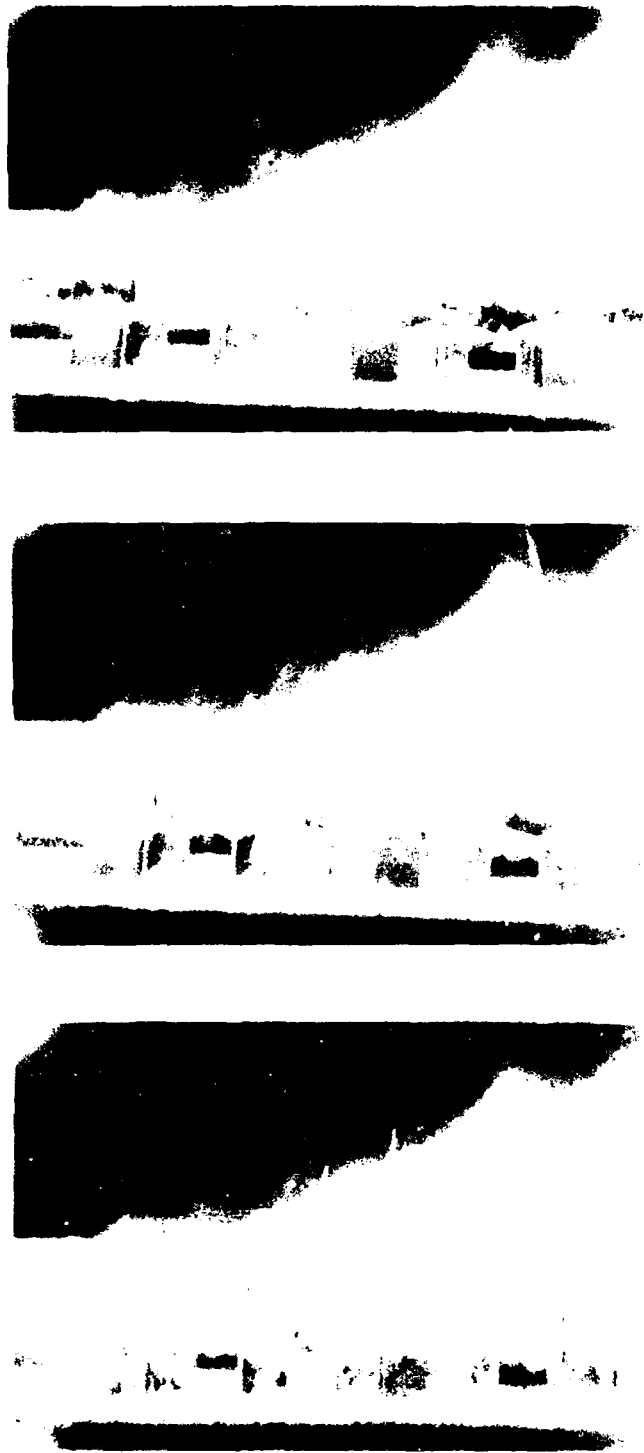


Figure 4.1. Motion-picture frames from  
Operation SNOWBALL, showing  
debris lofting.

#### 4.1.1 Data Presentation

The discrete debris trajectories associated with identical blast conditions were found to vary greatly. It is convenient, therefore, to study these trajectories in statistical groups rather than individually. Statistical presentations allow the results of different experiments to be compared; they also tend to eliminate anomalous trajectories that result from error.

All trajectories of debris from similar buildings exposed to the same blast were superimposed on a single figure, upon which the approximate bounds of plus and minus one standard deviation ( $\pm 1\sigma$ ) were constructed. Theoretically, about 68 percent of the trajectories should lie within these bounds. The lower bound, however, applies only to those trajectories that were observed; many were not.

A few individual trajectories are included in this chapter to illustrate how debris actually traveled. The individual trajectories presented are, for the most part, the highest ones observed in the various experiments.

#### 4.1.2 SNOWBALL 1/120-Scale Buildings

Figure 4.2 shows trajectories for a roof panel and a rafter from a building in the front row of the SNOWBALL complex. The panel and the rafter are shown in their observed positions at various times after the arrival of the shock front. As in the film sequence of Figure 4.1, lofting is evident in this figure.

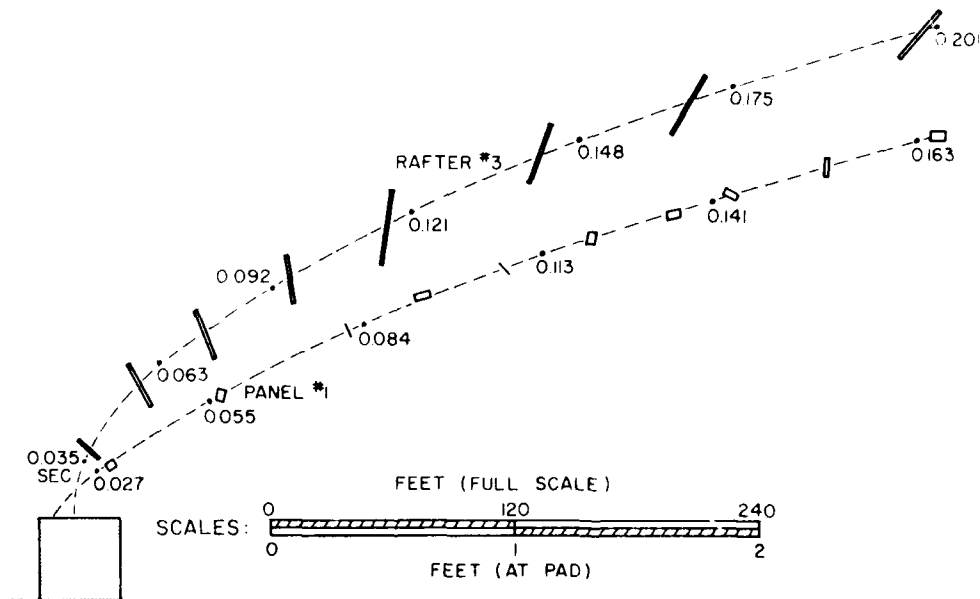


Figure 4.2. Roof-panel and roof-rafter trajectories from a front-row building of the SNOWBALL complex.

The trajectories observed in SNOWBALL were placed into two classes — those from the isolated building and the buildings in the front row of the complex, which might be called the "exposed" buildings, and those from all other buildings in the complex, which might be called the "sheltered" buildings. Figures 4.3(a) and (b) show the velocity bounds for roof-panel debris from the "exposed" and "sheltered" buildings, respectively.

A comparison of these results indicates (1) a higher upper-horizontal-velocity bound for the sheltered buildings; (2) similar lower-horizontal-velocity bounds; and (3) slightly higher vertical-velocity bounds for the exposed buildings. Lofting — indicated by high vertical velocities — occurs at the expense of some horizontal velocity: this may be why roof-panel debris from the exposed buildings, which exhibited lofting, also exhibited lower horizontal velocities.

Figures 4.4(a) and (b) show similar data for the SNOWBALL roof rafters. Only three roof-rafter trajectories were recorded for the buildings in rows 2 through 8 of the complex; hence, Figure 4.4(b) shows velocity-versus-time plots of these individual trajectories rather than statistical bounds.

The velocity bounds for the roof rafters from the exposed buildings tend to bracket the bounds for the roof panels from these buildings, showing a close statistical correspondence between the results for the rafters and the results for the panels. A similar comparison between rafters and panels of the sheltered buildings could not be made, because of the insufficient data obtained.

#### 4.1.3 DISTANT PLAIN, Event 2a, 1/50-Scale Buildings and PRAIRIE FLAT 1/8-Scale Buildings; High-Overpressure Sites

This and other sections that follow compare the results of pairs of tests that were designed to simulate the same full-scale blast conditions. The two parts of Figure 4.5 are drawn so that the same full-scale distances apply to both sets of trajectories. There are obvious differences among these trajectories and among the bounds of the velocity-versus-time plots (Figures 4.6 and 4.7). The differences are best seen in Figure 4.8, in which the velocity bounds for roof panels have been re-scaled for direct comparison between the two tests.

The horizontal-velocity bounds for the DISTANT PLAIN roof panels are above those for the PRAIRIE FLAT roof panels. Refer to Table 1.3, which should show whether differences in the full-scale simulated conditions explain the observed differences. The DISTANT PLAIN experiment simulated a 0.23-MT explosion that produced a 35-psi peak free-field overpressure; PRAIRIE FLAT simulated a 0.13-MT explosion that produced a 25-psi peak overpressure. The full-scale air velocity for the former should have been about 1.3 times that for the latter; this

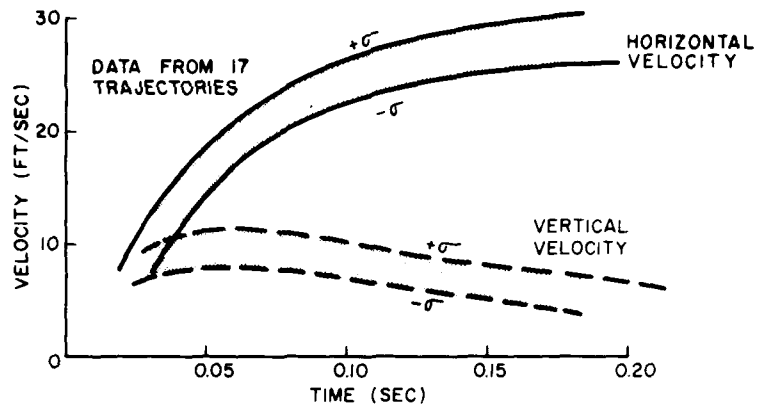


Figure 4.3(a). Bounds of velocity-versus-time plots for roof panels from exposed (front-row and isolated) buildings; Operation SNOWBALL.

8

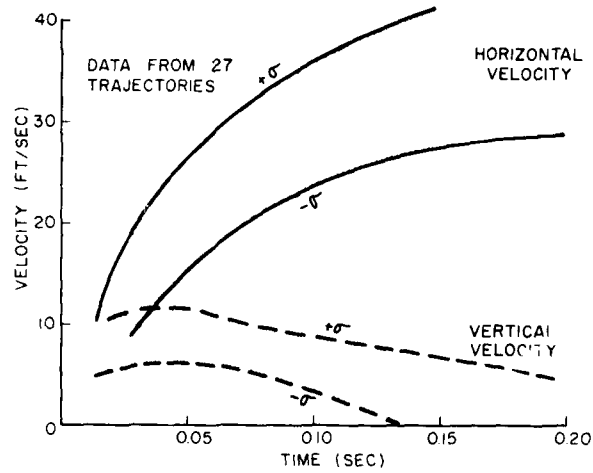


Figure 4.3(b). Bounds of velocity-versus-time plots for roof panels from sheltered buildings (rows 2 through 8 of complex); Operation SNOWBALL.

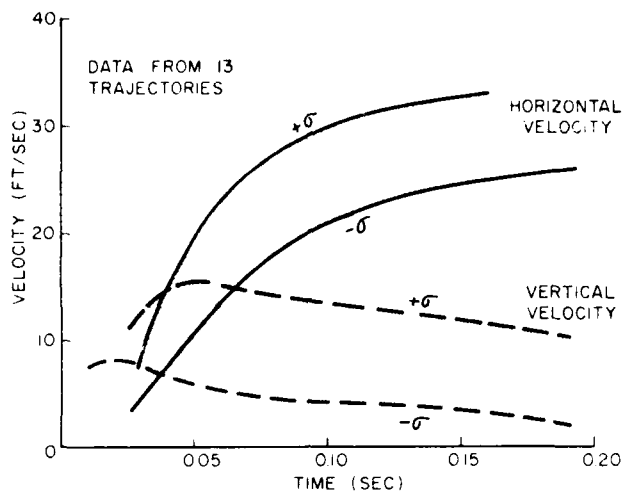


Figure 4.4(a). Bounds of velocity-versus-time plots for roof rafters from exposed buildings; Operation SNOWBALL.

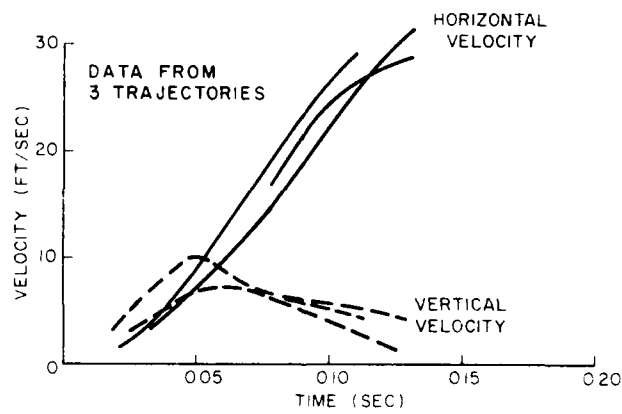


Figure 4.4(b). Velocity-versus-time plots for roof rafters from sheltered buildings; Operation SNOWBALL.

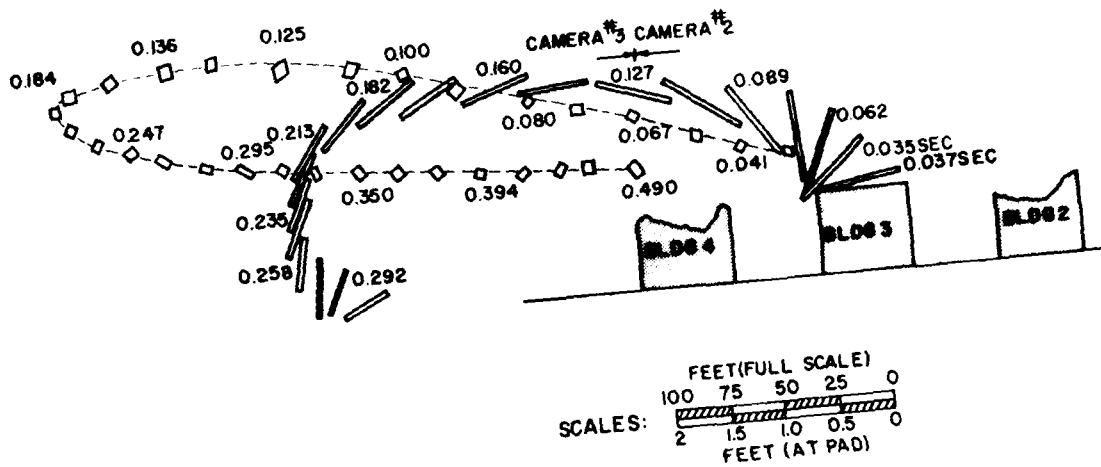


Figure 4.5(a). Roof-panel and roof-rafter trajectories, DISTANT PLAIN, Event 2a, 1/50-scale buildings; high-overpressure site.

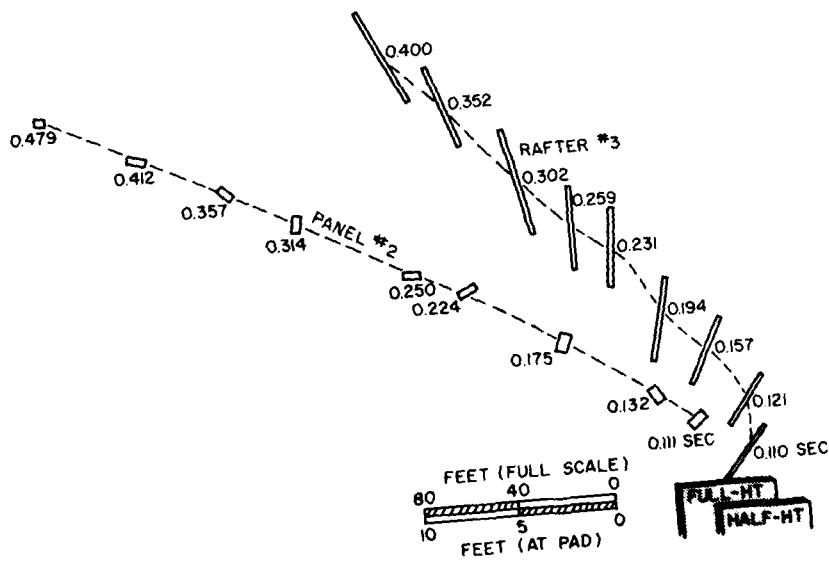


Figure 4.5(b). Roof-panel and roof-rafter trajectories, PRAIRIE FLAT 1/8-scale buildings; high-overpressure site.

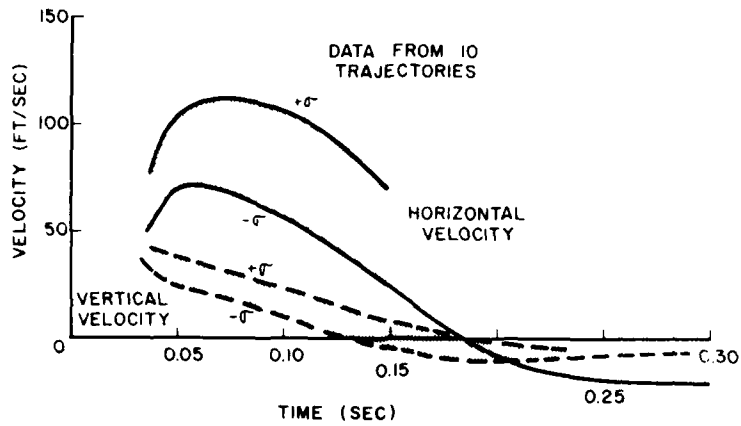


Figure 4.6(a). Bounds of velocity-versus-time plots for roof panels from 1/50-scale buildings; DISTANT PLAIN, Event 2a, high-overpressure site.

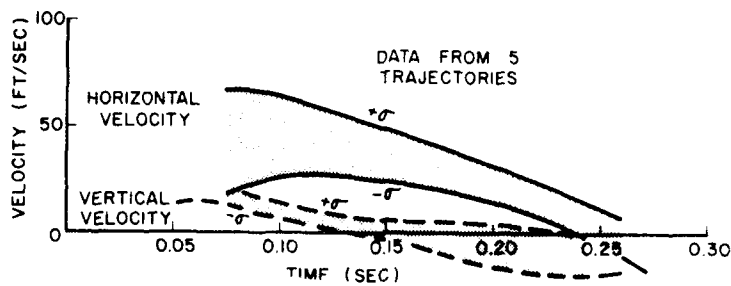


Figure 4.6(b). Bounds of velocity-versus-time plots for roof rafters from 1/50-scale buildings; DISTANT PLAIN, Event 2a, high-overpressure site.

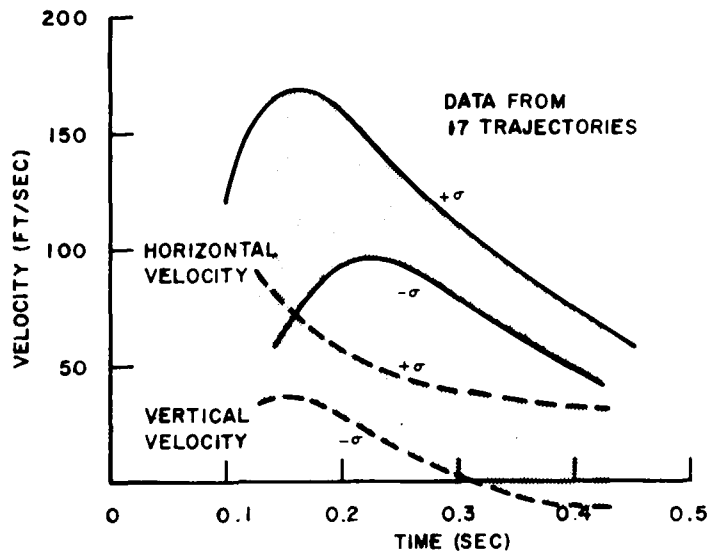


Figure 4.7(a). Bounds of velocity-versus-time plots for roof panels from 1/8-scale buildings; PRAIRIE FLAT high-overpressure site.

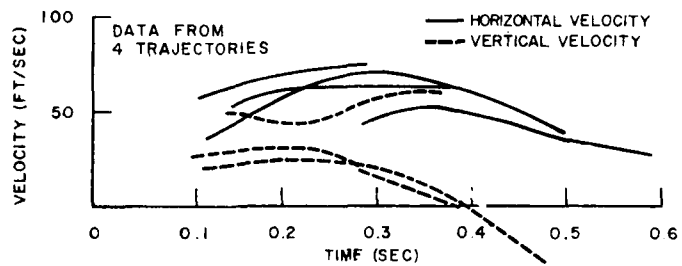


Figure 4.7(b). Velocity-versus-time plots for roof rafters from 1/8-scale buildings; PRAIRIE FLAT high-overpressure site.

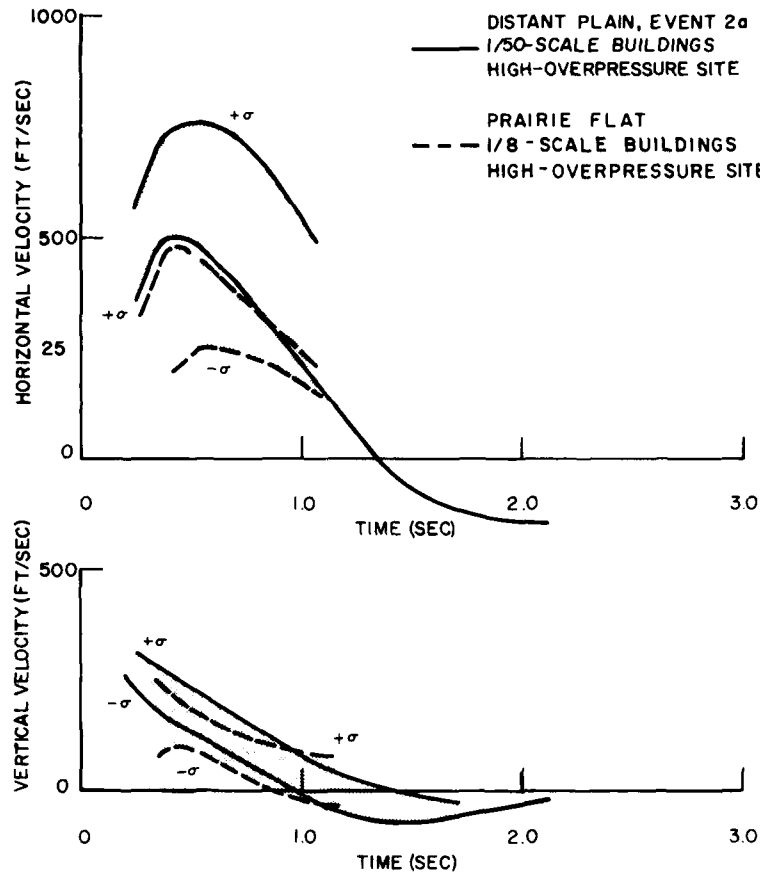


Figure 4.8. Comparison of full-scale velocity-versus-time bounds; DISTANT PLAIN, Event 2a, 1/50-scale buildings and PRAIRIE FLAT 1/8-scale buildings, high-pressure sites.

would have caused higher debris velocities in DISTANT PLAIN, which Figure 4.8 shows was the case.

The difference in simulated weapon yield indicates that the simulated blast duration should have been about 20 percent longer in DISTANT PLAIN than in PRAIRIE FLAT. This effect is not obvious in the data of Figure 4.8.

#### 4.1.4 DISTANT PLAIN, Event 2a, 1/50-Scale Buildings and PRAIRIE FLAT 1/8-Scale Buildings; Low-Overpressure Sites

Figures 4.9(a) and (b) show the trajectories of debris from these two experiments. Only two panels and one rafter were recorded in flight in the DISTANT PLAIN test; winds blew most of the roof panels away before the blast. Figure 4.10 shows the velocity-versus-time plots for these trajectories.

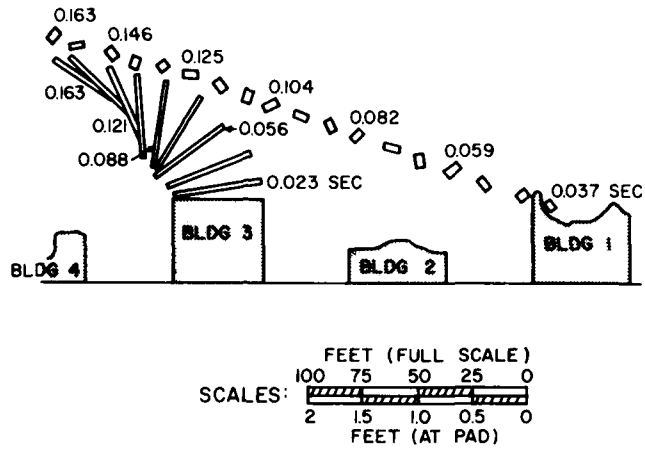


Figure 4.9(a). Roof-panel and roof-rafter trajectories, DISTANT PLAIN, Event 2a, 1/50-scale buildings; low-overpressure site.

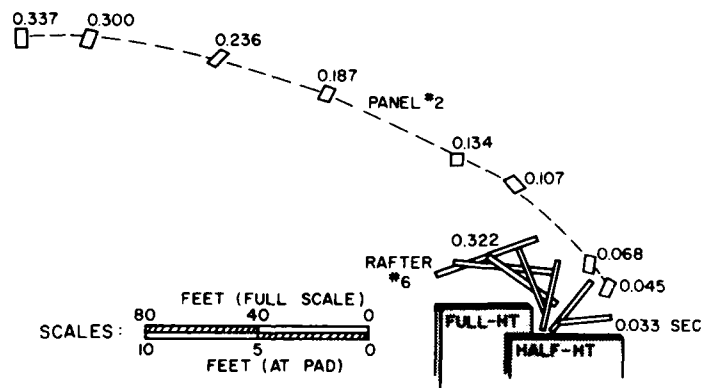


Figure 4.9(b). Roof-panel and roof-rafter trajectories, PRAIRIE FLAT 1/8-scale front block buildings; low-overpressure site.

The 1/8-scale models at the PRAIRIE FLAT low-overpressure site included two buildings with frame walls along with the block-wall buildings. Figure 4.11(a)

shows the velocity bounds for roof-panel debris from the frame models, and Figure 4.11(b) shows corresponding results for roof-panel debris from the block models.

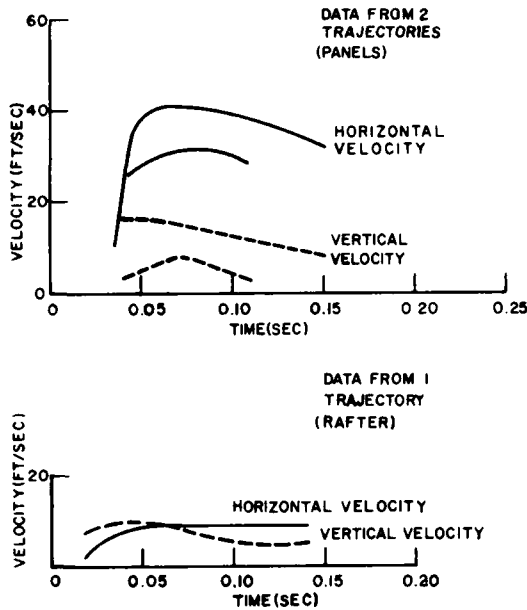


Figure 4.10. Velocity-versus-time plots for roof panels and one roof rafter from 1/50-scale buildings; DISTANT PLAIN, Event 2a, low-overpressure site.

The upper-horizontal-velocity bound and the vertical velocity bounds are lower for debris from the frame-building roofs than for debris from the block-building roofs. Lower vertical velocities for roof debris from the frame buildings would be expected: The frame walls collapse more quickly than the block walls, thereby disturbing the blast wave a shorter time. There is no apparent reason for the difference in horizontal velocities.

Since only one rafter was recorded in flight, no comparison of results for this kind of debris is possible.

Figure 4.12 shows the velocity bounds for debris from the PRAIRIE FLAT 1/8-scale block buildings and for debris from the DISTANT PLAIN 1/50-scale

block buildings. The velocity-versus-time graphs have been converted to the simulated full-scale values. From Table 1.3, the DISTANT PLAIN test simulated a 0.13-MT explosion resulting in a peak free-field overpressure of 19 psi at the low-overpressure model site; the PRAIRIE FLAT test simulated a 0.07-MT explosion and a peak overpressure of 10 psi. The full-scale air velocity at the DISTANT PLAIN site should have been about 60 percent greater than that at the PRAIRIE FLAT site, with correspondingly greater trajectory velocities. A comparison of the results in Figure 4.12 does not reveal this. The simulated blast duration in DISTANT PLAIN should have been about 20 percent longer than that in PRAIRIE FLAT, and Figure 4.12 does indicate this trend. Comparisons between these particular tests have limited value, unfortunately, because only two trajectories — a very poor statistical sample — were recorded in the DISTANT PLAIN event.

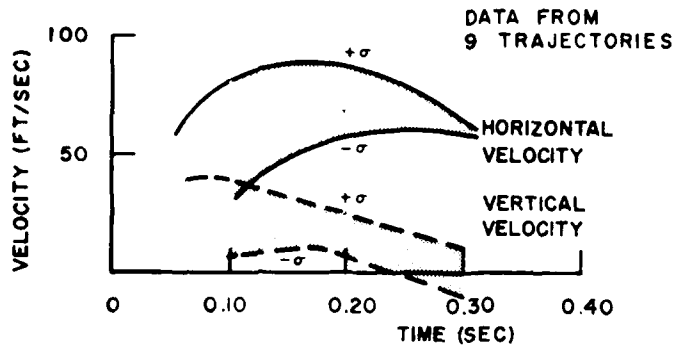


Figure 4.11(a). Bounds of velocity-versus-time plots for roof panels from 1/8-scale frame buildings; PRAIRIE FLAT low-overpressure site.

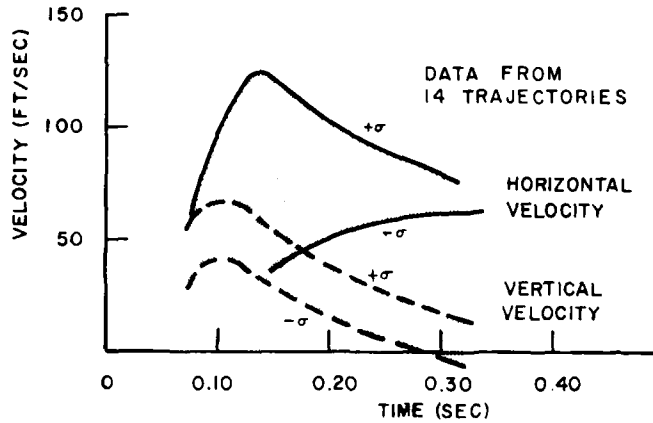


Figure 4.11(b). Bounds of velocity-versus-time plots for roof panels from 1/8-scale block buildings; PRAIRIE FLAT low-overpressure site.

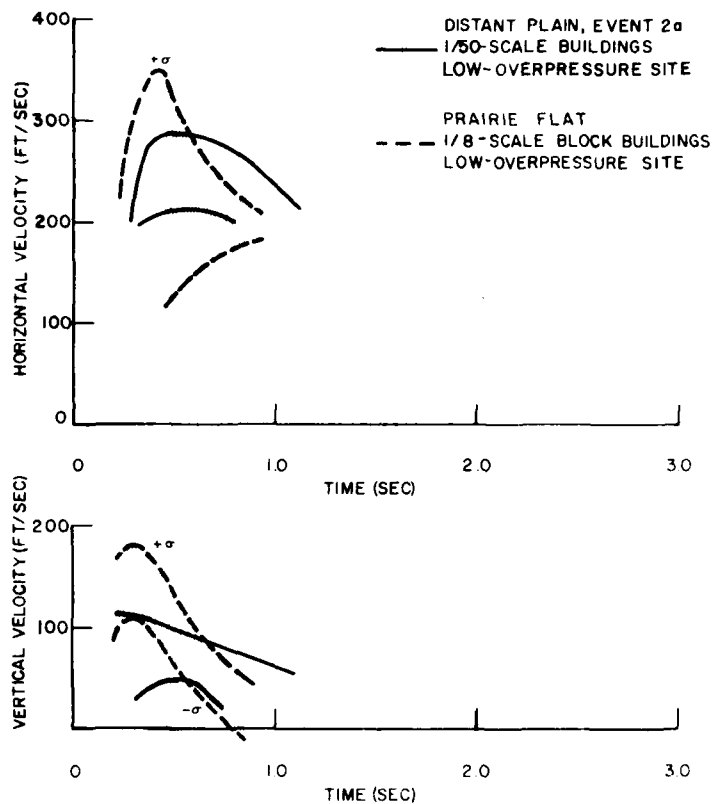


Figure 4.12. Comparison of full-scale velocity-versus-time plots, DISTANT PLAIN, Event 2a, 1/50-scale buildings, and bounds, PRAIRIE FLAT 1/8-scale block buildings, low-overpressure site.

#### 4.1.5 DISTANT PLAIN, Event 2a, 1/140-Scale Buildings and PRAIRIE FLAT 1/20-Scale Buildings

A comparison was made between the very small (1/140-scale) block buildings used in DISTANT PLAIN, Event 2a, and the 1/20-scale block buildings in PRAIRIE FLAT. Figure 4.13(a) shows roof-panel and rafter trajectories observed in the DISTANT PLAIN test; Figure 4.13(b) shows corresponding results from PRAIRIE FLAT.

It was possible to join two camera records taken during the DISTANT PLAIN test to obtain virtually complete trajectories for several pieces of debris. The rafter trajectory in Figure 4.13(a) clearly shows the turnaround caused by the negative phase of the blast.

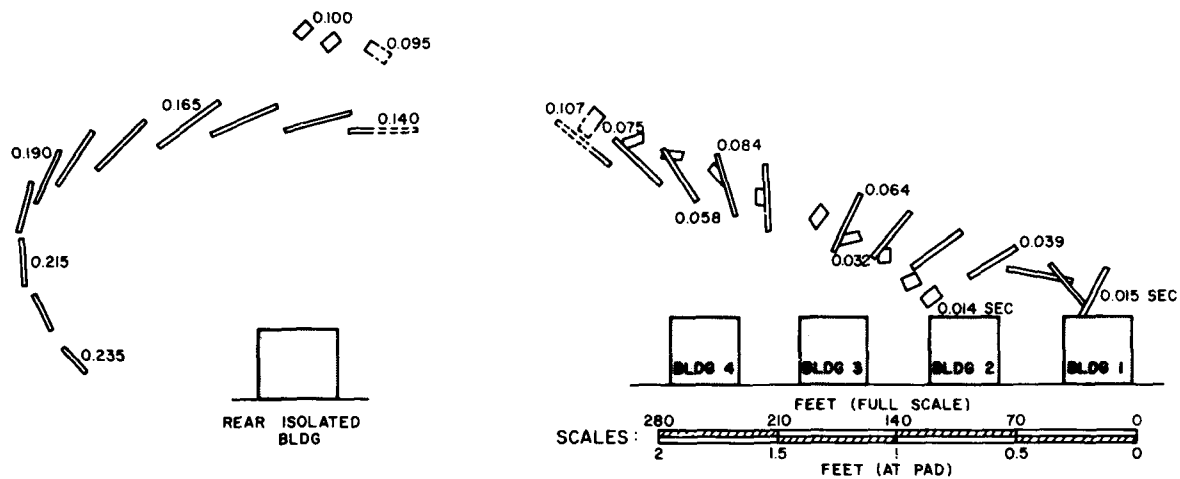


Figure 4.13(a). Roof-panel and roof-rafter trajectories, DISTANT PLAIN, Event 2a, 1/140-scale buildings.

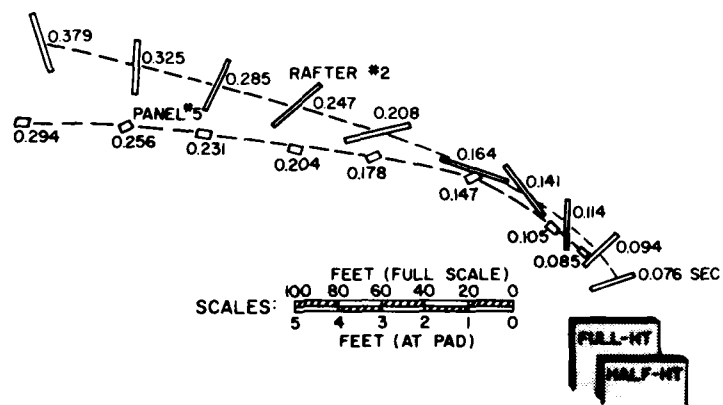


Figure 4.13(b). Roof-panel and roof-rafter trajectories, PRAIRIE FLAT 1/20-scale front buildings.

Figure 4.14(a) shows the  $\pm 1\sigma$  bounds of the velocity-versus-time plots for roof panels from the 1/140-scale DISTANT PLAIN buildings. Figure 4.14(b) shows the two velocity-versus-time plots for the only rafters that were observed in flight from these buildings. These curves fall within the bounds of data for the roof panels — a similarity not evident in Figures 4.15(a) and (b), which show comparable data for the 1/20-scale PRAIRIE FLAT models. Figure 4.16, in which the DISTANT PLAIN and PRAIRIE FLAT data have been converted to full-scale conditions, permits comparison of the velocity-versus-time results from the two events.

Table 1.3 shows that DISTANT PLAIN, Event 2a, simulated a 1.8-MT explosion producing 37 psi peak free-field overpressure; PRAIRIE FLAT simulated a 0.8-MT explosion producing 19 psi overpressure at the 1/20-scale-building site. The simulated air velocity in DISTANT PLAIN should have been about 70 percent greater than that in PRAIRIE FLAT, and the blast duration in DISTANT PLAIN should have been about 30 percent greater. There is some evidence that the DISTANT PLAIN simulated air velocity was higher, but not nearly by a margin of 70 percent; the velocity waveform in Figure 4.16, however, does show some evidence that the DISTANT PLAIN blast duration was greater.

Table 1.3 also shows that the simulated overpressure at the rear location of 1/50-scale buildings in DISTANT PLAIN was about the same as that at the 1/20-scale building site in PRAIRIE FLAT — about 20 psi. One would expect similar peak trajectory velocities in both cases. The values of the  $\pm 1\sigma$  velocity bounds, converted to full-scale units, are:

	<u>DISTANT PLAIN</u> (ft/sec)	<u>PRAIRIE FLAT</u> (ft/sec)
+ $\sigma$	300	500
- $\sigma$	200	300

This comparison is not conclusive, because the DISTANT PLAIN values are based on the observation of only two trajectories.

#### 4.2 Debris Clouds

Many of the model buildings were blown apart into so many pieces that it was impossible to trace individual trajectories. The walls of the DIAL PACK building, for example, were constructed much like the roofs and generated as much debris. Debris appeared on the high-speed film as clouds of building elements with which individual pieces could not be followed.

An alternative method of studying debris in flight, therefore, was to study the debris clouds. An imaginary grid was constructed in a vertical plane passing

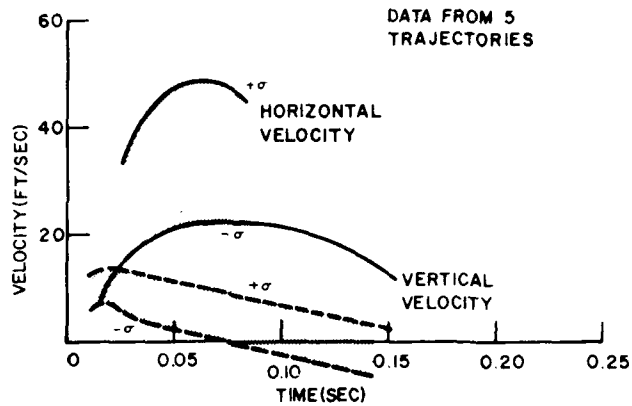


Figure 4.14(a). Bounds of velocity-versus-time plots for roof panels from 1/140-scale buildings; DISTANT PLAIN, Event 2a.

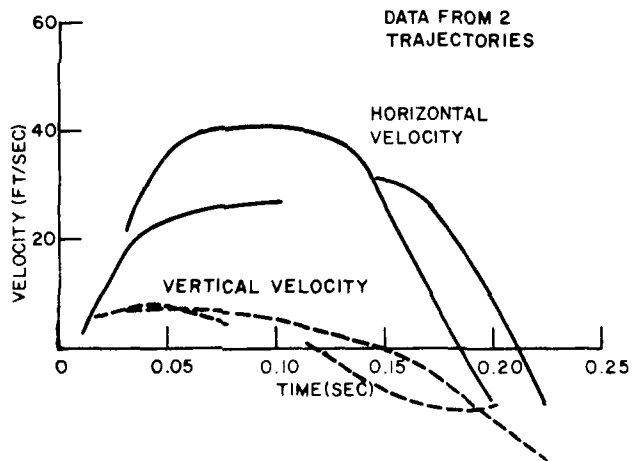


Figure 4.14(b). Velocity-versus-time plots for roof rafters from 1/140-scale buildings; DISTANT PLAIN, Event 2a.

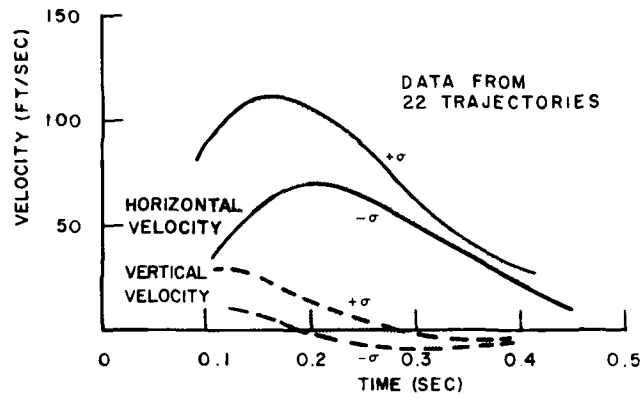


Figure 4.15(a). Bounds of velocity-versus-time plots for roof panels from 1/20-scale buildings; PRAIRIE FLAT.

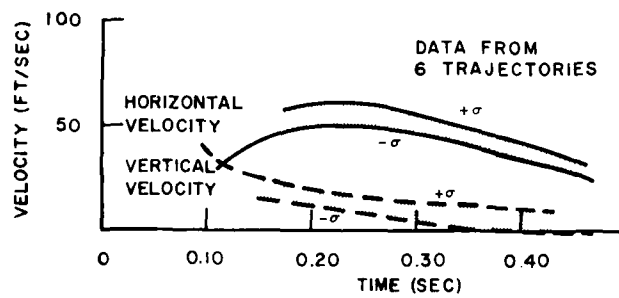


Figure 4.15(b). Bounds of velocity-versus-time plots for roof rafters from 1/20-scale buildings; PRAIRIE FLAT.

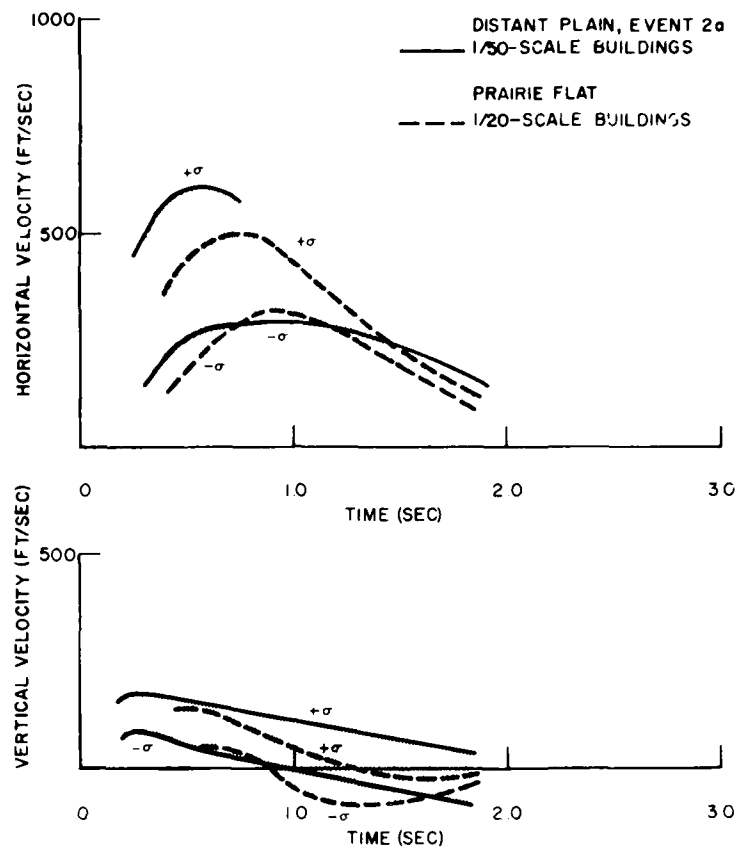


Figure 4.16. Comparison of full-scale velocity-versus-time bounds; DISTANT PLAIN, Event 2a, 1/140-scale buildings and PRAIRIE FLAT 1/20-scale buildings.

through the model buildings and ground zero. This grid, superimposed on the film frames, made it possible to count the number of pieces in the various grid squares at given times. A series of such grid counts thus approximated the travel of the debris cloud as the blast wave passed over the model buildings. Data were recorded until debris started leaving the field of view.

#### 4.2.1 DIAL PACK 1/120-Scale Buildings

The two DIAL PACK sites consisted of pairs of model buildings arranged in line at the crest of the slope, on the slope, and below the slope. Film records taken from the side show only one building at each position: the second building of each pair is hidden behind the first. (Figure 2.22 is a plan view that shows the model layout at this site.) The imaginary vertical grid running longitudinally along the pad was divided into 4-inch squares, equivalent to 40-foot squares in full scale.

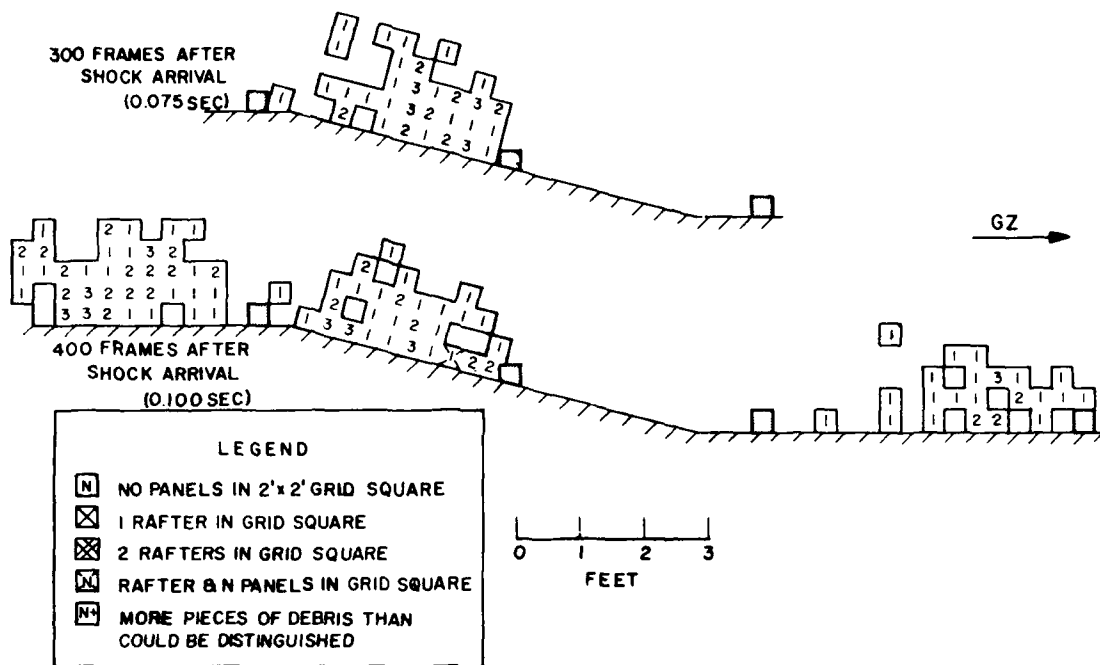


Figure 4.17. Airborne debris projected on a vertical plane: DIAL PACK 1/120-scale buildings.

Figure 4.17 shows the debris-cloud approximations at two times after the arrival of the blast wave. The top view shows the cloud, at 300 (film) frames after shock arrival, from the pair of buildings on the slope; the bottom view shows clouds from the buildings at the top, those on the slope, and those forward of the foot of the slope at 400 frames after shock arrival. (The buildings at the foot of the slope were not in proper camera view.)

The debris cloud from the buildings in front of the slope is similar to that from the buildings on the slope. The cloud from the buildings at the top of the slope shows that more debris traveled a bit higher and farther from these buildings.

Considerably fewer pieces of debris were generated from the 1/120-scale models than were generated from the 1/20-scale models, and it was possible to observe a few individual trajectories. These are included in Appendix J. One panel — apparently from a roof — followed a trajectory similar to those of the roof panels from buildings in Operation SNOWBALL. Another panel, which was observed to have come from a wall, accelerated more rapidly than any of the debris observed in the SNOWBALL test.

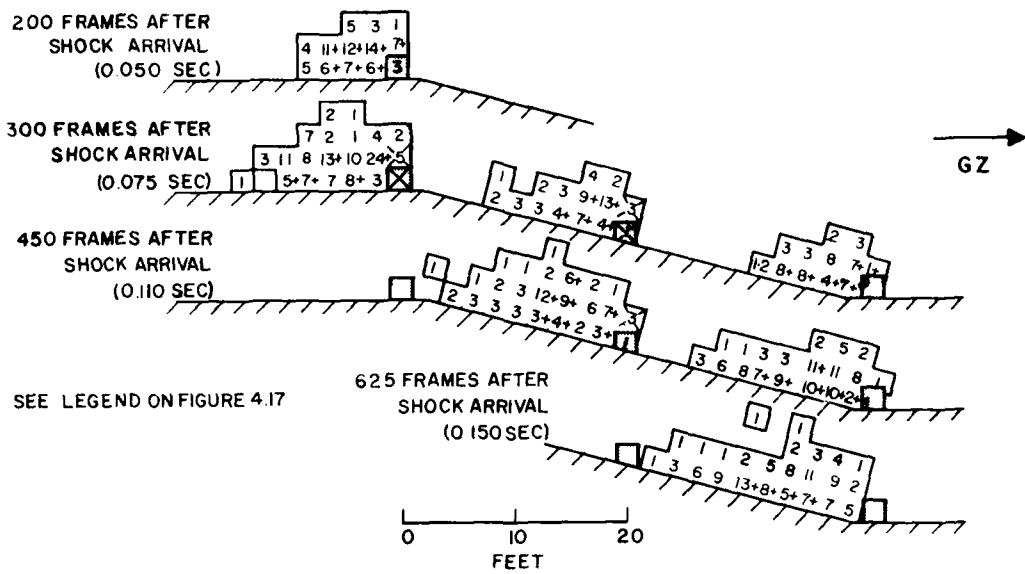


Figure 4.18. Airborne debris projected on a vertical plane: DIAL PACK 1/20-scale buildings.

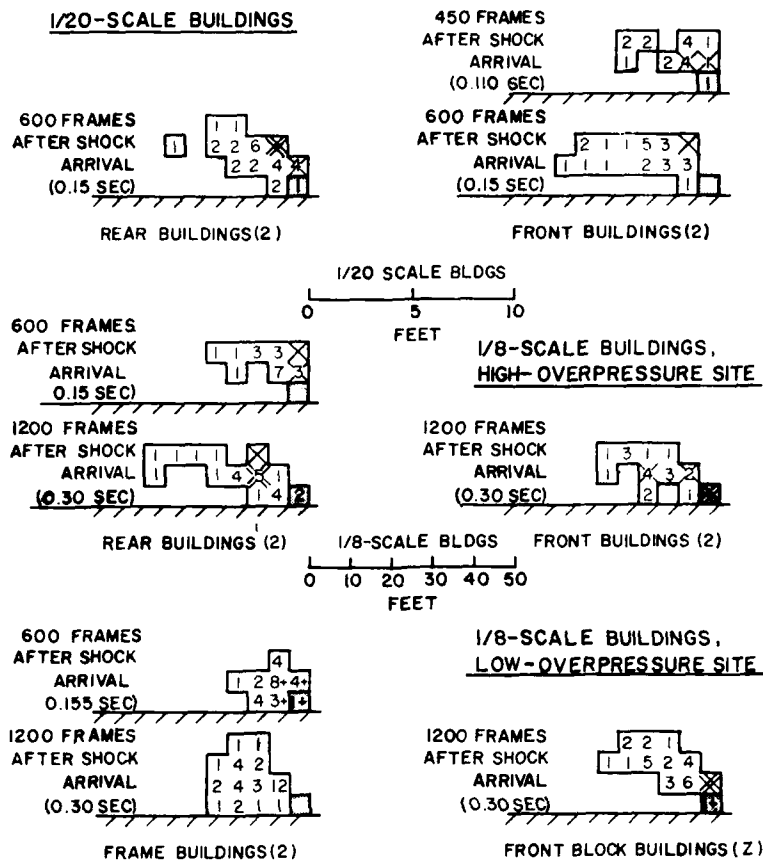
#### 4.2.2 DIAL PACK 1/20-Scale Buildings

Figure 4.18 shows the debris-cloud approximations at various times after the arrival of the blast wave. At this site the pair of buildings at the top of the slope, on the slope, and at the foot of the slopes were the ones observed by the cameras. It was possible to get data from all three pairs of buildings at 300 frames after shock arrival. At other times, it was possible to obtain data from only one or two of the three sites.

The debris cloud from the buildings at the base of the slope at 300 frames after shock arrival is similar to that from the buildings on the slope, as was true for the smaller models. Likewise, the cloud from the buildings at the top of the slope shows that the debris tended to travel higher and farther from these buildings. At 450 frames after shock arrival, there appears to be a greater difference between the debris clouds from the buildings at the foot of the slope and those on the slope; debris transport seems to be retarded by deflection of the blast flow at the foot of the slope.

#### 4.2.3 PRAIRIE FLAT 1/8- and 1/20-Scale Buildings

The PRAIRIE FLAT data already have been discussed. To obtain a check on the validity of the "debris cloud" concept used in DIAL PACK, the PRAIRIE FLAT data were converted to the same vertical-grid format. Figure 4.19 shows the results of this recasting of data.



SEE LEGEND ON FIGURE 4.17

Figure 4.19. Airborne debris projected on a vertical plane; PRAIRIE FLAT building sites.

Direct comparisons are possible between the 1/20-scale buildings in the two experiments, because the models were of the same size, at the same range from ground zero, and subjected to the same blast magnitude and resulting overpressure. The amounts of debris carried two and three building heights above ground were similar at the two sites. This is to be expected, since most of the debris at these heights probably consisted of lofted roof elements in both cases. Differences appear at lower elevations, where most of the DIAL PACK wall debris was observed. The DIAL PACK wall debris appeared to travel farther in the same time period than debris from the roof, probably because the wall elements were lighter and because they were not subjected to lofting to the degree that the roof elements were.

Figure 4.19 also shows the approximate debris clouds constructed for the 1/8-scale PRAIRIE FLAT buildings. The roof debris from these models followed the same tendency as debris from the 1/20-scale models: Regardless of scale, roof debris was lofted two to three building heights above ground.

## Chapter 5

### SUMMARY, CONCLUSIONS, AND RECOMMENDATIONS

#### 5.1 Hazard Prediction

The principal objective of all tests discussed in this report was to provide information that would aid in the prediction of debris hazards under nuclear-blast conditions — how far debris will travel, what form its trajectories will take, and how it is distributed. These kinds of information were obtained, with varying degrees of success, from scale-model buildings exposed to high-explosive simulated nuclear blasts in Operation SNOWBALL, Operation DISTANT PLAIN, Event PRAIRIE FLAT, and Event DIAL PACK at the Suffield Defense Research Establishment, Alberta, Canada, and Event SOTRAN at the White Sands Proving Grounds, New Mexico.

##### 5.1.1 Relating Model Elements to Real Materials

Determining how far debris will travel in a blast wave, an important aspect of hazard prediction, is achieved by scaling measured distances at the test site up to full size. Table 1.3 shows scaling factors, simulated blast yields, and peak overpressures. It would be important also, however, to know what real materials the model debris particles represented in full scale — that is, how the simulated full-scale debris densities or specific gravities compared with those of real building materials.

The relationships shown in Table 1.2 require that the ratios of the scale-model debris densities to those of their full-scale equivalents be the same as the ratios of the experimental peak air-blast densities to those of the simulated full-scale air-blast densities. The experiments were designed to satisfy this requirement, but Table 5.1, which summarizes the model and derived full-scale specific gravities, shows that constant values were not always attained. Simulated full-scale specific gravities for wall blocks ranged from 1.5 to 2.2, reasonably close to that of medium-hard brick (1.9). The simulations of frame construction, however, were not as good: Simulated full-scale specific gravities of roof panels ranged between 0.42 and 3.8, based upon a 1-inch-thick full-scale panel; the specific gravity of 3/4-inch plywood with some roofing material attached probably would range between 0.5 and 1.

Table 5.1  
SUMMARY OF SPECIFIC GRAVITIES OF MODEL ELEMENTS

Test	Bldg. Scale	Peak Over-Pressure (psi)	Wall Type	Specific Gravity of Model			$\rho_f/\rho_o$ (test)	$\rho_f/\rho_o$ (simulated)	Simulated (full-scale) Specific Gravities			$u_f/c_o$ (simulated)
				Wall Block	Roof* Panel	Wall* Panel			Wall Block	Roof* Panel	Wall* Panel	
SNOWBALL	1/120	1	Block	1.17	2.30	-	1.05	1.73	1.9	3.8	-	0.60
DISTANT PLAIN	1/140	1.7	Block	0.96	0.92	-	1.08	2.27	2.0	1.9	-	1.08
	1/50	1.7	Block	1.34	1.08	-	1.08	1.77	2.2	1.81	-	0.63
	1/50	3	Block	0.94	0.36	-	1.14	2.23	1.8	0.71	-	0.98
White Sands	1/33	2	Block	1.31	1.11	-	1.10	1.70	2.0	1.7	-	0.58
	1/33	3	Block	0.94	1.11	-	1.14	2.03	1.70	2.0	-	0.81
PRAIRIE FLAT	1/120	1	Block	1.17	0.92	-	1.05	1.73	1.9	1.5	-	0.60
	1/20	3	Block	1.12	0.42	-	1.14	1.77	1.8	0.66	-	0.63
	1/8	6	Block	0.97	0.33	-	1.26	1.97	1.5	0.52	-	0.76
	1/8	3	Block	1.34	0.33	-	1.14	1.45	1.7	0.42	-	0.39
	1/8	3	Frame	-	0.33	0.33	1.14	1.45	-	0.42	0.42	0.39
DIAL PACK	1/120	1	Frame	-	1.37	1.37	1.05	1.73	-	2.2	2.2	0.60
	1/20	3	Frame	-	0.55	0.20	1.14	1.77	-	0.86	0.28	-

\*Based upon 1-inch thickness, full scale. The equivalent model panel thickness is the scaling factor; e.g., SNOWBALL roof panels were 1/120-inch thick.

It was not always possible to find suitable materials for the models, especially the smaller ones. The roof panels were required to be so light that weights were necessary to keep them in place. On those models that incorporated frame walls, the simulated full-scale specific gravities of wall panels ranged between 0.42 and 2.2; a practical real value would be about 0.5.

### 5.1.2 Predicted Bounds of Roof-Debris Distributions

Figure 5.1 shows the radial displacement (distances along a radius from ground zero) of roof panels, converted to full scale and plotted versus the simulated nuclear weapon yield. The solid symbols represent the greatest observed distances traveled from the building of origin; the open symbols represent values obtained from integration of the velocity curves in Chapter 4. (The  $1\sigma$  bounds were used wherever possible.) Integration was carried out until velocity reached zero, which indicated the maximum travel distance; no negative travel was considered.

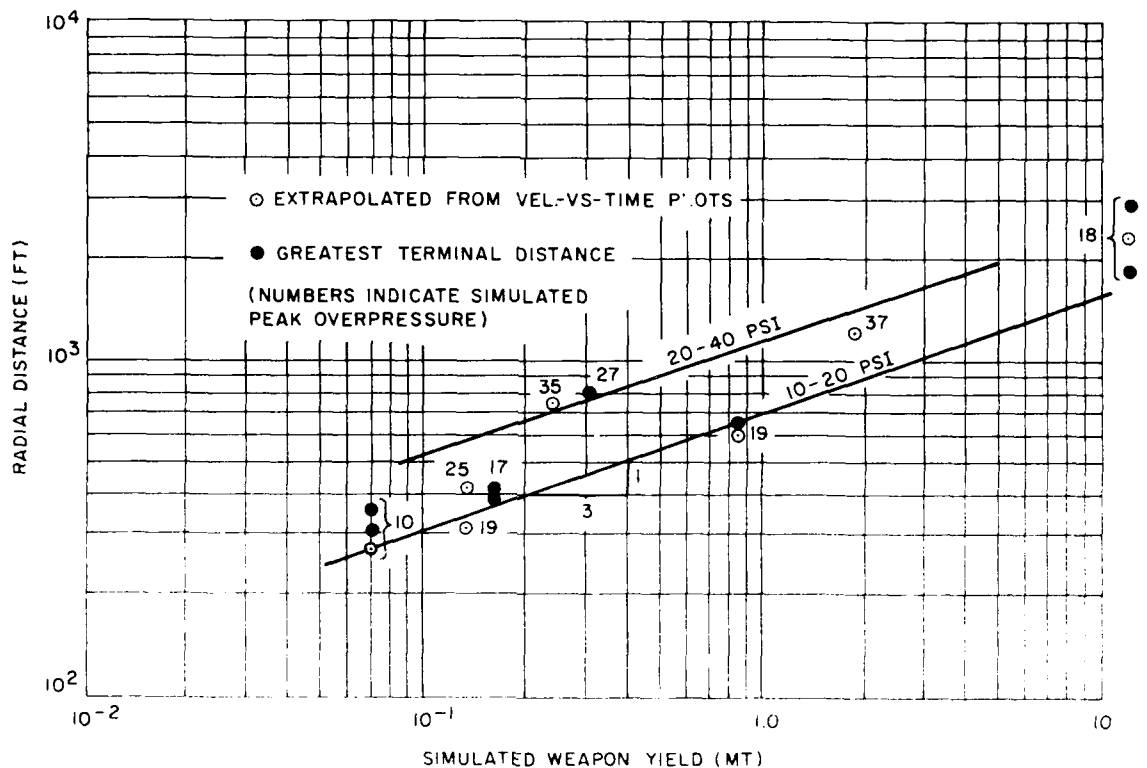


Figure 5.1. Maximum full-scale radial distances between roof-panel terminal locations and buildings of origin.

The maximum observed distances correlate well with the values obtained by integration. Radial distance tends to vary in direct proportion to the cube root of weapon yield, as does the blast duration. Maximum distance increases with increasing simulated overpressure, but data scatter prevents an accurate delineation of this relationship. One effect not evident on the figure is the variation of simulated debris density — by as much as a factor of 10.

Figure 5.2 shows the tangential spread (distances tangent to the blast front) of roof panels, plotted in the same format as that of Figure 5.1. One additional variable — the model-building height — was considered here. It appears that the tangential spread of debris depends only very little upon whether the building of origin was

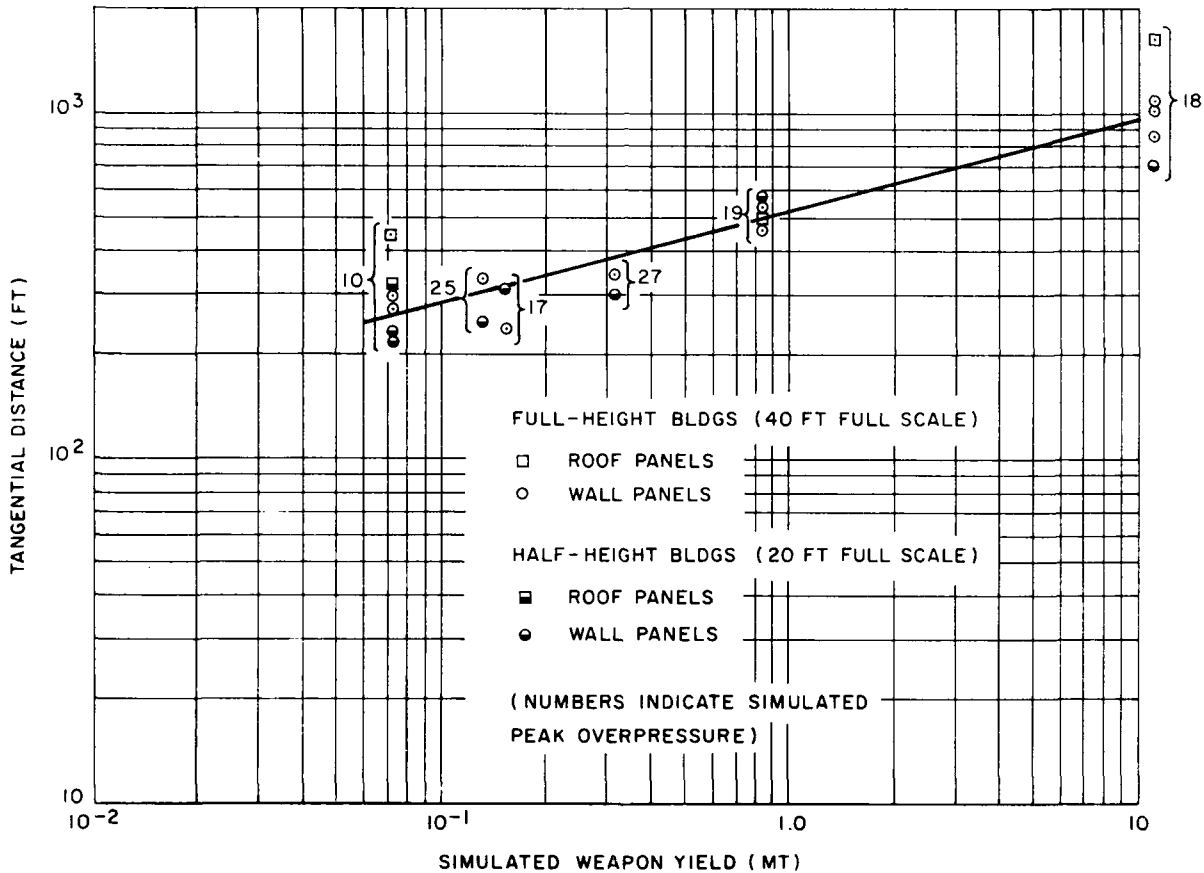


Figure 5.2. Maximum full-scale tangential distances between roof- and wall-panel terminal locations and buildings of origin.

a full-height or a half-height model; this agrees with the following postulated mechanism: Sideward (tangential) transport of debris is assumed to be related to the

lofting observed in high-speed film records — that is, the tendency of debris to be carried well above the building height. Two factors, then, tend to spread debris — (1) velocity imparted to the debris by disturbed blast conditions caused by the building of origin, and (2) lift effects that take place while the debris is in flight. The former factor should be independent of weapon yield, and the latter should be expected to vary with the blast duration (in other words, with the cube root of the weapon yield). The scatter of points on the figure indicates that the tangential spread of debris varied approximately with the fourth root of the weapon yield. The magnitude of peak overpressure does not appear to have had a significant effect on debris spread, at least for this range of data.

### 5.1.3 Predicted Bounds of Block-Debris Distributions

Figure 5.3 shows the radial displacement of wall blocks, plotted in the same format as that of the previous figures. Two distance corrections were made here

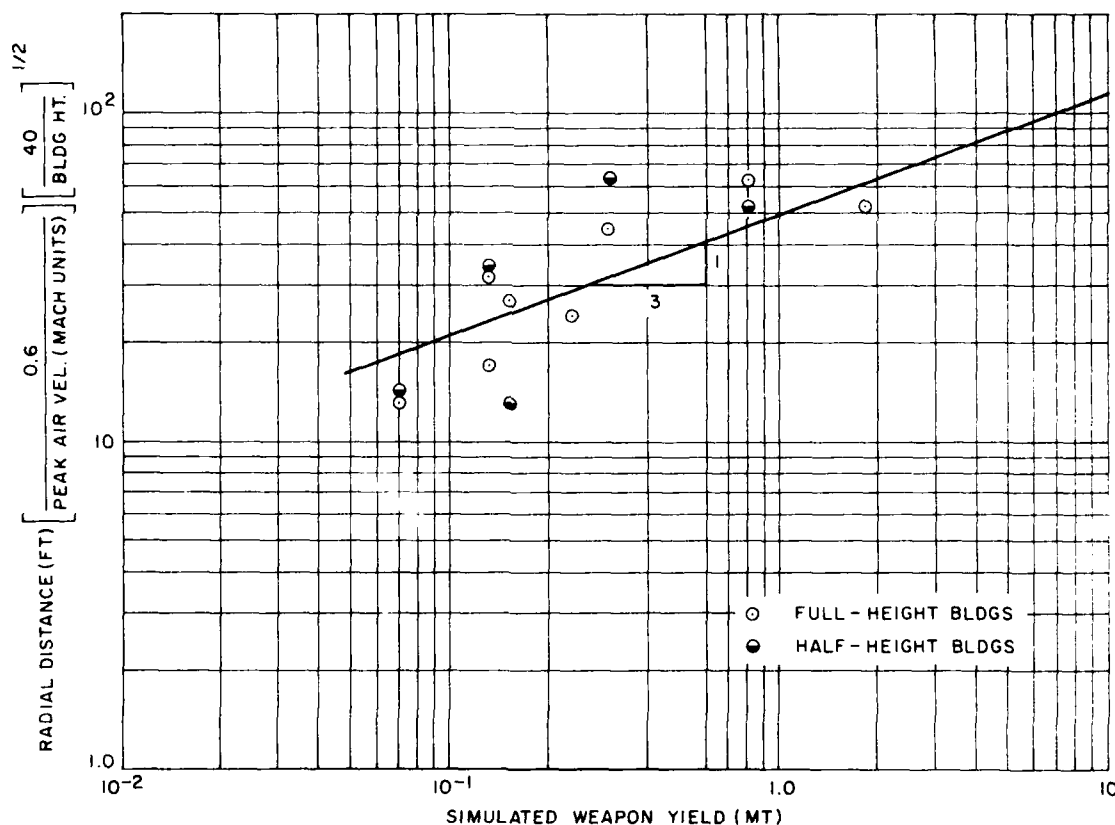


Figure 5.3. Maximum full-scale radial distances between wall-block terminal locations and buildings of origin.

so that all data could be represented by a single line: The radial distances were divided by the peak simulated air-blast velocity and by the square root of the building height. These corrections are based on the assumption that this type of debris rapidly reaches a peak velocity proportional to the air-blast velocity and that, subsequently, it undergoes free fall to earth. This assumption is an oversimplification; as a result, the data points still show considerable scatter. Reflected overpressure may have had some effect on debris travel, but the blocks displaced the farthest usually came from the edges of walls where the duration of reflected overpressure was short.

If the initial velocity of a block is assumed to result from an impulse, the peak velocity and, hence, the distance traveled, would be inversely proportional to the block's density. No correction was made here for simulated block density, however, because variations in model block density were small.

Figure 5.4 shows the tangential spread of wall blocks, the displacements again having been corrected as in Figure 5.3 to allow the representation of data by a single line. Less scatter appears here than in the previous figure. The line, which represents the average, is approximately proportional to the sixth root of the simulated weapon yield, rather than the fourth root, as was the case for roof-panel spread. This implies that lift, which is duration-dependent, had less of an effect on wall-block spread than on roof-panel spread — a conclusion that one is likely to draw intuitively.

The building-height correction (multiplying the tangential displacements by the square root of the building height) appears to have been reasonable, since the data for full-height and half-height buildings are nearly coincident.

Figures 5.1 through 5.4 permit the bounds of debris distributions to be determined for a variety of weapon yields and for typical kinds of debris. The corresponding peak overpressures, however, must be within the narrow range of 10 to 40 psi simulated in these tests. The information from the model tests that indicates how debris is distributed between these bounds is given in Chapter 3 and the appendices. Real buildings under blast conditions would not break up into discrete, uniform elements as the model buildings did; however, the data from the model tests can be used to estimate the distribution of assumed actual debris if the aerodynamic characteristics of such actual debris are similar to the characteristics of the model debris. For example, assume that a 10-MT nuclear blast producing a peak overpressure of 20 psi would tear about 5000 pieces of plywood from the roof of a masonry structure 20 feet high and 40 feet square in plan. These assumed full-scale conditions are similar to those simulated by the 1/120-scale half-height models in

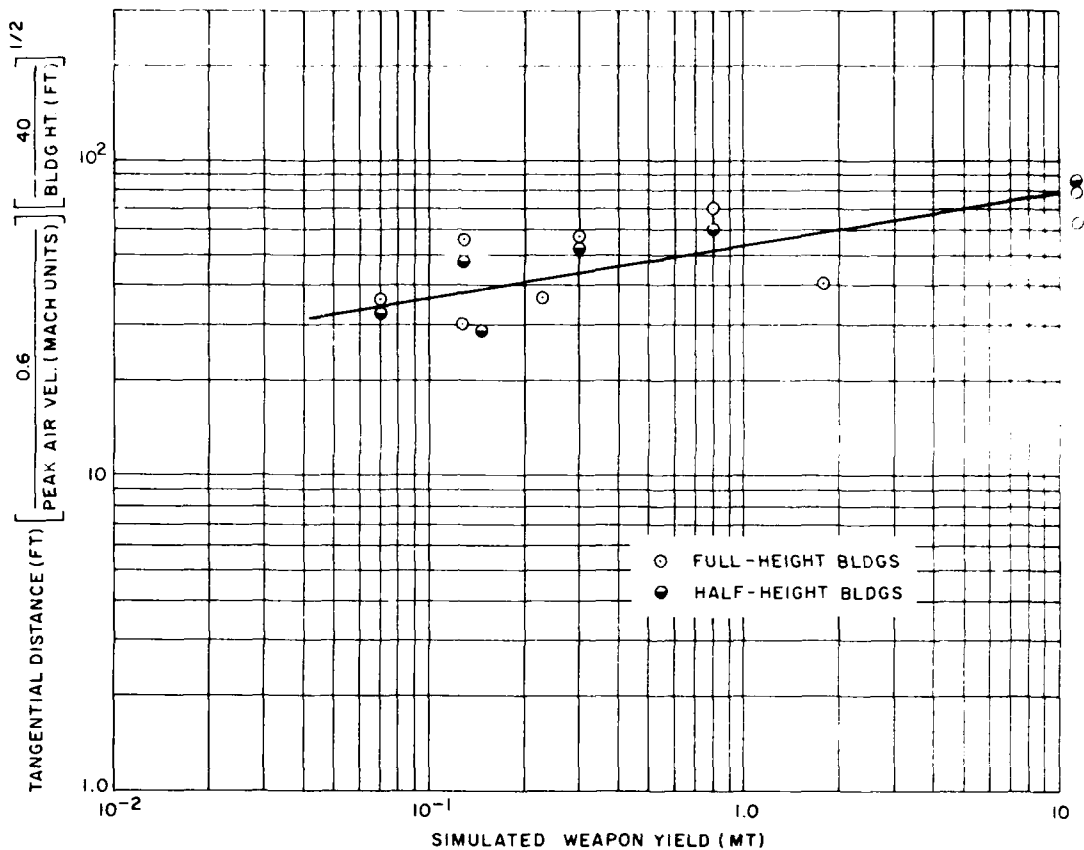


Figure 5.4. Maximum full-scale tangential distances between wall-block terminal locations and buildings of origin.

Event PRAIRIE FLAT. Figure 3.12 shows the distribution of 47 roof panels from building 15; each of these displaced model panels can be thought of as representing 100 pieces of actual debris from a real building. The distribution of actual debris, of course, would be spread out more uniformly over a similar full-scale area.

#### 5.1.4 Maximum Height of Debris Trajectories

As has been seen, debris can be lofted into high trajectories that may carry it to facilities well above the height of the debris source. The height to which debris travels, therefore, is another important aspect of hazard prediction.

What determines the height to which pieces of debris will travel? It is postulated that upward flight is initiated by vortices formed at the leading edge of a building as the blast wave passes. The lifting effect of these vortices is strongest on building elements near such leading edges — for example, roof panels near the side

of a building that faces the blast. Elements such as these were observed to have traveled the greatest distances in many instances during the scale-model tests.

A measure of the ultimate height attained by a piece of debris is its maximum vertical velocity.

Figure 5.5 shows ratios of maximum vertical debris velocities to peak air-blast velocity plotted versus simulated weapon yield. The maxima used were obtained directly from film records and from the  $+σ$  bounds of the data presented in Chapter 4. There is some indication that the velocity ratio depends upon debris

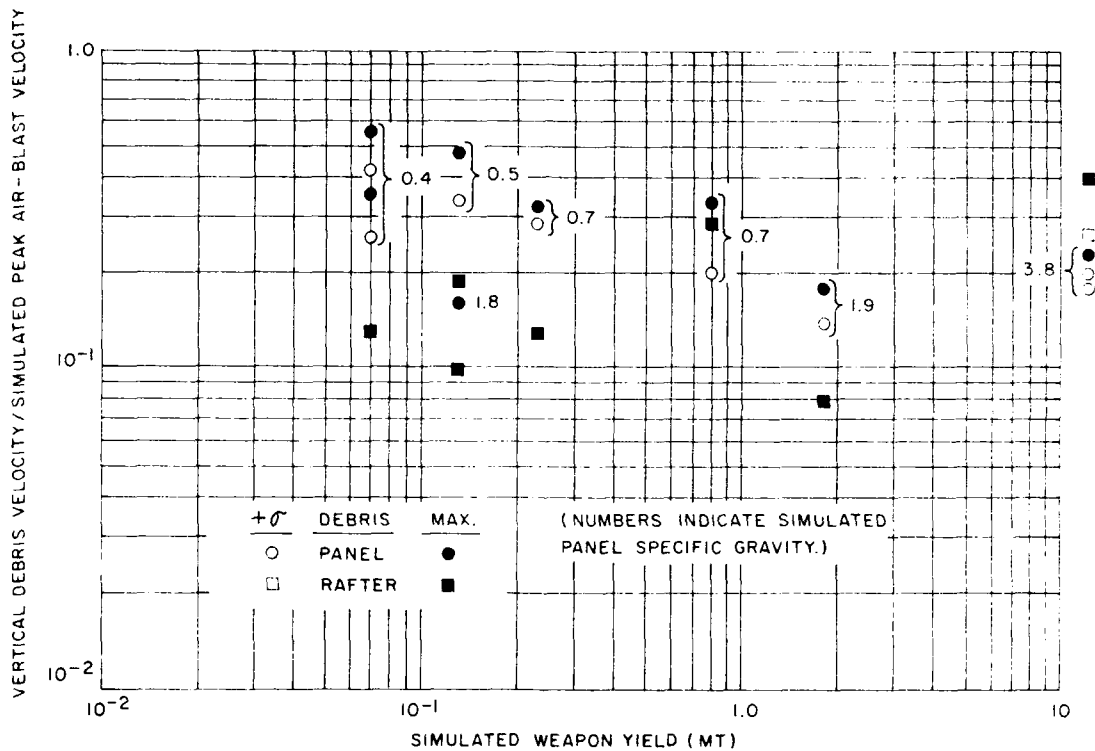


Figure 5.5. Ratios of maximum full-scale vertical debris velocities to simulated peak air velocity versus simulated weapon yield.

density (specific gravity) — a value of about 0.35 for specific gravities in the range of 0.4 to 0.7, and about 0.15 for a specific gravity of about 2.0. This is almost the inverse proportionality that would be expected if the debris were accelerated solely by an initial impulse. The data for the simulated 12-MT yield do not fit this trend, raising the possibility that both specific gravity and weapon yield influence vertical debris velocity. However, no consistent effect of yield is evident.

There is clearer evidence that weapon yield affects the maximum height to which debris will travel. Figure 5.6 shows data for the maximum trajectory height, converted to full scale, plotted versus simulated weapon yield. This figure also shows the effect of blast intensity; higher overpressures (air velocities) produce greater trajectory heights. Debris specific gravity also may have some effect, but data scatter masks it.

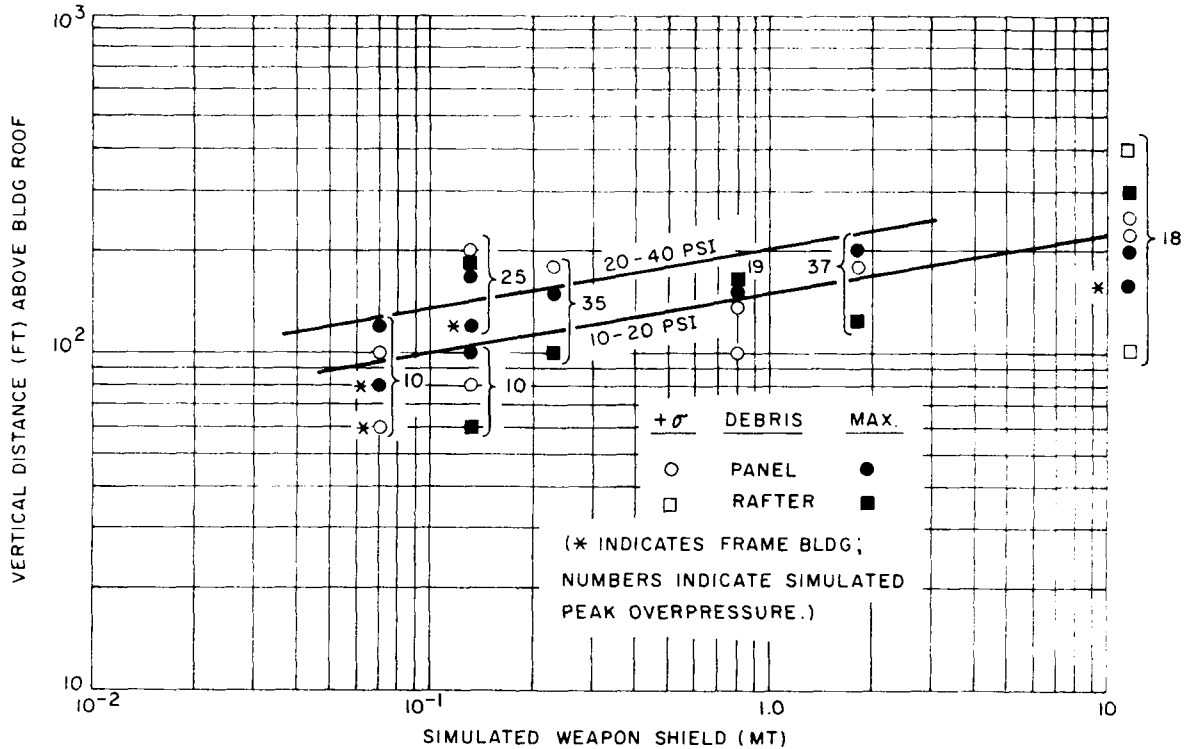


Figure 5.6 includes data from Event DIAL PACK in which trajectories were not plotted — where the number of pieces in flight at various times were determined from film records and plotted on imaginary vertical grids. (This is the "debris cloud" concept discussed in Chapter 4.)

#### 5.1.5 Influence of Site Factors on Debris Distribution

How do buildings in dense concentrations and buildings on or near sloping terrain react to blast? Results obtained from the complexes, where models were arranged in dense concentrations, show some evidence that outer buildings tend somewhat to shield those within the complex from the full force of the blast wave. Figure 5.7 illustrates this in simplified plan views of the SNOWBALL and PRAIRIE FLAT complexes. The boxes represent relative building positions, and the numbers within the boxes represent the maximum tangential spread of roof panels from each building in units of hundreds of feet. The spread of debris from buildings within each complex generally is lower than the spread from buildings at the front and rear and from the isolated buildings. There are exceptions: Two buildings well within the SNOWBALL complex had a spread of 1200 feet (full scale), which was exceeded only by one building in the front row. These anomalies may be the result of experimental inaccuracies or of wind damage that occurred before the test blast.

The maximum tangential spread of debris is the result of debris scattering caused by random lift forces. Debris scattering continues as long as debris is in flight — whether the post-blast air flow is away from or toward ground zero. Thus, the maximum tangential displacements are related to flight times. Maximum radial distances are strongly affected by the negative phase of the blast wave; in fact, the debris flights of longest duration may be of those pieces that are carried back by the negative phase and deposited near their buildings of origin.

Figure 5.8 shows that sloping terrain also has some effect on debris spread; this, in turn, implies that sloping terrain influences debris flight duration. At the DIAL PACK site that accommodated 1/20-scale models, the tangential debris spread from buildings at the base of the slope was not as great as those from the buildings on the separate flat pad, and the spread from the buildings at the top of the slope was greater than that from the buildings on the flat pad. These effects were not as pronounced for the 1/120-scale models. At both sites the tangential spread from buildings on slopes was about the same as that from buildings on flat terrain; this shows that the blast wave reorients itself in line with the slope as it travels along it. A slope like the one shown in Figure 5.8 offers no protection against debris unless the potential debris source is located right at the base of the slope.

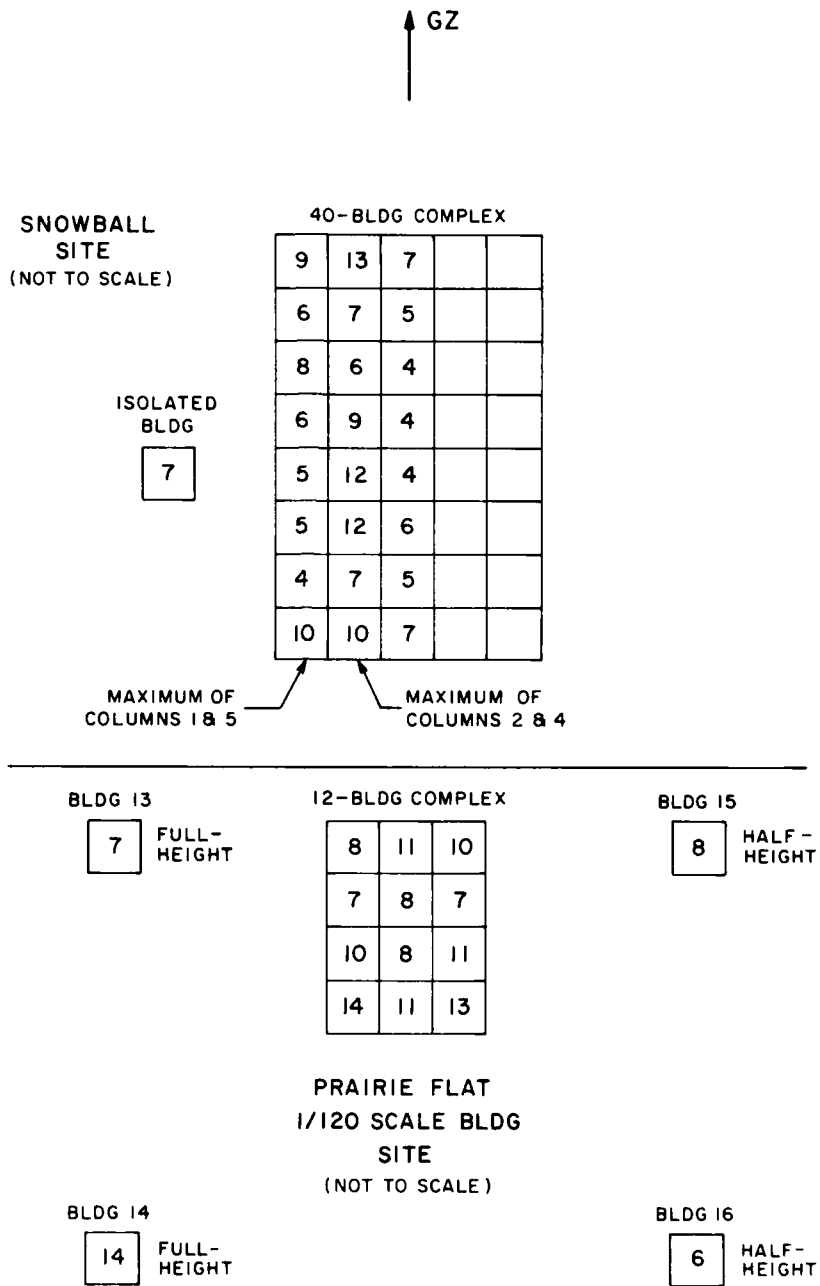


Figure 5.7. Maximum full-scale tangential distances between roof-panel terminal locations and buildings of origin; SNOWBALL and PRAIRIE FLAT 1/120-scale buildings.

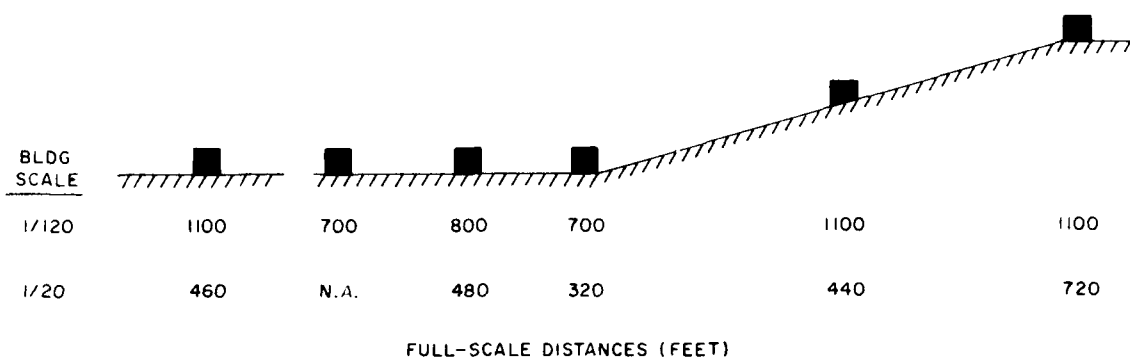


Figure 5.8. Maximum full-scale tangential distances between roof-panel terminal locations and buildings of origin; DIAL PACK 1/120-scale and 1/20-scale buildings.

## 5.2 Experimental Techniques

### 5.2.1 Model Construction

The methods of model-building construction that were developed during the course of these tests proved to be satisfactory and can be used in similar tests. Basically, the methods make use of weighted but completely separate roof panels and walls of interlocked blocks with cross-bracing or of frangible frame construction. Buildings with frame walls are more convenient to use than those with block walls, and, in general, they provide similar results.

### 5.2.2 Instrumentation and Data Collection

Since experience in the early tests showed that local winds could alter the distribution of deposited debris to an extent that would invalidate test results, plastic sheets weighted down with sand bags and other objects were used in the later tests to cover debris until weather conditions permitted debris collection. Debris was kept covered until it was logged. This procedure was crucial where very high winds prevailed after the test blast.

Filming techniques could be improved if similar tests are performed in the future. Had clearly visible distance marks been used near the models, it would have been possible to make more accurate linear measurements from the film frames. In several experiments, two buildings in line were viewed by a single camera. They were far enough apart to be distinguished by perspective on the film records, but the pieces of debris from them could not be distinguished with regard to building of origin on the film frames that showed them in flight. The cameras could have been

run slower, which would have permitted the use of films capable of better resolution. Color film has the advantage of allowing an observer to separate debris in flight from the background on film records.

An important consideration not included in these experiments is the time history of velocity and density in low-overpressure blast waves. Such information, which presently is not available, is necessary for an accurate determination of what full-scale blast conditions were simulated by the tests.

A technique using smoke trails or puffs to measure blast velocity was tried several times, without success. Actually, following the lightweight roof panels accomplished roughly the same thing. These elements did have finite mass, however, and were not accelerated instantly to the air-blast velocity. The air velocity and the horizontal debris velocity should be equal, though, where the debris velocity reaches its maximum; it is possible, therefore, to draw a line through the maxima of the various trajectories recorded in a given test and to then construct a curve from these maxima that approximates the actual air-velocity waveform. Figure 5.9 shows the results of doing this for the various tests. Velocities were divided by the

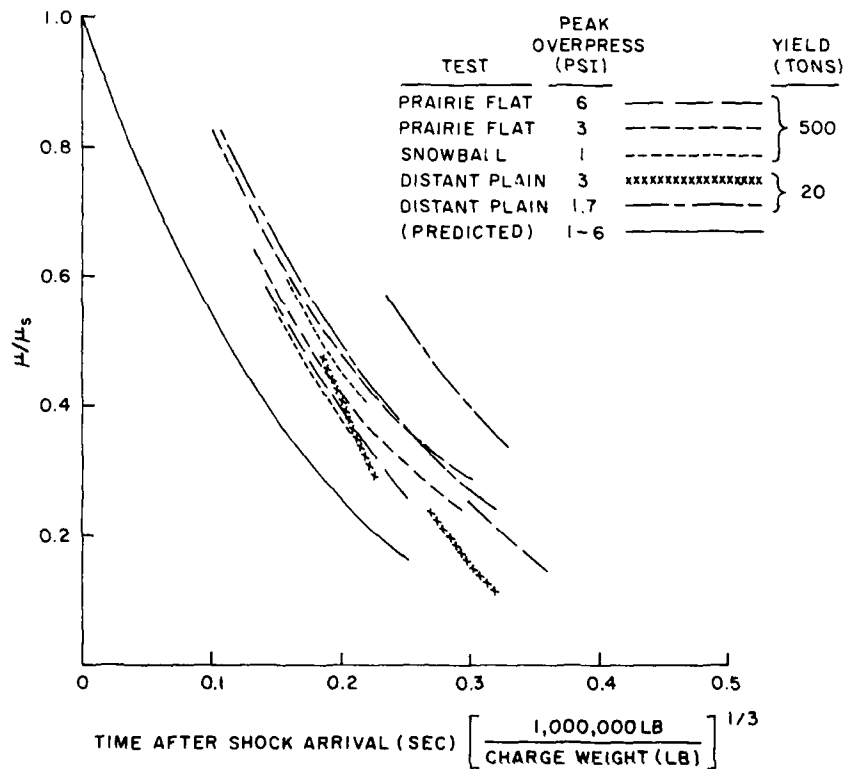


Figure 5.9. Comparison of air-velocity waveforms from various tests with the predicted waveform.

predicted air-particle velocity at each test site. Most of the experimental data lie within a relatively narrow band, which shows that variations in peak overpressure had little effect on the results. Data obtained from the 20-ton detonation agree well with data from the 500-ton detonations. One consistent difference in all the data is that, while the trend follows the predicted (solid-line) curve, the experimental results are shifted to the right. A satisfactory explanation of this shift has not yet been made. Data from the various tests were obtained with different cameras and reduced at different times by several people. Also, the various velocity curves resulting from different tests were constructed independently, before any thought was given to comparing them. These facts do not support a systematic bias in the construction of the curves, but such a bias appears to exist. Extrapolation of the curves in Figure 5.9 to the time of shock arrival indicates that the peak velocity would be about 20 percent greater than that predicted; this seems improbable. The questions that remain simply underscore the need for accurate field measurements in tests that may be made in the future.

### 5.3 Reproducibility and Consistency of Data

These experiments of scale-model buildings subjected to simulated nuclear blast conditions produced great amounts of data. How well can these data be relied on? It was not possible to perform statistical analyses on all the data in a reasonable time; however, the results obtained from certain 1/120-scale buildings in various tests were analyzed for consistency and reproducibility.

#### 5.3.1 Roof-Panel Distributions — 1/120-Scale Models

The roof-panel distributions from seven 1/120-scale buildings were examined in detail. These comprised the four isolated buildings in PRAIRIE FLAT, the two buildings nearest the blast (forward of the slope) in DIAL PACK, and the center building of the front row in the 40-building SNOWBALL complex. Some obvious candidates had to be eliminated: The isolated building in SNOWBALL was damaged by winds before the blast, and distributions from the two buildings on the separate flat pad in DIAL PACK were distorted by cross winds.

Figure 5.10 shows the statistical means of the roof-panel displacements from the seven buildings chosen for analysis, along with confidence levels of 0.5, 0.75, and 0.95 obtained with the "t" distribution procedure.<sup>1</sup> In this procedure it is assumed that the collection of radial (y) or tangential (x) displacements of roof panels from each building represents a sample equal in number to the numbers of panels drawn from a large population of displacements with unknown mean

<sup>1</sup>Fraser, D. A. S., Statistics: An Introduction, John Wiley & Sons, Inc., New York, 1958; pp. 204, 276-278.

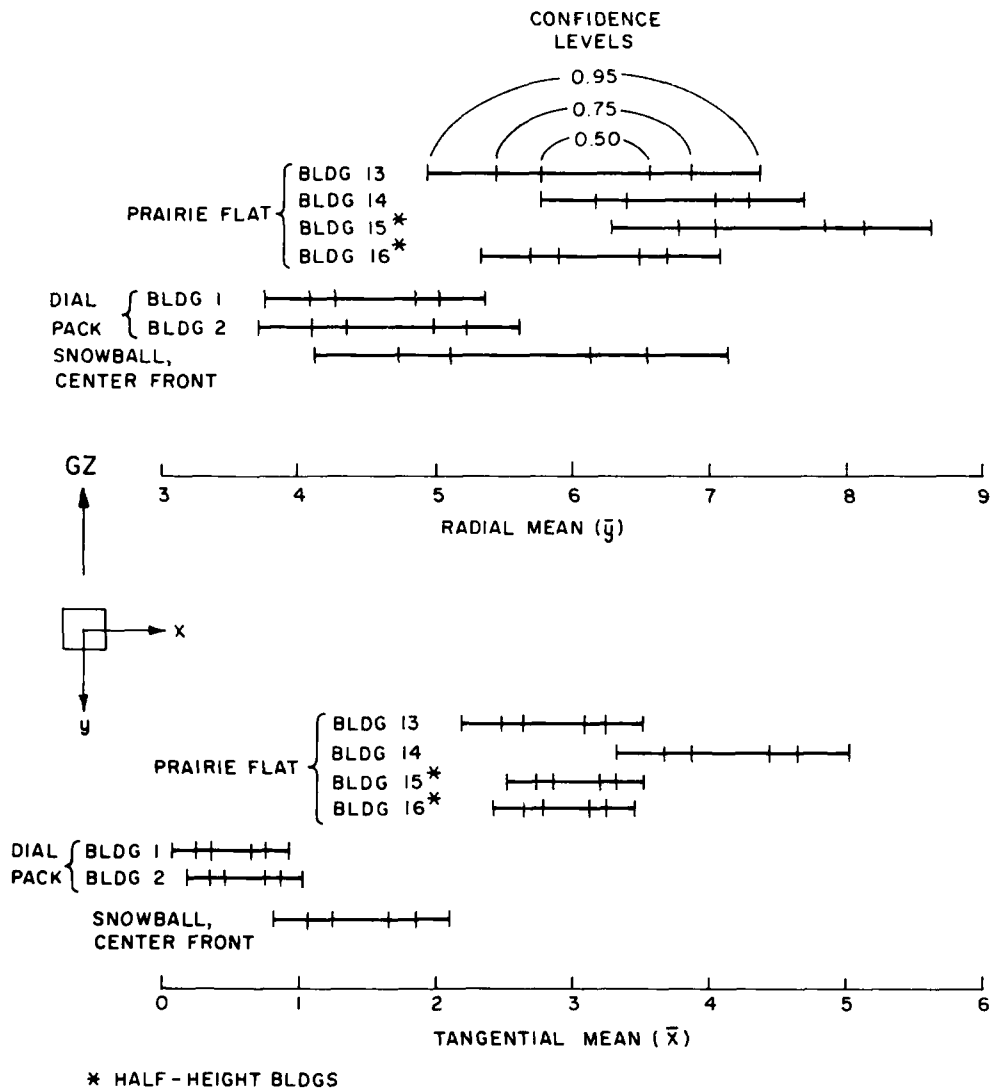


Figure 5.10. Comparison of the radial and tangential mean displacements of roof panels; SNOWBALL, PRAIRIE FLAT, and DIAL PACK 1/120-scale buildings.

distribution ( $\bar{y}$  or  $\bar{x}$ ). This actually was not the case; the data from each model building represented a unique set because of differences — usually small — in building construction and blast characteristics. These sets of data varied among themselves to a greater extent, therefore, than if they had been drawn from a single large population. The 0.5-level bounds imply a 50-percent probability that the mean of the postulated large population from which the sample for each roof was assumed to be taken lies within those bounds. Three of the four PRAIRIE FLAT buildings have

common radial-distance values within the 0.5-confidence-level bounds. If these four distributions had in fact represented samples from a single larger population, it would not be improbable that the 0.5-confidence-level bounds of one of the four would lie beyond the corresponding bounds for the other three. The potential error in assuming a single large population becomes greater when results of different tests are compared. Even so, the results from the seven buildings had common values lying within the 0.95-confidence-level bounds for radial distances. The bounds for the two DIAL PACK buildings are almost identical, which confirms that such experiments can be reproduced closely. The mean distributions for these two buildings are lower, probably because, as explained earlier, these were frame buildings.

Under perfectly symmetrical conditions, the means of the tangential distances should be zero. As Figure 5.10 shows, the means are not zero; this indicates disturbances by cross winds or the action of asymmetrical blast waves. The data for building 14 of PRAIRIE FLAT differ significantly from the data for the other three nearby buildings, illustrating that large discrepancies can occur in a small area. The tangential means for roof debris from the SNOWBALL and DIAL PACK buildings were closer to zero than those applicable to PRAIRIE FLAT; the conditions in the former tests evidently approached the ideal of perfect symmetry more closely. Again, the data for the two DIAL PACK buildings are almost identical.

Figure 5.11 shows the 0.95-confidence-level bounds for the variances (square of the standard deviation) of roof-panel displacements. These bounds were obtained from the chi-squared distribution technique.<sup>2</sup> The same rationale assumed for the "t" distribution of the statistical means applies here. In the radial direction, all seven buildings show common values within the confidence bounds. Results from the PRAIRIE FLAT buildings, however, include extremes almost as great as those from all buildings considered together.

Corresponding data for tangential spread show no common values lying within the 0.95-confidence-level bounds for all buildings. A good overlap of data is obtained, however, if building 14 of PRAIRIE FLAT is excluded.

### 5.3.2 Consistency with Other Data

The characteristics seen in the data for the seven selected 1/120-scale buildings recur throughout the data for other models and other tests. In some cases, differences in similarly obtained data occur that are difficult to understand; in other cases, samples of data are found that are almost identical. Generally, most of the

---

<sup>2</sup>Ibid., pp. 269, 279, 280.

data are consistent, and the reproducibility of results from one test to another (as indicated in Figures 5.10 and 5.11) is about as good as the consistency of results within a single test.

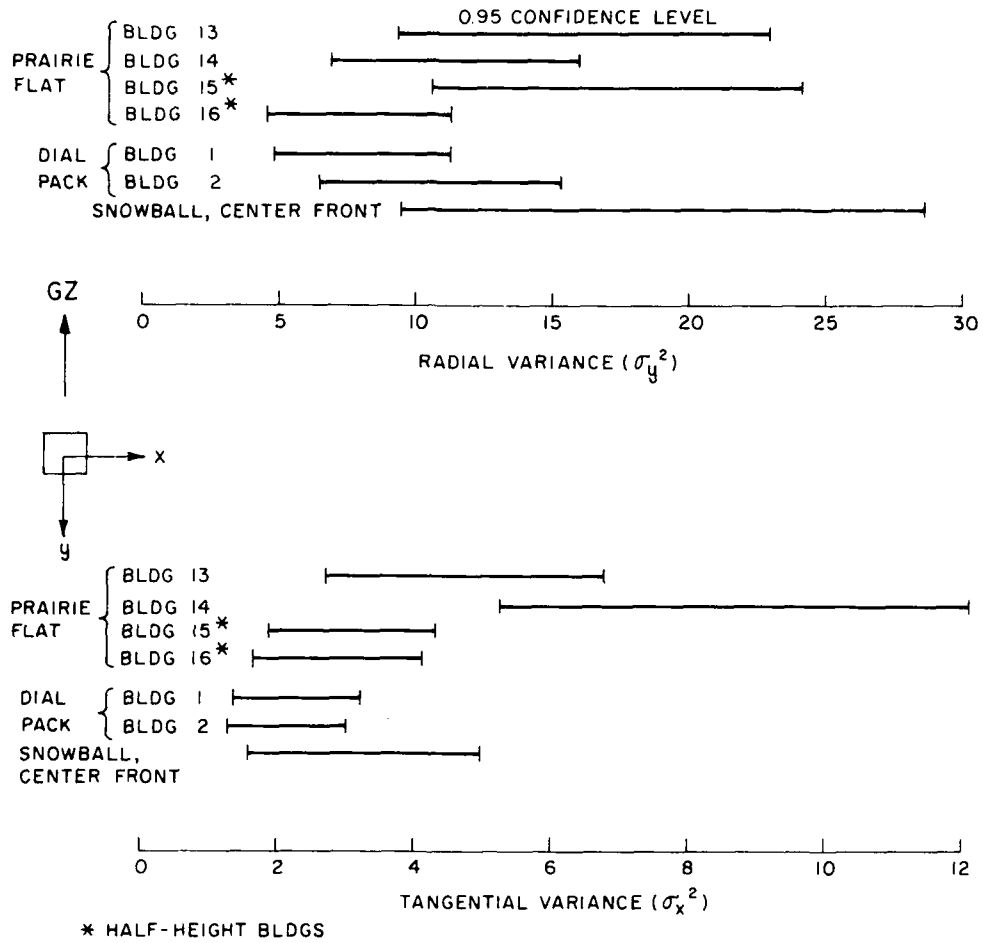


Figure 5.11. Comparison of the radial and tangential variances of roof panels; SNOWBALL, PRAIRIE FLAT, and DIAL PACK 1/120-scale buildings.

## DISTRIBUTION LIST

### DEPARTMENT OF DEFENSE

Defense Technical Information Center  
12 cy ATTN: DD

Defense Intelligence Agency  
ATTN: C. Wiehle  
ATTN: P. Johnson

Defense Nuclear Agency  
ATTN: DOST  
ATTN: SPTD, R. Webb  
4 cy ATTN: TITL  
5 cy ATTN: SPTD, T. Kennedy  
2 cy ATTN: SPSS  
2 cy ATTN: VLWS, M. Rubenstein  
2 cy ATTN: RATN

Field Command  
Defense Nuclear Agency  
ATTN: FCPR  
2 cy ATTN: FCTMD

Field Command  
Defense Nuclear Agency  
Livermore Division  
ATTN: FCPRL

Undersecretary of Def. for Rsch. & Engrg.  
ATTN: Stragic & Space Systems (OS)  
ATTN: ATSD (AE), Exec. Sec.

### DEPARTMENT OF THE ARMY

BMD Advanced Technology Center  
Department of the Army  
ATTN: Archives  
ATTN: M. Dembo

Harry Diamond Laboratories  
Department of the Army  
ATTN: DELHD-NP

U.S. Army Ballistic Research Labs  
5 cy ATTN: DRDAR-BLE, J. Keefer

U.S. Army Nuclear & Chemical Agency  
ATTN: C. Davidson

### DEPARTMENT OF THE AIR FORCE

Air Force Weapons Laboratory, AFSC  
ATTN: SUL

### DEPARTMENT OF THE NAVY

Naval Surface Weapons Center  
ATTN: Code F-31

### DEPARTMENT OF DEFENSE CONTRACTORS

BDM Corporation  
ATTN: C. Somers

Bell Telephone Laboratories, Inc.  
10 cy ATTN: E. Witt

General Electric Company-TEMPO  
10 cy ATTN: DASIAC

JAYCOR  
ATTN: Library

Lovelace Biomedical & Environmental Res. Inst., Inc.  
ATTN: D. Richmond

R & D Associates  
ATTN: C. MacDonald  
3 cy ATTN: P. Rausch

Science Applications, Inc.  
ATTN: M. Drake

Science Applications, Inc.  
ATTN: W. Layson

SRI International  
ATTN: J. Rempel  
2 cy ATTN: Library

### OTHER GOVERNMENT AGENCY

Federal Emergency Management Agency  
2 cy ATTN: G. Sisson

### FOREIGN ORGANIZATIONS

Atomic Weapons Research Establishment  
2 cy ATTN: N. Thumpston

Defense Research Establishment  
2 cy ATTN: J. Anderson

Ernst-Mach-Institut  
ATTN: H. Reichenback